

Georgia State University

ScholarWorks @ Georgia State University

---

Chemistry Dissertations

Department of Chemistry

---

6-12-2006

## On the Mechanistic Roles of the Protein Positive Charge Close to the N(1)Flavin Locus in Choline Oxidase

Mahmoud Ghanem

Follow this and additional works at: [https://scholarworks.gsu.edu/chemistry\\_diss](https://scholarworks.gsu.edu/chemistry_diss)

 Part of the [Chemistry Commons](#)

---

### Recommended Citation

Ghanem, Mahmoud, "On the Mechanistic Roles of the Protein Positive Charge Close to the N(1)Flavin Locus in Choline Oxidase." Dissertation, Georgia State University, 2006.  
doi: <https://doi.org/10.57709/1059246>

This Dissertation is brought to you for free and open access by the Department of Chemistry at ScholarWorks @ Georgia State University. It has been accepted for inclusion in Chemistry Dissertations by an authorized administrator of ScholarWorks @ Georgia State University. For more information, please contact [scholarworks@gsu.edu](mailto:scholarworks@gsu.edu).

**On the Mechanistic Roles of the Protein Positive Charge Close to the N(1) Flavin Locus in  
Choline Oxidase**

**by**

**Mahmoud Ghanem**

**Under the Direction of Dr. Giovanni Gadda**

**Abstract**

Choline oxidase catalyzes the oxidation of choline to glycine betaine. This reaction is of considerable medical and biotechnological applications, because the accumulation of glycine betaine in the cytoplasm of many plants and human pathogens enables them to counteract hyperosmotic environments. In this respect, the study of choline oxidase has potential for the development of a therapeutic agent that can specifically inhibit the formation of glycine betaine, and therefore render pathogens more susceptible to conventional treatment. The study of choline oxidase has also potential for the improvement of the stress resistance of plant by introducing an efficient biosynthetic pathway for glycine betaine in genetically engineered economically relevant crop plant. In this study, *codA* gene encoding for choline oxidase was cloned. The cloned gene was then used to express and purify the wild-type enzyme as well as to prepare selected mutant forms of choline oxidase. In all cases, the resulting enzymes were purified to high levels, allowing for detailed characterizations. The biophysical and biochemical analyses of choline oxidase variants in which the positively charged residue close to the flavin N(1) locus (His<sub>466</sub>) was removed (H466A) or reversed (H466D) suggest that in choline oxidase, His<sub>466</sub> modulates the electrophilicity of the bound flavin and the polarity of the active site, and

contributes to the flavinylation process of the covalently bound FAD as well as to the stabilization of the negative charges in the active site.

Biochemical, structural, and mechanistic relevant properties of selected flavoproteins with special attention to flavoprotein oxidases, as well as the biotechnological and medical relevance of choline oxidase, are presented in Chapter I. Chapter II summarizes all the experimental techniques used in this study. Chapter III-VII illustrate my studies on choline oxidase, including cloning, expression, purification and preliminary characterizations (Chapter III), spectroscopic and steady state kinetics (Chapter IV), the catalytic roles of His<sub>466</sub> and the effects of reversing the protein positive charge close to the flavin N(1) locus (Chapter V and VI), and the roles of His<sub>310</sub> with a special attention to its involvement in a proton-transfer network (Chapter VII). Chapter VIII presents a general discussion of the data presented.

INDEX WORDS: Choline Oxidase, Active Site Base, Flavin N(1) Locus, Proton-Transfer Network, Chemical Mechanism, Flavoprotein.

**On the Mechanistic Roles of the Protein Positive Charge Close to the N(1) Flavin Locus in  
Choline Oxidase**

**by**

**Mahmoud Ghanem**

**A Dissertation Submitted in Partial Fulfillment of the Requirements for the Degree of**

**Doctor of Philosophy**

**in the College of Arts and Sciences**

**Georgia State University**

**2006**

Copyright by

Mahmoud Ghanem and Dr. Giovanni Gadda

2006

**On the Mechanistic Roles of the Protein Positive Charge Close to the N(1) Flavin Locus in  
Choline Oxidase**

**by**

**Mahmoud Ghanem**

Research Advisor: Dr. Giovanni Gadda  
Committee Members: Dr. A.L. Baumstark  
Dr. Dabney W. Dixon  
Dr. Dale E. Edmondson

Electronic Version Approved by:

Office of Graduate Studies  
College of Arts and Sciences  
Georgia State University  
May 2006

## **Acknowledgments**

There are many people to acknowledge and thank as usual for their help and support throughout my period of study. My first acknowledgment and thanks goes to my advisor, Dr. Giovanni Gadda, for teaching and guiding me to become a mature and a successful scientist. I am extremely grateful to be your student for the last four years. From you, I have gained a deep sense of curiosity in acquiring knowledge in any scientific field. Additionally, from some thoughts and suggestions you have shared with me, as well as the ways you handle many things, I learned not only how to be a scientist, but also how to be a big-minded person. Most importantly, you were doing all of these in a very kind friendly way that always make me feel that you are not only my advisor that I learned from him everything in science but also you are really a great friend of mine that I can openly share with him my cheers and tears and always find a very good and mature opinions and suggestions.

I am also very thankful to my committee members, Dr. Baumstark, Dr. Dixon, and Dr. Edmondson, for your great suggestions for my project, and your constant support in all aspects during these years. All of you have inspired me to be a great scientist from a variety of aspects. I have truly felt the big and generous minds of a scientist from all of you. I have learned so much from each of you, which can be of benefit for my career and my whole life. Dr. Dixon, I have learned from you how to become a good scientific writer through your critical reading of my writing, also I will never forget the class that I attend it with you because it really benefit me in a way that you trained me how to think critically about my career. Dr. Edmondson, I will never forget your kind hosting of me in your laboratory while you was teaching me how to measure the Redox Potential of my enzyme, I really enjoyed that time in your laboratory and I also learned a

lot from you through your kind and generous suggestions either in your laboratory or through our regular flavin group meeting.

For the Egyptian Government, I am really very thankful to my government that supported me financially through my Ph.D. program here in the United States. I would like also to dedicate a special Thank to all the employees of the Egyptian Culture and Educational Bureau (ECEB) in Washington D.C. for providing me all kinds of supports and helping me to solve all sorts of problems that I ever faced through my Ph.D. program.

For my labmates, I had such a great time with all of you. Fan, Kevin, Nichole, Trang, Tran, Kunchala, Merid, Osbourne, and Steffan. All of you make the lab such an exciting place. As the one who had been with me the longest time, Fan, I am really glad to work with you. Not only were you always there for me since I joined the lab, but also you have been a great friend whom I can always rely on.

I also owe big thanks to my best friends, Mohamed Emara, Hassan Walley, and Hossam Ewis. During the years of my degree, with its ups and downs, you were always there for me like a family that I can share my cheers and tears, and a family that I can always count on. I enjoyed everyday being around you at the school. Mohamed, you are just a great friend that I knew since 16 years and I can always count on at any time. I will never forget how generous you were in helping me to settle down when I firstly came here to start my Ph.D. in the United State, and even before that time, I really owe you a big thank for all what you did for me, you are really a friend in needs.

Also, as the most important part of my life, my family, my mom Ms. Hossneya Kamal, my late dad Mr. Ghanem Mahmoud, my sister Ms. Eman Ghanem, my daughter (the sweetest person in my life) Yomna Ghanem, and my wife Ms. Maha Hosny. I really become speechless



when it comes to the time to acknowledge my family, because no words can address my sincere feeling toward all of them. Mom, you did a lot for me and you sacrifice your life for taking good care of me and my sister, without your endless supports and unconditional love, I could not have gotten this far. Yomna, you are always the sweetest person in my whole life and thinking about you and your future always encourage me to be more successful and proceed constantly in my career, you are really the light of my life. Eman, you are not only a great sister but also you are always a very close friend of mine that I can share with you everything in my life, also you usually care about me and my career in a way that I always mention that I am lucky because I have two mothers instead of one!! Maha, I owe you a big thank for your continuous love, supports and encouragements through these times. I am so grateful and fortunate to have all of you as the light of my life!

Best wishes to all the people, mentioned or not mentioned, who have been giving me supports, helps, and encouragements!

## Table of Contents

vii

Abstract.....	i
Acknowledgments.....	iv
Table of Contents.....	vii
List of Tables .....	xi
List of Figures .....	xiii
List of Schemes.....	xviii
Chapter I. Introduction.....	1
1.1. Flavoproteins.....	1
1.1.1. The Reactivity of Flavoproteins with Sulfite.....	7
1.1.2. Stabilization of Anionic Semiquinone by Flavoprotein Oxidases.....	10
1.1.3. Stabilization of the Benzoquinoid Anionic Form of 6- and 8-Substituted Hydroxy- and Mercaptoflavins by Flavoprotein Oxidases .....	12
1.1.4. Positive Charge in Proximity of N(1)-C(2)=O and Flavinylation .....	16
1.2. GMC Oxidoreductase Enzyme Superfamily .....	22
1.2.1. Glucose Oxidase .....	26
1.2.2. Cholesterol Oxidase .....	30
1.2.3. Cellobiose Dehydrogenase.....	32
1.2.4. Pyranose 2-Oxidase .....	34
1.2.5. Methanol Oxidase (Alcohol Oxidase) .....	36
1.3. Other Structurally and Mechanistically Relevant Flavoproteins .....	37
1.3.1. Glycolate Oxidase.....	38
1.3.2. Flavocytochrome $b_2$ .....	42

1.3.3. D-Amino Acid Oxidase .....	45
1.4. Choline Oxidase.....	49
1.4.1. X-ray Structure of Choline Oxidase .....	68
1.5. Choline Dehydrogenase .....	79
1.6. Biological Applications .....	85
1.6.1. Glycine Betaine as an Osmoprotectant .....	90
1.6.2. Biotechnological Application of Glycine Betaine .....	93
1.6.3. Biomedical Applications of Glycine Betaine .....	94
1.7. Goals .....	97
References.....	100
CHAPTER II. Material and Methods. ....	119
Materials .....	119
Instruments.....	120
Subcloning and cloning of <i>codA</i> .....	120
Enzyme preparation .....	124
Site-directed mutagenesis .....	125
Expression and purification of the mutated enzymes .....	126
Enzyme assays .....	126
Spectral studies .....	128
Potentiometric titrations.....	130
Steady state kinetics.....	131
Rapid kinetics.....	132
Data analysis .....	132

References.....	136
Chapter III. Cloning, Sequence Analysis, and Purification of Choline Oxidase From <i>Arthrobacter globiformis</i> : A Bacterial Enzyme Involved in Osmotic Stress Tolerance .....	138
Abstract.....	138
Introduction.....	139
Materials and Methods.....	141
Results.....	149
Discussion.....	156
Acknowledgments.....	160
References.....	161
Chapter IV. Spectroscopic and Kinetic Properties of Recombinant Choline Oxidase from <i>Arthrobacter globiformis</i> . ....	165
Abstract.....	165
Introduction.....	167
Experimental Procedures .....	170
Results.....	174
Discussion.....	190
Acknowledgment.....	195
References.....	196
Chapter V. On the Catalytic Role of the Conserved Active Site Residue His <sub>466</sub> of Choline Oxidase. ....	202
Abstract.....	202
Introduction.....	204

Experimental Procedures .....	208
Results.....	215
Discussion.....	230
Acknowledgment.....	238
References.....	239
Chapter VI. Effects of Reversing the Protein Positive Charge in Proximity of the N(1)-Flavin Locus of Choline Oxidase.....	244
Abstract.....	244
Introduction.....	246
Experimental Procedures .....	250
Results.....	256
Discussion.....	272
Acknowledgment.....	278
References.....	279
Chapter VII. On the Role of the Active Site Residue His310 of Choline Oxidase. ....	284
Abstract.....	284
Introduction.....	286
Experimental Procedures .....	290
Results.....	293
Discussion.....	300
References.....	304
Chapter VIII. General Discussion.....	305
References.....	317

## List of Tables

Table 1.1. Some Characteristic Properties of Selected Flavoproteins .....	11
Table 1.2. Examples of Flavoproteins Containing Covalently Linked Flavin Redox Centers <sup>a</sup> ...	18
Table 1.3. Some Structural and Mechanistic Features of Selected Flavoenzymes.....	37
Table 1.4. Inhibition Studies of Choline Oxidase at pH 6.5 <sup>a</sup> .....	56
Table 1.5. Steady State Kinetic Parameters for Choline and <i>N</i> -Substituted Choline Analogs as Substrates for Choline Oxidase at pH 8 <sup>a</sup> .....	57
Table 1.6. pH Dependence of Kinetic Isotope Effects at Different Oxygen Concentrations <sup>a</sup> .....	62
Table 1.7. pK <sub>a</sub> Values for Steady State Kinetic Parameters with Choline or 1,2-[ <sup>2</sup> H <sub>4</sub> ]-Choline as Substrate <sup>a</sup> .....	62
Table 1.8. NMR Determination of Hydration Ratio of Betaine Aldehyde and 3,3- Dimethylbutylraldehyde in Aqueous Solution <sup>a</sup> .....	66
Table 2.1. Oligonucleotide primers used for primer extension amplification and PCR of <i>codA</i> , as well as the mutagenesis for pET/ <i>codA</i> .....	122
Table 3.1. Oligonucleotide Primers Used for Primer Extension Amplification and PCR of <i>codA</i> . .....	143
Table 3.2. Purification of Recombinant <i>A. globiformis</i> Choline Oxidase Heterogously Expressed in <i>E. coli</i> .....	151
Table 4.1. Steady-State Kinetic Parameters for Recombinant Choline Oxidase with Choline or Betaine Aldehyde as Substrate at pH 7 <sup>a</sup> .....	185
Table 4.2. Product Inhibition Studies of Recombinant Choline Oxidase with Glycine Betaine <sup>a</sup>	186
Table 5.1. Steady State Kinetic Parameters of CHO-H466A and CHO-WT with Choline as Substrate at pH 7 <sup>a</sup> .....	223

Table 5.2. The Effect of Imidazole on the Turnover Number of CHO-H466A at Different pH Values <sup>a</sup> .....	223
Table 5.3. Substrate and Solvent Isotope Effects on the Oxidation of Choline Catalyzed by CHO-H466A.....	227
Table 6.1. Comparison of the Spectral Properties Parameters of CHO-H466D, CHO-H466A, and CHO-WT, at pH 6.....	259
Table 6.2. Midpoint Reduction-Oxidation Potentials for the Enzyme-FAD of Unliganded CHO-WT, CHO-H466A, and CHO-H466D, at pH 7 <sup>a</sup> .....	265
Table 7.1. Anaerobic Spectral Incubation of CHO-H310A with Choline <sup>a</sup> .....	299

## List of Figures

Figure 1.1. Structures of riboflavin, FMN, and FAD. ....	2
Figure 1.2. Representation of possible flavin-protein interactions. ....	3
Figure 1.3. Redox and ionization states of flavins.....	3
Figure 1.4. Spectra of glucose oxidase in the oxidized, semiquinone (anionic or neutral), and fully reduced states. ....	4
Figure 1.5. Artificial flavins that have been used as flavin replacements in flavoproteins. ....	4
Figure 1.6. Mode of reaction of sulfite with oxidized flavin. ....	9
Figure 1.7. Effect of sulfite on lactate oxidase. ....	9
Figure 1.8. Tautomeric and mesomeric forms of 8-mercaptoflavin. ....	13
Figure 1.9. Spectral changes upon binding of 8-mercapto-FAD to the apoprotein of glucose oxidase. ....	13
Figure 1.10. Structures of the neutral and the anionic form of 6-hydroxy- and 6-mercaptoflavins. .....	15
Figure 1.11. Mode of covalent attachment of flavin to the protein in flavoproteins. ....	17
Figure 1.12. Flavinylation mechanism of trimethylamine dehydrogenase.....	20
Figure 1.13. Mechanism of flavinylation of monomeric sarcosine oxidase and <i>N</i> - methyltryptophan oxidase.....	21
Figure 1.14. The three-dimensional structures of members of the GMC oxidoreductase enzyme superfamily. ....	23
Figure 1.15. The active site residues of GMC oxidoreductase enzyme superfamily. ....	25
Figure 1.16. Docking of $\beta$ -D-glucose to the pyranose 2-oxidase active site. ....	36



Figure 1.17. The three-dimensional structures of FMN-dependent enzymes that oxidize $\alpha$ -hydroxy acids.....	39
Figure 1.18. The hydrogen bonding pattern of the inhibitors at the active site of glycolate oxidase. ....	41
Figure 1.19. Schematic presentation of the proposed transition state of glycolate oxidase. ....	41
Figure 1.20. Active site of <i>R. gracilis</i> DAAO with D-3,3,3-F <sub>3</sub> -alanine bound (PDB code 1C0L). .....	47
Figure 1.21. pH-Dependence of the deuterium isotope effects. ....	58
Figure 1.22. pH dependence of <sup>D</sup> (k <sub>cat</sub> /K <sub>m</sub> ) and <sup>D</sup> k <sub>cat</sub> values with 1,2-[ <sup>2</sup> H <sub>4</sub> ]-choline as substrate for choline oxidase at 0.07 (□), 0.25 (■), 0.97 mM (○) and saturating (●) oxygen concentrations. ....	61
Figure 1.23. Three-dimensional structure of choline oxidase from <i>Arthrobacter globiformis</i> . ...	70
Figure 1.24. Rossmann fold (ADP-binding motif) structure of choline oxidase.....	71
Figure 1.25. Approximately orthogonal views of the 50 - 1.86 Å resolution electron density maps for the FAD isoalloxazine ring in choline oxidase. ....	73
Figure 1.26. Active site structures of choline oxidase, fitting with DMSO.....	73
Figure 1.27. Active site structures of choline oxidase, showing its cavity (A) and docking with choline (B). ....	77
Figure 1.28. Active site structures of choline oxidase showing the proton-transfer network. ....	78
Figure 1.29. UV-visible absorbance spectrum of choline dehydrogenase containing a His-tag from <i>Escherichia coli</i> K 12, in air saturated 100 mM potassium phosphate, pH 7.0, at 25 °C. .....	81
Figure 1.30. Alignment of choline oxidase with choline dehydrogenase.....	83

Figure 1.31. The surface of the monomeric structure of choline oxidase.....	84
Figure 1.32. Structures of selected osmoprotectants. ....	87
Figure 1.33. Osmostress response systems of <i>E. coli</i> . ....	88
Figure 1.34. Osmostress response systems of <i>Bacillus subtilis</i> . ....	89
Figure 1.35. Enhanced tolerance of transgenic <i>Arabidopsis</i> to salt stress. ....	92
Figure 3.1. Purification of recombinant <i>A. globiformis</i> choline oxidase heterogously expressed in <i>E. coli</i> . ....	151
Figure 3.2. MALDI-TOF mass spectrometric analysis of recombinant choline oxidase. ....	153
Figure 3.3. UV-Visible absorbance spectrum of recombinant choline oxidase. ....	155
Figure 3. 4. Alignment of choline oxidase with selected members of the GMC oxidoreductase enzyme superfamily. ....	159
Figure 4.1. Reaction of recombinant choline oxidase with sodium dithionite. ....	174
Figure 4.2. Circular dichroism spectrum of flavin semiquinone-containing choline oxidase. ...	176
Figure 4.3. Electron spin resonance spectrum of recombinant choline oxidase. ....	177
Figure 4. 4. Conversion of E-FAD <sub>ox/sq</sub> to E-FAD <sub>ox</sub> . ....	180
Figure 4. 5. Reaction of FAD <sub>ox</sub> -containing choline oxidase with sodium dithionite. ....	180
Figure 4.6. Reaction of choline oxidase with sulfite. ....	181
Figure 4.7. UV-Visible absorbance spectra of choline oxidase during turnover with choline..	183
Figure 4.8. pH Dependence of the $k_{cat}/K_m$ and $k_{cat}$ values for choline as substrate for recombinant choline oxidase.....	188
Figure 4.9. pH Dependence of the $k_{cat}/K_m$ values for oxygen with choline or betaine aldehyde as substrate for recombinant choline oxidase.....	188

Figure 4.10. pH Dependence of the apparent kinetic parameters of E-FAD <sub>ox/sq</sub> and E-FAD <sub>ox</sub> with choline as substrate. ....	189
Figure 4.11. pH Dependence of inhibition by glycine betaine. ....	189
Figure 5.1. The conserved active site residues in the GMC oxidoreductase superfamily. ....	205
Figure 5.2. Comparison of the spectral properties of CHO-H466A (solid curves) and CHO-WT (dotted curves). ....	217
Figure 5.3. Reaction of CHO-H466A with sulfite. ....	218
Figure 5.4. Effect of pH on the spectral properties of CHO-H466A and CHO-WT. ....	219
Figure 5.5. Potentiometric redox titration of CHO-H466A in complex with glycine betaine....	221
Figure 5.6. pH dependence of the imidazole-rescued activity of CHO-H466A. ....	224
Figure 5.7. pH dependence of $k_{cat}/K_m$ (●) and $k_{cat}$ (○) values of CHO-H466A for choline as substrate. ....	227
Figure 5.8. Binding of glycine betaine to CHO-H466A. ....	229
Figure 5.9. Proposed interaction of His <sub>466</sub> with the flavin N(5)-sulfite adduct. ....	232
Figure 6.1. Line draw showing the interaction of His <sub>466</sub> with the N(1)-C(2)=O locus of FAD and the choline alkoxide species in the transition state for the oxidation of choline catalyzed by choline oxidase. ....	249
Figure 6.2. Purification of CHO-H466D. ....	256
Figure 6.3. Comparison of the spectral properties of CHO-H466D, CHO-WT and CHO-H466A. ....	258
Figure 6.4. Stoichiometry and flavin content of CHO-H466D. ....	260
Figure 6.5. Effect of pH on the spectral properties of CHO-H466D. ....	262
Figure 6.6. Anaerobic reduction of CHO-H466A using xanthine and xanthine oxidase. ....	263

Figure 6.7. Potentiometric reduction titration of CHO-H466D in complex with choline. ....	263
Figure 6.8. Potentiometric reduction-oxidation titration of CHO-WT, CHO-H466A, and CHO-H466D. ....	266
Figure 6.9. Binding of choline to CHO-H466D. ....	269
Figure 6.10. Binding of glycine betaine to CHO-WT, CHO-H466A and CHO-H466D. ....	270
Figure 6.11. Reaction of CHO-H466D with sulfite. ....	271
Figure 7.1. Line draw showing the interaction of His <sub>466</sub> with the N(1)–C(2)=O locus of FAD and the choline alkoxide species in the transition state for the oxidation of choline catalyzed by choline oxidase. ....	288
Figure 7.2. Crystal structure of choline oxidase. ....	289
Figure 7.3. Expression and purification of CHO-H310A. ....	293
Figure 7.4. Spectral properties of CHO-H310A. ....	294
Figure 7.5. Anaerobic reaction of CHO-H310A with choline (1). ....	297
Figure 7.6. Anaerobic reaction of CHO-H310A with choline (2). ....	298
Figure 7.7. Anaerobic reaction of CHO-H310A with choline (3). ....	299

## List of Schemes

Scheme 1.1. Reactions catalyzed by GMC oxidoreductases. ....	24
Scheme 1.2. The enzymatic reaction catalyzed by glucose oxidase. ....	26
Scheme 1.3. Proposed mechanisms for alcohol oxidation by GMC enzymes. ....	29
Scheme 1.4. Reaction catalyzed by glycolate oxidase. ....	38
Scheme 1.5. Reaction catalyzed by flavocytochrome $b_2$ . ....	42
Scheme 1.6. Proposed mechanism of L-lactate oxidation by flavocytochrome $b_2$ . ....	44
Scheme 1.7. Reaction catalyzed by D-amino acid oxidase. ....	45
Scheme 1.8. Kinetic mechanism of D-amino acid oxidase. ....	45
Scheme 1.9. Proposed direct hydride transfer mechanism of D-amino acid oxidase. ....	48
Scheme 1.10. Reaction catalyzed by choline oxidase. ....	50
Scheme 1.11. Chemical mechanism of choline oxidase for oxidation of choline at pH 10. ....	59
Scheme 1.12. Proposed mechanism for the oxidation of betaine aldehyde catalyzed by choline oxidase. ....	66
Scheme 1.13. Proposed mechanism for the four-electron oxidation of choline to glycine betaine catalyzed by choline oxidase. ....	67
Scheme 1.14. Oxidation of choline to glycine-betaine catalyzed by choline dehydrogenase. ....	79
Scheme 3.1. Reaction catalyzed by choline oxidase. ....	140
Scheme 4.1. Reaction catalyzed by choline oxidase. ....	169
Scheme 4.2. Steady state kinetics for choline oxidase. ....	169
Scheme 5.1. Chemical mechanism for choline oxidation catalyzed by choline oxidase. ....	206
Scheme 5.2. Chemical reaction catalyzed by choline oxidase. ....	206

Scheme 5.3. Proposed role of His466 in stabilizing the transition state during the oxidation of choline catalyzed by choline oxidase.....	235
Scheme 6.1. Reaction catalyzed by choline oxidase.....	248
Scheme 6.2. Chemical mechanism for choline oxidation catalyzed by choline oxidase.....	249
Scheme 7.1. Reaction catalyzed by choline oxidase.....	288
Scheme 7.2. Proposed role of His <sub>310</sub> in the reaction catalyzed by choline oxidase.....	303
Scheme 8.1. Mechanism of oxidation of choline catalyzed by choline oxidase.....	316

## CHAPTER I

### Introduction

#### 1.1. Flavoproteins

Since the discovery and the chemical characterizations of flavins (Figure 1.1) in the 1930s, they have been known of being capable of both one- and two-electron transfer processes, and as playing a fundamental role in coupling the two-electron oxidation of many organic substrates to the one-electron transfers of the respiratory chain (1). The mode of interaction of the isoalloxazine nucleus of the flavin with the protein is the key determinant of the type of function carried out by a particular enzyme. From a chemical standpoint, the isoalloxazine moiety of the flavin is amphipathic, i.e., while the xylene moiety is hydrophobic and can interact with hydrophobic parts of the protein, the pyrimidine ring is hydrophilic and electron-deficient, enabling the formation of hydrogen bonds and electrostatic interactions with proteins (Figure 1.2) (2).

The flavin can exist in three different redox states, the oxidized, semiquinoid, and the fully reduced species (Figure 1.3). In addition, the semiquinone can exist in a neutral (blue) or anionic (red) form, with a  $pK_a$  of  $\sim 8.5$  in solution (3, 4). This  $pK_a$  can be significantly changed upon the binding of the flavin to a specific protein, i.e., while some enzymes can stabilize the neutral radical form over the whole pH range at which the enzyme is stable ( $pK_a \gg 8.5$ ), others stabilize the red anionic semiquinone species ( $pK_a \ll 8.5$ ). In some enzymes, among which glucose oxidase was the first example (5), the  $pK_a$  is in the detectable pH range, allowing the spectral characterizations of these two species (Figure 1.4).

At neutral pH, the pyrimidine moiety of the isoalloxazine nucleus is electron rich molecule in the reduced state with a negative charge at the N(1)-C(2)=O locus (anionic hydroquinone). A  $pK_a$  value of  $\sim 6.5$  was determined for the ionization of the N(1) locus of the reduced flavin (2). A powerful tool to probe the active center of many flavin enzymes before their crystal structures become available is the replacement of the native flavin by suitably modified flavins (6). Many flavoprotein enzymes, in which flavin cofactor is not covalently attached, can accept a chemically modified flavin ring structure into their active site (7). A large number of chemically modified flavins with different substituents at various positions around the isoalloxazine nucleus have become available (Figure 1.5). The use of chemically modified flavin substituents has proved to be of great value, since they can be used to probe the flavin environment at a specific position. In this regard, studies on the interactions of the flavin with the enzyme active site were initiated by the use of naturally occurring 6-OH and 8-OH flavin chromophores (8, 9). Edmondson et al., were first to probe the importance of the N(5) position in flavin coenzymes through the use of 5-deaza-FMN (10).

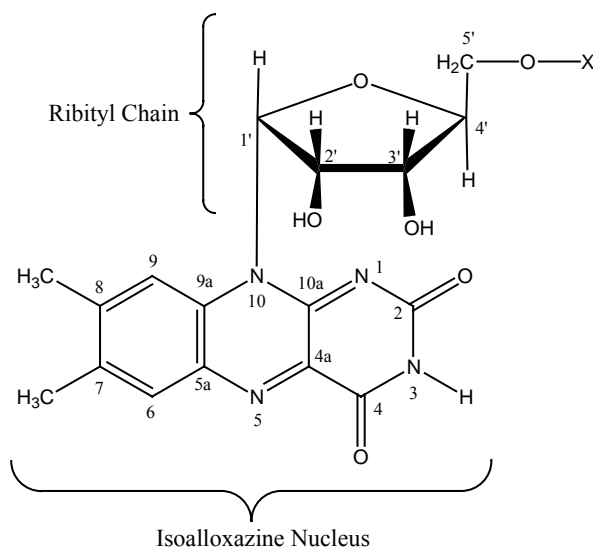


**Figure 1.1.** Structures of riboflavin, FMN, and FAD. Riboflavin, X = H; FMN, X =  $\text{PO}_3^{2-}$ ; FAD, X = ADP.



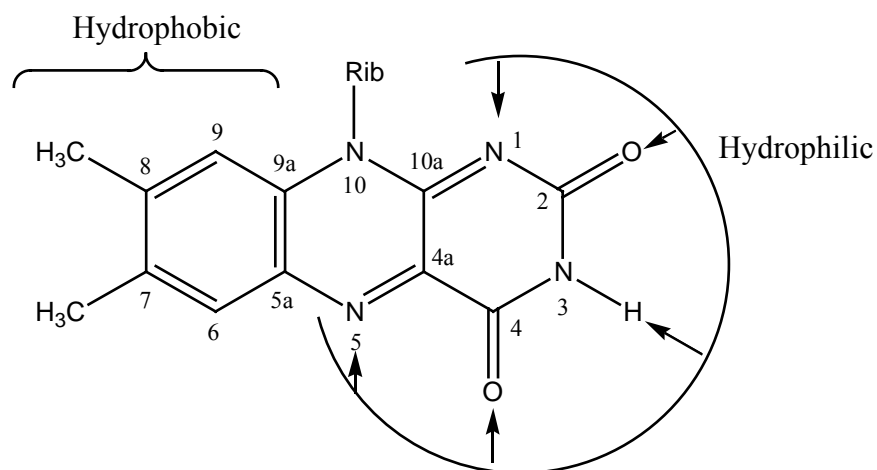


**Figure 1.2.** Representation of possible flavin-protein interactions. Modified from ref. (2).

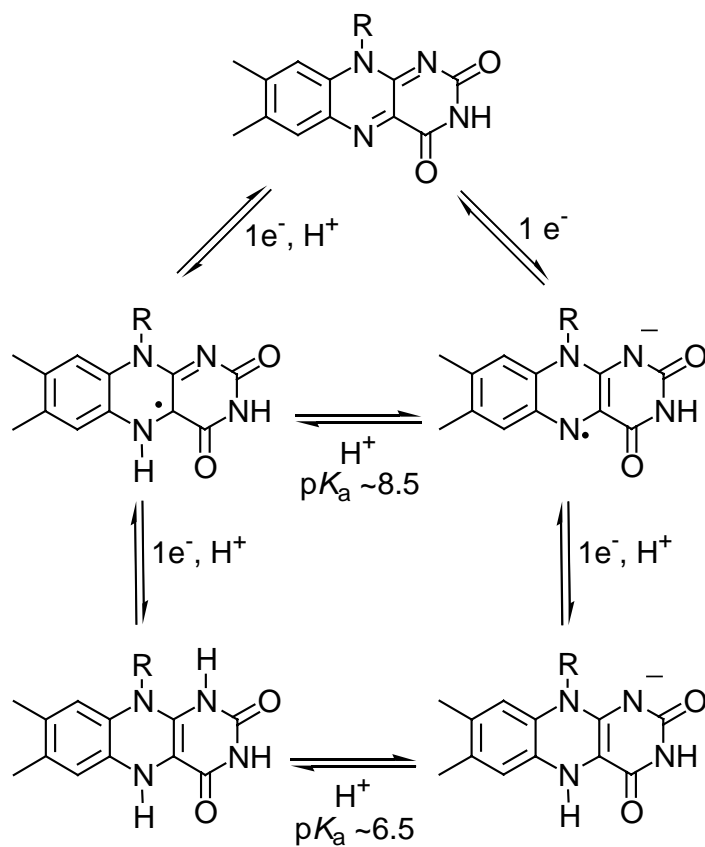


**Figure 1.3.** Redox and ionization states of flavins. Modified from ref. (2).

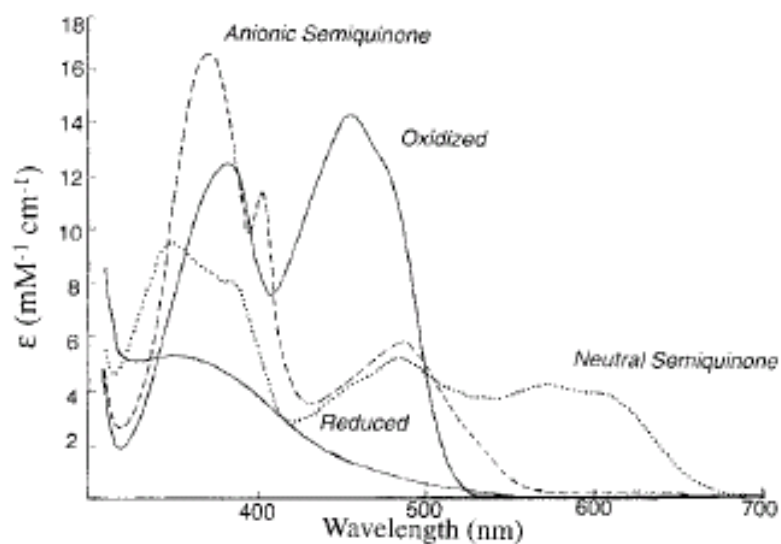


**Figure 1.4.** Spectra of glucose oxidase in the oxidized, semiquinone (anionic or neutral), and fully reduced states.

Taken without permission from ref. (5).

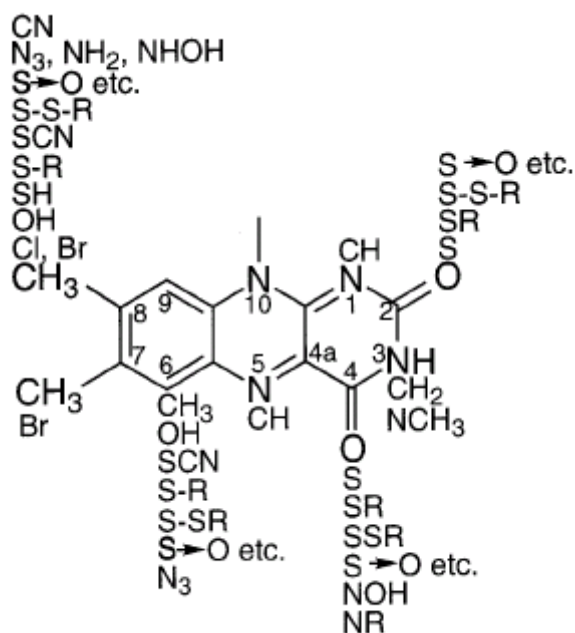


**Figure 1.5.** Artificial flavins that have been used as flavin replacements in flavoproteins.

Taken without permission from ref. (1).

Our understanding of the versatile chemistry of flavins and the mechanisms of action of flavoprotein enzymes has progressed significantly in the last 20 years, especially since the X-ray crystallographic structures of many flavoprotein enzymes have become available. Flavoenzymes can be grouped into relatively small number of classes, where members within the same class share several common properties, including the type of reactions that they catalyze, the nature of the auxiliary redox centers, and their ability to use molecular oxygen as electron acceptor (11). Simple flavoproteins have been classified on the basis of the reactivity of the reduced enzyme with molecular oxygen. This classification, as well as the common properties of each class, have been reviewed previously by Massey and Hemmerich (6), but for convenience they will be summarized here.

**Flavoprotein Monooxygenases.** In flavoprotein monooxygenases, such as *p*-hydroxybenzoate hydroxylase (PHBH) and bacterial luciferase, the reduced enzyme reacts with molecular oxygen with the formation of an observable C(4a)-hydroperoxide intermediate (11). In this class of enzymes, the physiological reductant for the reaction is either NADH or NADPH (11). The flavin hydroperoxide intermediate then transfers an oxygen atom to the substrate with the formation of a C(4a)-hydroxyflavin, which returns to its oxidized state upon dehydration. However, in the absence of the organic substrate, the flavin hydroperoxide can convert slowly to H<sub>2</sub>O<sub>2</sub> and oxidized flavin (11).

**Electron Transferases.** The flavoprotein electron transferases, such as flavodoxin, NADPH-cytochrome P-450 reductase, and ferredoxin-NADP<sup>+</sup> reductase, react slowly with oxygen with the production of flavin semiquinone and O<sub>2</sub><sup>-</sup>. Enzymes from this class are physiologically involved in single-electron transfer reactions. In addition, they all thermodynamically stabilize the blue neutral form of the flavin semiquinone species (11). The

use of chemically reactive flavins, such as 8-Cl-, 8-SCN-, or 8-SH, showed that the benzene ring of the flavin is the only solvent accessible part of the cofactor in that class of enzymes (2). The X-ray crystallographic data of flavodoxin and ferredoxin-NADP<sup>+</sup> reductase have strengthened that conclusion (12). In contrast to oxidases, enzymes from this group cannot stabilize either a flavin-N(5)-sulfite adduct or the benzoquinoid forms of 6- and 8-substituted flavins (2).

**Flavoprotein Oxidases.** In flavoprotein oxidases such as choline oxidase, glucose oxidase, cholesterol oxidase, pyranose 2-oxidase, glycolate oxidase, sarcosine oxidase, monoamine oxidase, and D-amino acid oxidase, to cite a few examples, the reduced enzyme reacts rapidly with molecular oxygen with the production of H<sub>2</sub>O<sub>2</sub> and the oxidized flavin, without the formation of any observable flavin intermediate (13).

Flavoprotein oxidases have been found to share many common properties (Table 1.1) including: 1) they all stabilize a flavin N(5)-sulfite adduct (14-22); 2) they all stabilize the red anionic semiquinone flavin radical on the one-electron reduction (16, 17, 22-25); and 3) they all stabilize the benzoquinoid anion forms of 6- and 8-substituted hydroxy- and mercaptosubstituted flavins (2, 9, 14, 18, 26, 27). In all the studied to date cases, the negative charge of the anionic flavin is localized at the N(1)-C(2)=O region of the isoalloxazine moiety (Figure 1.1) (2). These conclusions have led to the further interpretation that a positively charged locus of the protein electrostatically interacts with the pyrimidine ring of the flavin to stabilize the negative charge at the N(1)-C(2)=O locus of the anionic one- or two-electron reduced flavin (6, 14, 18-20). The mechanistic implications for a protein positive charge stabilizing a negative charge on the N(1) locus of the flavin are: to render flavin reduction thermodynamically favorable by elevating the midpoint reduction-oxidation potential of the bound flavin (18, 20, 26-29); to preferentially stabilize the anionic form of the reduced flavin that readily reacts with molecular oxygen (18, 20,

28, 29); and to facilitate the flavinylation process for those enzymes in which the flavin is covalently linked to the protein moiety (30). In the last few years, the X-ray crystal structures of many flavoprotein oxidases have been solved, clearly establishing that a positively charged amino acid residue or a dipole of an  $\alpha$ -helix is commonly oriented toward the N(1)-C(2)=O locus of the enzyme-bound flavin (31-40).

### 1.1.1. The Reactivity of Flavoproteins with Sulfite

One of the most notable features of flavoproteins is that while the free reduced flavin undergoes reaction readily with molecular oxygen, this property is retained only by some flavoproteins including, flavoprotein oxidases and flavoproteins monooxygenases. Until the discovery of the reactivity of sulfite with flavoproteins, no correlations have been found between oxygen reactivity and different properties of flavoenzymes, such as spectral properties, fluorescence, or nature of the flavin prosthetic group (FMN or FAD). The ability of sulfite ions to react with flavoproteins and to form a reversible flavin-N(5)-sulfite adduct has been examined in a large number of flavoenzymes (Figure 1.6) (19). This reaction was found to occur with a number of flavoprotein oxidases such as glucose oxidase ( $K_d = 0.72$  mM) (41), lactate oxidase ( $K_d = 28$  nM) (14), glycolate oxidase ( $K_d = 0.27$   $\mu$ M) (42), D- and L-amino acid oxidase ( $K_d = 3.4$  mM) (19, 43), cholesterol oxidase ( $K_d \sim 0.14$  and 24 mM for *Brevibacterium sterolicum* and *Streptomyces hygroscopicus* cholesterol oxidase, respectively) (16), monomeric sarcosine oxidase ( $K_d$  not determined due to the extremely slow complex formation) (22), and choline oxidase ( $K_d = 50$   $\mu$ M) [this study; (44)]. In all cases, it was found that the formation of the flavin-sulfite adduct is dependent on sulfite concentration, temperature, and pH, but it is not affected by oxygen or light (21).

Spectrophotometrically, the flavin-N(5)-sulfite adduct is characterized by a bleaching of the UV-visible absorbance spectrum of the enzyme-bound flavin, and the subsequent appearance of a new absorption band at ~320-330 nm, with a spectrum similar, but not identical, to the anionic reduced flavoprotein (Figure 1.7 and Figure 4.6; Chapter IV) (19, 44). It was also found that the formation of the reversible flavin-N(5)-sulfite adduct is a characteristic feature of those flavoenzymes that react readily with molecular oxygen as an electron acceptor (1, 2, 19, 21). In contrast, no sulfite reaction was observed with flavoprotein dehydrogenases (19, 21). Therefore, the formation of covalent N(5)-flavin adduct with sulfite has become a common feature that distinguishes flavoprotein oxidases from dehydrogenases (6, 19, 21). The oxidized flavin is electron deficient, and sulfite is a powerful nucleophile; thereby flavin in its oxidized state can react with either  $\text{SO}_3^{2-}$  or  $\text{HSO}_3^-$  (21). In addition, elemental analysis as well as the hydrolysis of the crystalline flavin-sulfite complex showed that one  $\text{SO}_3^{2-}$  was bound per flavin (21).

A linear correlation between the dissociation constant of the flavin-N(5)-sulfite adduct and the oxidation reduction potentials of the bound flavin has been proposed (21). Recently, a linear relationship was shown between the rate constants of flavin-N(5)-sulfite adduct formation ( $k_{\text{on}}$ ) and the midpoint redox potentials of enzyme bound flavins of the reconstituted lactate oxidase with different FMN analogs bearing various substitutions at the flavin 6- and 8-positions (45). In this study, the  $k_{\text{on}}$  values for sulfite formation showed a pattern similar to those of the  $k_{\text{red}}$  values for lactate, with increasing values as the redox potential was raised, until a breakpoint was reached at ~-120 mV, beyond which these values remain unchanged (45). The  $k_{\text{off}}$  values of sulfite, however, showed a consistent decrease with increasing the redox potentials of the enzyme-bound flavin with no obvious breakpoint (45). Interestingly, it was also proposed in this study that the linear relationship between the rate constants of flavin reductions and flavin-N(5)-

sulfite adduct formation and the flavin redox potential below the observed breakpoint indicated the development of significant negative charge in the transition states of the reactions (45).

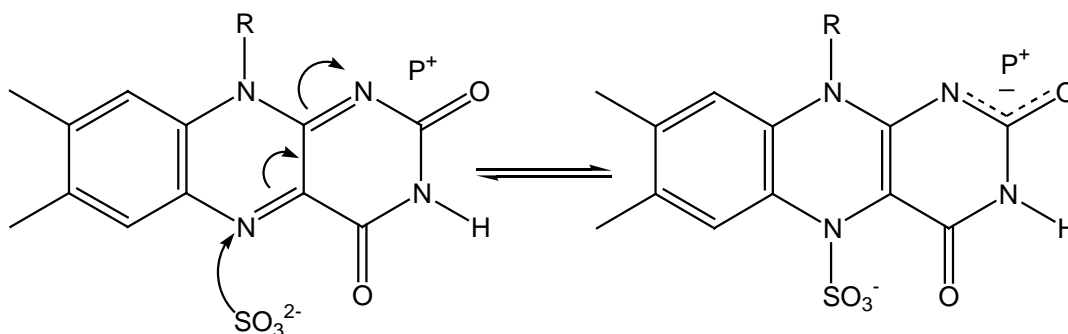


**Figure 1.6.** Mode of reaction of sulfite with oxidized flavin.  
 $P^+$ , protein positively charged amino acid residue or  $\alpha$ -helix dipole.

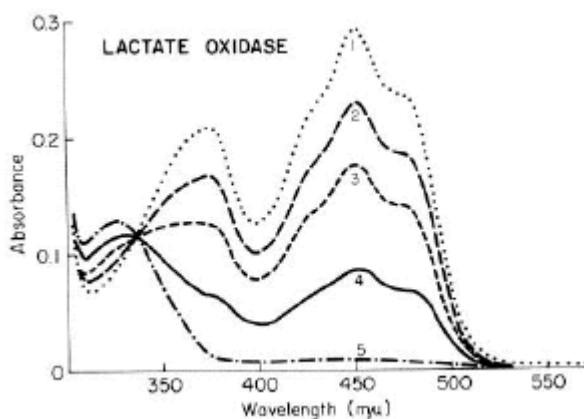


**Figure 1.7.** Effect of sulfite on lactate oxidase.  
*Curve 1*, untreated enzyme (24  $\mu\text{M}$  with respect to FMN content) in 100 mM sodium phosphate, pH 7, at 25  $^{\circ}\text{C}$ . *Curves 2 to 5*, after adding sodium sulfite to concentrations of 6.18  $\mu\text{M}$ , 12.3  $\mu\text{M}$ , 24.4  $\mu\text{M}$ , and 216  $\mu\text{M}$ , respectively. Taken without permission from ref. (19).

### 1.1.2. Stabilization of Anionic Semiquinone by Flavoprotein Oxidases

The flavosemiquinone forms of all the simple flavoproteins studied, i.e., flavoprotein oxidases, flavoprotein monooxygenases, and electron transferases, were either the anionic (red) or neutral (blue) semiquinone forms, each of which has very different and distinctive absorption spectra (Figure 1.4) (5). This conclusion has been supported by the use of model flavins to provide further evidence for the preferred tautomeric structures of the flavin radicals (Figure 1.3) (4, 46). In addition, it can be concluded, with few exceptions, that while the flavoprotein oxidases and hydroxylases stabilize the anionic form of the semiquinone upon the one-electron reduction of the enzymes, the flavoprotein dehydrogenases stabilize the neutral form of the semiquinone (Table 1.1) (1, 2, 19). With the exception of glucose oxidase, which showed an ionization with a  $pK_a$  value of  $\sim 7.5$  (Figure 1.4) (5), most of the flavoproteins studied did not show such ionization; instead, they either stabilize the anionic or the neutral radical species over the whole pH range at which the enzyme is stable. Therefore, it has been concluded that the particular protein to which the flavin is attached stabilizes either the anionic or the neutral semiquinone (19). Furthermore, it has been proposed that either a positively charged amino acid residue or a dipole of an  $\alpha$ -helix close to the flavin N(1) position is responsible for the thermodynamic stabilization of the anionic flavin semiquinone through an electrostatic interaction with the negative charge that develops at the N(1)-C(2)=O of flavosemiquinone species (16, 23, 24). A positively charged residue could also be responsible for the formation of flavin-N(5)-sulfite adduct by facilitating the nucleophilic attack of sulfite to the N(5) locus of the oxidized flavin.



**Table 1.1.** Some Characteristic Properties of Selected Flavoproteins

Flavoenzyme	Cofactor	Radical	N(5)-sulfite adduct	8-Mercapto- flavin	6-Mercapto- flavin	8-Hydroxy- flavin	6-Hydroxy- flavin
Choline oxidase <sup>a</sup>	FAD	Red	Yes	nd	nd	nd	nd
Glucose oxidase <sup>b</sup>	FAD	Red/Blue pK 7.3	Yes	Resolved benzoquinoid	nd	nd	Anion pK < 5.6
Cholesterol oxidase <sup>c</sup>	FAD	Red	Yes	Resolved benzoquinoid	nd	nd	nd
Glycolate Oxidase <sup>d</sup>	FMN	Red	Yes	Resolved benzoquinoid	nd	nd	nd
Lactate oxidase <sup>e</sup>	FMN	Red	Yes	Resolved benzoquinoid	Anion pK < 5	Anion pK < 4	Anion pK < 5
D-Amino acid oxidase <sup>f</sup>	FAD	Red	Yes	Resolved benzoquinoid	Anion pK < 5		Anion pK < 5
Sarcosine oxidase <sup>g</sup>	FAD	Red	Yes	nd	nd	nd	nd
Pyranose 2-oxidase <sup>h</sup>	FAD						
Polyamine oxidase <sup>i</sup>	FAD						
Vanillyl-alcohol oxidase <sup>j</sup>	FAD						
<i>p</i> -Hydroxy-benzoate hydroxylase <sup>k</sup>	FAD	Red/Blue	No	Thiolate			pK < 6.9
Ferredoxin-NADP <sup>+</sup> reductase <sup>l</sup>	FAD	Blue	No	Undefined benzoquinoid			Neutral pK ≥ 10
Glutathione reductase <sup>m</sup>	FAD	Red	No	Undefined benzoquinoid	Anion pK < 4.5		Binds poorly pK ~7.2
Flavodoxin <sup>n</sup>	FMN	Blue	No	Undefined benzoquinoid	Neutral pK 6.4	Neutral pK 6.1	Neutral pK ~9
Trimethylamine dehydrogenase <sup>o</sup>	FMN						
Dihydroorotate dehydrogenase <sup>p</sup>	FMN						
Flavocytochrome <i>b</i> <sub>2</sub> <sup>q</sup>	FMN						
Old yellow enzyme <sup>r</sup>	FMN	Red	No	Smooth benzoquinoid	Anion	Neutral pK 6.2	Anion pK 5.7

<sup>a</sup>, (25, 44, 47-49); <sup>b</sup>, (5, 18, 19, 50-52); <sup>c</sup>, (16); <sup>d</sup>, (2, 19, 42); <sup>e</sup>, (5, 18, 50-52); <sup>f</sup>, (5, 18, 50-52); <sup>g</sup>, (22); <sup>h</sup>, (31); <sup>i</sup>, (53); <sup>j</sup>, (54, 55); <sup>k</sup>, (18, 50-52); <sup>l</sup>, (5, 56); <sup>m</sup>, (57); <sup>n</sup>, (5, 18, 50-52); <sup>o</sup>, (30); <sup>p</sup>, (58, 59); <sup>q</sup>, (60, 61); <sup>r</sup>, (5, 18, 50-52); *nd*, not determined.

### 1.1.3. Stabilization of the Benzoquinoid Anionic Form of 6- and 8-Substituted Hydroxy- and Mercaptoflavins by Flavoprotein Oxidases

The use of modified flavin chromophores at the active sites of many flavoenzymes is a powerful tool to probe the protein microenvironment of the bound flavins (2). The presence of a positively charged amino acid or a dipole of an  $\alpha$ -helix at the active site of many flavoprotein oxidases was proposed long before the crystal structures of enzymes became available (6, 14, 18-20). This proposal was mainly based on the use of modified flavin chromophores that can exist in different tautomeric and/or mesomeric forms, such as 6- and 8- hydroxy and mercaptoflavins. As an example, 8-Mercaptoflavin has significant spectral differences between the neutral and the anionic species, as well as between the corresponding benzenoid and paraquinoid forms (Figure 1.8) (2). The spectral properties of these chromophores were confirmed by binding to flavoproteins with known crystal structure, such as flavodoxin, glutathione reductase, *p*-hydroxybenzoate hydroxylase, glucose oxidase, and riboflavin-binding protein (62-65). For both glutathione reductase and *p*-hydroxybenzoate hydroxylase, in which a positive charge from the  $\alpha$ -helix dipole is oriented toward the N(1)-C(2)=O locus of the bound flavin (63-65), the expected spectrum of the anionic paraquinoid species of 8-mercaptoflavin (species D, Figure 1.8) was obtained. Similarly, for flavodoxin, in which the flavin C(8) locus is solvent accessible (66), the expected spectrum of the anionic paraquinoid species of 8-mercaptoflavin (species C, Figure 1.8) was also obtained. The most significant effects of binding of 8-mercaptoflavin to the proteins were observed with both glucose oxidase (Figure 1.9) and riboflavin-binding protein. While in glucose oxidase the anionic paraquinoid resonance (species D, Figure 1.8) was stabilized, a typical spectrum corresponding to the neutral benzenoid form (species A, Figure 1.8) was obtained upon the binding of 8-mercaptoflavin to riboflavin-binding protein, consistent

with the preference of this protein to bind neutral flavin (67). The anionic paraquinoid form of 8-mercaptoflavin was also observed upon the binding of 8-mercaptoflavin to other flavoprotein oxidases, such as D-amino acid oxidase, lactate oxidase, and old yellow enzyme (18).

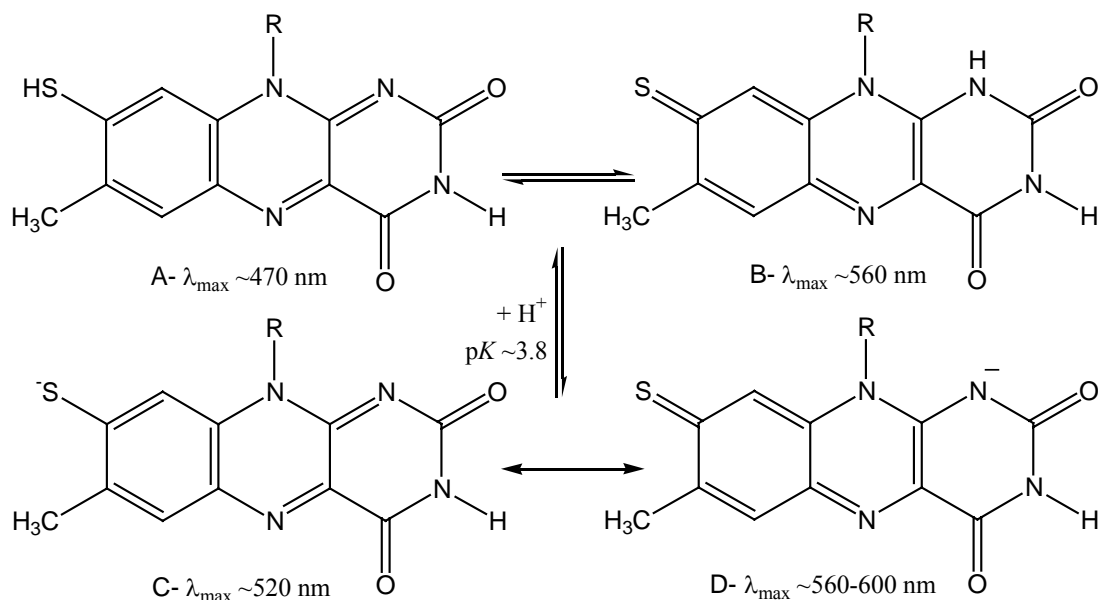


**Figure 1.8.** Tautomeric and mesomeric forms of 8-mercaptoflavin. *A*, neutral benzenoid species; *B*, neutral paraquinoid species; *C*, anionic benzenoid species (8-thiolate); *D*, anionic paraquinoid species. Modified from ref. (2).

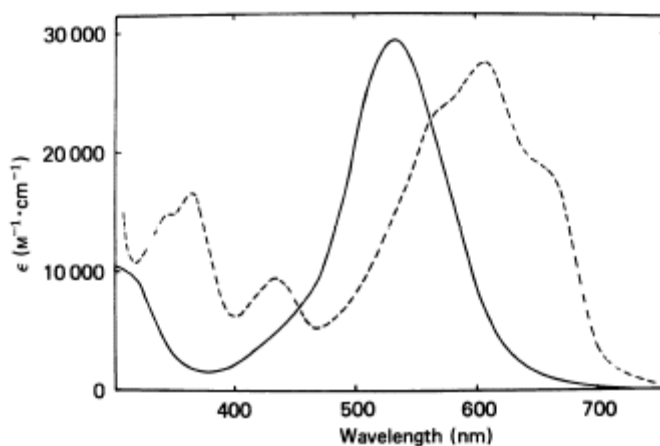


**Figure 1.9.** Spectral changes upon binding of 8-mercapto-FAD to the apoprotein of glucose oxidase. *Solid curve*, 8-mercapto-FAD; *broken curve*, bound to apo-glucose oxidase. Taken without permission from ref. (18).

Overall, by the use of 8-mercaptoflavin as a probe of the flavin microenvironment in many flavoproteins, three conclusions have been drawn. 1) The 8-thiolate (anionic) form of 8-mercaptoflavin (species C, Figure 1.8) is stabilized by flavoproteins that catalyze one-electron transfer reactions, such as flavodoxin and NADPH-cytochrome P-450 reductase (2, 6, 18). These proteins also stabilize the neutral (blue) semiquinone species upon reduction. 2) The anionic paraquinoid form of 8-mercaptoflavin (species D, Figure 1.8) is stabilized by flavoproteins of the oxidase/dehydrogenase class, such as glucose oxidase, lactate oxidase, D-amino acid oxidase, and old yellow enzyme (2, 6, 18). These proteins also stabilize the red anionic form of semiquinone and the flavin-N(5)-sulfite adduct as well. 3) Other flavoproteins do not conform to the classification above, showing properties of both classes, such as flavoprotein transhydrogenases and hydroxylases (Table 1.1) (18).

The effect of binding of 8-hydroxyflavins on flavoproteins could be explained by following the same principles and structures used with 8-mercaptoflavin. However, the spectral changes attributed to the ionized paraquinoid species of 6-hydroxyflavin are consistent with the charge being localized in the pyrimidine ring (8). This could be attributed to the difference between oxygen and sulfur in electronegativity and in undergoing  $\pi$ -interactions (2).

The effects of binding of 6-hydroxy- and 6-mercaptoflavin to flavoproteins could be also described by the same structures and reasoning used for 8-substituted analogs. In solution, while the neutral species is protonated at C(6) locus, the anionic form exhibits a longer (red shifted) wavelength absorbance spectrum, consistent with N(1)-blocked 6-hydroxyflavins (Figure 1.10) (9, 67, 68). Therefore, it has been suggested that the anionic paraquinoid species of 6-hydroxyflavin can provide significant information about the charge distribution around the bound flavin (2).

The microenvironment of the bound flavin could be also probed by monitoring the shifts in  $pK_a$  values of these oxidized flavin analogs upon binding to apoproteins (the  $pK_a$  values of 8-SH, 8-OH, 6-SH, and 6-OH flavin analogs are 3.8, 4.8, 5.9, and 7.1, respectively) (2).

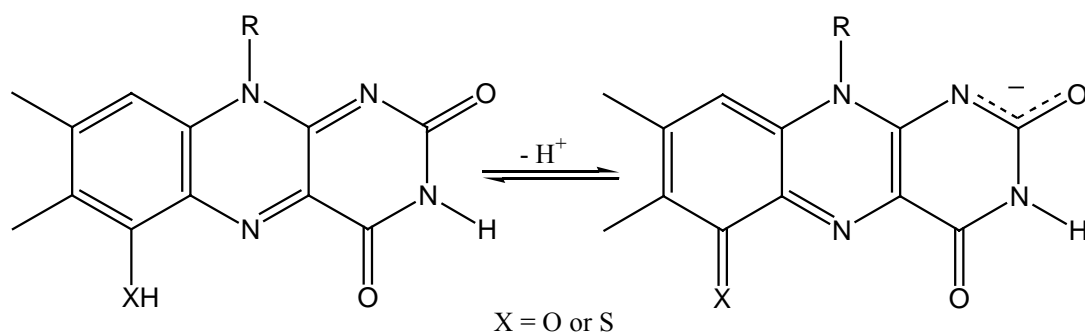


**Figure 1.10.** Structures of the neutral and the anionic form of 6-hydroxy- and 6-mercaptoflavins. Modified from ref. (2).

In conclusion, from the use of 6- and 8-substituted flavin analogs, along with the stabilization of the anionic flavin semiquinone radical or hydroquinone, and the flavin-N(5)-sulfite adduct as different probes for the flavin microenvironment of many flavoprotein before their X-ray crystal structures become available, it has been proposed that a flavoprotein with a positive charge (amino acid residue or  $\alpha$ -helix dipole) in the vicinity of the flavin N(1) locus should: 1) stabilize the anionic semiquinone as well as the hydroquinone species of flavin; 2) stabilize a reversible flavin-N(5)-sulfite adduct; 3) stabilize the benzoquinoid anion form of 8-mercaptoflavin; 4) lower the  $pK_a$  of the 6- and 8-substituted flavin analogs. Most interestingly, it was also proposed that protein-flavin interaction would enhance the uptake of the redox equivalents through position N(5) during catalysis, thereby a contribution on the redox potential of the enzyme-bound flavin should be also observed as well (18, 20, 26, 27, 69).

#### 1.1.4. Positive Charge in Proximity of N(1)-C(2)=O and Flavinylation

Singer and his coworkers firstly established the covalent attachment of flavins to proteins in 1955 in their study of mammalian succinate dehydrogenase enzyme (70-72). Subsequently, many flavoproteins have been identified as covalently attached to the flavin cofactors (FAD or FMN). In all the flavoproteins studied, the mode of covalent attachment of the flavin cofactor to the polypeptide chain of the host protein was found to be one of five modes (Figure 1.11), which are summarized for convenience in Table 1.2. These observations raised the question of the correlation between the covalent attachment of the flavin cofactor and the mechanism of the resulting enzyme. Williamson and Edmondson, by studying the effects of pH on the oxidation-reduction potentials of 8 $\alpha$ -*N*-imidazolylflavins showed that as the pH increases, the redox potential decreases (73). This result strongly suggests that the modulation of the flavin microenvironment through the histidyl group  $pK_a$  of the 8 $\alpha$ -*N*-imidazolylflavins could influence the oxidation-reduction potential of the flavin (73). In addition, Edmondson and de Francesco, by studying modified aminoacyl flavins, have proposed a correlation between the covalent attachment of the flavins and their redox properties (74). The results obtained in their studies showed that the oxidation-reduction potentials of aminoacyl flavins were ~50-60 mV more positive compared to the unmodified flavins. Furthermore, a number of recent studies of flavin-dependent enzymes containing covalently bound flavins, namely cholesterol oxidase (75), vanillyl-alcohol oxidase (54), and *p*-cresol methylhydroxylase (76), showed that, irrespective of the type of flavin linkage and protein, the removal of the covalent linkage between the flavin and the enzyme results in a decrease of the  $E'_m$ , 7 value for the bound flavin of ~100 mV. Therefore, a clear correlation between the covalent attachment of the flavin cofactor and the protein and the oxidation-reduction potentials of the formed enzymes could be made.

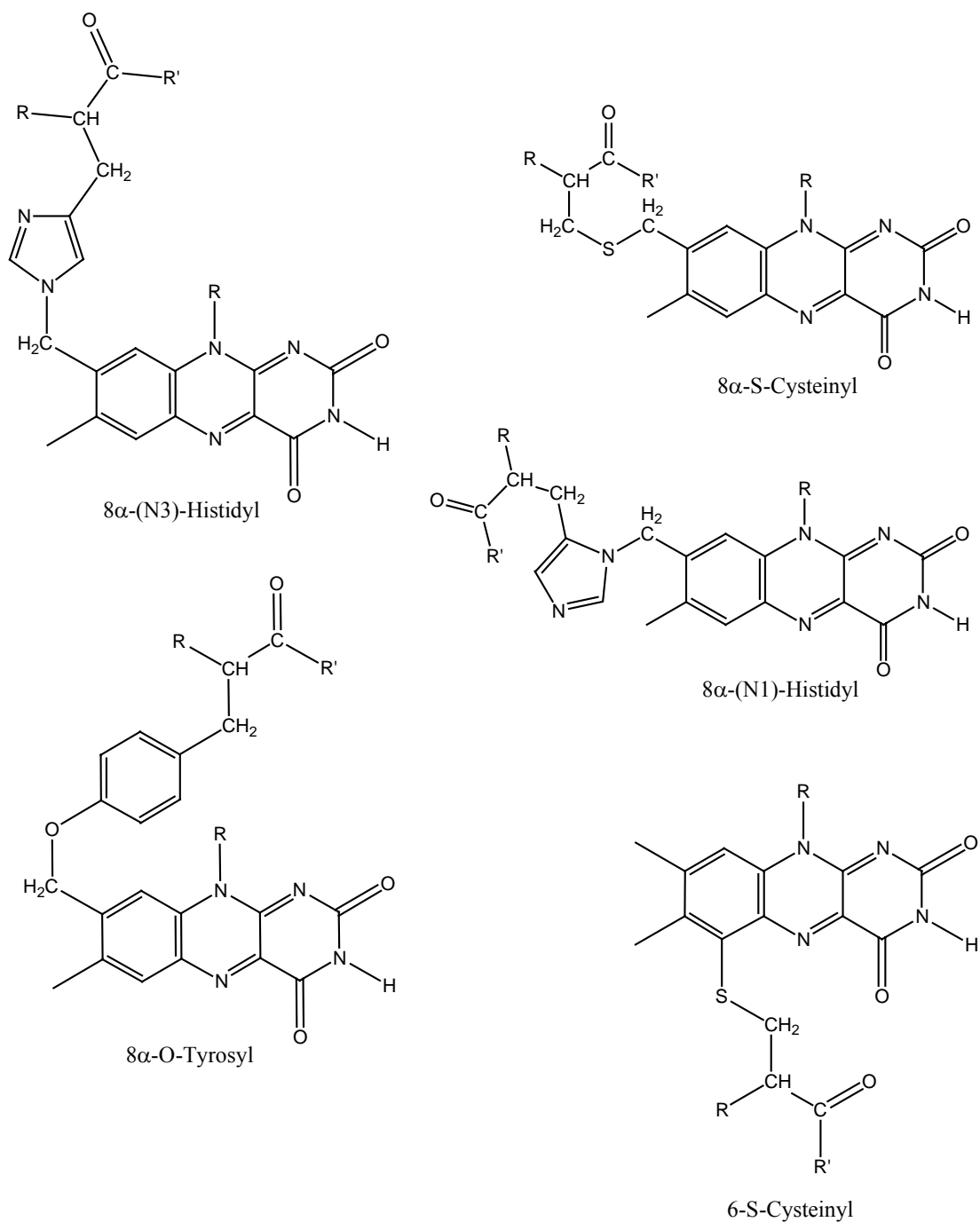


**Figure 1.11.** Mode of covalent attachment of flavin to the protein in flavoproteins.

**Table 1.2.** Examples of Flavoproteins Containing Covalently Linked Flavin Redox Centers<sup>a</sup>

Mode of Attachment	Enzyme	References
6-S-Cysteinylyl FMN	Dimethylamine dehydrogenase	(77)
	Trimethylamine dehydrogenase	(30)
8- $\alpha$ - <i>NI</i> -Histidyl FAD	Cholesterol oxidase	(75, 78)
	Thiamin dehydrogenase	(79, 80)
	L-Galactonolactone oxidase	(81)
8- $\alpha$ - <i>N3</i> -Histidyl FAD	Choline oxidase	(82)
	Pyranose 2-oxidase	(31)
	Fumarate reductase	(83)
	Sarcosine dehydrogenase	(84)
	Succinate dehydrogenase	(85)
	Vanillyl-alcohol oxidase	(54, 55)
	6-Hydroxy-D-nicotine oxidase	(86)
8- $\alpha$ - <i>O</i> -Tyrosyl-FAD	D-Gluconolactone oxidase	(87)
	<i>p</i> -Cresol methylhydroxylase	(88)
8- $\alpha$ -S-Cysteinylyl FAD	Monoamine oxidase A	(89, 90)
	Monoamine oxidase B	(89, 90)
	Monomeric sarcosine oxidase	(91)

<sup>a</sup> Modified from ref. (92).



The mechanism of covalent flavinylation has been proposed and reviewed in several flavoproteins, among which *p*-cresol methylhydroxylase (8- $\alpha$ -*O*-Tyrosyl-FAD) (88), 6-hydroxy-D-nicotine oxidase (8- $\alpha$ -*N*3-Histidyl FAD) (86), monomeric sarcosine oxidase (8- $\alpha$ -S-Cysteiny FAD) (91), trimethylamine dehydrogenase (6-S-Cysteiny FMN) (30), and *N*-methyltryptophan oxidase (8- $\alpha$ -S-Cysteiny FAD) (93). In all these cases, it was suggested that a positively charged amino acid residue in proximity to the N(1)-C(2)=O region of the bound flavin is important to stabilize the negative charge that develops at the N1/C2 region during the flavinylation reaction and is therefore suggested to facilitate flavinylation of the enzyme (30, 86, 88, 91, 92). For *p*-cresol methylhydroxylase, Arg447 was found to be located at a distance of  $\sim 3$  Å from the N1/C2 locus of the bound flavin (88). This residue was proposed to facilitate the flavinylation process by stabilizing the negative charge that develops at the N(1)-C(2)=O locus of the iminoquinone methide flavin intermediate during the flavinylation process (88). Similarly, Arg67, which is located in the vicinity of the N(1)-C(2)=O locus of the bound flavin of 6-hydroxy-D-nicotine oxidase, was identified as being critical for the flavinylation process (94). Mutagenesis studies of that residue have demonstrated the requirement of a positive charge at this position (N1/C2) to facilitate the flavinylation process (94). Furthermore, Mewies et al., in their studies of the differentially charged mutants at position 222 of trimethylamine dehydrogenase, concluded that the positively charged guanidino group of Arg222 stabilizes the negative charge as it develops at the N1 position of FMN during flavinylation of the enzyme (Figure 1.12) (30). When Arg222 was substituted with Lys (R222K) a significant decrease in the amount of the active flavinylated enzyme was observed. However, the removal or reversal of that positive charge, as in case of R222V and R222E, resulted in the production of completely

inactive enzymes that were totally devoid of FMN, consistent with a critical role of such positively charged residue at this position (30).

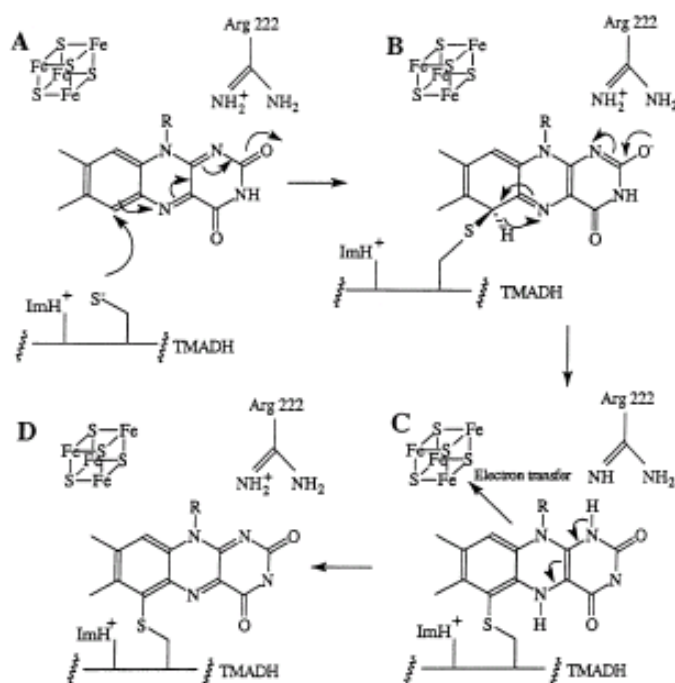


**Figure 1.12.** Flavinylation mechanism of trimethylamine dehydrogenase.

*ImH<sup>+</sup>*, the protonated imidazole side-chain of residue His29 that is thought to assist in the nucleophilic attack of Cys30 at the C6 atom of flavin by formation of an imidazolium/thiolate ion-pair. The role of Arg-222 in stabilizing negative charge as it develops at the N1/O2 positions of the flavin is shown. Re-oxidation of the reduced flavin is by internal electron transfer to the 4Fe-4S center. Taken without permission from ref. (30).

A self-catalytic flavinylation mechanism was also proposed for monomeric sarcosine oxidase (8- $\alpha$ -S-Cysteinyl FAD) through the FAD interactions with the positive side chains and the helix dipole (95). The X-ray crystal structure of monomeric sarcosine oxidase showed that FAD is covalently attached to Cys315 (22, 91). In addition, the crystal structure also showed that the bound FAD is located in a highly basic environment that contains seven basic residues.

Lys348 was found to be located at a distance of  $\sim 2.8$  Å from the N(1) locus of the bound FAD and hydrogen bonded to C(2)=O of the flavin ring (22, 91). Similarly, the positive charge of the  $\alpha$ -helix dipole ( $\alpha$ F4) was also found to be pointed to the same C(2)=O locus of the bound flavin (22, 91). Therefore it was proposed that the negative charge that develops on the N(1)-C(2)=O region of the isoalloxazine ring during the process of covalent flavinylation of monomeric sarcosine oxidase is stabilized by the positive charge of Lys348 together with the positive charge of the  $\alpha$ -helix dipole and that this stabilization facilitates the flavinylation process (95).

Recently, it was observed that the addition of a small excess of sodium borohydride to either monomeric sarcosine oxidase or its homologue, *N*-methyltryptophan oxidase, followed by the binding of substrate and reaction with oxygen, resulted in a tautomeric rearrangement reaction of 3,4-dihydroflavin to 1,5-dihydroflavin (Figure 1.13) (93). Intermediate I (Figure 1.13) in the proposed tautomerization mechanism of 1,3-dihydroflavin was found to be similar to the quinonoid flavin intermediate produced in the flavinylation process of monomeric sarcosine oxidase (95). Therefore, this tautomerization reaction provided insight for a similar flavin tautomerization reaction that has been proposed as a key step during the covalent flavinylation process of these enzymes.

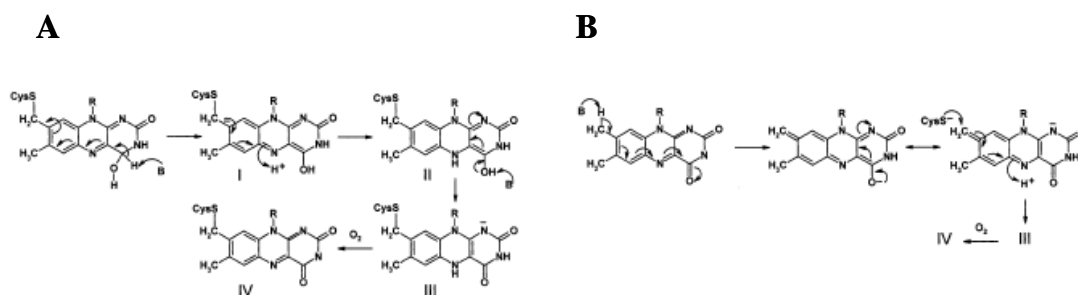


**Figure 1.13.** Mechanism of flavinylation of monomeric sarcosine oxidase and *N*-methyltryptophan oxidase.

*A*, mechanism of tautomerization of 3,4-dihydroflavin to an air sensitive 1,5-dihydroflavin; *B*, the mechanism proposed for the covalent attachment of flavin to MSOX or MTOX. Taken without permission from ref. (93).

## 1.2. GMC Oxidoreductase Enzyme Superfamily

The Glucose-Methanol-Choline (GMC) oxidoreductase enzyme superfamily is composed of a group of flavoenzymes that are able to catalyze the conversion of alcohols to the corresponding aldehydes or ketones (Scheme 1.1) (96). This family includes glucose oxidase (34, 39, 62), cholesterol oxidase (16, 38, 97, 98), cellobiose dehydrogenase (32, 99), pyranose 2-oxidase (31, 33, 100), methanol oxidase (101), choline dehydrogenase (96, 102, 103) (see detailed description in Section 1.5), and choline oxidase (25, 47, 48) (see detailed description in Section 1.4). The X-ray crystal structures of glucose oxidase (39, 62), cholesterol oxidase (97), cellobiose dehydrogenase (32), pyranose 2-oxidase (31, 33), and choline oxidase<sup>1</sup>, showed a *p*-hydroxybenzoate hydroxylase (PHBH) – like fold in the monomeric structures of these enzymes (Figure 1.14). In addition, the overall structures of these enzymes showed that with the exception of pyranose 2-oxidase, which has a tetrameric structure, they all share dimeric structures, and the polypeptide chain of each monomer folds into two domains, a highly conserved FAD binding domain and a substrate binding domain. Although GMC enzymes exhibit little sequence similarity in their substrate binding domains, the crystal structures of choline oxidase, glucose oxidase, cholesterol oxidase, cellobiose dehydrogenase, and pyranose 2-oxidase show that they all share highly conserved catalytic sites, suggesting a similar activation mechanism for the oxidation of their substrates (Figure 1.15) (31-33, 39, 62, 97). Although the X-ray crystal structure of methanol oxidase has not been solved, an unambiguous mechanism has been proposed for that enzyme, which will be discussed in this chapter (see 1.2.5). However, the mechanism of other GMC oxidoreductase enzymes with known structures is still ambiguous

---

<sup>1</sup> Recently, the X-ray crystal structure of choline oxidase has been resolved at 1.86 Å resolution (Lountos, G. T., Fan, F., Gadda, G., and Orville, A. M; unpublished data; see Section 1.4.1. for detailed description).

because of the masking of their catalytic steps (reductive or oxidative process) by other rate limiting steps in their reaction mechanisms (104-106).

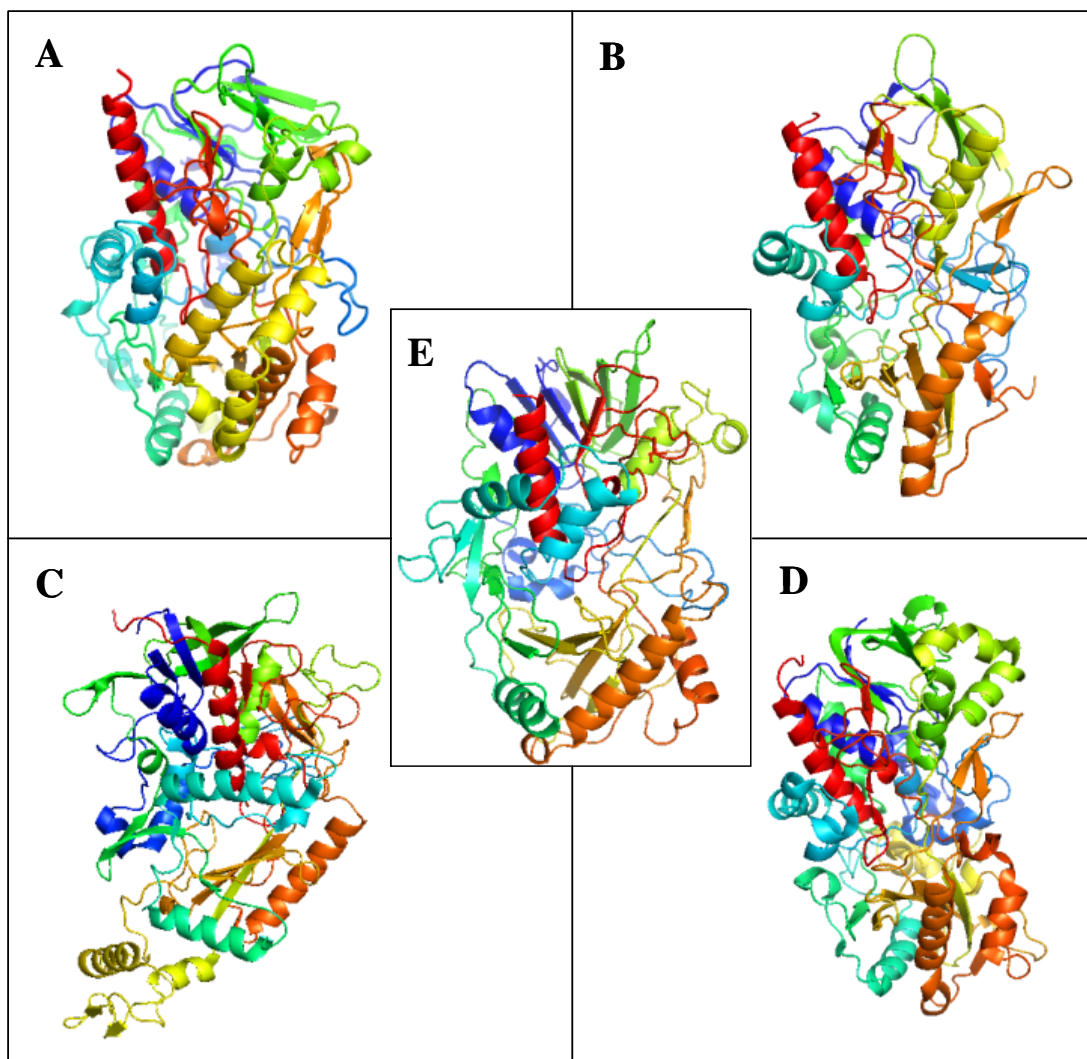
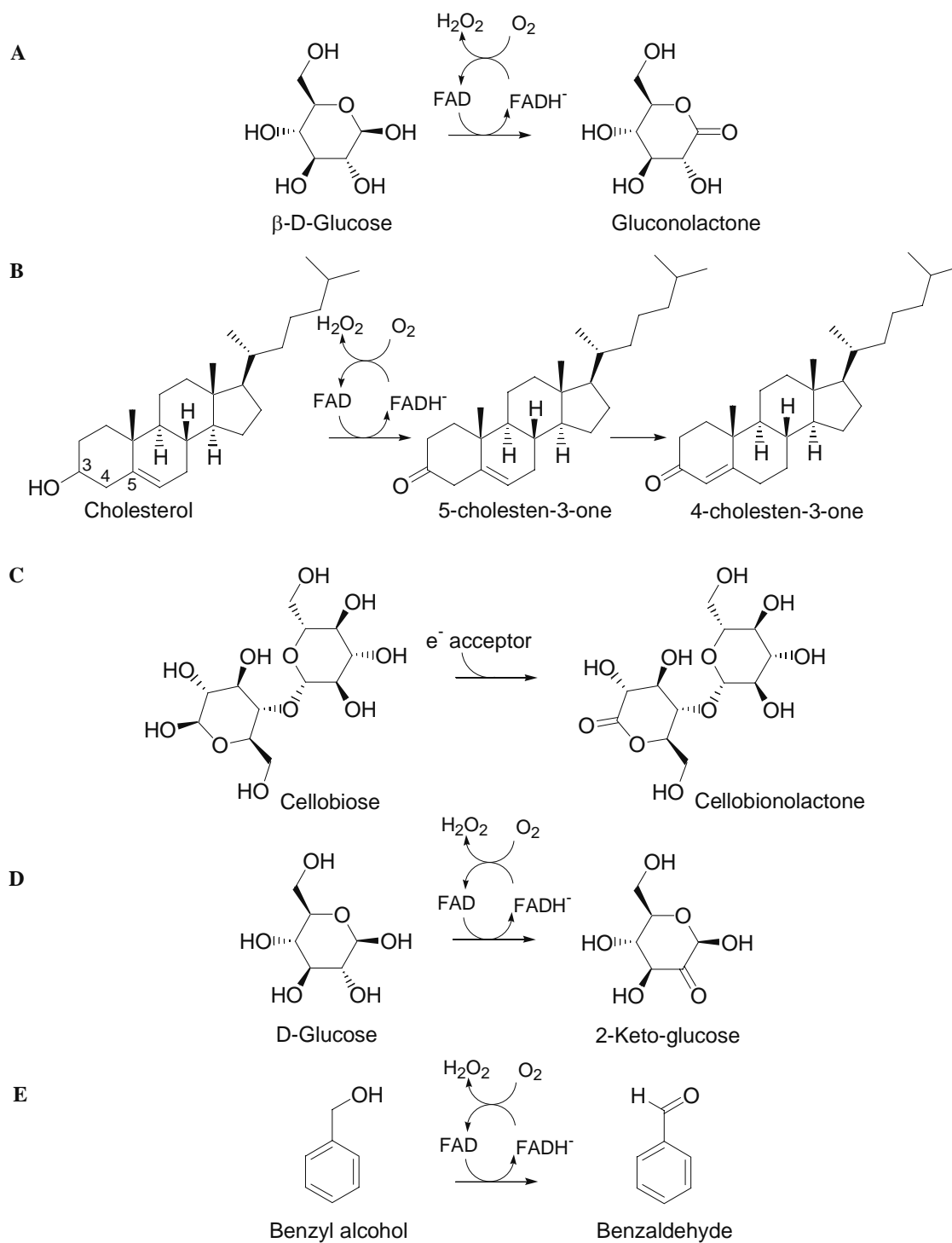


**Figure 1.14.** The three-dimensional structures of members of the GMC oxidoreductase enzyme superfamily.

*A*, glucose oxidase from *Aspergillus niger* (PDB code 1CF3); *B*, cholesterol oxidase from *Streptococcus* (PDB code 1COY); *C*, pyranose 2-oxidase from *Trametes ochracea* (PDB code 1TT0); *D*, cellobiose dehydrogenase from *Phanerochaete chrysosporium* (PDB code 1NAA); *E*, choline oxidase from *Arthrobacter globiformis* (Lountos, G. T., Fan, F., Gadda, G., and Orville, A. M; unpublished data).



**Scheme 1.1.** Reactions catalyzed by GMC oxidoreductases.

*A*, Glucose oxidase; *B*, cholesterol oxidase; *C*, cellobiose dehydrogenase; *D*, pyranose-2 oxidase; *E*, methanol oxidase (alcohol oxidase).

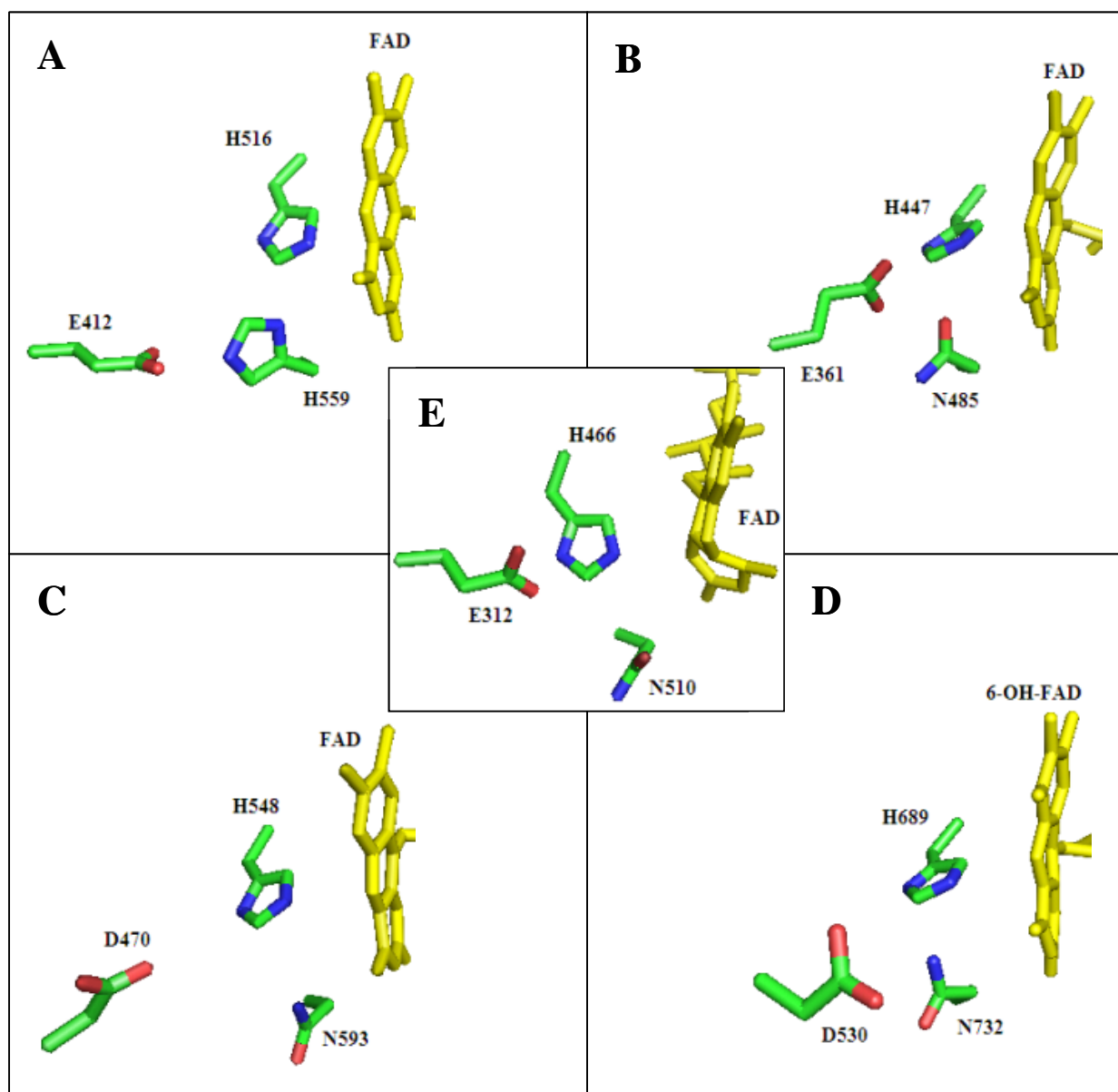
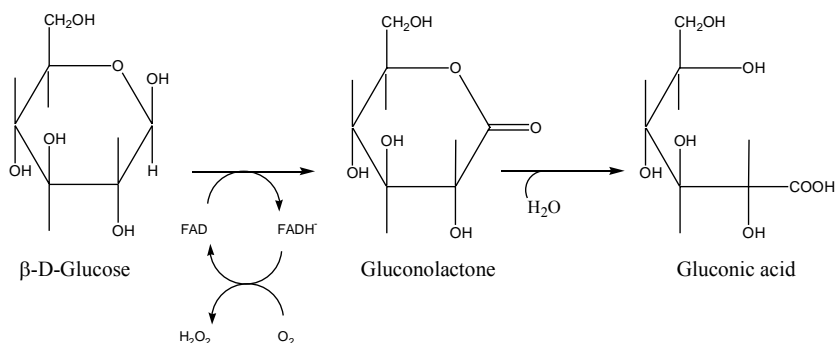


**Figure 1.15.** The active site residues of GMC oxidoreductase enzyme superfamily.

*A*, Glucose oxidase from *Aspergillus niger* (PDB code 1CF3); *B*, cholesterol oxidase from *Brevibacterium sterolicum* (PDB code 1COY); *C*, pyranose 2-oxidase from *Trametes ochracea* (PDB code 1TT0); *D*, cellobiose dehydrogenase from *Phanerochaete chrysosporium* (PDB code 1NAA); *E*, choline oxidase from *Arthrobacter globiformis* (Lountos, G. T., Fan, F., Gadda, G., and Orville, A. M; unpublished data).

### 1.2.1. Glucose Oxidase

Glucose oxidase (E.C. 1.1.3.4) is an FAD-dependent enzyme that catalyzes the oxidation of  $\beta$ -D-glucose to  $\delta$ -gluconolactone (Scheme 1.2) (62). Glucose oxidase is used in commercial applications, such as the production of gluconic acid (a food preservative), and as an important biosensor for the quantitative determination of glucose in bodily fluid, foodstuffs, beverages and fermentation liquors (62, 107). The active form of the enzyme has been identified and purified from several molds. The most common fungal sources of glucose oxidase are *Penicillium amagasakiense* and *Aspergillus niger* (108-110). In addition, the enzyme has been recently purified from *Phanerochaete chrysosporium* and *Talaromyces flavus* fungi as well (62). Glucose oxidases from *Penicillium amagasakiense* and from *Aspergillus niger* showed high degrees of identity (66%) and similarity (79%) (111) and comparable kinetic parameters (112).



**Scheme 1.2.** The enzymatic reaction catalyzed by glucose oxidase.



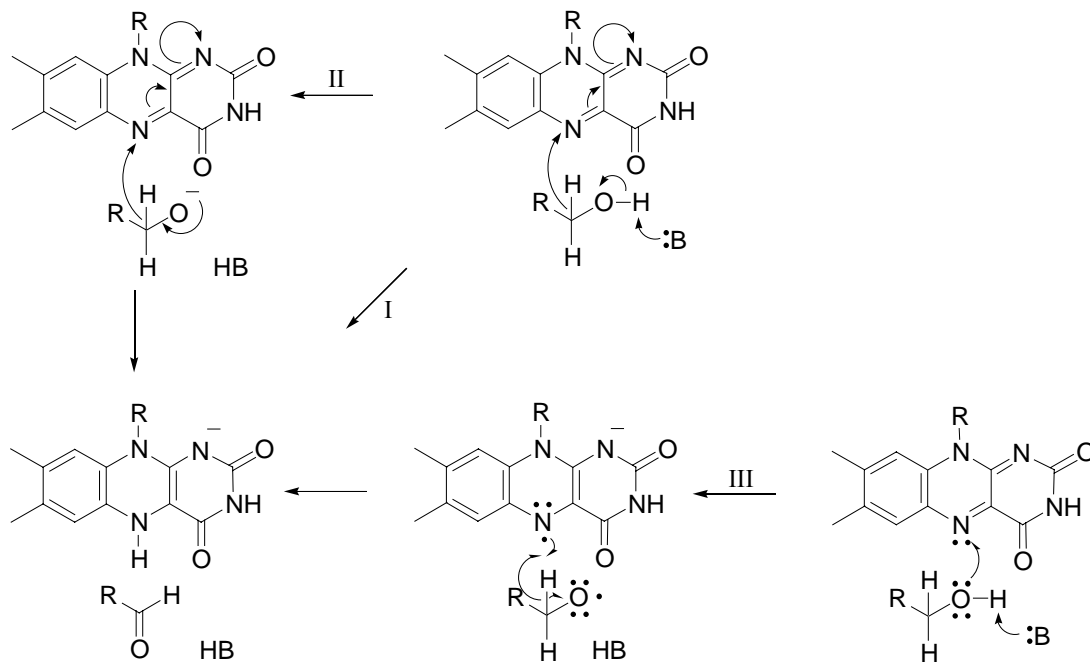
Glucose oxidase is a homodimer with molecular mass ranging from 150 to 180 kDa, depending on the degree of glycosylation. Each monomer contains one tightly attached but not covalently bound FAD (109). The X-ray structural data of glucose oxidase revealed that the monomeric molecule has a compact spheroid structure with PHBH fold (Figure 1.14) (62). The prosthetic group of the enzyme, FAD, was found to be located near the dimer interface, but without actual interaction with this interface (62). His516, His559, and Glu412 were identified as highly conserved residues in the active site of glucose oxidase with respect to other GMC enzymes (Figure 1.15) (62). His516, which is fully conserved among the seven GMC enzymes, was proposed as the catalytic base that abstracts the proton from the substrate hydroxyl group and initiates the reductive half-reaction in which the substrate glucose is oxidized to gluconolactone with the subsequent reduction of the bound FAD (39, 62, 104, 111). The results obtained from both the pH profiles and the kinetic isotope effects of the mutant enzyme (H516A) with respect to wild-type enzyme suggested that the protonated form of this highly conserved active site histidine residue functions also as a general acid during the oxidative half-reaction (111, 113). NMR studies on the anaerobically reduced species of glucose oxidase at pH 5.6 indicated the presence of a negative charge at the N(1)-C(2)=O locus of the bound flavin, which is stabilized by a positively charged residue (114). The crystal structure of the enzyme showed that His516<sup>Nε2</sup> is located at a distance of ~3.8 Å from the N(1) locus of the flavin and therefore could stabilize in its protonated state the negative charge developing on the N(1)-C(2)=O locus of the flavin (62).

The other active site histidine residue, His559, was found to be hydrogen bonded with Glu412 and a water molecule (W110) (62). The studies that preceded the elucidation of the X-ray crystal structure of glucose oxidase suggested that the carboxylate group of glutamate at

position 412 of glucose oxidase plays a major role in substrate binding and specificity (104). The modeled enzyme-substrate complex structure of glucose oxidase revealed that substrate binding to the enzyme was banned upon protonation of Glu412, which in turn disrupted the hydrogen bond with His559 and resulted in reorganization of the active site (39). It was also found that the binding of  $\beta$ -D-glucose to the active site was stabilized by hydrophobic contacts to Phe414, Trp426, as well as to Tyr68 and FAD. In addition to these important hydrophobic interactions, hydrogen bonds were also observed between glucose and several residues in the active site such as, Tyr68, Asn514, Arg512, His516, His559, and Thr/Ser110 (39). The disruptions of these hydrogen bonds via mutagenesis or by the use of substrate analogs resulted in significant decrease in the binding affinity and specificity of the substrate to the active site of the enzyme (39). Arg512 and Asn514 were also found to be involved in substrate binding. This study also showed that there is a direct interaction between the substrate and His516 (39), which differs from the water-mediated interaction between substrate and enzyme in cholesterol oxidase (97, 115).

Mechanistically, the chemical reaction catalyzed by glucose oxidase can be summarized as follows. 1) During the reductive half-reaction, after the substrate glucose binds to the free enzyme, it is oxidized to gluconolactone with the subsequent reduction of the bound FAD. 2) During the oxidative half-reaction, the reduced enzyme-bound flavin complexed with the oxidized substrate releases product, with the subsequent oxidation of the reduced flavin by molecular oxygen (second substrate) and with the production of hydrogen peroxide, consistent with a ping-pong oxidation mechanism of glucose catalyzed by glucose oxidase (116). Kinetic isotope effects studies with either glucose or 2-deoxyglucose as substrate showed that while with glucose the product release is a first order rate-limiting step of the reaction, with 2-deoxyglucose

substrate oxidation becomes partially rate limiting for the overall turnover of the enzyme; the product release does not limit the enzyme turnover (116). pH dependence studies on kinetic parameters ( $k_{\text{cat}}$  and  $k_{\text{cat}}/K_m$ ) of glucose oxidase showed that with increasing pH, the reoxidation of the enzyme in the oxidative half-reaction becomes rate limiting rather than the product release (117). Kinetic isotope effects showed a small ratio of  $\sim 2\text{--}3$  comparing 1- $^2\text{H}$ -D-glucose (deuterated substrate) and D-glucose, which in turn hindered the accurate determination of the chemical mechanism of glucose oxidase (104). In contrast, no solvent deuterium isotope effect has been detected on any step in the mechanism with either glucose or 2-deoxyglucose as substrate (104). These results clearly suggest that the OH and CH bonds are cleaved in different steps in catalysis (Scheme 1.3, pathway II) (104, 118).



**Scheme 1.3.** Proposed mechanisms for alcohol oxidation by GMC enzymes.

*I*, Hydride transfer mechanism; *II*, Asynchronous hydride transfer mechanism; *III*, Oxygen radical mechanism.

### 1.2.2. Cholesterol Oxidase

Cholesterol oxidase (E.C. 1.1.3.6) is an FAD-containing enzyme that catalyzes the oxidation and subsequent isomerization of the *trans*  $\Delta^5$ - $\Delta^6$ -3 $\beta$ -hydroxysteroids to the corresponding  $\Delta^4$ - $\Delta^5$ -3-ketosteroids (Scheme 1.1). Cholesterol oxidase has been isolated from several microbial sources including *Streptomyces* sp., *Brevibacterium*, *Pseudomonas*, *Rhodococcus*, and *Schizophyllum* (16). Cholesterol oxidase has also shown a wide range of industrial and clinical applications (16). Although the enzyme has shown a wide range of substrate steroid specificities, the presence of a 3 $\beta$ -hydroxyl group on the substrate steroid ring is essential for enzymatic activity (119-121). The highest enzymatic activity is observed when cholesterol is used as a substrate.

Structurally, cholesterol oxidase is a dimeric protein with a monomeric molecular mass of ~55 kDa, and one FAD molecule for each monomer (97). The mode of FAD attachment to the enzyme differs in enzymes from different sources, i.e., while FAD is uncovalently bound to cholesterol oxidase from *Streptomyces* sp., the crystal structure of cholesterol oxidase from *Brevibacterium sterolicum* showed that FAD is covalently attached to the protein backbone via an 8-hyridinyl-FAD residue (122). The X-ray crystal structure of cholesterol oxidase from either *Streptomyces* sp. or *B. sterolicum* shows that the monomeric molecule has a compact spheroid structure with PHBH fold (Figure 1.14) (40, 97). The prosthetic group of the enzyme, FAD, was found to be deeply buried in the protein structure and was involved in extensive contacts, mainly with the FAD binding domain (40, 97). In addition, the highly conserved active site residues of cholesterol oxidase compared to other GMC enzymes have been identified to be His447, Asn485, and Glu361 (Figure 1.15) (40, 97). A hydrogen bonding network between these conserved residues along with Wat541 has been previously proposed to help the substrate

positioning and to coordinate general base and electrophilic catalysis (105). Furthermore, hydrogen bonding between the side chain of Asn485 and the  $\pi$  system of bound FAD that modulates the redox potential in the reaction catalyzed by cholesterol oxidase was also proposed by Yin et al. (115).

The role of the fully conserved active site residue His447 (Figure 1.15) was extensively studied through the kinetic characterizations of His447 mutant enzymes (105). The results suggested that His447 might have the potential to act as the general base that abstract the substrate hydroxyl proton to initiate catalysis (105). However, the recent availability of a crystal structure of an unliganded form of cholesterol oxidase at sub-Ångstrom resolution ( $\sim 0.9$  Å), in which it was shown that the N $\epsilon$ 2 position of the active site His<sub>447</sub> residue pointing at the substrate hydroxyl group is protonated (35), clearly does not support this histidine residue acting as a specific base in catalysis. These structural observations prompted the authors to suggest that the conserved histidine residue might act as a hydrogen bond donor to the hydroxyl oxygen of the substrate, which would assist in positioning the substrate with respect to the flavin for efficient catalysis (35). His447 was accordingly suggested to play two roles. The first role is to position the substrate with respect to the flavin and Glu361. The second role is to increase the basicity of Wat541 instead of being a general base directly (35); i.e., His447 plays a role in a network of hydrogen bonds rather than acting directly as a catalytic base that abstracts the hydroxyl proton from the steroid during hydride transfer (105, 106). Most interestingly, the X-ray crystal structure of cholesterol oxidase also showed that His447<sup>N $\epsilon$ 2</sup> is located at a distance of  $\sim 3.9$  Å from the N(1) locus of the flavin (35, 97); therefore it could stabilize in its protonated state the negative charge in proximity of N(1)-C(2)=O locus of the bound flavin. This point, however, has not been addressed in any study.

Mechanistically, and based on the structural studies, Li et al. proposed a radical mechanism for cholesterol oxidase (97), with a single electron being transferred from the hydroxyl oxygen of the substrate to the flavin, followed by the transfer of the proton from C3 of the substrate to the N5 position of the flavin ring (Scheme 1.3, pathway III). Alternatively, a hydride transfer mechanism was also proposed (97). In this case, the abstraction of the substrate hydroxyl proton prompts the transfer of the hydride to the flavin moiety (Scheme 1.3, pathway I). Similar to glucose oxidase, an unambiguous characterization of the chemical mechanism for CH bond cleavage in cholesterol oxidase was also limited due to the substrate isomerization step occurring after the cholesterol oxidation being slow. Indeed, kinetic isotope effects showed a small deuterium isotope effect of  $\sim 2.2$  with  $3\alpha$ -[ $^2\text{H}$ ]-cholesterol, and no solvent isotope effects for the wild type enzyme (105).

### 1.2.3. Cellobiose Dehydrogenase

Cellobiose dehydrogenase (E.C. 1.1.99.18) is an extracellular flavocytochrome that is secreted by various cellulolytic fungi (123). Cellobiose dehydrogenase has been purified from various filamentous fungi of which the enzyme from the white-rot fungus, *Phanerochaete chrysosporium*, is the best characterized (123, 124). Similar to cellulases, the expression of cellobiose dehydrogenase is triggered by the presence of cellulose in the medium and repressed in the presence of glucose (125). FAD and porphyrin IX are the two cofactors of the enzyme; these have been reported to interact with two distinct domains of the single polypeptide chain of cellobiose dehydrogenase (125, 126). These two domains are connected by a glycosylated, hydroxyamino-rich linker peptide, which is highly susceptible to cleavage by pepsin, allowing the separations of these two domains (125, 126). Recently, the X-ray crystal structure of each of

the two separate domains, the flavin domain (32), and the heme domain (127), has been reported. The crystal structure of the flavoprotein domain of the enzyme showed an overall fold that is similar to that of other members of GMC family, i.e., a PHBH fold (32). Similar to other GMC enzymes, the monomeric polypeptide chain folds into two structurally distinct domains, the FAD binding and the substrate binding domains (Figure 1.14). The uncovalently attached FAD was found as 6-hydroxy FAD, consistent with the spectral properties of the flavin chromophore (32). In addition, the isoalloxazine ring of the bound flavin was found to be sharply bent along N(5)-N(10) axis (butterfly bending). The partial positive charge provided from the dipole of an  $\alpha$ -helix, which is located in proximity of N(1)-C(2)=O of the bound flavin, together with the butterfly bending of the flavin ring, were suggested to modulate the redox potential of the semiquinone as well as the hydroquinone of the bound flavin (32). Two highly conserved and critical residues have been identified in the active site of cellobiose dehydrogenase, which are His689 and Asn732 (Figure 1.15). Both residues form hydrogen bonds to W1214 (32). Based on the structural data and site directed mutagenesis studies, His689, which is fully conserved among the GMC family, was suggested to play the role of the general base that abstracts the substrate hydroxyl proton to initiate catalysis (32, 128). Moreover, site directed mutagenesis studies of the conserved active site residue Asn732 suggested that this residue plays an important role for the positioning of the substrate 1- $\alpha$ H and 1- $\beta$ -OH relative to FAD and His689, respectively, which in turn promotes the deprotonation as well as the oxidation of the substrate (128). The X-ray crystallographic structure of the flavin domain of cellobiose dehydrogenase showed that His689<sup>Ne2</sup> is located at a distance of  $\sim 4$  Å from the N(1) locus of the flavin (32). Therefore, His689 in its protonated state could stabilize the negative charge that develops in proximity of N(1)-C(2)=O locus of the bound flavin.

Mechanistically, the crystal structure of the flavoprotein domain of cellobiose dehydrogenase with bound inhibitor (cellobiono-1,5-lactam) suggested a hydride transfer mechanism for the dehydrogenation of the substrate (99). In this mechanism, His689 acts as a general base that abstracts the substrate hydroxyl proton, followed by a concerted hydride transfer from the axially aligned C(1)-H of the substrate to the flavin N(5) via a transition state characterized by partial planarization of C(1) (Scheme 1.3, pathway I) (99).

#### 1.2.4. Pyranose 2-Oxidase

Pyranose 2-oxidase (EC 1.1.3.10) is a 270 kDa homotetramer, which catalyzes the oxidation of several aldopyranoses regioselectively at the C2 position to the corresponding 2-ketoaldoses and with the production hydrogen peroxide (Scheme 1.1) (33, 100). Pyranose 2-oxidase is located in the hyphal periplasmic space and it is widely distributed among wood-degrading basidiomycetes (129). Pyranose 2-oxidase has been purified and characterized from various fungi, among which *Phanerochaete chrysosporium* and *Trametes ochracea* are the best studied and have three-dimensional structures available (33, 100). Besides oxidizing a number of pyranose sugars at the C2 position, pyranose 2-oxidase acts also on the C3 position of certain substrates such as 2-deoxy-D-glucose, 2-keto-D-glucose and methyl  $\beta$ -D-glucosides (130, 131). In addition, it has been shown that the enzyme is able to utilize not only oxygen but also various quinones as electron acceptors (132). Therefore, it has been proposed that pyranose 2-oxidase might be involved in ligninolysis as an H<sub>2</sub>O<sub>2</sub>-producing enzyme and as a quinone-reducing enzyme (132).

The monomeric structure of pyranose 2-oxidase folds similarly to other GMC oxidoreductase enzymes (Figure 1.14). The FAD molecule is buried inside the protein, and is



covalently bound via its 8 $\alpha$ -methyl group to N $^{\epsilon 2}$  of His167, resulting in 8 $\alpha$ -(N3)-histidyl flavinylation of the enzyme (133). Similar to cellobiose dehydrogenase (32), a butterfly bending of the isoalloxazine ring of the flavin cofactor was also observed but to a lesser extent with pyranose 2-oxidase (33). A water molecule (W678) was observed to form a hydrogen bond with the N5 atom of the FAD isoalloxazine (33). This bending of the isoalloxazine ring has been explained due to the presence of acetate in the active site, which originates from the acetate buffer used for crystallization (33). Acetate ( $K_{is} = 9.3$  mM) and other organic monocarboxylic acids such as propionate, formate, and valerate have been determined to be competitive inhibitors with respect to  $\beta$ -D-glucose as substrate for pyranose 2-oxidase (33). The highly conserved active site residues of pyranose 2-oxidase have been identified to be His548 and Asn593 (Figure 1.15) (33). In addition, His548, which is fully conserved throughout the GMC family, has been proposed to play the role of the catalytic base that abstracts the substrate hydroxyl proton during catalysis (33). Mechanistically, the putative docking model of  $\beta$ -D-glucose into the active site of pyranose 2-oxidase showed that the  $\beta$ -hydrogen atom of either C2 or C3 of glucose points directly toward the N5 atom of isoalloxazine nucleus of the bound FAD (Figure 1.16). Accordingly, a hydride transfer mechanism was proposed for the oxidation of glucose catalyzed by pyranose 2-oxidase (Scheme 1.3, pathway I) (33).

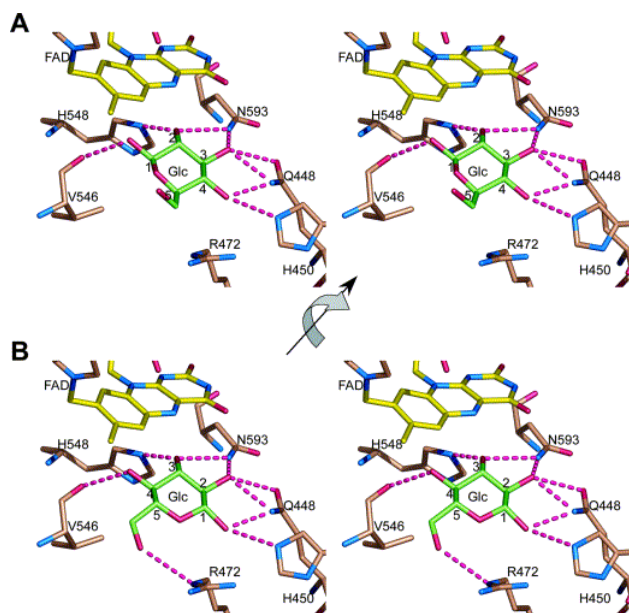


**Figure 1.16.** Docking of  $\beta$ -D-glucose to the pyranose 2-oxidase active site. *A*, Glucose oriented for oxidation at C2. *B*, Glucose oriented for oxidation at C3. Taken without permission from Ref. (33).

### 1.2.5. Methanol Oxidase (Alcohol Oxidase)

Although the X-ray crystallographic structure of methanol oxidase has not been solved yet, unambiguous mechanistic characterization of the enzyme from *Hansenula polymorpha* has been performed (101). This study was performed through the use of substrate and solvent kinetic isotope effects with benzyl alcohol as a substrate or its analogues (101). With benzyl alcohol as substrate, a deuterium isotope effect value of 1.0 and a solvent isotope effect of 2.0 were observed, suggesting that CH bond cleavage is masked and that OH bond cleavage is a rate-limiting step. With 2-substituted ethyl alcohol as substrate, however, the primary deuterium isotope effects increased to  $\sim 5$ , while solvent isotope effects decreased to  $\sim 1$ . Based on these results, an asynchronous hydride transfer mechanism was suggested (Scheme 1.3, pathway II). In short, the OH bond is cleaved prior to the CH bond cleavage, forming an alkoxide intermediate (101).

### 1.3. Other Structurally and Mechanistically Relevant Flavoproteins

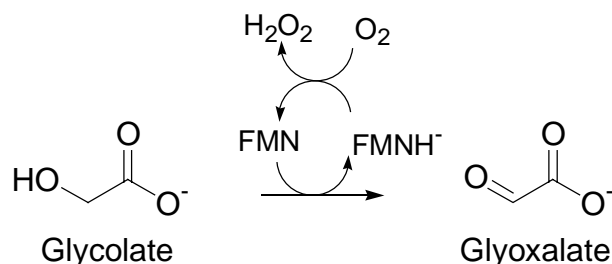
In this section, some of the structurally and mechanistically relevant flavoenzymes will be discussed in details in the following sub-sections. Those flavoenzymes have been kinetically well studied and their three dimensional structures are available. Thereby, providing insights on the correlation between their structure and the mechanism of reactions that they catalyzed with respect to GMC oxidoreductase superfamily to which choline oxidase belong. For convenience, all the structurally and mechanistically relevant features of selected flavoenzymes including GMC family members are summarized in Table 1.3.

**Table 1.3.** Some Structural and Mechanistic Features of Selected Flavoenzymes

Flavoenzyme (PDB file)	Cofactor	Folding topology	Protein residue contacting N(1)-C(2)=O	Proposed mechanism	Ref
Choline Oxidase (na)	FAD	PHBH	$\alpha$ -Helix/His466	Asynchronous hydride transfer	(134-138)
Glucose Oxidase (1CF3)	FAD	PHBH	$\alpha$ -Helix/His516	Concerted hydride transfer	(62)
Cholesterol Oxidase (1COY)	FAD	PHBH	$\alpha$ -Helix/His447	Hydride transfer	(97, 139)
Cellobiose Dehydrogenase (1NAA)	FAD	PHBH	$\alpha$ -Helix/His689	Hydride transfer	(32, 99)
Pyranose 2-Oxidase (1TT0)	FAD	PHBH	$\alpha$ -Helix/His548	Hydride transfer	(33, 100)
D-Amino Acid Oxidase (1DDO)	FAD	PHBH	$\alpha$ -Helix/Arg285	Concerted hydride transfer	(37, 140)
Polyamine Oxidase (1B37)	FAD	PHBH	$\alpha$ -Helix		(53)
Monomeric Sarcosine Oxidase (1L9F)	FAD	PHBH	$\alpha$ -Helix/K348	Polar /Hydride transfer	(95)
<i>p</i> -Hydroxybenzoate Hydroxylase (1PHH)	FAD	PHBH			(141, 142)
Vanillyl-Alcohol Oxidase (2VAO)	FAD	2 domains $\alpha + \beta$	R504		(143, 144)
Flavocytochrome $b_2$ (1FCB)	FMN	$(\alpha/\beta)_8$ Barrel	K349	Asynchronous hydride transfer	(60, 61)
Glycolate Oxidase (1GOX)	FMN	$(\alpha/\beta)_8$ Barrel	K230	Hydride transfer	(145, 146)
Trimethylamine Dehydrogenase (2TMD)	FMN	$(\alpha/\beta)_8$ Barrel	R222		(30, 147)
Dihydroorotate Dehydrogenase (2DOR)	FMN	$(\alpha/\beta)_8$ Barrel	K164		(58, 59)
Old yellow Enzyme (1OYB)	FMN	$(\alpha/\beta)_8$ Barrel	R243		(148)

### 1.3.1. Glycolate Oxidase

Glycolate oxidase (E. C. 1.1.3.15) is an FMN dependent enzyme that catalyzes the oxidation of the  $\alpha$ -hydroxy acid glycolates to the corresponding  $\alpha$ -keto acids (glyoxalates) (Scheme 1.4) (36, 42). Glycolate oxidase is a member of the family of the  $\alpha$ -hydroxy acid oxidases. In plants, the oxidation of glycolates to glyoxalates catalyzed by the peroxisomal glycolate oxidase is considered as a key step in photorespiration (36). In animals, the enzyme is located in liver peroxisomes; it is involved in oxalate production and is therefore related to oxalate-mediated disorders, including renal lithiasis and hyperoxaluria (36, 146).



**Scheme 1.4.** Reaction catalyzed by glycolate oxidase.

Glycolate oxidase in solution is a homotetramer/octamer with molecular mass of  $\sim 43$  kDa for each monomer (36). Similar to other members of the  $\alpha$ -hydroxy acid oxidase family, the X-ray crystal structure of spinach glycolate oxidase showed that the polypeptide chain of the enzyme folds into the  $(\alpha\beta)_8$  barrel structural motif (Figure 1.17) (149, 150). However, additional helices were observed besides the  $(\alpha\beta)_8$  barrel, forming a “lid” structure that covers the top of the active site (149). The FMN cofactor molecule is deeply buried in the barrel, with only the N5 atom being exposed to the solvent (149). Most interestingly, Lys230, which is located near the  $\text{N}(1)-\text{C}(2)=\text{O}$  of the bound FMN, has been proposed to stabilize the negative charge that develops in proximity of  $\text{N}(1)-\text{C}(2)=\text{O}$  locus of the bound flavin (Figure 1.17) (17, 36, 42, 149,

150). This positively charged side chain in this region has also been proposed to be responsible for some of the typical flavoprotein oxidase characteristics such as the formation of flavin-N(5)-sulfite adducts and the stabilization of the red anionic flavin semiquinone and of the benzoquinoid form of 8-mercaptoflavin (2). It has been shown that glycolate oxidase maintains all these features and thereby can be considered as a typical member of this class of flavoproteins (42).

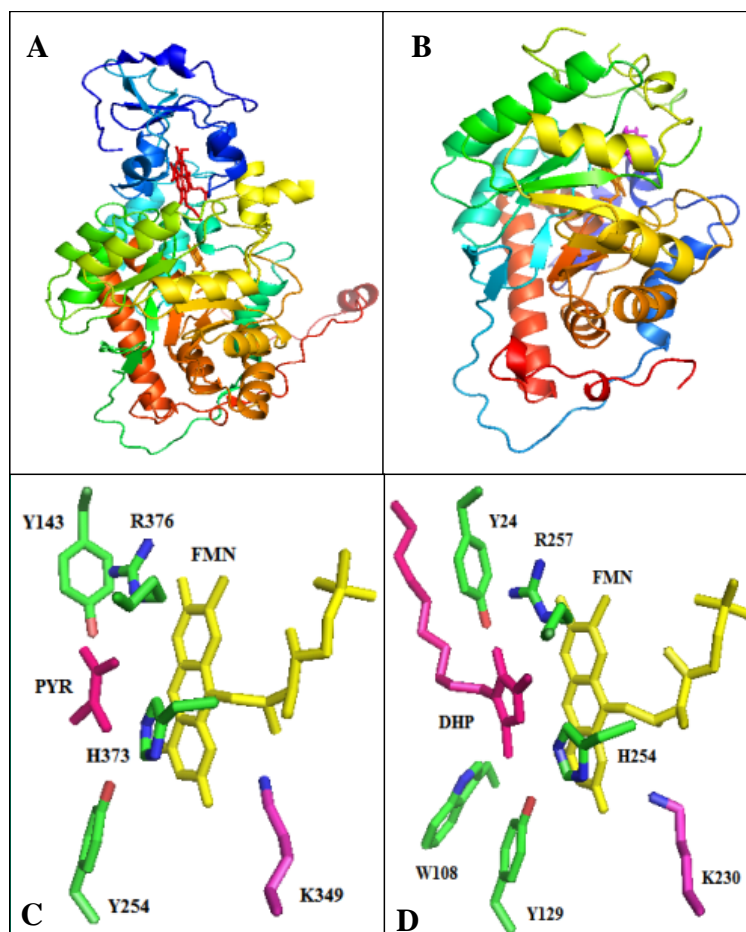


**Figure 1.17.** The three-dimensional structures of FMN-dependent enzymes that oxidize  $\alpha$ -hydroxy acids.

*A* and *C*, flavocytochrome  $b_2$  from *Saccharomyces cerevisiae* (PDB code 1FCB); *B* and *D*, glycolate oxidase from spinach (PDB code 1AL8); *PYR*, pyruvic acid; *DHP*, 3-decyl-2,5-dioxo-4-hydroxy-3-pyrroline (TKP).

The detailed structural investigation of the active site of glycolate oxidase showed that a number of residues are conserved in comparison with other FMN-dependent  $\alpha$ -hydroxy acid oxidizing enzymes (Figure 1.17) (17, 36, 149, 150). The positively charged residues Arg257 and Arg164, along with Tyr24, were proposed to interact with the carboxylate-group of the substrate (Figure 1.17) (36). Glycolate oxidase was also crystallized in complex with two inhibitors, 3-decyl-2,5-dioxo-4-hydroxy-3-pyrroline (TKP) or 4-carboxy-5-(1-pentyl)hexylsulfanyl-1,2,3-triazole (TACA) (Figure 1.18) (146). The carboxyl group of the ligands was observed to form hydrogen bonds with the side chains of Arg257 and Tyr24, as well as that of Arg164. The only notable exception was Trp108, which, while it forms hydrogen bond with TKP, it is not interacting with TACA (146). Therefore, it has been suggested that Trp108 is playing an important role in determining the substrate specificity via size exclusion (146).

Mechanistically, it has been proposed based on the available structural data that the carboxyl part of glycolate is bound to Arg257 and Tyr24, while the hydroxyl group bound to Tyr129 (Figure 1.19). Site directed mutagenesis studies of Tyr24 and Tyr129 confirmed these assumptions, and also indicated a role for Tyr129 in stabilizing the transition state intermediate during catalysis (17, 145). In addition, His254 was proposed to be responsible for proton abstraction from the substrate during catalysis (36, 146). Previously, a carbanion mechanism was generally accepted for the catalytic mechanism of glycolate oxidase. Although little kinetic characterization of glycolate oxidase is available, the carbanion mechanism was proposed for glycolate oxidase in analogy to previous studies on flavocytochrome  $b_2$ , which suggested that the substrate  $\alpha$ -proton is abstracted by the conserved His254 prior to the electron transfer to FMN (36). However, there is no firm evidence that rules out a hydride transfer mechanism for glycolate oxidase (151). Therefore, the mechanism of glycolate oxidase is still ambiguous,

although a hydride transfer mechanism seems to be more likely for glycolate oxidase as the case of the most recently proposed mechanism for flavocytochrome  $b_2$  (152), yet more detailed studies with glycolate oxidase have to be carried out to validate this mechanism.

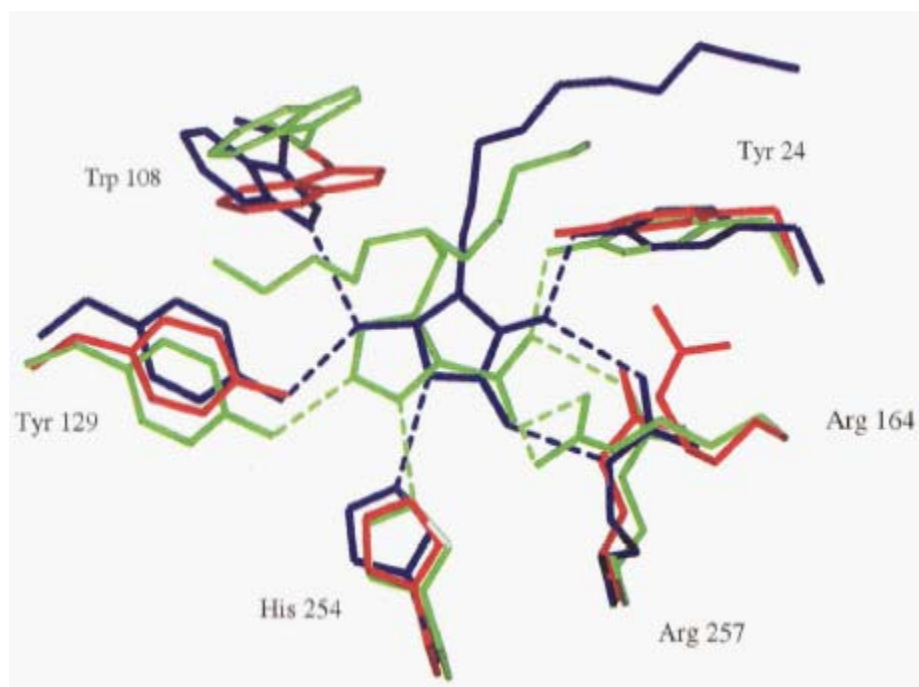


**Figure 1.18.** The hydrogen bonding pattern of the inhibitors at the active site of glycolate oxidase.

The holoenzyme is colored red, the TACA complex green, and the TKP complex blue. Distances less than 3.2 Å from the inhibitors are marked with dashed lines. Taken without permission from ref. (146).

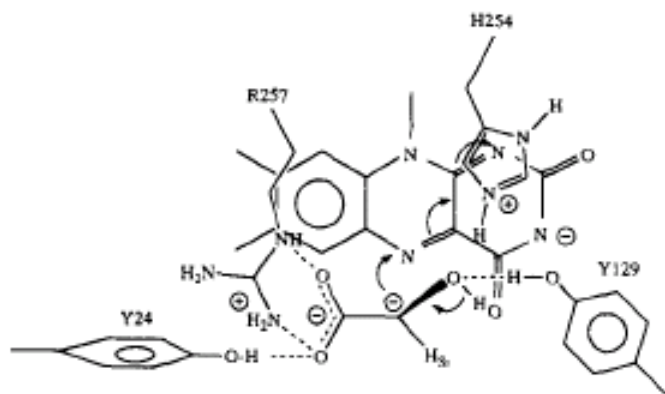
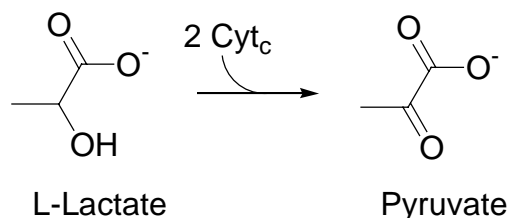


**Figure 1.19.** Schematic presentation of the proposed transition state of glycolate oxidase. Taken without permission from ref. (146).

### 1.3.2. Flavocytochrome $b_2$

Flavocytochrome  $b_2$  (E. C. 1.1.2.3) is the best studied member of the  $\alpha$ -hydroxy acid oxidases family. Flavocytochrome  $b_2$  is an FMN-dependent enzyme that catalyzes the oxidation of L-lactate to pyruvate (Scheme 1.5), which is the product of lactate oxidation for the Krebs cycle (153). The expression of flavocytochrome  $b_2$  is induced by oxygen and L-lactate (154). Besides its role in producing pyruvate, flavocytochrome  $b_2$  also participates in a short electron transport chain involving cytochrome  $c$  and cytochrome oxidase. This leads to the transfer of the reducing equivalents gained from L-lactate oxidation to oxygen, yielding one molecule of ATP for every L-lactate molecule consumed (155). Flavocytochrome  $b_2$  is a homotetramer with a molecular mass of ~58 kDa for each monomer. Each monomer contains two noncovalently bound cofactors, FMN and heme (155).



**Scheme 1.5.** Reaction catalyzed by flavocytochrome  $b_2$ .

The X-ray crystallographic structure of flavocytochrome  $b_2$  showed that each subunit of the tetrameric structure of the enzyme folds into two domains, the heme-binding domain (11 kDa at N-terminal) and the flavin-binding domain (45 kDa at C-terminal). The two domains are connected by a short, yet flexible, hinge peptide (61). In addition, the polypeptide chain of the flavin domain folds into an  $(\alpha/\beta)_8$  barrel structure, consistent with other members of the  $\alpha$ -hydroxy acid oxidases family (Figure 1.17) (61). The FMN cofactor molecule was found to be

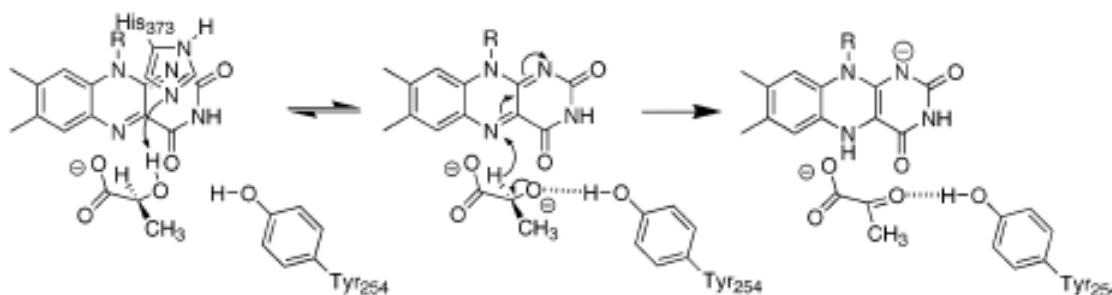


buried in the central  $\beta$ -barrel, suggesting that the flavin cofactor is sequestered from the solvent (61).

The X-ray crystallographic structure of the enzyme complexed with its product pyruvate implied that the product is stabilized in the active site of the enzyme through the interactions of its carboxylate group with the side chains of Arg376 and Tyr143 (Figure 1.17), suggesting an important role for Arg376 and Tyr143 in substrate binding and specificity (61). On the other hand, His373 and Tyr254 were observed to interact with the ketooxygen atom of pyruvate and were therefore suggested to play important roles in catalysis (Figure 1.17) (61, 154). It was proposed that Lys349, which was found to be located close to the N(1)-C(2)=O locus of the bound FMN, is responsible for the stabilization of the anionic semiquinone and hydroquinone as well as the formation of a tight flavin-N(5)-sulfite adduct through its electrostatic interactions with the negative charge that develops at that region (Figure 1.17) (61).

Mechanistically, kinetic characterizations were carried out on the wild type enzyme and enzymes containing mutations on catalytic relevant residues, such as His373 and Tyr254, to gain insights into flavocytochrome  $b_2$  (156). Kinetic studies on the mutant form of the proposed active site histidine, H373Q, showed  $\geq 10^5$  decrease in the rate of lactate oxidation compared to the wild type enzyme (156), suggesting an important role of His373 in catalysis. However, this does not distinguish between the postulated carbanion mechanism and the hydride transfer mechanism. Sobrado et al. performed a thorough mechanistic characterization of flavocytochrome  $b_2$  using kinetic isotope effects as probes, via both steady state and pre-steady state kinetics (60). The results obtained from these studies suggested that the CH and OH bonds are cleaved in a stepwise manner during catalysis. However the kinetic characterization of the mutant form of enzyme in which Tyr254 was replaced with phenylalanine (Y254F) was

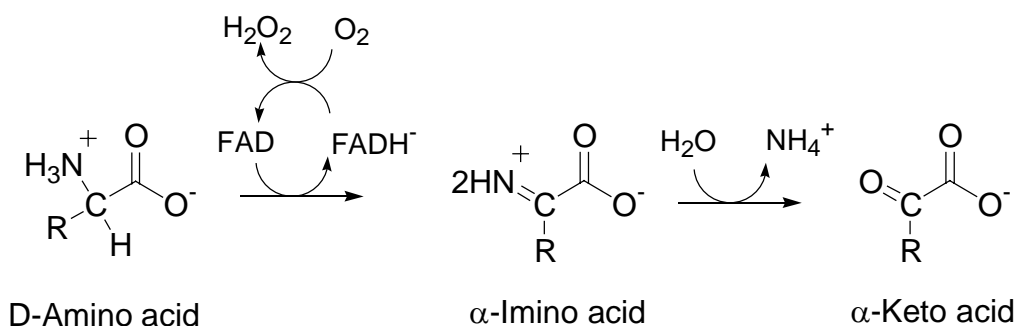
consistent with the cleavages of OH and CH bonds becoming concerted compared to the wild type enzyme (152). This change was explained with a reduced stabilization of the alkoxide intermediate in the phenylalanine variant, which is formed after the proton abstraction by His373 in a hydride transfer mechanism (Scheme 1.6). Tyr254 was therefore suggested to play a role in stabilizing the alkoxide intermediate by forming a hydrogen bond with the charged lactate hydroxyl oxygen. The alternative carbanion mechanism appears unlikely because it is hard to reconcile with the more concerted mechanism observed in the Y254 mutant enzyme. If a carbanion mechanism were adopted by the enzyme, losing the interaction between Tyr254 and substrate hydroxyl oxygen should substantially slow down the latter step and result in more stepwise CH and OH bond cleavages (152). Based on these observations, the authors suggested a stepwise hydride transfer as the mechanism for the chemical step in wild type flavocytochrome  $b_2$  and, by extension, the family of enzymes that oxidizes  $\alpha$ -hydroxy acids (Scheme 1.6).



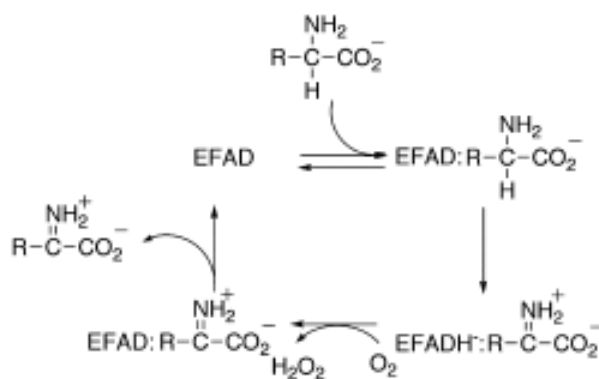
**Scheme 1.6.** Proposed mechanism of L-lactate oxidation by flavocytochrome  $b_2$ . Taken without permission from ref. (152).

### 1.3.3. D-Amino Acid Oxidase

D-Amino acid oxidase (EC 1.4.3.3, DAAO) catalyzes the dehydrogenation of D-isomers of amino acids to the corresponding  $\alpha$ -imino acids, which after subsequent hydrolysis yield  $\alpha$ -keto acids and ammonia (Scheme 1.7). The kinetic mechanism of DAAO, as is common in flavoprotein oxidases, is divided into a reductive half-reaction, in which the amino acid is oxidized with the concomitant reduction of the bound flavin, and an oxidative half-reaction, in which the reduced flavin is oxidized by molecular oxygen with the subsequent release of the product (Scheme 1.8). This FAD-dependent enzyme was shown to play a vital role in the modulation of serine levels in mammalian brain (157, 158).



**Scheme 1.7.** Reaction catalyzed by D-amino acid oxidase.



**Scheme 1.8.** Kinetic mechanism of D-amino acid oxidase.  
Taken without permission from ref. (140).

Although the enzyme is well studied, no unequivocal mechanism for the dehydrogenation of the substrate has yet been established (28, 140, 159). Over the years, two different mechanisms have been proposed for the reaction catalyzed by this flavoprotein oxidase: the hydride transfer mechanism and the carbanion mechanism. Evidence that favors a direct hydride transfer mechanism comes from the transfer of the  $\alpha$ -hydrogen of the substrate to the C(5) position of the enzyme reconstituted with 5-deaza-FAD (160). Similarly, the elimination of halide from  $\beta$ -chloro-D-alanine validates the hypothesis that the reductive half-reaction of DAAO involves the initial formation of a carbanion intermediate after the abstraction of the  $\alpha$ -hydrogen of the substrate as a proton (161). Finally, a direct hydride transfer mechanism was considered in which  $\alpha$ -H<sup>+</sup> abstraction is coupled with the hydride transfer (162).

Two different research groups have described the X-ray crystallographic structure of DAAO from pig kidney with the inhibitor benzoate bound (37, 163). The X-ray structure of the enzyme showed that there is no active site residue properly placed to act as a base for carbanion formation. The only notable interaction of the inhibitor with the active site residue includes the carboxylic group of benzoate with Arg283 and Tyr228 (37, 163). A similar interaction was observed between the carboxylic group of D-3,3,3-F<sub>3</sub>-alanine and the homologous arginine and tyrosine residues (Arg285 and Tyr223) in a recent structure of DAAO from *Rhodotorula gracilis* (Figure 1.20) (164). In addition, the amino group of D-3,3,3-F<sub>3</sub>-alanine was also observed to form a hydrogen bond with a water molecule and the carbonyl oxygen of Ser335 (164). In all structures the carbon atom of the inhibitor, which corresponds to the  $\alpha$ -carbon of the amino acid substrate, was found to be located at a distance of  $\sim 3.4$  Å from the N(5) of the isoalloxazine ring of the bound flavin (37, 163, 164). These structural data clearly suggest a direct hydride transfer mechanism as well as argue against the carbanion mechanism that was proposed earlier.

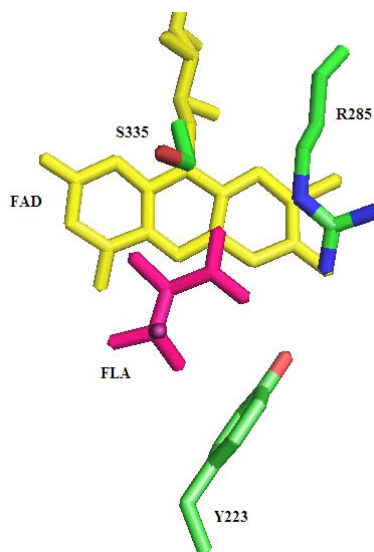
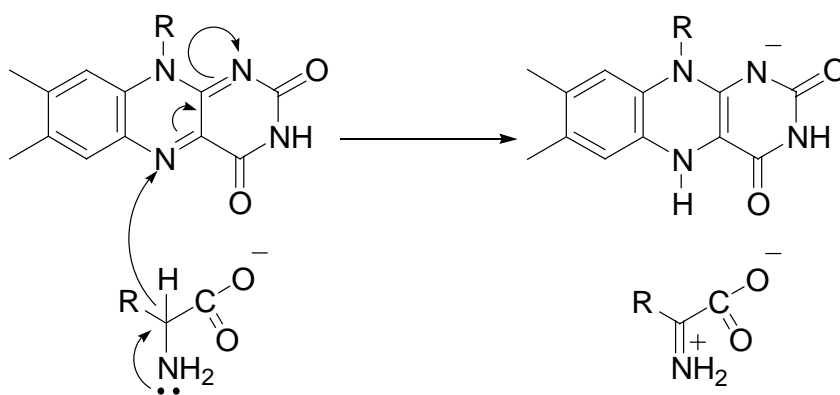


**Figure 1.20.** Active site of *R. gracilis* DAAO with D-3,3,3-F<sub>3</sub>-alanine bound (PDB code 1C0L). FLA, D-3,3,3-F<sub>3</sub>-alanine.

The currently available structures of DAAO from different sources in complex with ligands have showed that Arg285 interacts with the carboxylate group of the ligand and that the negative charge that develops at the vicinity of N(1)-C(2)=O locus of the bound flavin is stabilized by the dipole of  $\alpha$ -helix F5 (37, 163). This result argued against the previously proposed role of Arg285 in stabilizing the negative charge that develops in proximity of N(1) locus of the bound flavin. Consequently, this result disagreed with the involvement of Arg285 in the stabilization of the anionic flavin semiquinone and hydroquinone, and for the formation of tight flavin-N(5)-sulfite adduct as well as in the modulation of the electrophilicity of the bound flavin by increasing the oxidation-reduction potentials of the bound FAD (165). Recently, Pollegioni et al., through their biochemical and spectroscopic analyses of different mutant forms of DAAO in which Arg285 was replaced by selected residues (R285A, R285K, and R285D), concluded that in the free enzyme, Arg285 is still involved in the stabilization of the negative charge on the N(1)-C(2)=O locus of the flavin (159). This conclusion was based on the assumption that although the guanidinium group of Arg285 was found to be located at a distance

of  $\sim 7$  Å from the N(1)-C(2)=O locus of the flavin in the structures of the enzyme in complex with substrate or ligands, in the absence of substrate or ligands the side chain of Arg285 would be able to rotate to a distance of  $\sim 3$  Å from the N(1)-C(2)=O locus of flavin (159). The role of Arg285 in stabilizing the negative charge at the vicinity of the N(1)-C(2)=O locus of the bound flavin in DAAO is still ambiguous due to the unavailability of the X-ray crystal structure of the unliganded enzyme

Fitzpatrick and his co-workers in the last few years have performed a thorough kinetics characterization of DAAO by using substrate and solvent kinetic isotope effects approaches to probe the order of CH bond cleavage and the C=N bond formation (140, 166-168). The results obtained from the analysis of isotope effects studies agree well with the structural studies allowed Fitzpatrick to conclude that the mechanism of DAAO is a direct hydride mechanism, in which both the CH bond cleavage and the C=N bond formation occur in the same transition state (Scheme 1.9). In agreement with this conclusion, a recent computational studies also suggested a direct hydride transfer mechanism involving the anionic form of the amino acid substrate (169).



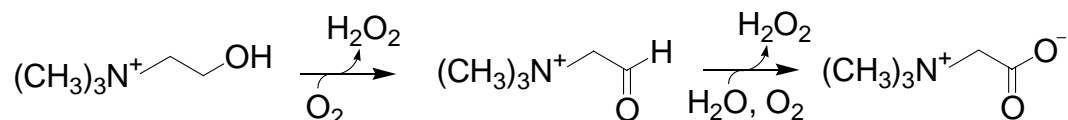
**Scheme 1.9.** Proposed direct hydride transfer mechanism of D-amino acid oxidase.

#### 1.4. Choline Oxidase

Mann et al. first reported the isolation of choline oxidase in 1938. In that study, choline oxidase of rat liver was shown to be a typical dehydrogenase (170). It was assumed that choline oxidase system was composed of choline dehydrogenase, cytochrome c, and cytochrome oxidase. The oxidation of choline was inhibited by betaine, as well as the  $\text{HNMe}_3^+$  (trimethylammonium) and  $\text{NH}_4^+$  ions. In addition, it was also concluded that the trimethylammonium headgroup of choline is important for the specific binding of the substrate to the enzyme (170). A second active form of choline oxidase, which oxidized choline to betaine aldehyde with the uptake of one or two mol of oxygen at pH 6.7 or 7.8, respectively, was also isolated from rat liver in 1938 (171). This form of active choline oxidase was also found in rat kidney but not in blood, muscle, or brain (171).

The *Arthrobacter globiformis* choline oxidase was first purified by fractionations with ammonium sulfate and acetone, followed by column chromatography using the anionic exchanger DEAE-cellulose and gel filtration Sephadex G-200 columns (172). The purified enzyme showed absorbance maxima at 363 and 450 nm, consistent with the purified protein being a flavoenzyme (172). The enzyme showed a molecular mass of ~71 kDa by SDS-PAGE and ~83 kDa by gel filtration, and an isoelectric point (pI) around pH 4.5 (172). The catalytic activity of the purified enzyme was tested using either choline or betaine aldehyde as substrate. The enzymatic activity assays showed the ability of choline oxidase to utilize both choline and betaine aldehyde as substrate, with the subsequent production of glycine betaine (172). On the other hand, the enzymatic activity of choline oxidase was significantly decreased by using a number of substrate analogs, suggesting high substrate specificity of the enzyme for either choline (100%) or betaine aldehyde (46%) (172). A  $K_m$  value of 1.2 mM and 8.7 mM was

determined for choline and betaine aldehyde, respectively. Therefore, it was proposed that choline oxidase from *Arthrobacter globiformis* catalyzes the oxidation of choline or betaine aldehyde with the production of glycine betaine in a reaction where oxygen is acting as electron acceptor and with the production of hydrogen peroxide (Scheme 1.10) (172, 173).



**Scheme 1.10.** Reaction catalyzed by choline oxidase.

The prosthetic group of *A. globiformis* choline oxidase was also investigated by subjecting the enzyme to trypsin-chymotrypsin digestion (82). One of the purified peptide fragments yielded a UV-visible absorbance spectrum similar to that of flavin (FMN or FAD). To identify whether the prosthetic group of choline oxidase was FMN or FAD, the fluorescence intensity of the purified flavin peptide was tested after enzymatic hydrolysis with nucleotide pyrophosphatase at pH 3. The flavin fluorescence intensity increased by 2-fold upon releasing AMP by hydrolysis with nucleotide pyrophosphatase, consistent with FAD rather than FMN being the cofactor (82). The position of flavin attachment was investigated using aminoacyl riboflavin, for which covalent linkage occurs at the 8 $\alpha$ -methylene group of the isoalloxazine ring (82). The fluorescence excitation spectrum of aminoacyl riboflavin along with the purified flavin peptide of choline oxidase at pH 3 showed a ~25 nm hypsochromic shift of the visible peak centered at 346 nm as compared to free riboflavin (from 373 nm to 346 nm), suggesting that in choline oxidase flavinylation occurs at the 8 $\alpha$ -methylene group of the isoalloxazine moiety (82). To establish whether N(1) or N(3) of the histidine residue of the protein bound to the 8 $\alpha$ -



methylene group of FAD, reduction with sodium borohydride and the fluorescence properties of the bound flavin were examined. The purified flavin peptide was not reduced with sodium borohydride, consistent with the covalently bound flavin isolated from the *A. globiformis* choline oxidase being 8 $\alpha$ -[N(3)-histidyl]-FAD. Indeed, it had been reported previously that the N(1) isomer of histidyl flavin can be reduced with borohydride and its fluorescence is quenched, while the N(3) isomer cannot (174). The electrophoretic mobility of the hydrolysate of the methylated histidylflavin of choline oxidase from *Alcaligenes* sp. at pH 6.25 also confirmed 8 $\alpha$ -[N(3)-histidyl]-FAD as the prosthetic group (25). The covalently bound FAD showed maxima at 358 and 453 nm and a shoulder at 480 nm, with a stoichiometric amount of 1 mol of FAD per mol of enzyme. Furthermore, the covalently bound FAD was reduced anaerobically upon addition of choline or betaine aldehyde, and re-oxidized upon aeration (25).

A comprehensive study on the spectroscopic properties of choline oxidase from *Alcaligenes* sp. was conducted for better understanding of the properties of the covalently bound FAD of choline oxidase (48). The authors drew several conclusions based on the spectroscopic properties of the covalently bound FAD. 1) Choline oxidase from *Alcaligenes* sp. was able to stabilize the anionic flavin semiquinone as an intermediate during the course of the enzyme reduction using either dithionite or by photo-irradiating the enzyme in the presence of EDTA. 2) The presence of a catalytic amount (3.7  $\mu$ M) of free riboflavin significantly enhanced the photoreduction rate not only to the semiquinone state but also to the fully reduced form of flavin. 3) The produced semiquinone did not showed any reactivity toward the substrates choline or betaine aldehyde and most importantly, did not show any reactivity toward oxygen, which is an unusual feature among flavoprotein oxidases. 4) The oxidized enzyme was able to form a complex with glycine betaine (the product of the reaction); the dissociation constant of such

complex was determined through spectroscopic titration to be 17 mM at pH 7.5. 5) No significant anionic semiquinone was observed upon the reduction of the enzyme-bound glycine betaine by either dithionite or by photoreduction in the presence of EDTA. 6) The biphasic reactivity of the fully reduced form of the enzyme-bound glycine betaine toward oxygen (rapid and slow phases) led the authors to propose a mechanism for the photoreaction of the enzyme-product complex, wherein a C(4a)-adduct (slowly reacting with oxygen) and the fully reduced flavin via an N(5)-adduct (rapidly reacting with oxygen) were formed (48).

In the past 10 years, studies on choline oxidase were mainly focused on the biotechnological applications of the enzyme (175-179), which will be discussed in detail in Section 1.5.

In a recent study by Rand et al. aimed at identifying the type of flavin linkage as well as the amino acid residue to which FAD is attached in choline oxidase from *A. globiformis*, it was concluded that choline oxidase contains 8 $\alpha$ -[N(1)-histidyl]-FAD at position 87 in the polypeptide chain (49). The results obtained in this study were mainly dependent on the nucleotide sequence of *codA* gene coding for *A. globiformis* choline oxidase, which had been previously reported in Genbank (accession number X84895) (180). The sequencing analysis of the recently cloned *codA* gene from *A. globiformis* genome in our laboratory indicated that the nucleotide sequence of *codA* originally reported in GenBank (accession number X84895) contains seven flaws, resulting in a translated protein with a significantly altered amino acid sequence between position 298 and 410. Therefore, the results obtained here in this study might lack of accuracy. Indeed, the recently solved X-ray crystal structure of *A. globiformis* choline oxidase showed that FAD is covalently linked to His99<sup>N<sub>62</sub></sup> (for details see 1.4.1), confirming the inaccuracy of the results obtained in that study.

Recently, the kinetic mechanism of the commercially available choline oxidase from *A. globiformis* (Sigma-Aldrich, St. Louis, MO) was characterized in our laboratory using different kinetic approaches (181, 182). The steady state kinetic data showed that choline oxidase catalyzed the four-electron oxidation of choline to the carboxylic acid glycine betaine. This reaction occurs through two sequential flavin-linked hydride transfers from choline and the resulting betaine aldehyde intermediate to molecular oxygen (181). In addition, pH and deuterium kinetic isotope effects studies on the oxidation of choline to betaine aldehyde in air saturated buffer showed that a catalytic base with an apparent  $pK_a$  value of  $\sim 8$  is required for the oxidation of choline to glycine betaine. When the pH is at least one pH unit below the  $pK_a$  of such catalytic base, the C-H bond cleavage becomes fully rate limiting for catalysis (182). In that study, from an analysis of the amino acid sequence of choline oxidase from *A. globiformis*<sup>2</sup> (180) with respect to other members of GMC oxidoreductase superfamily (39, 97, 105, 183), histidine 466 was proposed to act as the catalytic base in choline oxidase (182).

Choline oxidase from *A. globiformis* was recently cloned in our laboratory (47). The recombinant enzyme was expressed and purified to high purity and quantity, allowing detailed biophysical, biochemical, and spectroscopic characterizations of the enzyme, as well as mechanistic and structural studies with site-directed mutants (44, 47, 137, 138). These studies will be discussed in detail in Chapters 3-7.

In a recent study that has been carried out in our laboratory on the recombinant enzyme, choline and glycine betaine analogs have been used as substrates and inhibitors for the enzyme at pH 6.5 to probe the structural determinants that are relevant for substrate specificity and binding

---

<sup>2</sup> The sequencing analysis of the recently cloned *codA* gene from *A. globiformis* genome in our laboratory indicated that the nucleotide sequence of *codA* originally reported in GenBank (accession number X84895) contains seven flaws, resulting in a translated protein with a significantly altered amino acid sequence between position 298 and 410 (46).

(184). As shown in Table 1.4, the  $K_{is}$  values that were determined for the competitive inhibition patterns of glycine betaine, *N,N*-dimethylglycine, or *N*-methylglycine with respect to choline were found to increase monotonically with decreasing number of methyl groups, consistent with the importance of the trimethylammonium moiety of the ligand for substrate binding (Table 1.4) (184). On the other hand, the  $K_{is}$  values did not show any changes upon substituting glycine betaine with inhibitors containing methyl, ethyl, allyl, and 2-amino-ethyl esters, which strongly suggests that the acetate moiety of the ligand does not participate in substrate binding (Table 1.4) (184). In agreement with the inhibition data, the second-order rate constants  $k_{cat}/K_m$  (which reflect the specificity of the enzyme for the organic substrate) decreased upon using *N,N*-dimethylethanolamine and *N*-methylethanolamine as substrate with respect to choline (Table 1.5) (184). In addition to the methyl groups of the trimethylammonium moiety, the positive charge on the same moiety has also been shown to be important for substrate binding and specificity. When choline was substituted with its isosteric analogue 3,3-dimethyl-1-butanol as substrate for choline oxidase, a significant decrease in both the turnover number ( $k_{cat}$ ) and the  $k_{cat}/K_m$  values were observed (Table 1.5) (184). These results suggest that the positive charge on the trimethylammonium headgroup of the substrate is important for substrate binding and catalysis (184). An energetic contribution of  $\sim 29 \text{ kJ mol}^{-1}$  was determined from the kinetic data for the interaction of the quaternary ammonium portion of the substrate with the active site of choline oxidase, i.e.,  $\sim 7 \text{ kJ mol}^{-1}$  from each methyl group and  $\sim 8 \text{ kJ mol}^{-1}$  from the positive charge (184). This value compares well with the value of  $\sim 33 \text{ kJ mol}^{-1}$  that was determined before for the contribution of the quaternary ammonium moiety of acetylcholine in acetylcholinesterase (185, 186). Similar observations have also been reported before for enzymes that use molecules containing choline moiety as substrates, including acetylcholine, phosphatidylcholine, and

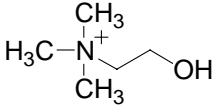
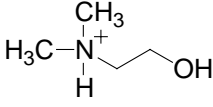
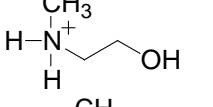
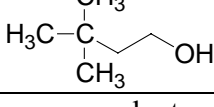
phosphocholine (185-188). Among these enzymes, phospholipase C, acetyl-cholinestrane, and CTP:phosphocholine cytidyltranseferase have been well characterized for the substrate binding properties (185-188). The X-ray crystal structures of those enzymes complexed with their specific inhibitors suggested that the trimethylammonium headgroup of the ligands is stabilized by  $\pi$ -cation interaction to specific active site aromatic residues (185-188).

**Table 1.4.** Inhibition Studies of Choline Oxidase at pH 6.5 <sup>a</sup>

Inhibitor	Structure	Type of inhibition	$K_{is}$ , mM	$R^2$
Glycine betaine	$\begin{array}{c} \text{CH}_3 \\   \\ \text{H}_3\text{C}-\text{N}^+-\text{CH}_2-\text{COO}^- \\   \\ \text{CH}_3 \end{array}$	competitive	$15 \pm 2$	0.984
<i>N,N</i> -Dimethylglycine	$\begin{array}{c} \text{CH}_3 \\   \\ \text{H}_3\text{C}-\text{N}^+-\text{CH}_2-\text{COO}^- \\   \\ \text{CH}_3 \end{array}$	competitive	$57 \pm 1$	0.995
<i>N</i> -Methylglycine	$\begin{array}{c} \text{H} \\   \\ \text{H}_3\text{C}-\text{N}^+-\text{CH}_2-\text{COO}^- \\   \\ \text{H} \end{array}$	competitive	$405 \pm 2$	0.998
Tetramethylamine	$\begin{array}{c} \text{CH}_3 \\   \\ \text{H}_3\text{C}-\text{N}^+-\text{CH}_3 \\   \\ \text{CH}_3 \end{array}$	competitive	$11 \pm 1$	0.997
Trimethylamine	$\begin{array}{c} \text{CH}_3 \\   \\ \text{H}_3\text{C}-\text{N}^+-\text{H} \\   \\ \text{CH}_3 \end{array}$	competitive	$2.4 \pm 0.2$	0.998
Dimethylamine	$\begin{array}{c} \text{CH}_3 \\   \\ \text{H}_3\text{C}-\text{N}^+-\text{H} \\   \\ \text{H} \end{array}$	competitive	$6 \pm 1$	0.998
Methylamine	$\begin{array}{c} \text{H} \\   \\ \text{H}_3\text{C}-\text{N}^+-\text{H} \\   \\ \text{H} \end{array}$	competitive	$26 \pm 1$	0.996
Trimethylethylamine	$\begin{array}{c} \text{CH}_3 \\   \\ \text{H}_3\text{C}-\text{N}^+-\text{C}_2\text{H}_5 \\   \\ \text{CH}_3 \end{array}$	competitive	$13 \pm 2$	0.988
Dimethylethylamine	$\begin{array}{c} \text{CH}_3 \\   \\ \text{H}_3\text{C}-\text{N}^+-\text{C}_2\text{H}_5 \\   \\ \text{H} \end{array}$	competitive	$9 \pm 1$	0.995
Methylethylamine	$\begin{array}{c} \text{H} \\   \\ \text{H}_3\text{C}-\text{N}^+-\text{C}_2\text{H}_5 \\   \\ \text{H} \end{array}$	competitive	$8 \pm 1$	0.995
Allyltrimethylamine	$\begin{array}{c} \text{CH}_3 \\   \\ \text{H}_3\text{C}-\text{N}^+-text{CH}_2-\text{CH}=\text{CH}_2 \\   \\ \text{CH}_3 \end{array}$	competitive	$15 \pm 1$	0.999
2-Amino-trimethylethylamine	$\begin{array}{c} \text{CH}_3 \\   \\ \text{H}_3\text{C}-\text{N}^+-text{CH}_2-\text{CH}_2-\text{NH}_3^+ \\   \\ \text{CH}_3 \end{array}$	competitive	$9 \pm 1^b$	0.993

<sup>a</sup> Choline oxidase activity was measured at varying concentrations of both choline and inhibitor in air-saturated 50 mM sodium pyrophosphate, pH 6.5 and 25 °C. <sup>b</sup> Value determined for the protonated form of 2-amino-trimethylethylamine. Modified from ref. (184).

**Table 1.5.** Steady State Kinetic Parameters for Choline and *N*-Substituted Choline Analogs as Substrates for Choline Oxidase at pH 8<sup>a</sup>

Substrate	Structure	$k_{cat}$ , s <sup>-1</sup>	$k_{cat}/K_m$ , M <sup>-1</sup> s <sup>-1b</sup>	$R^2$
Choline		86 ± 1	200,000 ± 10,000	0.995
<i>N,N</i> -Dimethylethanolamine		5.9 ± 0.1	18,400 ± 300	0.996
<i>N</i> -Methylethanolamine		0.37 ± 0.01	710 ± 10	0.994
3,3-Dimethyl-1-butanol		8.0 ± 0.1	7,900 ± 980	0.980

<sup>a</sup> Choline oxidase activity was measured at varying concentrations of organic substrate and oxygen in 50 mM sodium pyrophosphate, pH 8, and 25 °C. <sup>b</sup>  $k_{cat}/K_m$  is the  $k_{cat}/K_m$  value for the organic substrate. Modified from ref. (184).

In a subsequent study by our group, primary deuterium and solvent kinetic isotope effects were used to investigate the mechanism of substrate oxidation (CH and OH bond cleavages) by recombinant choline oxidase using both rapid kinetics and steady-state kinetics techniques (134). That study showed that in the reductive half-reaction, the CH bond cleavage is not masked by other kinetic steps as indicated by the pH independent value (in the pH range 6.5-10) of  $\sim 10.6$  for  $^D(k_{\text{cat}}/K_m)$  with deuterated choline (Figure 1.21) (134). In good agreement with that value, at pH 10 a  $^Dk_{\text{red}}$  value of  $\sim 8.9$  was also determined for the anaerobic reduction of the bound-flavin by choline, irrespective of whether protio or deuterated solvent was used (134). In addition, the study also showed that while the  $^Dk_{\text{cat}}$  and  $^{D_2O}k_{\text{cat}}$  values were 7.3 and 1.1, respectively, the  $^{D_2O}(k_{\text{cat}}/K_m)$  and the  $^{D_2O}k_{\text{red}}$  values were equal to unity with either choline or deuterated choline (134). Overall, the results obtained have indicated that chemical steps of choline oxidation catalyzed by choline oxidase are fully rate limiting for both the overall turnover and the reductive half-reaction in which choline is oxidized to betaine aldehyde. In addition, the removal of the substrate hydroxyl proton and the hydride transfer from the substrate  $\alpha$ -carbon to the N(5) locus of the flavin cofactor occur in a stepwise fashion with the formation of a transient alkoxide intermediate species (Scheme 1.11) (134).

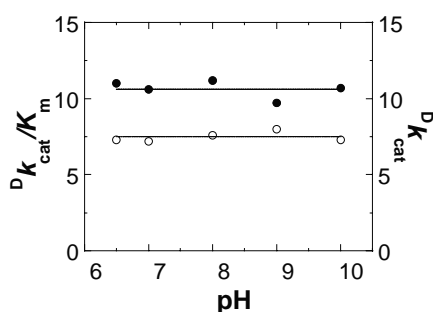
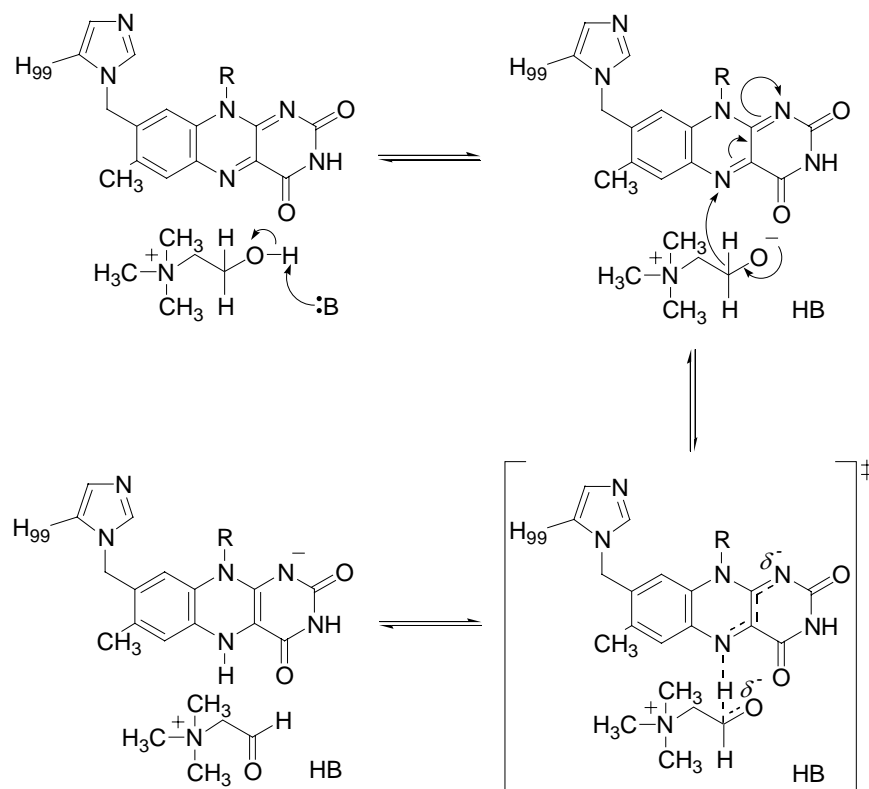


**Figure 1.21.** pH-Dependence of the deuterium isotope effects.

pH-dependence of the deuterium isotope effects on  $k_{\text{cat}}/K_m$  (●) and  $k_{\text{cat}}$  (○) values. Activity assays of choline oxidase were performed in 50 mM buffer with choline and 1,2- $^{[2H_4]}$ -choline as substrate, at 25 °C. Data were fit by  $y = 10.6$  and  $y = 7.5$  for  $k_{\text{cat}}/K_m$  and  $k_{\text{cat}}$  values, respectively. Taken without permission from ref. (134).





**Scheme 1.11.** Chemical mechanism of choline oxidase for oxidation of choline at pH 10. Modified from ref. (134).

In another recent study on recombinant choline oxidase, the effects of temperature and oxygen concentration on the kinetic isotope with deuterated choline have been investigated (135). At saturating oxygen concentrations, the  $^Dk_{\text{cat}}$  and the  $^D(k_{\text{cat}}/K_m)$  values with 1,2- $^{2}\text{H}_4$ -choline were pH-independent, whereas at oxygen concentration  $\leq 0.97$  mM, they decreased at high pH to limiting values that depended on oxygen concentration (Figure 1.22 and Table 1.6) (135). In addition, the  $k_{\text{cat}}$  and  $k_{\text{cat}}/K_m$  pH profiles also showed similar patterns reaching plateaus at high pH. By using choline as a substrate at oxygen concentration of  $\leq 0.25$  mM, both the limiting  $k_{\text{cat}}/K_m$  at high pH and the  $\text{pK}_a$  values moved to lower values (Table 1.7) (135). These data suggested that oxygen availability is the major determinant that dictates whether the reduced enzyme-betaine aldehyde complex proceeds forward to catalysis or reverts to the oxidized

enzyme-choline alkoxide complex during turnover of the enzyme with choline (135). To test the involvement of quantum mechanical tunneling in the hydride transfer mechanism catalyzed by choline oxidase, the effect of temperature on the  $^Dk_{\text{cat}}$  and the  $^D(k_{\text{cat}}/K_m)$  values at saturating oxygen concentration were determined (135). The effect of temperature on the kinetic isotope effects can provide evidence on whether hydride transfer occurs quantum mechanically or by following the classical over-the barrier behavior (135). The  $^D(k_{\text{cat}}/K_m)$  was temperature dependent and with value similar to the isotope effects on the preexponential factors ( $A_H'/A_D'$ ). The large isotope effect on the preexponential factors ( $A_H'/A_D'$ ) determined from the temperature dependence of the  $k_{\text{cat}}/K_m$  values with choline and 1,2- $[-^2\text{H}_4]$ -choline, with a value of  $\sim 14$ , rules out a classical over-the-barrier behavior for hydride transfer, for which  $A_H'/A_D'$  values between 0.7 and 1.7 are expected (135). Similar enthalpies of activation ( $\Delta H^\ddagger$ ) with values of  $18 \pm 2$  and  $18 \pm 5 \text{ kJ mol}^{-1}$  were determined for choline and 1,2- $[-^2\text{H}_4]$ -choline, respectively. Overall, these data suggested that the reversible hydride transfer mechanism of choline catalyzed by choline oxidase occurred quantum mechanically. In such mechanism, the tunneling behavior of the hydride transfer is mainly affected by the distance between the hydride donor and acceptor (135).

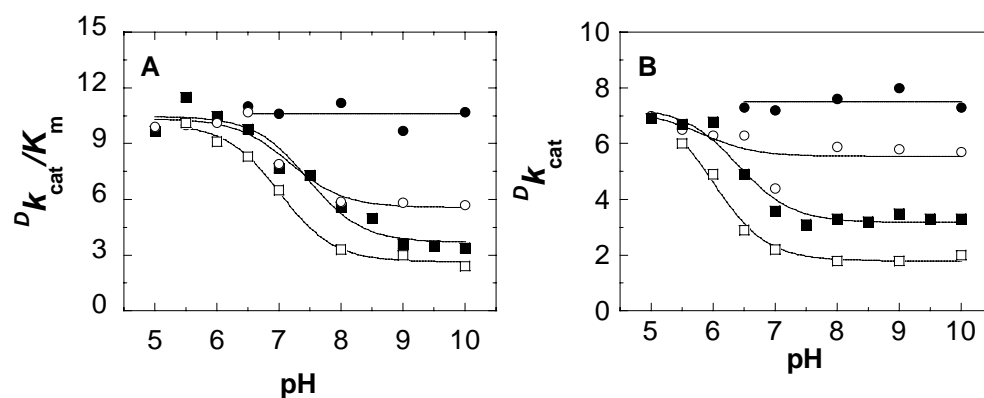


**Figure 1.22.** pH dependence of  $D(k_{cat}/K_m)$  and  $Dk_{cat}$  values with 1,2- $[^2H_4]$ -choline as substrate for choline oxidase at 0.07 ( $\square$ ), 0.25 ( $\blacksquare$ ), 0.97 mM ( $\circ$ ) and saturating ( $\bullet$ ) oxygen concentrations. Activity assays of choline oxidase were performed in 50 mM buffer with choline or 1,2- $[^2H_4]$ -choline as substrate, at 25 °C. Taken without permission from ref. (135).

**Table 1.6.** pH Dependence of Kinetic Isotope Effects at Different Oxygen Concentrations <sup>a</sup>

[O <sub>2</sub> ], mM	<sup>D</sup> ( <i>k</i> <sub>cat</sub> / <i>K</i> <sub>m</sub> )			<sup>D</sup> <i>k</i> <sub>cat</sub>		
	<i>Y</i> <sub>L</sub> <sup>b</sup>	<i>Y</i> <sub>H</sub> <sup>b</sup>	p <i>K</i> <sub>a</sub>	<i>Y</i> <sub>L</sub>	<i>Y</i> <sub>H</sub>	p <i>K</i> <sub>a</sub>
∞ <sup>c</sup>	10.6 ± 0.6	10.6 ± 0.6	n.a. <sup>d</sup>	7.5 ± 0.3	7.5 ± 0.3	n.a. <sup>d</sup>
0.97	10.3 ± 0.4	5.6 ± 0.4	7.2 ± 0.3	7.2 ± 1.0	5.5 ± 0.3	5.9 ± 0.9
0.25	10.5 ± 0.4	3.7 ± 0.4	7.5 ± 0.2	7.3 ± 0.3	3.2 ± 0.2	6.3 ± 0.1
0.07	10.1 ± 0.2	2.6 ± 0.2	7.2 ± 0.2	7.5 ± 0.6	1.8 ± 0.1	6.0 ± 0.1

<sup>a</sup> Conditions: 50 mM buffer, pH from 5 to 10 and 25 °C. <sup>b</sup> *Y*<sub>L</sub> and *Y*<sub>H</sub> are the limiting values at low and high pH, respectively. <sup>c</sup> Data are from ref. (134). <sup>d</sup> n.a., not applicable. Taken without permission from ref. (135).

**Table 1.7.** p*K*<sub>a</sub> Values for Steady State Kinetic Parameters with Choline or 1,2-[<sup>2</sup>H<sub>4</sub>]-Choline as Substrate <sup>a</sup>

substrate	[O <sub>2</sub> ], mM	<i>k</i> <sub>cat</sub> / <i>K</i> <sub>m</sub> , M <sup>-1</sup> s <sup>-1</sup>		<i>k</i> <sub>cat</sub> , s <sup>-1</sup>	
		p <i>K</i> <sub>a</sub>	<i>Y</i> <sup>b</sup>	p <i>K</i> <sub>a</sub>	<i>Y</i> <sup>b</sup>
choline	∞ <sup>c</sup>	7.6 ± 0.2	130,000 ± 30,000	7.1 ± 0.1	58 ± 8
	0.97	7.5 ± 0.1	150,000 ± 13,000	6.9 ± 0.1	41 ± 3
	0.25	7.3 ± 0.1	66,000 ± 9,000	6.5 ± 0.1	21 ± 1
	0.07	7.0 ± 0.1	47,000 ± 5,000	6.0 ± 0.1	6.6 ± 0.3
1,2-[ <sup>2</sup> H <sub>4</sub> ]-choline	∞ <sup>c</sup>	7.8 ± 0.2	14,000 ± 5,000	7.1 ± 0.2	7.5 ± 1.2
	0.97	7.5 ± 0.2	29,000 ± 6,000	7.0 ± 0.1	7.6 ± 0.9
	0.25	7.6 ± 0.1	18,000 ± 3,000	6.9 ± 0.1	6.7 ± 0.4
	0.07	7.6 ± 0.1	18,000 ± 3,000	6.7 ± 0.1	3.6 ± 0.2

<sup>a</sup> Conditions: 50 mM buffer, pH from 5 to 10 and 25 °C. <sup>b</sup> *Y*, limiting value at high pH. <sup>c</sup> Data are from ref. (134). Taken without permission from ref. (135).

Recently, another study on recombinant choline oxidase was carried out in our laboratory aimed at understanding the mechanism of betaine aldehyde oxidation through the kinetic and spectroscopic analyses of the oxidation of betaine aldehyde and its isosteric analog 3,3-dimethylbutyraldehyde (136). While the anaerobic stopped-flow mixing of the enzyme with either choline or betaine aldehyde at pH 8 resulted in complete reduction of the bound flavin with similar  $k_{\text{red}}$  values  $\geq 48 \text{ s}^{-1}$ , only 10 to 26% of the enzyme-bound flavin was reduced by 3,3-dimethylbutyraldehyde between pH 6 and 10 (136). In addition, 3,3-dimethylbutyraldehyde was found to act as a competitive inhibitor *versus* choline in the reaction catalyzed by choline oxidase (136). At air-saturation oxygen concentrations, the pH dependence of the kinetic parameters  $k_{\text{cat}}$  and  $k_{\text{cat}}/K_{\text{m}}$  with betaine aldehyde indicated that a catalytic base with  $\text{p}K_{\text{a}}$  value of  $\sim 6.7$  is required for the oxidation of betaine aldehyde catalyzed by choline oxidase (136). Previous studies showed that, at saturating oxygen concentrations, flavin reduction is the rate-limiting for the overall turnover number of betaine aldehyde, with a limiting value of  $135 \text{ s}^{-1}$ , at high pH (134). Because  $k_{\text{cat}}/K_{\text{O}_2}$  value for the oxidation of the reduced enzyme bound betaine aldehyde complex ( $k_5$ ) is  $\sim 9 \times 10^4 \text{ M}^{-1} \text{ s}^{-1}$  (44), therefore, the rate constant for oxidation of the reduced enzyme bound betaine aldehyde at a concentration of oxygen of 0.25 mM at 25 °C (atmospheric conditions) is expected to be  $\sim 22 \text{ s}^{-1}$ . Accordingly, the apparent  $\text{p}K_{\text{a}}$  value observed in the  $k_{\text{cat}}/K_{\text{m}}$  pH profile of betaine aldehyde would be perturbed to lower values by 0.85 pH unit with respect to the intrinsic  $\text{p}K_{\text{a}}$  value of 7.5, which has been recently determined from the  $k_{\text{cat}}/K_{\text{m}}$  pH profile with choline and its analogues as substrate for choline oxidase (44, 184). Therefore, it was proposed that an active site base triggers the hydride transfer mechanism of betaine aldehyde, which is most likely the same base that triggers the hydride transfer mechanism of choline (136). The NMR spectroscopic analyses of both betaine aldehyde and its isosteric analog 3,3-

dimethylbutyraldehyde revealed that while betaine aldehyde exists predominantly (99%) as a diol form in aqueous solution, 3,3-dimethylbutyraldehyde favors the aldehyde ( $\geq 65\%$ ) over the hydrated form in the pH range between 6 and 10 (Table 1.8) (136). Overall, the results obtained in this study suggested that choline oxidase oxidizes the hydrated form of betaine aldehyde through a base-catalyzed hydride transfer mechanism from the organic substrate to the enzyme-bound flavin (Scheme 1.12) (136).

Overall, based on the results obtained from the different biochemical and kinetic studies carried on the wild-type as well as some selected mutant proteins of choline oxidase (this thesis), our proposed model of the mechanism of reactions for the four-electron oxidation of choline to glycine betaine catalyzed by choline oxidase can be summarized as follows. 1) During the reductive half-reaction, an unidentified active site base with a  $pK_a$  of 7.5 activates the alcohol substrate with formation of an alkoxide species (species 1 and 2 in Scheme 1.13) (44, 134). 2) This alkoxide intermediate is transiently stabilized in the active site through electrostatic interaction with the N $\epsilon$ 2 atom of the imidazolium side chain of His<sub>466</sub> (species 3 in Scheme 1.13, Chapter 5) (137). 3) Similarly, the protonated His<sub>466</sub> also stabilizes electrostatically the negative charge that develops on the N(1)-C(2)=O locus of the reduced flavin (anionic species) through its N $\epsilon$ 2 atom (species 3 in Scheme 1.13, Chapter 6) (138). 4) The hydride transfer from the  $\alpha$ -carbon of the substrate to the N(5) locus of the bound flavin occurs quantum mechanically from the activated choline alkoxide species (species 3 in Scheme 1.13) (135). 5) During the oxidative half-reaction, the electron delocalization from the N(1) locus of the anionic hydroquinone along with the proton transfer from the unidentified catalytic base result in the formation of the C(4a)-hydroperoxo-flavin (species 5 in Scheme 1.13). 6) The highly unstable C(4a)-hydroperoxo-flavin abstracts the second proton from the hydride at the N(5) locus of the FAD with the subsequent

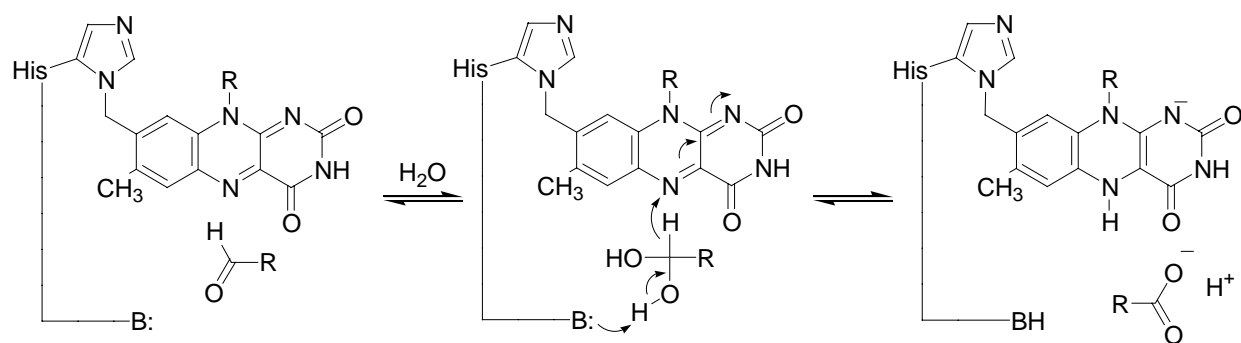
release of  $\text{H}_2\text{O}_2$  and the formation of oxidized enzyme-bound FAD (species 6 and 7 in Scheme 1.13). 7) Finally, the oxidation of the hydrated betaine aldehyde occurs through a base catalyzed transfer of a hydride ion from the organic substrate to the enzyme-bound FAD, with a mechanism that is similar to that proposed for the oxidation of choline as proposed recently in a study by our group on the mechanism of aldehyde oxidation (*136*).

**Table 1.8.** NMR Determination of Hydration Ratio of Betaine Aldehyde and 3,3-Dimethylbutylaldehyde in Aqueous Solution <sup>a</sup>

pD	betaine aldehyde [diol]/[aldehyde]	3,3-dimethylbutylaldehyde [diol]/[aldehyde]
5.9	nd <sup>b</sup>	0.42
6.9	99	nd
7.3	99	0.35
8.5	99	0.27
9.5	99	0.22
10.7	99	0.20
12.1	99	0.14

<sup>a</sup> Conditions: 50 mM aldehyde, dissolved in 99.9% D<sub>2</sub>O, at 25 °C.

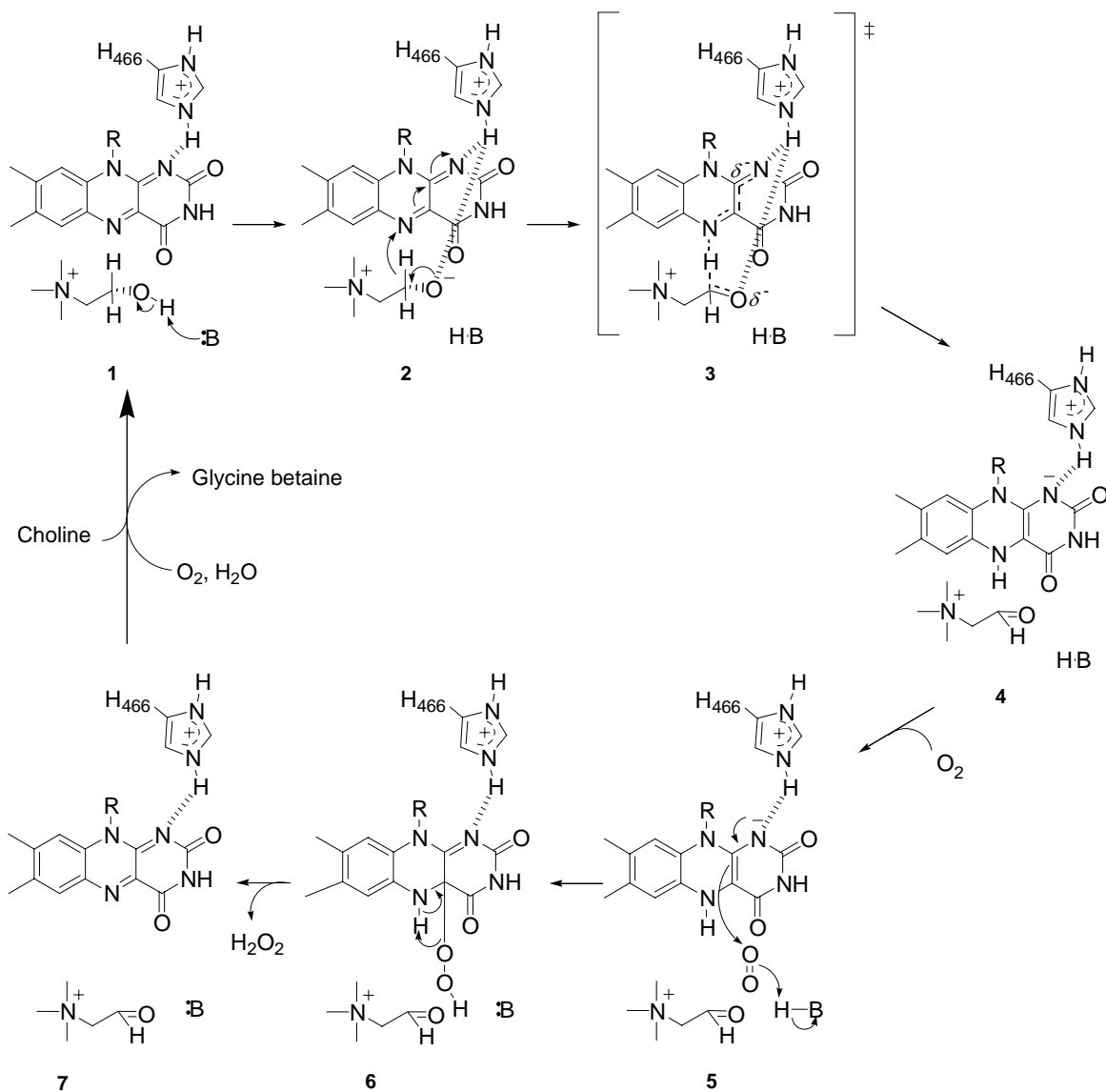
<sup>b</sup> nd, not determined. Taken without permission from ref. (136).



**Scheme 1.12.** Proposed mechanism for the oxidation of betaine aldehyde catalyzed by choline oxidase.

Taken without permission from ref. (136).





**Scheme 1.13.** Proposed mechanism for the four-electron oxidation of choline to glycine betaine catalyzed by choline oxidase.

### 1.4.1. X-ray Structure of Choline Oxidase

The X-ray crystallographic structure of choline oxidase from *A. globiformis* was recently determined at 1.86 Å resolution (George Lountos, Fan Fan, Giovanni Gadda, and Allen M. Orville, unpublished results).

**Overall structure.** The crystal structure of choline oxidase at resolution of 1.86 Å was solved by molecular replacement using the coordinates of glucose oxidase [1CF3, (39)] as a template. The crystallographic data confirmed our previously obtained results for the oligomerization state of the enzyme in solution (47), and showed that choline oxidase has a dimeric structure, with approximate dimensions of 88 Å x 70 Å x 46 Å (Figure 1.23). The two monomers interact with each other in an antiparallel manner. The overall structure of choline oxidase was found to be similar to the PHBH-fold (*p*-hydroxy-benzoate hydroxylase) previously reported for other GMC enzymes (31, 33, 34, 39, 62, 97). In addition, the polypeptide chain of each monomer folded into two domains, the substrate-binding domain and the FAD binding domain, with the active site being located between these two domains (Figure 1.23).

**Flavin-binding domain.** The flavin-binding domain comprises residues 1-159, 201-311, and 464-527. The secondary structure of the flavin-binding domain consists of six-stranded β-sheets flanked by three-stranded antiparallel β-sheets and α-helices, consistent with other GMC enzymes (Figure 1.23) (31, 33, 34, 39, 62, 97). In addition, a typical Rossmann fold (βαβ) (residues 16-44) was observed for the binding of the ADP sp. of the FAD (Figure 1.24). This ADP-binding motif includes the highly conserved sequence, GXGXXG (residues 20-25: GGGSAG). Among these residues, Ser23 forms several interactions with the flavin, with its main chain being 3.3 Å from the first phosphate group of the ADP moiety, and its side chain being 2.7 and 3.4 Å from the oxygen atoms of ribityl (O4\*) and second phosphate group of ADP,

respectively (Figure 1.24). Glu44<sup>O<sub>62</sub></sup> is located 2.7 and 3.2 Å from the ribose O2' and O3', respectively, of the adenosine sp. (Figure 1.24). With the exception of these two residues, no direct interactions between the enzyme and flavin adenine and ribitol were observed, which clearly shows the importance of covalent flavinylation in positioning the FAD in choline oxidase. For other GMC enzymes, in which FAD is not covalently attached to the protein such as, glucose oxidase and cellobiose dehydrogenase, intensive interactions were observed between the enzyme and the flavin. The increased interactions may compensate the noncovalently linked FAD in glucose oxidase and cellobiose dehydrogenase (189-192). A conserved loop structure composed of residues 65 – 95, which covers the entrance of the active site, was also observed (Figure 1.23). A similar active site loop structure was reported before for cholesterol oxidase (193). In that enzyme it was proposed through mutagenesis studies that such loop plays an important role in facilitating the movement of the substrate into and of the product out of the enzyme active site (193).

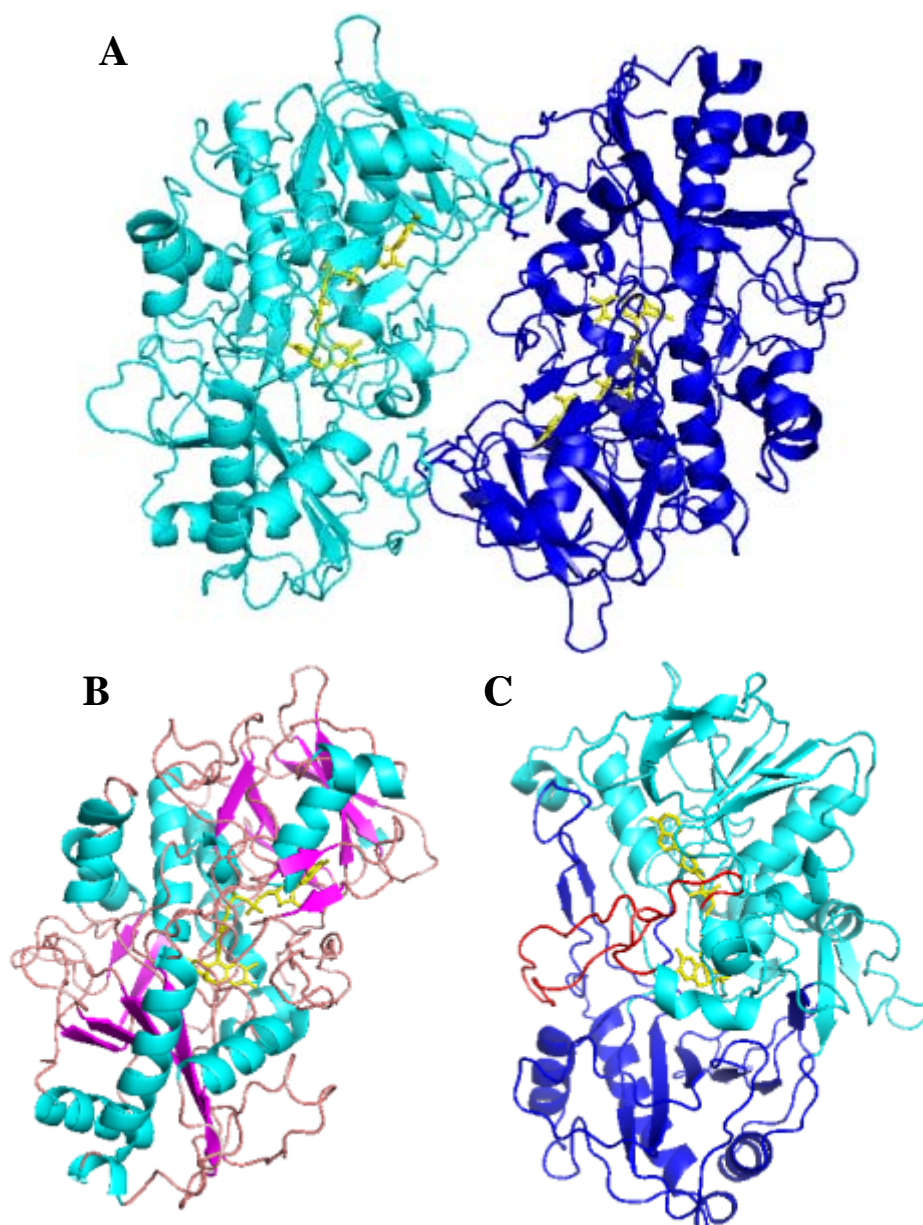


**Figure 1.23.** Three-dimensional structure of choline oxidase from *Arthrobacter globiformis*. Choline oxidase is shown in dimeric (A) and monomeric (B and C) structures. In B, the structure is colored by secondary structure elements (cyan:  $\alpha$ -helix, magenta:  $\beta$ -sheet, wheat: loop); in C, the structure is rotated by  $\sim 45^\circ$  with respect to the structure in B, and colored to show different domains (blue: substrate binding domain, cyan: flavin binding domain, red: active site loop structure). In all structures, the FAD molecule is colored in yellow.

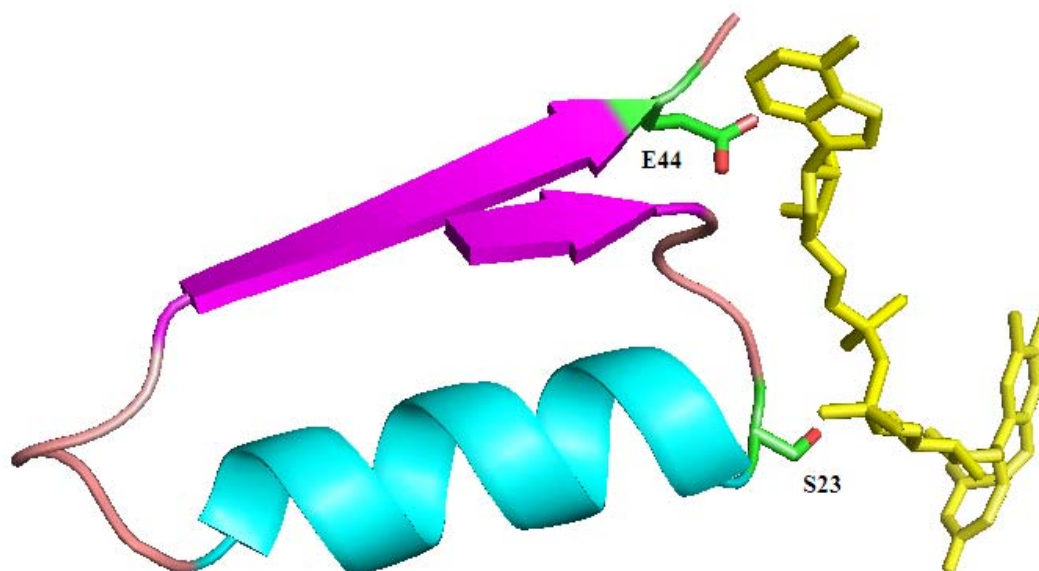


**Figure 1.24.** Rossmann fold (ADP-binding motif) structure of choline oxidase. Rossmann fold ( $\beta\alpha\beta$ ) (*cyan*:  $\alpha$ -helix, *magenta*:  $\beta$ -sheet, *wheat*: loop); the FAD molecule is colored in yellow.

Electron density clearly showed that the FAD is covalently linked to His99<sup>Nε2</sup> (Figure 1.25). This result disagrees with a previous mass spectrometric study on choline oxidase, which concluded that choline oxidase contains 8α-[N(1)-histidyl]-FAD at position 87 in the polypeptide chain (49). The electron density maps shown in Figure 1.25 demonstrate that the isoalloxazine ring of the bound flavin is not planar. The plane of the pyrimidine ring was at an angle of  $\sim 130^\circ$  with respect to the relatively flat piperazine and dimethylbenzene rings (Figure 1.25). The pyrimidine ring was also significantly distorted from planarity with a “half-boat” configuration. All atoms in the distorted pyrimidine ring were in the same plane with the exception of C4a, which was observed as  $sp^3$  hybridized. In addition, the C10a was also observed as partially  $sp^3$  hybridized. This structure is significantly different from both the oxidized flavin, and the reduced flavins, which typically exhibit an angle of  $\sim 150^\circ$  along the N5-N10 axis defined

by the dimethylbenzene and pyrimidine rings (194-196). A possible rationale that explains such an unusual distortion of the flavin in choline oxidase is that it could be due the formation of flavin-C4a- and C10a-adducts. The formation of the FAD-C4a-O<sub>2</sub> *in situ* could occur in two steps: 1) the bound FAD is reduced by the high brilliance synchrotron X-ray (photoreduction); 2) molecular oxygen within the aerobic crystal diffuses to the C4a position of the reduced FAD resulting in the formation of a FAD-C4a-O-O<sup>-</sup> adduct (197, 198). Further studies are currently underway to investigate the possible reasons of such unusual flavin distortion in choline oxidase.

**Substrate-binding domain.** The substrate-binding domain of choline oxidase consists of residues 160-200 and 312-463. It comprises three  $\alpha$ -helices and a slightly distorted five-stranded  $\beta$ -sheet; two strands in the  $\beta$ -sheet form the bottom of the active site. A large hydrophobic residue, Trp331, was observed within  $\beta$ -sheet strand, which lies about  $\sim 8.5$  Å from FAD. This distance fits well with substrate choline sandwiched between Trp331 and FAD, consistent with the role of Trp331 in substrate binding. In addition to Trp331, a number of hydrophobic residues were observed also in the active site in the substrate binding domain, including, Trp330, Ile333, Tyr352, as well as Phe357 (Figure 1.26). Furthermore, Glu312 was also observed in the substrate binding domain facing towards the active site, suggesting a role of this residue in facilitating substrate binding (*vide infra*).

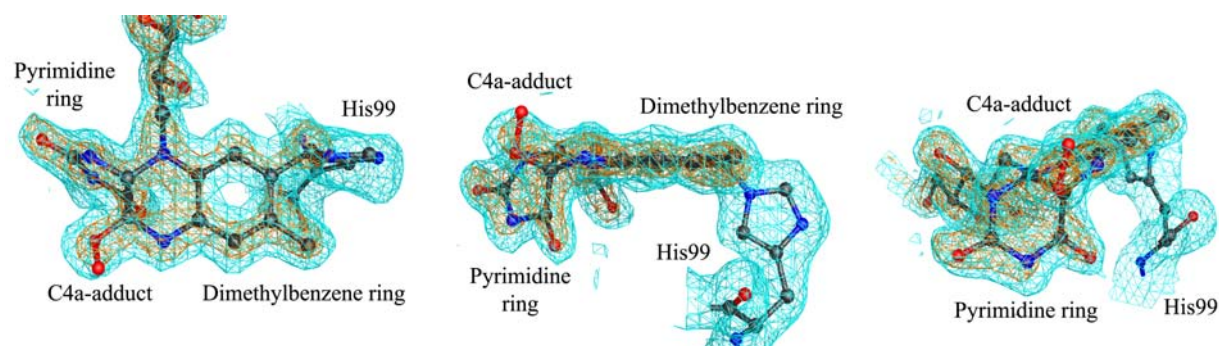


**Figure 1.25.** Approximately orthogonal views of the 50 - 1.86 Å resolution electron density maps for the FAD isoalloxazine ring in choline oxidase. The refined atomic model is shown superimposed with C, N, and O atoms are colored grey, blue and red, respectively. From Lountos, G. T., Fan, F., Gadda, G., and Orville, A. M.; unpublished data.

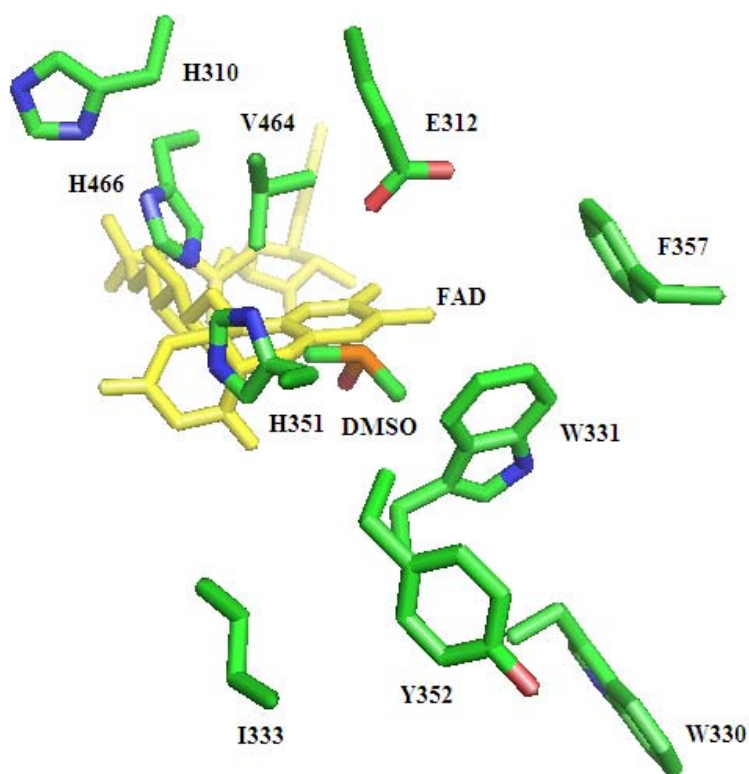


**Figure 1.26.** Active site structures of choline oxidase, fitting with DMSO. The important residues from substrate- and FAD-binding domains are shown.

**Active site.** The enzyme active site is located between the substrate binding domain and the flavin binding domain, with a conserved loop structure (residues 65-95) covering its entrance (Figure 1.23). One water molecule was observed in the enzyme active site, consistent with other GMC enzymes such as glucose oxidase, cholesterol oxidase, pyranose 2-oxidase, and cellobiose dehydrogenase (31, 33, 34, 39, 62, 97). Electron density showed a small molecule, not from the enzyme in the active site. By carefully reviewing all the reagents used in crystallization, DMSO was observed to fit well within the observed density map (Figure 1.26). The substrate choline was docked into the structure based on the density map with DMSO (Figure 1.27). Two histidine residues, His351 and His466, were also observed in the active site of choline oxidase (Figure 1.27). Earlier mechanistic studies on cholesterol oxidase, cellobiose dehydrogenase, and glucose oxidase, suggested that a histidine residue, which is fully conserved within the GMC family and corresponds to His466 of choline oxidase, might act as the specific base that participates in the oxidation of the alcohol substrate (39, 105, 113, 128, 199, 200). However, our recent biochemical and mechanistic studies of His466 mutant proteins (CHO-H466A and CHO-H466D) suggested that His466 is most likely not the active site base that abstracts the substrate hydroxyl proton during catalysis (these studies will be discussed in detail in Chapters 5 and 6). The X-ray crystallographic structure of the enzyme docked with choline showed that while His466 is located at a distance of  $\sim 4.8$  Å from the hydroxyl group of the docked substrate choline, His351 is located at a distance of  $\sim 3.3$  Å from the same region. Therefore, His351 might function as the specific base that abstracts the hydroxyl proton of the substrate during catalysis. Val464 is also likely to interact with choline, as suggested by the close distances to choline, i.e., 2.5 Å from its main chain and 3.5 Å from its side chain (Figure 1.27).



As pointed out earlier, the trimethylammonium headgroup of choline is the major determinant for substrate binding and specificity (184). The X-ray structural data of choline oxidase showed that three residues (Glu312, Trp331, and Phe357) are located close to the trimethylammonium moiety of the docked choline in the active site (Figure 1.27). In this respect, these three residues are likely to be the components of the previously proposed  $\pi$ -cation interactions of the substrate to selected active site residues of the enzyme (184), i.e. Glu312 can form an ion pair with the positive charge of the trimethylammonium moiety, and the two hydrophobic residues can interact with the methyl groups to form  $\pi$ -cation interactions, which in turn facilitates the substrate binding and positioning for catalysis. Similar observations have been reported before in many choline-binding enzyme such as phospholipase C, CTP: phosphocholine cytidyltransferase, and acetyl-cholinesterase, where  $\pi$ -cation interactions between their substrates and specific active site residues were the major determinant for substrate binding and specificity (185-188).

The X-ray crystallographic data of choline oxidase also showed that the N $\epsilon$ 2 atom of the conserved active site residue His466 is located at a distance of  $\sim 3.3$  Å from the N(1) locus of the enzyme-bound FAD (Figure 1.28), consistent with other GMC enzymes (31, 33, 34, 39, 62, 97), and suggesting an important role of such residue in catalysis and modulation of the bound flavin as well (this hypothesis will be discussed in details in Chapter 5 and 6). Most interestingly, the X-ray structure of choline oxidase showed that another histidine residue, His310, is located at a distance of  $\sim 2.9$  Å from His466 (His466<sup>N $\delta$ 1</sup>-His310<sup>N $\delta$ 1</sup>) (Figure 1.28). Polarographic preliminary results on the enzyme obtained by substituting His310 by an alanine residue showed that the purified mutant enzyme completely lost its catalytic activity with choline as a substrate. Spectrophotometrically, CHO-H310A was still able to bind choline with the subsequent

reduction of the enzyme-bound flavin, which occurred relatively slower than that of wild-type choline oxidase (16 h vs 1 s) and in a biphasic way. These results, together with the structural information, suggest an essential role of His310 in catalysis and the modulation of the enzyme-bound flavin, which will be discussed in detail in Chapter 7.

In conclusion, the X-ray crystallographic structure of choline oxidase was resolved at 1.86 Å resolution. The overall structure of choline oxidase resembles that of PHBH as previously observed for other GMC enzymes. A covalent linkage between the His99<sup>Nε2</sup> and FAD<sup>C8M</sup> atoms was observed. The electron density maps for the FAD reveal an unusually distorted isoalloxazine ring system that can be rationalized as a C4a- or C10a-covelant adduct. The substrate choline was docked into the active site of choline oxidase structure based on the density map of DMSO, which was found in the active site structure. The resulting orientation of substrate is consistent with His351 being the active site catalytic base that abstracts the substrate hydroxyl proton during catalysis. The distance and the orientation of the Glu312, Trp331, and Phe357 to the trimethylammonium headgroup of choline are consistent with  $\pi$ -cation interactions between the quaternary ammonium moiety of the substrate and these residues. The distance between the modeled choline  $\alpha$ -carbon and flavin N5 locus was found to be  $\sim 3$  Å, consistent with hydride transfer mechanism for the oxidation of choline catalyzed by choline oxidase. This in turn, also provides structural basis for the tunneling behavior of hydride transfer.

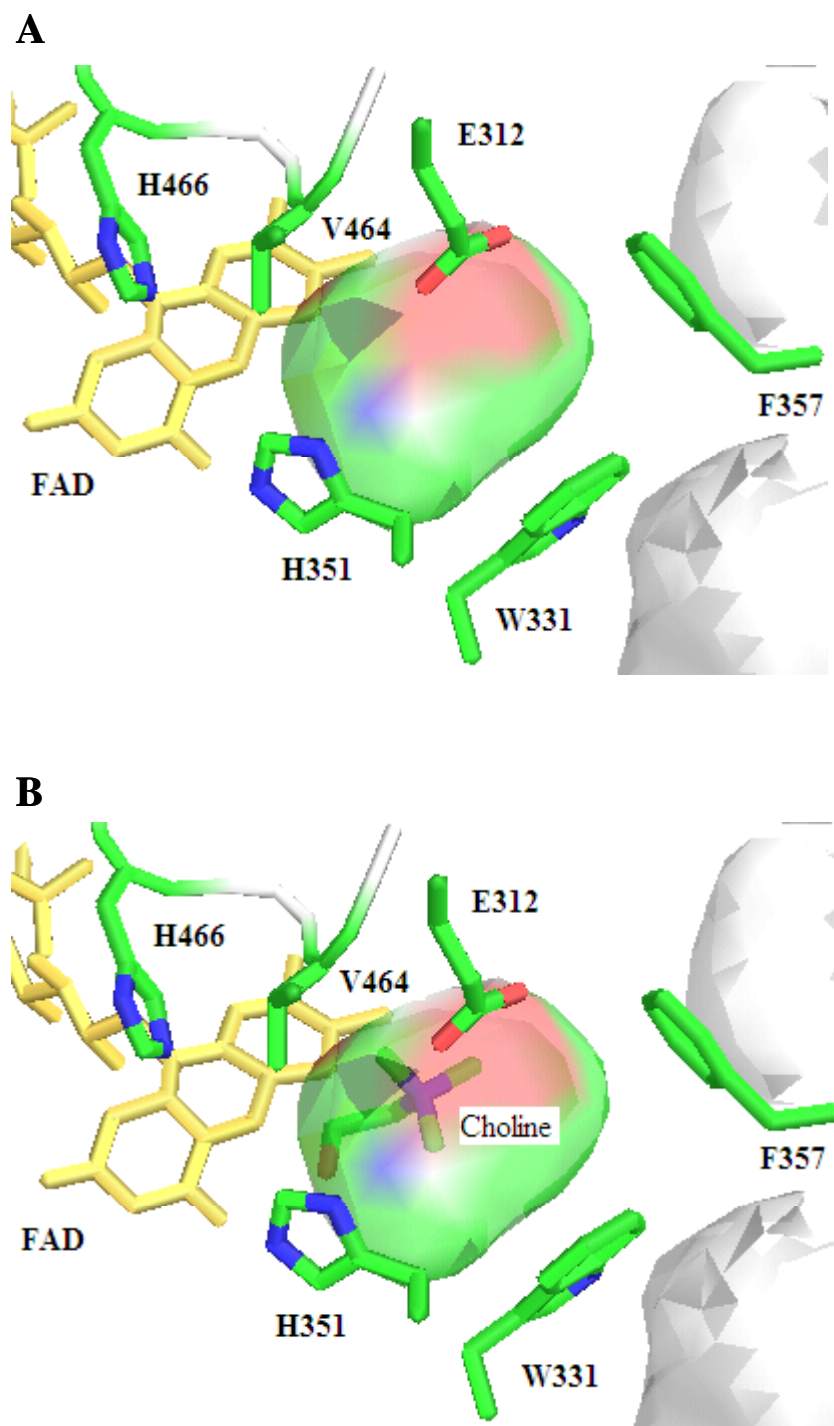


**Figure 1.27.** Active site structures of choline oxidase, showing its cavity (A) and docking with choline (B).

The important residues from the substrate- and FAD-binding domains are shown.

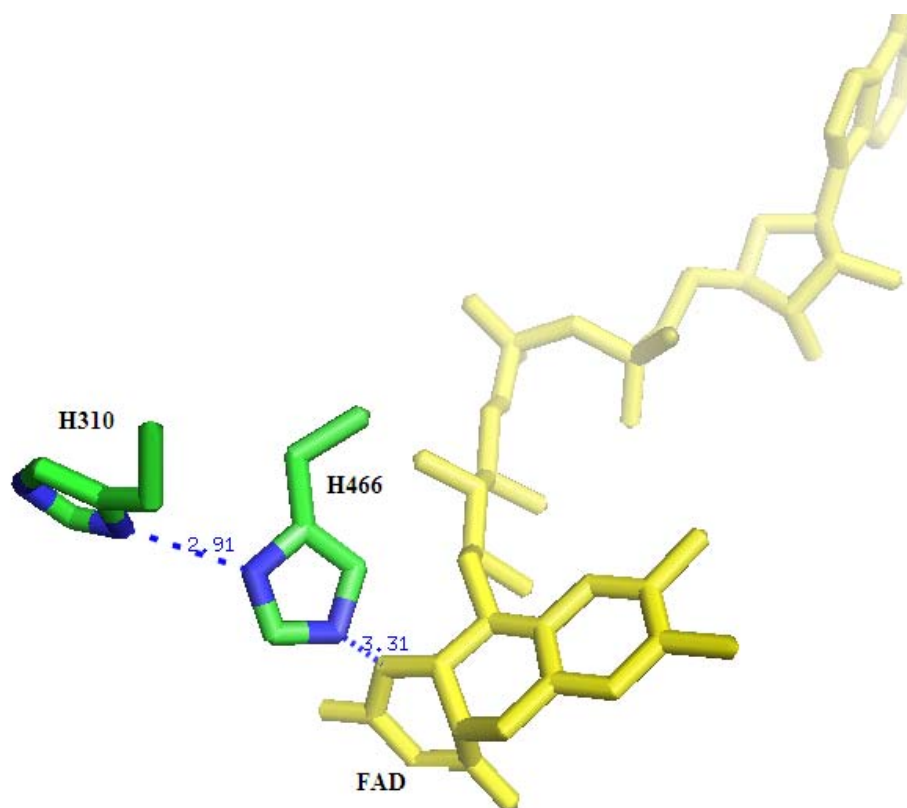
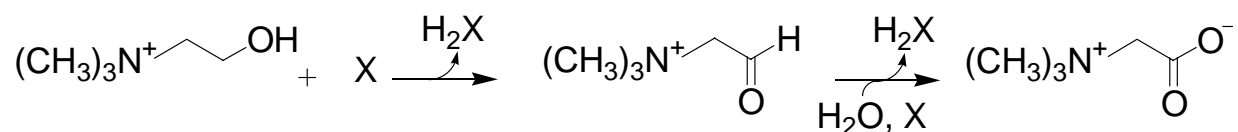


**Figure 1.28.** Active site structures of choline oxidase showing the proton-transfer network.

### 1.5. Choline Dehydrogenase

Choline dehydrogenase (E.C. 1.1.99.1) is an inner mitochondrial membrane protein that catalyzes the four-electron oxidation of choline to glycine betaine via a betaine aldehyde intermediate and requires an electron acceptor other than oxygen (103, 201, 202) (Scheme 1.14). This reaction is of considerable interest for both biomedical and biotechnological applications, because the reaction product, glycine betaine, enables tolerances towards various environmental stresses, such as hypersalinity and low and high temperatures in both transgenic plants (176-179) and pathogens (203-205) (see Section 1.6).



**Scheme 1.14.** Oxidation of choline to glycine-betaine catalyzed by choline dehydrogenase. X, Primary electron acceptor. Modified from ref. (102).

To date, no in depth biochemical or kinetic characterization has been performed on choline dehydrogenase, mainly due to the difficulty in its purification because of the instability of the enzyme *in vitro*. Although choline dehydrogenase has been grouped in the GMC flavin-dependent oxidoreductase superfamily (96), the presence of FAD as a cofactor is still ambiguous for this enzyme. Pyrroloquinoline quinone (PQQ) has been proposed to be the prosthetic group of the purified *Pseudomonas* choline dehydrogenase (103). Choline dehydrogenase has been also purified from rat liver mitochondria (201). The purified enzyme from either rat liver mitochondria or from *Pseudomonas* sp. showed to use phenazine methosulfate as a primary electron acceptor instead of oxygen (103, 201). In another study, the mitochondrial choline dehydrogenase showed a similar  $k_{\text{cat}}$  and  $K_{\text{m}}$  (0.8 mM) values with either phenazine methosulfate or ubiquinone as electron acceptors at infinite concentration (206).

Recently, we have reported the first recombinant choline dehydrogenase expressed and purified in *E. coli* by cloning the *betA* gene that codes for choline dehydrogenase from the moderate halophile *Halomonas elongata* (102). The purified enzyme showed its ability to react with either choline or betaine aldehyde as substrate with similar specificities, using phenazine methosulfate as the primary electron acceptor. Similar to the *Pseudomonas* enzyme, no evidence for the presence of FAD was observed in *H. elongata* choline dehydrogenase. The enzyme also showed ability to react with molecular oxygen as electron acceptor, but with four- to seven-fold decrease in  $k_{\text{cat}}$  values with respect to phenazine methosulfate (10.9 vs 1.5  $\mu\text{mol of O}_2/\text{min}/\text{mg}$  for choline as substrate, and 5.7 vs 1.4  $\mu\text{mol of O}_2/\text{min}/\text{mg}$  for betaine aldehyde as substrate, in 50 mM potassium phosphate, pH 7, at 25 °C), suggesting that the enzyme can act as an oxidase when electron acceptors other than molecular oxygen are not available (102).

Choline dehydrogenase from *E. coli* K12 was also cloned, and expressed in *E. coli* strain BL21(DE3) in our laboratory (Powell, N., Dissertation, Chemistry Department, Georgia State University). The recombinant enzyme was partially purified, and showed a molecular mass of ~62 kDa on SDS-PAGE. The partially purified enzyme also showed ability to react with both choline and betaine aldehyde as substrate, and to utilize either phenazine methosulfate or molecular oxygen as primary electron acceptor. The UV-visible absorbance spectrum of the purified enzyme showed absorbance maxima at ~275, ~375, and ~455 nm, as expected for a flavin-containing enzyme, but with relative intensities of the peaks in the near UV and visible regions of the spectrum suggesting that the bound flavin was present as a mixture of oxidized and anionic semiquinone states (Figure 1.29) (Powell, N., Dissertation, Chemistry Department, Georgia State University). This recombinant form choline dehydrogenase was highly unstable *in vitro*, which hindered any further biochemical and mechanistic investigations of that enzyme.

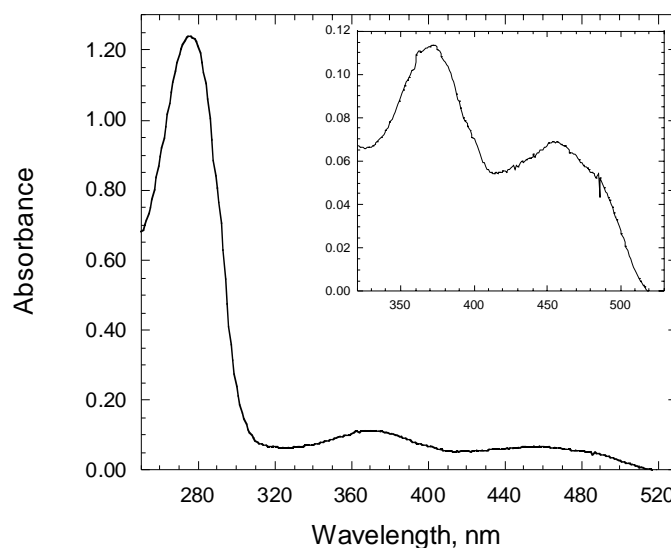


**Figure 1.29.** UV-visible absorbance spectrum of choline dehydrogenase containing a His-tag from *Escherichia coli* K 12, in air saturated 100 mM potassium phosphate, pH 7.0, at 25 °C. Taken from (Powell, N.; Dissertation, Chemistry Department, Georgia State University).

The amino acid sequence alignment comparison of choline oxidase from *A. globiformis* with choline dehydrogenase from *H. elongata* and choline dehydrogenase from *E. coli* revealed that the identities and the similarities between choline oxidase and choline dehydrogenase are 35% and 65%, respectively (Figure 1.30). The amino acid sequence alignment comparison of the two enzymes showed highly conserved residues in both the flavin binding domain and the active site of the enzymes (Figure 1.30). Due to the important roles of glycine betaine in bacterial survival under stressful environmental conditions (see Section 1.6 for details), the study of choline dehydrogenase has potential for the development of therapeutic agents that can inhibit the biosynthesis of glycine betaine in many humans' pathogenic diseases. However, due to the high insolubility and instability of choline dehydrogenase, studies of cytosolic choline oxidase, which shares ~65% similarity with choline dehydrogenase and catalyzes the same enzymatic

reaction, can shed light on the catalytic properties of choline dehydrogenase. The analysis of the sequence alignment comparison of choline oxidase with choline dehydrogenase showed that the major difference between the two proteins is limited to a short hydrophobic peptide (23 residues), which is absent in choline oxidase (Figure 1.30). This peptide might play an important role in anchoring choline dehydrogenase to the mitochondrial membrane. In addition, the crystal structure of choline oxidase showed that this region is located on the surface of the protein (Figure 1.31). Therefore, it is conceivable that a soluble and stable choline dehydrogenase might be obtained by mutagenizing choline dehydrogenase through the deletion of the nucleotides encoding for such short hydrophobic peptide.



CHO-Ag	MHIDNIENLSDRF	FDYIVVGGGSAGAAVAARLSEDP	PAVSVALVEAGPDD	RGVPEVLQ	LDR	60
CHD-He	-----MSQATE	FDYIIIGAGSAGNVLATRLTED	SDVSVLLLEAGGPDY	RFDFR	QMPA	53
CHD-Ec	-----MQFDYIIIGAGSAGNVLATRLTED	PNTSVLLLEAGGPDY	RFDFR	QMPA		49
		. . . . .	:***:::*.***. .:***:*. .** *:*** *			
CHO-Ag	WMELLESG--	YDWDYPIEPQ-ENGNSFMHARAKVMGGCSSHNSCIAFWAPRED	LDEWEA			117
CHD-He	ALAYPLQGKRYNWAFETD	PEPHMDNRRMECGRGKGLGSSSLINGMCYIRGNALDYDHWAK				113
CHD-Ec	ALAFPLQGKRYNWAFETEPEPFMNNRRMECGRGKGLGSSSLINGMCYIRGNALDLNWAQ					109
		:	* *	: *	: *	
CHO-Ag	KYGATGWNAEAAWPLYKRLETNEDAGPDAPHHGD	SGPVHLMNVPPKDPTGVALLDACEQA				177
CHD-He	QPGLEEDWYLSCLPYFKKSET-RDIGPNDYHGGD	GPVSVTPKAGNNPLYRTFIEAGKQA				172
CHD-Ec	EPGLEENWSYLDCLPYRKAET-RDMGENDYHGGD	GPVSVTTSKPGVNPLFEAMIEAGVQA				168
		: *	*	. *	::: ***. * :	**
CHO-Ag	GIPRAKFN	TGTTVVNGANFFQINRRADGTRSSSSVS	YIHPIVEQENFTLLTGLRARQLVF			237
CHD-He	GYPETEDVNGYQQE-GFGPMDRFVTPKGRRASTAR	GYLDTAKQRSNLTIETRAVTDVIEF				231
CHD-Ec	GYPRTDDLNGYQQE-GFGPMDRTVTPQGRRASTAR	GYLDQAKSRPNLTIRTHAMTDHIIF				227
		* * . . . *	. * . :	. * *::: . * . . :	*::: *	:
CHO-Ag	DADRRCTGVDIVDSAFGHTRHRLTARNEVV	LSTGAIDTPKLLMLSGIGPAAHLAEHGIEVL				297
CHD-He	EGKR-AVGVRYEQKQG--PKQARARREVLLCGGAIAS	PQILQRSVGNPEWLKELGIPV				288
CHD-Ec	DGKR-AVGVEWLEGDSTIPTRATANKEVLLCAGAIAS	PQILQRSVGNAEALLAEFDIPLV				286
		: . . *	. * :	. * . *::: . * . *::: *	. * *	:
CHO-Ag	VDSPGVGEHLQDHPEGVVQFEAKQPM	-----VAESTQWWEIG				334
CHD-He	HELPGVGENLQDHLEMYIQYECKEPTISLYPALQWYNQPKIGAEWLFG	GTGVGASNQFESC				348
CHD-Ec	HELPGVGENLQDHLEMYLQYECKEPTISLYPALQWYNQPKIGAEWLFG	GTGVGASNHFEAG				346
		:	*****:*** *	:***:***:		
CHO-Ag	IFTPTEDGLDRPDLMMHYGSVPFDMNTLRHGYPTTENG	FSLTPNVTHARSRGTVRLRSRD				394
CHD-He	GFIRSRDDEEWPNLQYHFLPIAISYNGK--SAVQA	HGFQAHVGSMSRSGRIRLTSKD				405
CHD-Ec	GFIRSRREEFAWPNIQYHFLPVAINYNGS--NAVKE	HGFQCHVGSMSRSPSRGHVRIKSRD				403
		*	: :	*::: *	: . . . . *	. . . *::: . : *::: *::: *
CHO-Ag	FRDKPMVDPRYFTDPEGHDMRVMVAGIRKAREIAAQ	PAMAEWTGRELSPGVEAQTDEELQ				454
CHD-He	PHAAPSILFNMAKEK--DWEEFRDAIRLTREIIAQ	PAFDTRYRGREISPGPDVQSDEELD				463
CHD-Ec	PHQHPAILFNYSHEQ--DWQEFRDAIRITREIMHQ	PALDQYRGREISPGVECQTDEQLD				461
		:	*	:	. *::: . . *	. . . *::: *::: *::: *::: *
CHO-Ag	DYIRKTHNTVYHPVGTVRMGAVEDEMSPLDPELRVK	GVTGLRVADASVMPEHVTVPNIT				514
CHD-He	NFVKQHAETAAYHPCGSCRMG--EGDMAVTDAQ	RGVHGLEGLRVVDASLFPVIPTGNLNAP				521
CHD-Ec	EFVRNHAETAHFPCGTCMKG--YDEMSVVDGEGRVHGLEGLRVVDAS	IMPQIITGNLNAT				519
		:::: . : . *::: *	: *::: . : *::: *::: *::: *			
CHO-Ag	VMMIGERCADLIRSARAGETTTADAELSAALA----					546
CHD-He	TIMLAEKIADRIRGREPLPRASVDYYVANGAPAKQAS					558
CHD-Ec	TIMIGEKIADMIRGQALPRSTAGYFVANGMPVRAKK					556
		. : *::: *::: ** *	. . . : . . . :			

**Figure 1.30.** Alignment of choline oxidase with choline dehydrogenase.

CHO-Ag, choline oxidase from *A. globiformis* (GenBank accession no. **AAP68832**); CHD-He, choline dehydrogenase from *Halomonas elongata* (GenBank accession no. **CAB77176**); CHD-Ec, choline dehydrogenase from *Escherichia coli* (GenBank accession no. **P17444**). *Yellow highlighted sequence*, conserved flavin binding domain; *gray highlighted sequence*, conserved active site; *cyan highlighted sequence*, site of the major differences between CHO and CHD; \*, identical residues; :, conserved substitution; ., semi-conserved substitution.

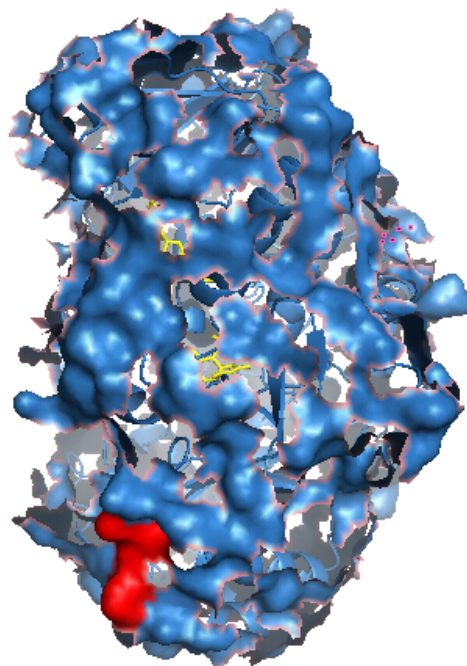


**Figure 1.31.** The surface of the monomeric structure of choline oxidase. Red highlighted residues, are Pro322, Met323, Val324, and Ala325. The FAD molecule is colored in yellow.

## 1.6. Biological Applications

The chemical reaction catalyzed by choline oxidase is of considerable interest for biotechnological and biomedical applications, because accumulation of glycine betaine in many economically relevant crop plants and human pathogens enables their stress resistance toward hyperosmotic environments (207). Therefore, the study of choline oxidase has potential for the development of therapeutic agents that inhibit the biosynthesis of glycine betaine and render pathogenic bacteria susceptible to either conventional treatments or the innate immune system, and for the improvement of water stress resistance in genetically engineered crops lacking efficient glycine betaine biosynthetic systems.

The exposure of microorganisms to high osmolality environments enhances rapid fluxes of water outside the cell, thereby resulting in dehydration and reduction in turgor of the cytoplasm. Microorganisms counteract the outflow of water from their cytoplasm by increasing the uptake of potassium ions and organic osmolytes (also called compatible solutes or osmoprotectants) to increase their intracellular solute pool and prevent the cytoplasmic outflow of water (208). Osmoprotectants are defined as exogenously provided organic solutes that promote bacterial growth under hyperosmotic environments. These compounds may act as precursors that can be enzymatically converted into compatible solutes or they may themselves be compatible solutes (207). The intracellular uptake of compatible solutes is not restricted to bacteria but is also used as a common strategy among fungi, plants, animals, and even human cells to compensate the adverse effects of high osmolality and high ionic strength (209, 210). In microorganisms, only a limited number of organic compounds serve as compatible solutes, including sugars (trehalose), free amino acids (glutamate and proline) and derivatives thereof (proline betaine and ecotine), polyols (glycerol and glucosylglycerol), and quaternary amines and

their sulfonium analogs (glycine betaine, carnitine, and dimethylsulfoniopropionate) (Figure 1.32) (207). In general, compatible solutes are highly soluble and at physiological pH their net charges are equal to zero. Compatible solutes can reach high intracellular concentration without interfering with the vital physiological functions of the cells (211). Glycine betaine (*N,N,N*-trimethylglycine) is one of the most commonly used compatible solutes that is accumulated in the cytoplasm of microorganisms to counteract hyperosmotic environments (212).

In microorganisms, the intracellular accumulation of glycine betaine is achieved either through transporters (osmotically stimulated uptake systems) that enhance the intracellular uptake of exogenous glycine betaine across the cell membrane or by endogenous intracellular biosynthetic pathways (207). In *E. coli* and *Salmonella typhimurium*, two transporters are mainly responsible for the intracellular uptake of exogenous glycine betaine across the cell membrane, ProP and ProU (Figure 1.33). The penetration of exogenous glycine betaine through the outer membrane of those two bacterial species is achieved by passive diffusion through the nonspecific porin transporters, i.e., OmpC and OmpF (Figure 1.33). The expression of porin structural genes is regulated by medium osmolality. OmpC synthesis prevails in hypertonic media, while the production of OmpF predominates under hypotonic environments (213). *E. coli* can synthesize glycine betaine by the two-step oxidation of its precursor choline catalyzed by the membrane bound choline dehydrogenase (Figure 1.33) (214). A limited number of other bacterial strains such as *A. globiformis*, *H. elongata*, *S. aureus*, and *P. aeruginosa* can also accumulate glycine betaine intracellularly by stepwise methylation of glycine (204, 215). In *Bacillus subtilis*, while the intracellular uptake of proline is controlled by the highly substrate-specific transport system OpuE (osmoprotectants uptake), the intracellular uptake of glycine betaine is controlled by 3 highly effective transporters, OpuA, OpuC, and OpuD, which enhance the exogenous uptake of

glycine betaine from the environment up to a cellular concentration level that exceed 1 M under osmotic stress conditions (Figure 1.34) (207).

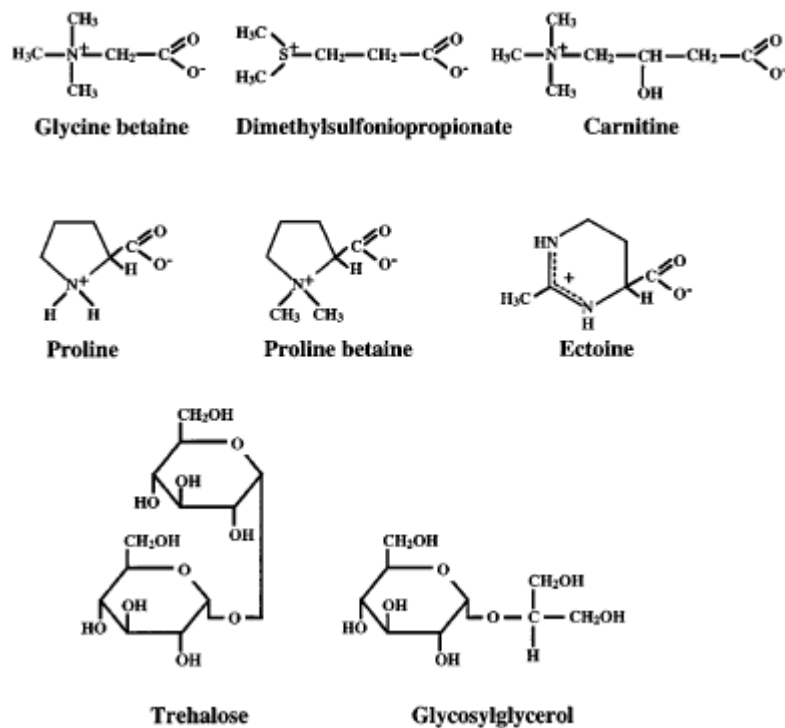


**Figure 1.32.** Structures of selected osmoprotectants.  
Taken without permission from ref. (207).

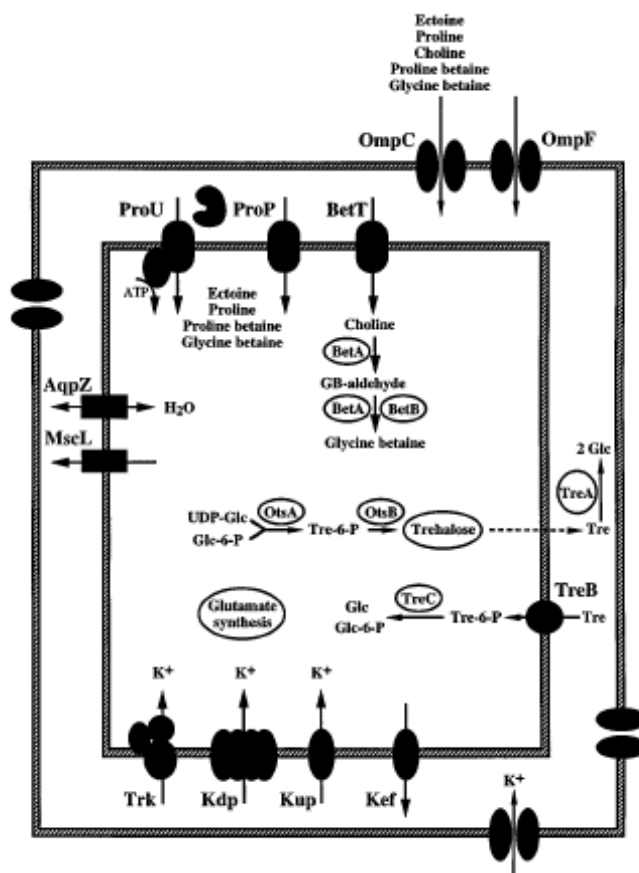


**Figure 1.33.** Osmostress response systems of *E. coli*.

*GB* glycine betaine, *Glc* glucose, *Glc-6-P* glucose-6-phosphate, *Tre* trehalose, *Tre-6-P* trehalose-6-phosphate, *UDP-Glc* uridine diphosphate-glucose. Taken without permission from ref. (207).

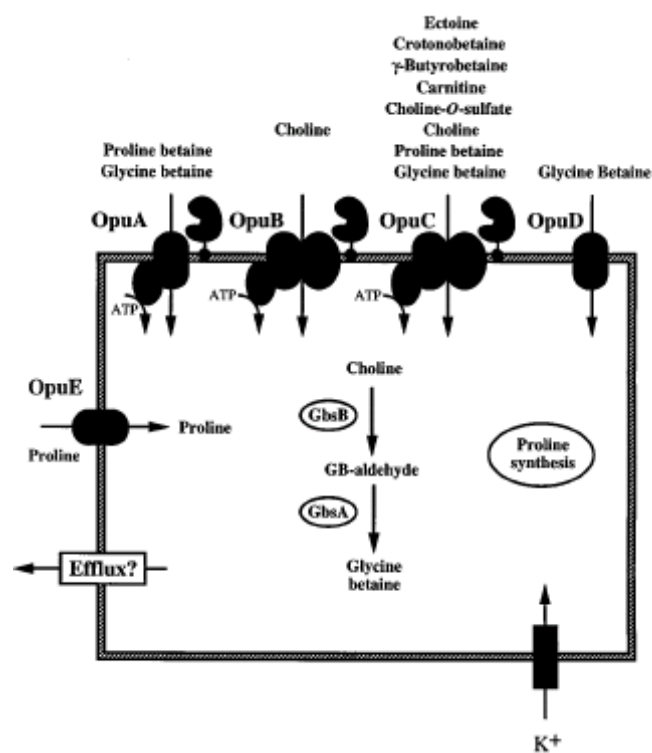


**Figure 1.34.** Osmostress response systems of *Bacillus subtilis*.  
Taken without permission from ref. (207).

### 1.6.1. Glycine Betaine as an Osmoprotectant

Glycine betaine (*N,N,N*-trimethylglycine) is a zwitterionic molecule that is widely distributed in a large variety of microorganisms, animals, and plants. The high intracellular concentration of glycine betaine does not interfere with the normal physiological functions within the cytoplasm of the cells but instead it maintains cell turgor and stabilizes the structure and function of several macromolecules (216). Consequently, the intracellular accumulation of glycine betaine enhances cells growth and proliferation under stress conditions. Glycine betaine acts as an osmoprotectant by stabilizing the highly ordered structures of proteins and membranes, particularly the quaternary structures of complex proteins (212).

The osmoprotective effects of glycine betaine on bacteria (*E. coli*) were first reported in an experiment that showed that in the presence of glycine betaine in the medium, *E. coli* can grow under inhibitory high concentration of NaCl (0.8 M) (217). Cayley *et al.* reported that the amount of glycine betaine increased monotonically in the cytoplasm of *E. coli* K12 with increasing osmolality (218). Similarly, it was observed that glycine betaine was responsible for the survival of the halophilic bacterium *Halomonas elongata* in a salinity range of 0.1-4 M NaCl (219). It has also been reported that the addition of glycine betaine can restore the depreciated growth rate of *E. coli* under high osmolality (211, 220). Such reversion of the inhibitory effect of high osmolality was also observed in other non-halophilic bacteria, such as *Bacillus subtilis*, and *Salmonella oranienburg* (221, 222).

In plants, glycine betaine has been shown to be a critical determinant of stress tolerance. The presence of glycine betaine as osmoprotectant is usually associated with enhanced growth and germination of plants in dry or saline environments (210). Moreover, the exogenous inclusion of glycine betaine has shown a significant effect on the growth and survival of a wide



range of plants under different stress conditions (178). The protective functions of glycine betaine for plants were confirmed by transforming betaine-synthesizing genes into plants that were deficient in glycine betaine. The gene that encodes for choline oxidase (*codA*), which converts choline to glycine betaine, has been the most commonly used in these transformations. The transformation of *Arabidopsis thaliana* with the *codA* gene from *Arthrobacter globiformis* resulted in a significant accumulation of glycine betaine in different organs of the transformed plants (178). The transgenic *Arabidopsis* have shown a significant tolerance to high-salt conditions (100 - 600 mM NaCl) during seed germination and during the growth of seedlings and mature plants (Figure 1.35) (178). Similarly, the imbibition and the germination of the seeds as well as the growth of the seedlings of transgenic plants showed enhanced tolerance to non-freezing low temperatures (5 °C) compared to those of wild-type plants (175, 178). In addition, the accumulation of glycine betaine in transgenic *Arabidopsis* plants resulted in a considerable tolerance to high-temperature (35-42 °C) during imbibition and germination (176). Finally, transformed *Arabidopsis thaliana* has shown a significant tolerance to high-intensity light stresses compared to wild type plants, which results from the fast recovery of the photosystem II complex from the light-induced inactivated state (177). Therefore, the accumulation of glycine betaine in many pathogens and plants enables their stress-resistance towards hyperosmotic environments.

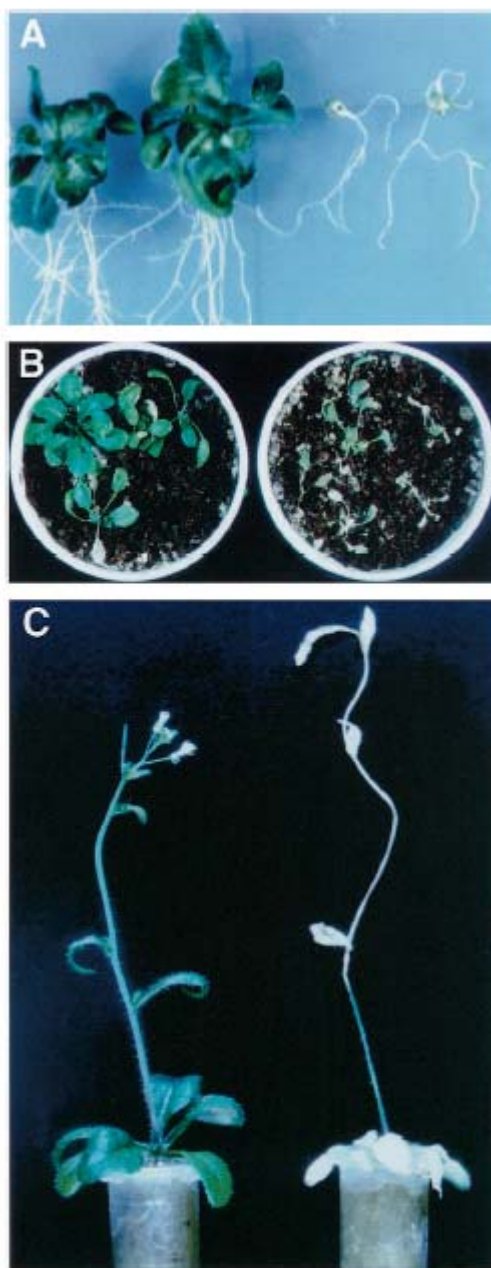


**Figure 1.35.** Enhanced tolerance of transgenic *Arabidopsis* to salt stress.

Enhanced tolerance to salt at various developmental stages of transgenic *Arabidopsis* that accumulates GB as a consequence of the introduction of the *codA* gene from *A. globiformis*. A, Seeds were germinated on gel-solidified medium supplemented with 100 mM NaCl and incubated for 20 d. The left two plants are transformed plants and the right two plants are wild type. B, Two-week-old seedlings were exposed to 600 mM NaCl for 4 h, and after transferring to normal conditions they were allowed to grow for 3 weeks. Left, Transformed plants; right, wild-type plants. C, Thirty-day-old plants were watered with 200 mM NaCl for 10 d. Left, Transformed plant; right, wild-type plant. Taken without permission from ref. (216).

### 1.6.2. Biotechnological Application of Glycine Betaine

Several economically relevant crop plants such as soybean, rice, and potato are deficient in osmoprotectants (223). As previously discussed (Section 1.6.1), several studies have strongly confirmed that glycine betaine is one of the most potent osmoprotectant in transgenic plants. Genetically engineered plants are expected to accumulate glycine betaine in their cytoplasm due to their inability to catabolize glycine betaine. Consequently, numerous studies have been carried out with the goal of genetically engineering increased stress tolerance in economically relevant crop plants (176, 177, 180, 224-226).

The introduction of betaine-producing enzymes (choline dehydrogenase) enhanced the survival of transgenic tobacco under varying salinity and temperature conditions (224). Transgenic lines of *Indica rice* have been transformed with the *codA* gene from *Arthrobacter globiformis* (227). The exposure of the genetically modified plants to salt stress (0.15 M NaCl) for one week, followed by a recovery period, showed that more than 50% of the transgenic plants could survive salt stress and set seed whereas wild-type plants failed to recover (227).

Recently, tomato plants, which normally do not accumulate glycine betaine and are susceptible to chilling stress, have been transformed with the *codA* gene from *Arthrobacter globiformis* (228). The genetically engineered plants have shown a notable improvement of chilling stress tolerance compared to wild-type plants in various developmental phases. The overall yield of the transgenic tomato plants during reproduction was enhanced by an average of 10–30% more fruit following chilling stress. It has been assumed that the increased levels of H<sub>2</sub>O<sub>2</sub> in *codA* transgenic plants, as a byproduct of choline oxidase-catalyzed glycine betaine synthesis, might activate an H<sub>2</sub>O<sub>2</sub>-inducible protective mechanism, resulting in improved chilling and oxidative tolerances in glycine betaine accumulating *codA* transgenic plants. Overall, the

introduction of a biosynthetic pathway of glycine betaine into tomato through genetic engineering is a valuable approach for improving chilling tolerance (228).

### **1.6.3. Biomedical Applications of Glycine Betaine**

The accumulation of the major osmoprotectant glycine betaine has been observed in a number of human pathogens, including *Listeria monocytogenes*, *Staphylococcus aureus*, and *Pseudomonas aeruginosa* (203, 205, 208). Hyperosmolarity is frequently encountered at human infection sites (229), where glycine betaine precursors, i.e., choline, acetylcholine, phosphatidylcholine, and phosphorylcholine, are abundant (230-232). Therefore, pathogens can employ these precursors not only to produce glycine betaine as a potent osmoprotectant, but also as carbon and nitrogen sources to survive at infectious sites.

*P. aeruginosa* is a human opportunistic microbe, which causes a variety of human systemic infections. For *P. aeruginosa*, glycine betaine does not only act as the major osmoprotectant of the pathogen, but it also serves as a metabolic intermediate as well (215). To examine the role of glycine betaine accumulation for bacterial growth under stressful infectious conditions, disulfiram was tested as an inhibitor for *P. aeruginosa* betaine aldehyde dehydrogenase (an enzyme that catalyzes the last irreversible step of glycine betaine synthesis from choline), with the goal of development of potent therapeutic agents for *P. aeruginosa* infection (215). Although *in vivo* studies are necessary before drawing any further conclusions, disulfiram totally and irreversibly inhibited the activity of betaine aldehyde dehydrogenase, suggesting a significant role for this inhibitor as an antimicrobial agent.

Several studies have shown that *L. monocytogenes*, which is causative agent of human food poisoning, can survive and tolerate a variety of environmental stress conditions due to the accumulation of glycine betaine (233, 234). The intracellular accumulation of glycine betaine in

the cytoplasm of *L. monocytogenes* enables the pathogens to tolerate not only external adverse environmental conditions such as high or low temperature prior to ingestion to host, but also the internal environment within the host with high salt concentration ranges from 0.3 to 0.7 M (205). The effects of glycine betaine accumulation on the virulence of *L. monocytogenes* were studied by mutating the glycine betaine transporter OpuC. In murine studies, the mutated pathogen showed a significant reduction in glycine betaine accumulation as well as a significant decrease of the bacterial colonies in small intestine of the host cell (205). These results strongly suggest an important role of glycine betaine synthesis in the virulence of pathogen.

*E. coli* is considered as the most frequent causative agent of human urinary tract infections. The osmolality of human urine can widely vary in a range between 0.04 to 1.4 mol/kg (235, 236). The human urinary tract experiences a wide range of pH fluctuations upon washing with urine that contains high levels of organic acid. The pH of human urine can vary between 5 to 8, depending on the nature of ingested diet (235). As a direct prove of the role of glycine betaine in enhancing the ability of *E. coli* to survive and grow in human urinary tract, glycine betaine was detected to be accumulated during the growth of *E. coli* in medium containing 1.2 M NaCl (235).

*Staphylococcus aureus* is now considered as the second most common cause (after *E. coli*) of urinary tract infection. This organism is also considered the most osmotolerant among the non-halophilic eubacteria (204). *S. aureus* has also shown its ability to withstand a wide range of osmolarity, it can grow well either at high (3.5 M NaCl) or low osmolalities, consistent with a highly developed system in regulating cytoplasmic osmolality (204). The urinary isolates of *S. aureus* accumulate glycine betaine in both the presence and absence of osmotic stress.

Unlike *E. coli*, *S. aureus* did not accumulate other betaines in presence of glycine betaine, suggesting the crucial role of glycine betaine for the survival and pathogenicity of *S. aureus* (204).

Overall, the accumulation of glycine betaine in many human pathogenic bacteria, which enables their growth and survival at human infection sites under hyperosmotic conditions, points potential of studying choline oxidase or its analog choline dehydrogenase for the development of therapeutic agents that inhibit the formation of glycine betaine and render pathogenic bacteria susceptible to either conventional treatments or the innate immune system.

## 1.7. Goals

Choline oxidase (E.C. 1.1.3.17) from *A. globiformis* is a flavin-dependent enzyme that catalyzes the four-electron oxidation of choline to glycine betaine, one of a limited number of compounds that accumulates to high levels in the cytoplasm of cells to counteract the adverse effects of hyperosmotic environments (207). The accumulation of glycine betaine has been observed in a number of human pathogenic bacteria, such as *Staphylococcus aureus*, *Mycobacterium tuberculosis*, *Pseudomonas aeruginosa*, *Listeria monocytogenes*, *Enterococcus faecalis*, *Klebsiella pneumoniae*, *Vibrio* sp. and *E. coli* O157: H7 (203-205, 208, 235, 237, 238). Osmotic stress conditions are frequently observed at human infection sites where glycine betaine precursors, i.e., choline and its analogues, are very abundant (229, 230, 232). Consequently, the study of choline oxidase or its analog choline dehydrogenase has potential for the development of therapeutic agents that inhibit the formation of glycine betaine and render pathogenic bacteria susceptible to either conventional treatments or the innate immune system. Furthermore, the recent findings that many crop plants accumulate glycine betaine in their cytoplasm in response to adverse environmental conditions, such as high or low temperature, high salts, and water deficiency, have motivated considerable interest in studying glycine betaine biosynthesis, with the objective of genetically engineering enhanced resistance towards environmental stress in economically relevant crop plants (176, 177, 180, 224-226).

Up to 2003, despite a wealth of studies on the biomedical and biotechnological applications of the enzyme, minimal biochemical and mechanistic studies on choline were reported. The biotechnological and biomedical potentials for choline oxidase require a meticulous biochemical, biophysical, kinetic, and structural characterization of the enzyme, which is the goal of this study. This study will provide a solid background for the different

biomedical and biotechnological applications of choline oxidase. It will also provide new insights for other flavoproteins that are structurally and functionally related to choline oxidase.

The biophysical, biochemical, structural, and mechanistic characterization of an enzyme usually require large quantities of the pure, active and stable form of such enzyme. Consequently, the first step in this project was aimed to clone *codA* gene that encodes for choline oxidase from *A. globiformis*. The cloned gene can then be used not only for production of enzyme, but also for the preparation of a number of mutant forms of choline oxidase to investigate the role of specific active site residues. In addition, efficient approaches for protein expression and purification, which can provide large quantities of pure and stable the enzymes, are required as well.

For a newly purified enzyme, it is important to understand firstly the different biophysical, biochemical, spectrophotometrical, kinetic, and mechanistic properties of the wild-type form prior of the further investigation of the role of specific active site residues by preparing different mutant forms of the enzyme. Thus, biophysical, biochemical, spectrophotometrical, kinetic, and mechanistic properties of the wild-type choline oxidase were studied in parallel with similar studies on selected mutant forms of the enzyme. From a structural standpoint, the X-ray crystallographic structures of most flavoprotein oxidases including choline oxidase (George Lountos, Fan Fan, Giovanni Gadda, and Allen M. Orville; unpublished results) have shown that a positively charge amino acid residue or a dipole of an  $\alpha$ -helix is oriented to the N(1)-C(2)=O locus of the enzyme-bound flavin (31-33, 35-40, 95, 183), with mechanistic implications for the modulation of flavin reactivity. While the effects of replacing the positive charge with a neutral amino acid on the flavin properties have been investigated for lactate monooxygenase (239), no studies have addressed the characterization of the flavin properties of an oxidase in which the



positive charge close to the flavin N(1) was reversed. The main goals of this study were aimed to obtain insights on the roles played by the positively charged conserved active site residue, His<sub>466</sub>, proximal to the N(1) locus of the bound flavin in choline oxidase; and for the first time to characterize a flavoprotein oxidase with a negative charge near the flavin N(1) locus. Mutant forms of choline oxidase were prepared in which the conserved active site residue, His<sub>466</sub>, was substituted with either a neutral (alanine) or a negatively charged (aspartate) amino acid, followed by the biophysical, biochemical and mechanistic characterizations of those mutant forms with respect to the wild-type choline oxidase.

Since unambiguous biochemical, structural, and mechanistic characterizations of other related flavoprotein oxidases that oxidize alcohols were hindered, the biochemical and the mechanistic studies of wild-type choline oxidase along with its active site mutants can shed light on other flavoproteins that are structurally and functionally related to choline oxidase. Interestingly, for the first time obtaining insights for flavoprotein oxidase with a negative charge near the flavin N(1) locus. From biotechnological and biomedical standpoints, these biochemical and mechanistic studies of choline oxidase will be the foundation for future rational design of efficient transition state analogs and inhibitors that could be used for the development of therapeutic agents that inhibit the formation of glycine betaine, and in turn render pathogenic bacteria susceptible to conventional treatments.

## References

- (1) Massey, V. (2000) The chemical and biological versatility of riboflavin. *Biochem. Soc. Trans.* 28, 283-96.
- (2) Ghisla, S., and Massey, V. (1986) New flavins for old: artificial flavins as active site probes of flavoproteins. *Biochem. J.* 239, 1-12.
- (3) Draper, R. D., and Ingraham, L. L. (1968) A potentiometric study of the flavin semiquinone equilibrium. *Arch. Biochem. Biophys.* 125, 802-8.
- (4) Ehrenberg, A., Müller, F., and Hemmerich, P. (1967) Basicity, visible spectra, and electron spin resonance of flavosemiquinone anions. *Eur. J. Biochem.* 2, 286-93.
- (5) Massey, V., and Palmer, G. (1966) On the existence of spectrally distinct classes of flavoprotein semiquinones. A new method for the quantitative production of flavoprotein semiquinones. *Biochemistry* 5, 3181-9.
- (6) Massey, V., and Hemmerich, P. (1980) Active-site probes of flavoproteins. *Biochem. Soc. Trans.* 8, 246-57.
- (7) Merrill, A. H., Jr., Lambeth, J. D., Edmondson, D. E., and McCormick, D. B. (1981) Formation and mode of action of flavoproteins. *Annu. Rev. Nutr.* 1, 281-317.
- (8) Ghisla, S., and Mayhew, S. G. (1976) Identification and properties of 8-hydroxyflavin--adenine dinucleotide in electron-transferring flavoprotein from *Peptostreptococcus elsdenii*. *Eur. J. Biochem.* 63, 373-90.
- (9) Mayhew, S. G., Whitfield, C. D., Ghisla, S., and Schuman-Jorns, M. (1974) Identification and properties of new flavins in electron-transferring flavoprotein from *Peptostreptococcus elsdenii* and pig-liver glycolate oxidase. *Eur. J. Biochem.* 44, 579-91.
- (10) Edmondson, D. E., Barman, B., and Tollin, G. (1972) On the importance of the N-5 position in flavin coenzymes. Properties of free and protein-bound 5-deaza analogs. *Biochemistry* 11, 1133-8.
- (11) Massey, V. (1995) Introduction: flavoprotein structure and mechanism. *Faseb J.* 9, 473-5.
- (12) Karplus, P. A., Daniels, M. J., and Herriott, J. R. (1991) Atomic structure of ferredoxin-NADP<sup>+</sup> reductase: prototype for a structurally novel flavoenzyme family. *Science* 251, 60-6.
- (13) Massey, V. (1994) Activation of molecular oxygen by flavins and flavoproteins. *J. Biol. Chem.* 269, 22459-62.

- (14) Fitzpatrick, P. F., and Massey, V. (1983) The reaction of 8-mercaptoflavins and flavoproteins with sulfite. Evidence for the role of an active site arginine in D-amino acid oxidase. *J. Biol. Chem.* 258, 9700-5.
- (15) Gadda, G., and Fitzpatrick, P. F. (1998) Biochemical and physical characterization of the active FAD-containing form of nitroalkane oxidase from *Fusarium oxysporum*. *Biochemistry* 37, 6154-64.
- (16) Gadda, G., Wels, G., Pollegioni, L., Zucchelli, S., Ambrosius, D., Pilone, M. S., and Ghisla, S. (1997) Characterization of cholesterol oxidase from *Streptomyces hygroscopicus* and *Brevibacterium sterolicum*. *Eur. J. Biochem.* 250, 369-76.
- (17) Macheroux, P., Kieweg, V., Massey, V., Soderlind, E., Stenberg, K., and Lindqvist, Y. (1993) Role of tyrosine 129 in the active site of spinach glycolate oxidase. *Eur. J. Biochem.* 213, 1047-54.
- (18) Massey, V., Ghisla, S., and Moore, E. G. (1979) 8-Mercaptoflavins as active site probes of flavoenzymes. *J. Biol. Chem.* 254, 9640-50.
- (19) Massey, V., Müller, F., Feldberg, R., Schuman, M., Sullivan, P. A., Howell, L. G., Mayhew, S. G., Matthews, R. G., and Foust, G. P. (1969) The reactivity of flavoproteins with sulfite. Possible relevance to the problem of oxygen reactivity. *J. Biol. Chem.* 244, 3999-4006.
- (20) Müller, F. (1972) On the interaction of flavins with phosphine-derivatives. *Z. Naturforsch [B]* 27, 1023-6.
- (21) Müller, F., and Massey, V. (1969) Flavin-sulfite complexes and their structures. *J. Biol. Chem.* 244, 4007-16.
- (22) Wagner, M. A., Trickey, P., Chen, Z. W., Mathews, F. S., and Jorns, M. S. (2000) Monomeric sarcosine oxidase: 1. Flavin reactivity and active site binding determinants. *Biochemistry* 39, 8813-24.
- (23) Brühmüller, M., Möhler, H., and Decker, K. (1972) Covalently bound flavin in D-6-hydroxynicotine oxidase from *Arthrobacter oxidans*. *Z. Naturforsch [B]* 27, 1073-4.
- (24) Gomez-Moreno, C., Choy, M., and Edmondson, D. E. (1979) Purification and properties of the bacterial flavoprotein: thiamin dehydrogenase. *J. Biol. Chem.* 254, 7630-5.
- (25) Ohta-Fukuyama, M., Miyake, Y., Emi, S., and Yamano, T. (1980) Identification and properties of the prosthetic group of choline oxidase from *Alcaligenes sp.* *J. Biochem. (Tokyo)* 88, 197-203.
- (26) Massey, V., and Ghisla, S. (1983) in *Biological Oxidations* (Sund, H., and Ullrich, V., Eds.) pp 114-139, Springer, Berlin.

- (27) Müller, F., Ghisla, S., and Bacher, A. (1986) in *Wasserlösliche Vitamine* (Isler, O., Brubacher, G., and Ghisla, S., Eds.), Thieme, Stuttgart.
- (28) Fraaije, M. W., and Mattevi, A. (2000) Flavoenzymes: diverse catalysts with recurrent features. *Trends Biochem. Sci.* 25, 126-32.
- (29) Trimmer, E. E., Ballou, D. P., Galloway, L. J., Scannell, S. A., Brinker, D. R., and Casas, K. R. (2005) Aspartate 120 of *Escherichia coli* Methylenetetrahydrofolate Reductase: Evidence for Major Roles in Folate Binding and Catalysis and a Minor Role in Flavin Reactivity. *Biochemistry* 44, 6809-22.
- (30) Mewies, M., Packman, L. C., Mathews, F. S., and Scrutton, N. S. (1996) Flavinylation in wild-type trimethylamine dehydrogenase and differentially charged mutant enzymes: a study of the protein environment around the N1 of the flavin isoalloxazine. *Biochem. J.* 317, 267-72.
- (31) Bannwarth, M., Bastian, S., Heckmann-Pohl, D., Giffhorn, F., and Schulz, G. E. (2004) Crystal structure of pyranose 2-oxidase from the white-rot fungus *Peniophora* sp. *Biochemistry* 43, 11683-90.
- (32) Hallberg, B. M., Henriksson, G., Pettersson, G., and Divne, C. (2002) Crystal structure of the flavoprotein domain of the extracellular flavocytochrome cellobiose dehydrogenase. *J. Mol. Biol.* 315, 421-34.
- (33) Hallberg, B. M., Leitner, C., Haltrich, D., and Divne, C. (2004) Crystal structure of the 270 kDa homotetrameric lignin-degrading enzyme pyranose 2-oxidase. *J. Mol. Biol.* 341, 781-96.
- (34) Hecht, H. J., Schomburg, D., Kalisz, H., and Schmid, R. D. (1993) The 3D structure of glucose oxidase from *Aspergillus niger*. Implications for the use of GOD as a biosensor enzyme. *Biosens Bioelectron* 8, 197-203.
- (35) Lario, P. I., Sampson, N., and Vrielink, A. (2003) Sub-atomic resolution crystal structure of cholesterol oxidase: what atomic resolution crystallography reveals about enzyme mechanism and the role of the FAD cofactor in redox activity. *J. Mol. Biol.* 326, 1635-50.
- (36) Lindqvist, Y., and Branden, C. I. (1989) The active site of spinach glycolate oxidase. *J. Biol. Chem.* 264, 3624-8.
- (37) Mattevi, A., Vanoni, M. A., Todone, F., Rizzi, M., Teplyakov, A., Coda, A., Bolognesi, M., and Curti, B. (1996) Crystal structure of D-amino acid oxidase: a case of active site mirror-image convergent evolution with flavocytochrome  $b_2$ . *Proc. Natl. Acad. Sci. U S A* 93, 7496-501.
- (38) Vrielink, A., Lloyd, L. F., and Blow, D. M. (1991) Crystal structure of cholesterol oxidase from *Brevibacterium sterolicum* refined at 1.8 Å resolution. *J. Mol. Biol.* 219, 533-54.

- (39) Wohlfahrt, G., Witt, S., Hendle, J., Schomburg, D., Kalisz, H. M., and Hecht, H. J. (1999) 1.8 and 1.9 Å resolution structures of the *Penicillium amagasakiense* and *Aspergillus niger* glucose oxidases as a basis for modelling substrate complexes. *Acta Crystallogr. D. Biol. Crystallogr.* 55, 969-77.
- (40) Yue, Q. K., Kass, I. J., Sampson, N. S., and Vrielink, A. (1999) Crystal structure determination of cholesterol oxidase from *Streptomyces* and structural characterization of key active site mutants. *Biochemistry* 38, 4277-86.
- (41) Swoboda, B. E., and Massey, V. (1966) On the reaction of the glucose oxidase from *Aspergillus niger* with bisulfite. *J. Biol. Chem.* 241, 3409-16.
- (42) Macheroux, P., Massey, V., Thiele, D. J., and Volokita, M. (1991) Expression of spinach glycolate oxidase in *Saccharomyces cerevisiae*: purification and characterization. *Biochemistry* 30, 4612-9.
- (43) Massey, V., Curti, B., and Ganther, H. (1966) A temperature-dependent conformational change in D-amino acid oxidase and its effect on catalysis. *J. Biol. Chem.* 241, 2347-57.
- (44) Ghanem, M., Fan, F., Francis, K., and Gadda, G. (2003) Spectroscopic and kinetic properties of recombinant choline oxidase from *Arthrobacter globiformis*. *Biochemistry* 42, 15179-88.
- (45) Yorita, K., Misaki, H., Palfey, B. A., and Massey, V. (2000) On the interpretation of quantitative structure-function activity relationship data for lactate oxidase. *Proc. Natl. Acad. Sci. U S A* 97, 2480-5.
- (46) Müller, F., Hemmerich, P., and Ehrenberg, A. (1968) Light absorption of flavosemiquinone metal chelates. *Eur. J. Biochem.* 5, 158-64.
- (47) Fan, F., Ghanem, M., and Gadda, G. (2004) Cloning, sequence analysis, and purification of choline oxidase from *Arthrobacter globiformis*: a bacterial enzyme involved in osmotic stress tolerance. *Arch. Biochem. Biophys.* 421, 149-58.
- (48) Ohta, M., Miura, R., Yamano, T., and Miyake, Y. (1983) Spectroscopic studies on the photoreaction of choline oxidase, a flavoprotein, with covalently bound flavin. *J. Biochem. (Tokyo)* 94, 879-92.
- (49) Rand, T., Halkier, T., and Hansen, O. C. (2003) Structural characterization and mapping of the covalently linked FAD cofactor in choline oxidase from *Arthrobacter globiformis*. *Biochemistry* 42, 7188-94.
- (50) Claiborne, A., Massey, V., Fitzpatrick, P. F., and Schopfer, L. M. (1982) 2-Thioflavins as active site probes of flavoproteins. *J. Biol. Chem.* 257, 174-82.
- (51) Massey, V., Claiborne, A., Biemann, M., and Ghisla, S. (1984) 4-Thioflavins as active site probes of flavoproteins. General properties. *J. Biol. Chem.* 259, 9667-78.

- (52) Schopfer, L. M., Massey, V., and Claiborne, A. (1981) Active site probes of flavoproteins. Determination of the solvent accessibility of the flavin position 8 for a series of flavoproteins. *J. Biol. Chem.* 256, 7329-37.
- (53) Binda, C., Coda, A., Angelini, R., Federico, R., Ascenzi, P., and Mattevi, A. (1999) A 30-angstrom-long U-shaped catalytic tunnel in the crystal structure of polyamine oxidase. *Structure* 7, 265-76.
- (54) Fraaije, M. W., van den Heuvel, R. H., van Berkel, W. J., and Mattevi, A. (1999) Covalent flavinylation is essential for efficient redox catalysis in vanillyl-alcohol oxidase. *J. Biol. Chem.* 274, 35514-20.
- (55) de Jong, E., van Berkel, W. J., van der Zwan, R. P., and de Bont, J. A. (1992) Purification and characterization of vanillyl-alcohol oxidase from *Penicillium simplicissimum*. A novel aromatic alcohol oxidase containing covalently bound FAD. *Eur. J. Biochem.* 208, 651-7.
- (56) Zanetti, G., Massey, V., and Curti, B. (1983) FAD analogues as mechanistic and 'binding-domain' probes of spinach ferredoxin-NADP<sup>+</sup> reductase. *Eur. J. Biochem.* 132, 201-5.
- (57) Zanetti, G., Beretta, C., and Malandra, D. (1986) Properties of rabbit liver glutathione reductase reconstituted with FAD analogs. *Arch. Biochem. Biophys.* 244, 831-7.
- (58) Rowland, P., Björnberg, O., Nielsen, F. S., Jensen, K. F., and Larsen, S. (1998) The crystal structure of *Lactococcus lactis* dihydroorotate dehydrogenase A complexed with the enzyme reaction product throws light on its enzymatic function. *Protein Sci.* 7, 1269-79.
- (59) Björnberg, O., Rowland, P., Larsen, S., and Jensen, K. F. (1997) Active site of dihydroorotate dehydrogenase A from *Lactococcus lactis* investigated by chemical modification and mutagenesis. *Biochemistry* 36, 16197-205.
- (60) Sobrado, P., Daubner, S. C., and Fitzpatrick, P. F. (2001) Probing the relative timing of hydrogen abstraction steps in the flavocytochrome *b*<sub>2</sub> reaction with primary and solvent deuterium isotope effects and mutant enzymes. *Biochemistry* 40, 994-1001.
- (61) Xia, Z. X., and Mathews, F. S. (1990) Molecular structure of flavocytochrome *b*<sub>2</sub> at 2.4 Å resolution. *J. Mol. Biol.* 212, 837-63.
- (62) Hecht, H. J., Kalisz, H. M., Hendle, J., Schmid, R. D., and Schomburg, D. (1993) Crystal structure of glucose oxidase from *Aspergillus niger* refined at 2.3 Å resolution. *J. Mol. Biol.* 229, 153-72.
- (63) Hofsteenge, J., Vereijken, J. M., Weijer, W. J., Beintema, J. J., Wierenga, R. K., and Drenth, J. (1980) Primary and tertiary structure studies of *p*-hydroxybenzoate hydroxylase from *Pseudomonas fluorescens*. Isolation and alignment of the CNBr

- peptides; interactions of the protein with flavin adenine dinucleotide. *Eur. J. Biochem.* 113, 141-50.
- (64) Schulz, G. E., Schirmer, R. H., and Pai, E. F. (1982) FAD-binding site of glutathione reductase. *J. Mol. Biol.* 160, 287-308.
  - (65) Wierenga, R. K., Drenth, J., and Schulz, G. E. (1983) Comparison of the three-dimensional protein and nucleotide structure of the FAD-binding domain of *p*-hydroxybenzoate hydroxylase with the FAD- as well as NADPH-binding domains of glutathione reductase. *J. Mol. Biol.* 167, 725-39.
  - (66) Burnett, R. M., Darling, G. D., Kendall, D. S., LeQuesne, M. E., Mayhew, S. G., Smith, W. W., and Ludwig, M. L. (1974) The structure of the oxidized form of clostridial flavodoxin at 1.9-Å resolution. *J. Biol. Chem.* 249, 4383-92.
  - (67) Ghisla, S., Massey, V., and Yagi, K. (1986) Preparation and some properties of 6-substituted flavins as active site probes for flavin enzymes. *Biochemistry* 25, 3282-9.
  - (68) Schöllnhammer, G., and Hemmerich, P. (1974) Nucleophilic addition at the photoexcited flavin cation: synthesis and properties of 6- and 9-hydroxy-flavocoenzyme chromophores. *Eur. J. Biochem.* 44, 561-77.
  - (69) Mayhew, S. G., Foust, G. P., and Massey, V. (1969) Oxidation-reduction properties of flavodoxin from *Peptostreptococcus elsdenii*. *J. Biol. Chem.* 244, 803-10.
  - (70) Kearney, E. B., and Singer, T. P. (1955) On the prosthetic group of succinic dehydrogenase. *Biochim. Biophys. Acta.* 17, 596-7.
  - (71) Singer, T. P., Kearney, E. B., and Massey, V. (1956) Observations on the flavin moiety of succinic dehydrogenase. *Arch. Biochem. Biophys.* 60, 255-7.
  - (72) Singer, T. P., Kearney, E. B., and Zastrow, N. (1955) Isolation and properties of succinic dehydrogenase. *Biochim. Biophys. Acta.* 17, 154-5.
  - (73) Williamson, G., and Edmondson, D. E. (1985) Effect of pH on oxidation-reduction potentials of 8  $\alpha$ -*N*-imidazole-substituted flavins. *Biochemistry* 24, 7790-7.
  - (74) Edmondson, D. E., and De Francisco, R. (1992) structure, synthesis, and physical properties of covalently bound flavins and 6- and 8-hydroxyflavins, in *Chemistry and Biochemistry of Flavoenzymes* (Muller, F., Ed.) pp 73-103, CRC Press, Boca Raton, Florida.
  - (75) Motteran, L., Pilone, M. S., Molla, G., Ghisla, S., and Pollegioni, L. (2001) Cholesterol oxidase from *Brevibacterium sterolicum*. The relationship between covalent flavinylation and redox properties. *J. Biol. Chem.* 276, 18024-30.

- (76) Efimov, I., Cronin, C. N., and McIntire, W. S. (2001) Effects of noncovalent and covalent FAD binding on the redox and catalytic properties of *p*-cresol methylhydroxylase. *Biochemistry* 40, 2155-66.
- (77) Yang, C. C., Packman, L. C., and Scrutton, N. S. (1995) The primary structure of *Hyphomicrobium* X dimethylamine dehydrogenase. Relationship to trimethylamine dehydrogenase and implications for substrate recognition. *Eur. J. Biochem.* 232, 264-71.
- (78) Kenney, W. C., Singer, T. P., Fukuyama, M., and Miyake, Y. (1979) Identification of the covalently bound flavin prosthetic group of cholesterol oxidase. *J. Biol. Chem.* 254, 4689-90.
- (79) Kenney, W. C., Edmondson, D. E., and Seng, R. L. (1976) Identification of the covalently bound flavin of thiamin dehydrogenase. *J. Biol. Chem.* 251, 5386-90.
- (80) Edmondson, D. E., and Kenney, W. C. (1976) Identification and properties of 8 $\alpha$ -(N(1)-histidyl)-riboflavin: the flavin component of thiamine dehydrogenase and beta-cyclopiasonate oxidocyclase. *Biochem. Biophys. Res. Commun.* 68, 242-8.
- (81) Kenney, W. C., Edmondson, D. E., Singer, T. P., Nishikimi, M., Noguchi, E., and Yagi, K. (1979) Identification of the covalently-bound flavin of L-galactonolactone oxidase from yeast. *FEBS Lett.* 97, 40-2.
- (82) Ohishi, N., and Yagi, K. (1979) Covalently bound flavin as prosthetic group of choline oxidase. *Biochem. Biophys. Res. Commun.* 86, 1084-8.
- (83) Cole, S. T. (1982) Nucleotide sequence coding for the flavoprotein subunit of the fumarate reductase of *Escherichia coli*. *Eur. J. Biochem.* 122, 479-84.
- (84) Wittwer, A. J., and Wagner, C. (1981) Identification of the folate-binding proteins of rat liver mitochondria as dimethylglycine dehydrogenase and sarcosine dehydrogenase. Purification and folate-binding characteristics. *J. Biol. Chem.* 256, 4102-8.
- (85) Walker, W. H., and Singer, T. P. (1970) Identification of the covalently bound flavin of succinate dehydrogenase as 8- $\alpha$ -(histidyl) flavin adenine dinucleotide. *J. Biol. Chem.* 245, 4224-5.
- (86) Brandsch, R., and Bichler, V. (1991) Autoflavinylation of apo6-hydroxy-D-nicotine oxidase. *J. Biol. Chem.* 266, 19056-62.
- (87) Singer, T. P., and McIntire, W. S. (1984) Covalent attachment of flavin to flavoproteins: occurrence, assay, and synthesis. *Methods Enzymol.* 106, 369-78.
- (88) Kim, J., Fuller, J. H., Kuusk, V., Cunane, L., Chen, Z. W., Mathews, F. S., and McIntire, W. S. (1995) The cytochrome subunit is necessary for covalent FAD attachment to the flavoprotein subunit of *p*-cresol methylhydroxylase. *J. Biol. Chem.* 270, 31202-9.



- (89) Kearney, E. B., Salach, J. I., Walker, W. H., Seng, R., and Singer, T. P. (1971) Structure of the covalently bound flavin of monoamine oxidase. *Biochem. Biophys. Res. Commun.* 42, 490-6.
- (90) Nagy, J., and Salach, J. I. (1981) Identity of the active site flavin-peptide fragments from the human "A"-form and the bovine "B"-form of monoamine oxidase. *Arch. Biochem. Biophys.* 208, 388-94.
- (91) Wagner, M. A., Khanna, P., and Jorns, M. S. (1999) Structure of the flavocoenzyme of two homologous amine oxidases: monomeric sarcosine oxidase and N-methyltryptophan oxidase. *Biochemistry* 38, 5588-95.
- (92) Mewies, M., McIntire, W. S., and Scrutton, N. S. (1998) Covalent attachment of flavin adenine dinucleotide (FAD) and flavin mononucleotide (FMN) to enzymes: the current state of affairs. *Protein Sci.* 7, 7-20.
- (93) Khanna, P., and Jorns, M. S. (2003) Tautomeric rearrangement of a dihydroflavin bound to monomeric sarcosine oxidase or N-methyltryptophan oxidase. *Biochemistry* 42, 864-9.
- (94) Mauch, L., Bichler, V., and Brandsch, R. (1990) Lysine can replace arginine 67 in the mediation of covalent attachment of FAD to histidine 71 of 6-hydroxy-D-nicotine oxidase. *J. Biol. Chem.* 265, 12761-2.
- (95) Trickey, P., Wagner, M. A., Jorns, M. S., and Mathews, F. S. (1999) Monomeric sarcosine oxidase: structure of a covalently flavinylated amine oxidizing enzyme. *Structure Fold Des.* 7, 331-45.
- (96) Cavener, D. R. (1992) GMC oxidoreductases. A newly defined family of homologous proteins with diverse catalytic activities. *J. Mol. Biol.* 223, 811-4.
- (97) Li, J., Vrielink, A., Brick, P., and Blow, D. M. (1993) Crystal structure of cholesterol oxidase complexed with a steroid substrate: implications for flavin adenine dinucleotide dependent alcohol oxidases. *Biochemistry* 32, 11507-15.
- (98) Sampson, N. S., and Vrielink, A. (2003) Cholesterol oxidases: a study of nature's approach to protein design. *Acc. Chem. Res.* 36, 713-22.
- (99) Hallberg, B. M., Henriksson, G., Pettersson, G., Vasella, A., and Divne, C. (2003) Mechanism of the reductive half-reaction in cellobiose dehydrogenase. *J. Biol. Chem.* 278, 7160-6.
- (100) De Koker, T. H., Mozuch, M. D., Cullen, D., Gaskell, J., and Kersten, P. J. (2004) Isolation and purification of pyranose 2-oxidase from *Phanerochaete chrysosporium* and characterization of gene structure and regulation. *Appl. Environ. Microbiol.* 70, 5794-800.
- (101) Menon, V., Hsieh, C. T., and Fitzpatrick, P. F. (1995) Substituted alcohols as mechanistic probes of alcohol oxidase. *Bioorg. Chem.* 23, 42-53.

- (102) Gadda, G., and McAllister-Wilkins, E. E. (2003) Cloning, Expression, and Purification of Choline Dehydrogenase from the Moderate Halophile *Halomonas elongata*. *Appl. Environ. Microbiol.* 69, 2126-32.
- (103) Russell, R., and Scopes, R. K. (1994) Use of hydrophobic chromatography for purification of the membrane-located choline dehydrogenase from a *Pseudomonas* strain. *Bioseparation* 4, 279-84.
- (104) Bright, H. J., and Gibson, Q. H. (1967) The oxidation of 1-deuterated glucose by glucose oxidase. *J. Biol. Chem.* 242, 994-1003.
- (105) Kass, I. J., and Sampson, N. S. (1998) Evaluation of the role of His447 in the reaction catalyzed by cholesterol oxidase. *Biochemistry* 37, 17990-8000.
- (106) Kass, I. J., and Sampson, N. S. (1998) The important of Glu361 position in the reaction catalyzed by cholesterol oxidase. *Bioorg. Med. Chem. Lett.* 8, 2663-8.
- (107) Crueger, A., and Crueger, W. (1990) Glucose-transforming enzymes, in *Microbial Enzyme and Biotechnology* (Fogarty, W. M., and Kelly, C. T., Eds.) pp 177-277, Elsevier Applied Science, London and New York.
- (108) Kusai, K., Sekuzu, I., Hagihara, B., Okunuki, K., Yamauchi, S., and Nakai, M. (1960) Crystallization of glucose oxidase from *Penicillium amagasakiense*. *Biochim. Biophys. Acta* 40, 555-7.
- (109) Pazur, J. H., and Kleppe, K. (1964) The Oxidation Of Glucose And Related Compounds By Glucose Oxidase From *Aspergillus Niger*. *Biochemistry* 3, 578-83.
- (110) Swoboda, B. E., and Massey, V. (1965) Purification And Properties Of The Glucose Oxidase From *Aspergillus Niger*. *J. Biol. Chem.* 240, 2209-15.
- (111) Kiess, M., Hecht, H. J., and Kalisz, H. M. (1998) Glucose oxidase from *Penicillium amagasakiense*. Primary structure and comparison with other glucose-methanol-choline (GMC) oxidoreductases. *Eur. J. Biochem.* 252, 90-9.
- (112) Kalisz, H. Z., Hendle, J., and Schmid, R. D. (1997) Structural and biochemical properties of glycosylated and deglycosylated glucose oxidase from *Penicillium amagasakiense*. *Appl. Microbiol. Biotechnol.* 47, 502-7.
- (113) Roth, J. P., and Klinman, J. P. (2003) Catalysis of electron transfer during activation of O<sub>2</sub> by the flavoprotein glucose oxidase. *Proc. Natl. Acad. Sci. U S A* 100, 62-7.
- (114) Sanner, C., Macheroux, P., Rüterjans, H., Müller, F., and Bacher, A. (1991) <sup>15</sup>N- and <sup>13</sup>C-NMR investigations of glucose oxidase from *Aspergillus niger*. *Eur. J. Biochem.* 196, 663-72.

- (115) Yin, Y., Sampson, N. S., Vrielink, A., and Lario, P. I. (2001) The presence of a hydrogen bond between asparagine 485 and the pi system of FAD modulates the redox potential in the reaction catalyzed by cholesterol oxidase. *Biochemistry* 40, 13779-87.
- (116) Gibson, Q. H., Swoboda, B. E., and Massey, V. (1964) Kinetics and Mechanism of Action of Glucose Oxidase. *J. Biol. Chem.* 239, 3927-34.
- (117) Weibel, M. K., and Bright, H. J. (1971) The glucose oxidase mechanism. Interpretation of the pH dependence. *J. Biol. Chem.* 246, 2734-44.
- (118) Fitzpatrick, P. F. (2001) Substrate Dehydrogenation by Flavoproteins. *Acc. Chem. Res.* 34, 299-307.
- (119) Brooks, C. J., and Smith, A. G. (1975) Cholesterol oxidase. Further studies of substrate specificity in relation to the analytical characterisation of steroids. *J. Chromatogr.* 112, 499-511.
- (120) Kamei, T., Takiguchi, Y., Suzuki, H., Matsuzaki, M., and Nakamura, S. (1978) Purification of 3 $\beta$ -hydroxysteroid oxidase of *Streptomyces violascens* origin by affinity chromatography on cholesterol. *Chem. Pharm. Bull. (Tokyo)* 26, 2799-2804.
- (121) Smith, A. G., and Brooks, C. J. (1975) Studies of the substrate specificity of cholesterol oxidase from *Nocardia erythropolis* in the oxidation of 3-hydroxy steroids. *Biochem. Soc. Trans.* 3, 675-7.
- (122) Pollegioni, L., Gadda, G., Ambrosius, D., Ghisla, S., and Pilone, M. S. (1999) Cholesterol oxidase from *Streptomyces hygroscopicus* and *Brevibacterium sterolicum*: effect of surfactants and organic solvents on activity. *Biotechnol. Appl. Biochem.* 30, 27-33.
- (123) Henriksson, G., Johansson, G., and Pettersson, G. (2000) A critical review of cellobiose dehydrogenases. *J. Biotechnol.* 78, 93-113.
- (124) Bao, W., Usha, S. N., and Renganathan, V. (1993) Purification and characterization of cellobiose dehydrogenase, a novel extracellular hemoflavoenzyme from the white-rot fungus *Phanerochaete chrysosporium*. *Arch. Biochem. Biophys.* 300, 705-13.
- (125) Li, B., Nagalla, S. R., and Renganathan, V. (1996) Cloning of a cDNA encoding cellobiose dehydrogenase, a hemoflavoenzyme from *Phanerochaete chrysosporium*. *Appl. Environ. Microbiol.* 62, 1329-35.
- (126) Henriksson, G., Pettersson, G., Johansson, G., Ruiz, A., and Uzcategui, E. (1991) Cellobiose oxidase from *Phanerochaete chrysosporium* can be cleaved by papain into two domains. *Eur. J. Biochem.* 196, 101-6.
- (127) Hallberg, B. M., Bergfors, T., Backbro, K., Pettersson, G., Henriksson, G., and Divne, C. (2000) A new scaffold for binding haem in the cytochrome domain of the extracellular flavocytochrome cellobiose dehydrogenase. *Structure* 8, 79-88.

- (128) Rotsaert, F. A., Renganathan, V., and Gold, M. H. (2003) Role of the flavin domain residues, His689 and Asn732, in the catalytic mechanism of cellobiose dehydrogenase from *Phanerochaete chrysosporium*. *Biochemistry* 42, 4049-56.
- (129) Giffhorn, F. (2000) Fungal pyranose oxidase: occurrence, properties and biotechnical applications in carbohydrate chemistry. *Appl. Microbiol. Biotechnol.* 54, 727-40.
- (130) Volc, J., Sedmera, P., Havlicek, V., Prikrylova, V., and Daniel, G. (1995) Conversion of D-glucose to D-erythro-hexose-2,3-diulose (2,3-diketo-D-glucose) by enzyme preparations from basidiomycete *Oudemansiella mucida*. *Carbohydr. Res.* 278, 59-70.
- (131) Freimund, S., Huwig, A., Giffhorn, F., and Kopper, S. (1998) Rare keto-aldehydes from enzymatic oxidation: substrate and oxidation products of pyranose 2-oxidase. *Chem. Eur. J.* 4, 2442-55.
- (132) Leitner, C., Volc, J., and Haltrich, D. (2001) Purification and characterization of pyranose oxidase from the white rot fungus *Trametes multicolor*. *Appl. Environ. Microbiol.* 67, 3636-44.
- (133) Halada, P., Leitner, C., Sedmera, P., Haltrich, D., and Volc, J. (2003) Identification of the covalent flavin adenine dinucleotide-binding region in pyranose 2-oxidase from *Trametes multicolor*. *Anal. Biochem.* 314, 235-42.
- (134) Fan, F., and Gadda, G. (2005) On the catalytic mechanism of choline oxidase. *J. Am. Chem. Soc.* 127, 2067-74.
- (135) Fan, F., and Gadda, G. (2005) Oxygen- and temperature-dependent kinetic isotope effects in choline oxidase: correlating reversible hydride transfer with environmentally enhanced tunneling. *J. Am. Chem. Soc.* 127, 17954-61.
- (136) Fan, F., Germann, M. W., and Gadda, G. (2006) Mechanistic studies of choline oxidase with betaine aldehyde and its isosteric analogue 3,3-dimethylbutyraldehyde. *Biochemistry* 45, 1979-86.
- (137) Ghanem, M., and Gadda, G. (2005) On the catalytic role of the conserved active site residue His466 of choline oxidase. *Biochemistry* 44, 893-904.
- (138) Ghanem, M., and Gadda, G. (2006) Effects of reversing the protein positive charge in proximity of the N(1)-flavin locus of choline oxidase. *Biochemistry* 45, 3437-47.
- (139) Vrielink, A., and Sampson, N. (2003) Sub-Ångstrom resolution enzyme X-ray structures: is seeing believing? *Curr. Opin. Struct. Biol.* 13, 709-15.
- (140) Fitzpatrick, P. F. (2004) Carbanion versus hydride transfer mechanisms in flavoprotein-catalyzed dehydrogenations. *Bioorg. Chem.* 32, 125-39.

- (141) Schreuder, H. A., Hol, W. G., and Drenth, J. (1988) Molecular modeling reveals the possible importance of a carbonyl oxygen binding pocket for the catalytic mechanism of *p*-hydroxybenzoate hydroxylase. *J. Biol. Chem.* 263, 3131-6.
- (142) Schreuder, H. A., van der Laan, J. M., Hol, W. G., and Drenth, J. (1988) Crystal structure of *p*-hydroxybenzoate hydroxylase complexed with its reaction product 3,4-dihydroxybenzoate. *J. Mol. Biol.* 199, 637-48.
- (143) Mattevi, A., Fraaije, M. W., Coda, A., and van Berkel, W. J. (1997) Crystallization and preliminary X-ray analysis of the flavoenzyme vanillyl-alcohol oxidase from *Penicillium simplicissimum*. *Proteins* 27, 601-3.
- (144) Mattevi, A., Fraaije, M. W., Mozzarelli, A., Olivi, L., Coda, A., and van Berkel, W. J. (1997) Crystal structures and inhibitor binding in the octameric flavoenzyme vanillyl-alcohol oxidase: the shape of the active-site cavity controls substrate specificity. *Structure* 5, 907-20.
- (145) Stenberg, K., Clausen, T., Lindqvist, Y., and Macheroux, P. (1995) Involvement of Tyr24 and Trp108 in substrate binding and substrate specificity of glycolate oxidase. *Eur. J. Biochem.* 228, 408-16.
- (146) Stenberg, K., and Lindqvist, Y. (1997) Three-dimensional structures of glycolate oxidase with bound active-site inhibitors. *Protein Sci.* 6, 1009-15.
- (147) Barber, M. J., Neame, P. J., Lim, L. W., White, S., and Matthews, F. S. (1992) Correlation of x-ray deduced and experimental amino acid sequences of trimethylamine dehydrogenase. *J. Biol. Chem.* 267, 6611-9.
- (148) Fox, K. M., and Karplus, P. A. (1994) Old yellow enzyme at 2 Å resolution: overall structure, ligand binding, and comparison with related flavoproteins. *Structure* 2, 1089-105.
- (149) Lindqvist, Y. (1989) Refined structure of spinach glycolate oxidase at 2 Å resolution. *J. Mol. Biol.* 209, 151-66.
- (150) Lindqvist, Y., and Branden, C. I. (1980) Structure of glycolate oxidase from spinach at a resolution of 5.5 Å. *J. Mol. Biol.* 143, 201-11.
- (151) Ghisla, S., and Massey, V. (1989) Mechanisms of flavoprotein-catalyzed reactions. *Eur. J. Biochem.* 181, 1-17.
- (152) Sobrado, P., and Fitzpatrick, P. F. (2003) Solvent and primary deuterium isotope effects show that lactate CH and OH bond cleavages are concerted in Y254F flavocytochrome *b*<sub>2</sub>, consistent with a hydride transfer mechanism. *Biochemistry* 42, 15208-14.
- (153) Appleby, C. A., and Morton, R. K. (1954) Crystalline cytochrome *b*<sub>2</sub> and lactic dehydrogenase of yeast. *Nature* 173, 749-52.

- (154) Cunane, L. M. (2002) Crystallographic study of the recombinant flavin-binding domain of baker's yeast *favocytochrome b<sub>2</sub>*: Comparison with the intact wild type enzyme. *Biochemistry* 41, 4264-72.
- (155) Jacq, C., and Lederer, F. (1974) Cytochrome *b<sub>2</sub>* from bakers' yeast (L-lactate dehydrogenase). A double-headed enzyme. *Eur. J. Biochem.* 41, 311-20.
- (156) Gaume, B., Sharp, R. E., Manson, F. D., Chapman, S. K., Reid, G. A., and Lederer, F. (1995) Mutation to glutamine of histidine 373, the catalytic base of flavocytochrome *b<sub>2</sub>* (L-lactate dehydrogenase). *Biochimie* 77, 621-30.
- (157) Schell, M. J., Molliver, M. E., and Snyder, S. H. (1995) D-serine, an endogenous synaptic modulator: localization to astrocytes and glutamate-stimulated release. *Proc. Natl. Acad. Sci. U S A* 92, 3948-52.
- (158) Wolosker, H., Blackshaw, S., and Snyder, S. H. (1999) Serine racemase: a glial enzyme synthesizing D-serine to regulate glutamate-N-methyl-D-aspartate neurotransmission. *Proc. Natl. Acad. Sci. U S A* 96, 13409-14.
- (159) Molla, G., Porrini, D., Job, V., Motteran, L., Vegezzi, C., Campaner, S., Pilone, M. S., and Pollegioni, L. (2000) Role of arginine 285 in the active site of *Rhodotorula gracilis* D-amino acid oxidase. A site-directed mutagenesis study. *J. Biol. Chem.* 275, 24715-21.
- (160) Hersh, L. B., and Jorns, M. S. (1975) Use of 5-deazaFAD to study hydrogen transfer in the D-amino acid oxidase reaction. *J. Biol. Chem.* 250, 8728-34.
- (161) Walsh, C. T., Schonbrunh, A., and Abeles, R. H. (1971) Studies on the mechanism of action of D-amino acid oxidase evidence for removal of substrate  $\alpha$ -hydrogen as a proton. *J. Biol. Chem.* 246, 6855-66.
- (162) Miura, R., and Miyake, Y. (1987) <sup>13</sup>C-NMR studies of porcine kidney D-amino acid oxidase reconstituted with <sup>13</sup>C-enriched flavin adenine dinucleotide. Effects of competitive inhibitors. *J. Biochem. (Tokyo)* 101, 581-9.
- (163) Mizutani, H., Miyahara, I., Hirotsu, K., Nishina, Y., Shiga, K., Setoyama, C., and Miura, R. (1996) Three-dimensional structure of porcine kidney D-amino acid oxidase at 3.0 Å resolution. *J. Biochem. (Tokyo)* 120, 14-7.
- (164) Umhau, S., Pollegioni, L., Molla, G., Diederichs, K., Welte, W., Pilone, M. S., and Ghisla, S. (2000) The X-ray structure of D-amino acid oxidase at very high resolution identifies the chemical mechanism of flavin-dependent substrate dehydrogenation. *Proc. Natl. Acad. Sci. U S A* 97, 12463-8.
- (165) Van den Berghe-Snorek, S., and Stankovich, M. T. (1985) Thermodynamic control of D-amino acid oxidase by benzoate binding. *J. Biol. Chem.* 260, 3373-9.

- (166) Denu, J. M., and Fitzpatrick, P. F. (1994) Intrinsic primary, secondary, and solvent kinetic isotope effects on the reductive half-reaction of D-amino acid oxidase: evidence against a concerted mechanism. *Biochemistry* 33, 4001-7.
- (167) Denu, J. M., and Fitzpatrick, P. F. (1994) pH and kinetic isotope effects on the oxidative half-reaction of D-amino-acid oxidase. *J. Biol. Chem.* 269, 15054-9.
- (168) Denu, J. M., and Fitzpatrick, P. F. (1992) pH and kinetic isotope effects on the reductive half-reaction of D-amino acid oxidase. *Biochemistry* 31, 8207-15.
- (169) Tilocca, A., Gamba, A., Vanoni, M. A., and Fois, E. (2002) First-principles molecular dynamics investigation of the D-amino acid oxidative half-reaction catalyzed by the flavoenzyme D-amino acid oxidase. *Biochemistry* 41, 14111-21.
- (170) Mann, P. J. G., Woodward, H. E., and Quastel, J. H. (1938) Hepatic oxidation of choline and arsenocholine. *Biochem. J.* 32, 1024-32.
- (171) Bernheim, F., and Bernheim, M. L. C. (1938) The choline oxidase of liver. *Am. J. Physiol.* 121, 55-60.
- (172) Ikuta, S., Imamura, S., Misaki, H., and Horiuti, Y. (1977) Purification and characterization of choline oxidase from *Arthrobacter globiformis*. *J. Biochem. (Tokyo)* 82, 1741-9.
- (173) Ikuta, S., Matuura, K., Imamura, S., Misaki, H., and Horiuti, Y. (1977) Oxidative pathway of choline to betaine in the soluble fraction prepared from *Arthrobacter globiformis*. *J. Biochem. (Tokyo)* 82, 157-63.
- (174) Edmondson, D. E., Kenney, W. C., and Singer, T. P. (1976) Structural elucidation and properties of 8 alpha-(N1-histidyl)riboflavin: the flavin component of thiamine dehydrogenase and beta-cyclopiazonate oxidocyclase. *Biochemistry* 15, 2937-45.
- (175) Alia, Hayashi, H., Chen, T., and Murata, N. (1998) Transformation with a gene for choline oxidase enhances the cold tolerance of *Arabidopsis* during germination and early growth. *Plant Cell Environ.* 21, 232-39.
- (176) Alia, Hayashi, H., Sakamoto, A., and Murata, N. (1998) Enhancement of the tolerance of *Arabidopsis* to high temperatures by genetic engineering of the synthesis of glycinebetaine. *Plant J.* 16, 155-61.
- (177) Alia, Kondo, Y., Sakamoto, A., Nonaka, H., Hayashi, H., Saradhi, P. P., Chen, T. H., and Murata, N. (1999) Enhanced tolerance to light stress of transgenic *Arabidopsis* plants that express the *codA* gene for a bacterial choline oxidase. *Plant Mol. Biol.* 40, 279-88.
- (178) Hayashi, H., Alia, Mustardy, L., Deshnum, P., Ida, M., and Murata, N. (1997) Transformation of *Arabidopsis thaliana* with the *codA* gene for choline oxidase; accumulation of glycinebetaine and enhanced tolerance to salt and cold stress. *Plant J.* 12, 133-42.

- (179) He, P. M., Zhang, D. B., Liang, W. Q., Yao, Q. H., and Zhang, R. X. (2001) Expression of Choline Oxidase Gene (*codA*) Enhances Salt Tolerance of the Tobacco. *Sheng Wu Hua Xue Yu Sheng Wu Wu Li Xue Bao (Shanghai)* 33, 519-24.
- (180) Deshnum, P., Los, D. A., Hayashi, H., Mustardy, L., and Murata, N. (1995) Transformation of *Synechococcus* with a gene for choline oxidase enhances tolerance to salt stress. *Plant Mol. Biol.* 29, 897-907.
- (181) Gadda, G. (2003) Kinetic mechanism of choline oxidase from *Arthrobacter globiformis*. *Biochim. Biophys. Acta* 1646, 112-8.
- (182) Gadda, G. (2003) pH and deuterium kinetic isotope effects studies on the oxidation of choline to betaine-aldehyde catalyzed by choline oxidase. *Biochim. Biophys. Acta* 1650, 4-9.
- (183) Hecht HJ, K. H., Hendle J, Schmid RD, Schomburg D. (1993) Crystal structure of glucose oxidase from *Aspergillus niger* refined at 2.3 Å resolution. *J. Mol. Biol.* 229, 153-172.
- (184) Gadda, G., Powell, N. L., and Menon, P. (2004) The trimethylammonium headgroup of choline is a major determinant for substrate binding and specificity in choline oxidase. *Arch. Biochem. Biophys.* 430, 264-73.
- (185) Harel, M., Kryger, G., Rosenberry, T. L., Mallender, W. D., Lewis, T., Fletcher, R. J., Guss, J. M., Silman, I., and Sussman, J. L. (2000) Three-dimensional structures of *Drosophila melanogaster* acetylcholinesterase and of its complexes with two potent inhibitors. *Protein Sci.* 9, 1063-72.
- (186) Pomponi, M., Sacchi, S., Colella, A., Patamia, M., and Marta, M. (1998) The role of TRP84 in catalytic power and the specificity of AChE. *Biophys. Chem.* 72, 239-46.
- (187) Kwak, B. Y., Zhang, Y. M., Yun, M., Heath, R. J., Rock, C. O., Jackowski, S., and Park, H. W. (2002) Structure and Mechanism of CTP: Phosphocholine Cytidylyltransferase (LicC) from *Streptococcus pneumoniae*. *J. Biol. Chem.* 277, 4343-50.
- (188) Martin, S. F., Follows, B. C., Hergenrother, P. J., and Trotter, B. K. (2000) The choline binding site of phospholipase C (*Bacillus cereus*): insights into substrate specificity. *Biochemistry* 39, 3410-5.
- (189) Hecht, H. J., Kalisz, H. M., Hendle, J., Schmid, R. D., and Schomburg, D. (1993) Crystal structure of glucose oxidase from *Aspergillus niger* refined at 2.3 Å resolution. *J. Mol. Biol.* 229, 153-172.
- (190) Hecht, H. J., Schomburg, D., Kalisz, H., and Schmid, R. D. (1993) The 3D structure of glucose oxidase from *Aspergillus niger*. Implications for the use of GOD as a biosensor enzyme. *Biosens. Bioelectron.* 8, 197-203.



- (191) Wohlfahrt, G., Witt, S., Hendle, J., Schomburg, D., Kalisz, H. M., and Hecht, H. J. (1999) 1.8 and 1.9 Å resolution structures of the *Penicillium amagasakiense* and *Aspergillus niger* glucose oxidases as a basis for modelling substrate complexes. *Acta Crystallogr. D. Biol. Crystallogr.* 55, 969-977.
- (192) Hallberg, B. M., Leitner, C., Haltrich, D., and Divne, C. (2004) Crystal structure of the 270 kDa homotetrameric lignin-degrading enzyme pyranose 2-oxidase. *J Mol Biol* 341, 781-96.
- (193) Sampson, N. S., Kass, I. J., and Ghoshroy, K. B. (1998) Assessment of the role of an omega loop of cholesterol oxidase: a truncated loop mutant has altered substrate specificity. *Biochemistry* 37, 5770-8.
- (194) Dixon, D. A., Lindner, D. L., Branchaud, B., and Lipscomb, W. N. (1979) Conformations and electronic structures of oxidized and reduced isoalloxazine. *Biochemistry* 18, 5770-5.
- (195) Fraaije, M. W., and Mattevi, A. (2000) Flavoenzymes: diverse catalysts with recurrent features. *Trends Biochem. Sci.* 25, 126-132.
- (196) Zheng, Y.-J., and Ornstein, R. L. (1996) A Theoretical Study of the Structures of Flavin in Different Oxidation and Protonation States. *J. Am. Chem. Soc.* 118, 9402-9408.
- (197) Kemal, C., and Bruice, T. C. (1976) The chemistry of an N5-methyl-1,5-dihydroflavin and its aminium cation radical. *J. Am. Chem. Soc.* 98, 3955-64.
- (198) Kemal, C., and Bruice, T. C. (1976) Simple synthesis of a 4a-hydroperoxy adduct of a 1,5-dihydroflavine: preliminary studies of a model for bacterial luciferase. *Proc. Natl. Acad. Sci. USA* 73, 995-9.
- (199) Su, Q., and Klinman, J. P. (1999) Nature of oxygen activation in glucose oxidase from *Aspergillus niger*: the importance of electrostatic stabilization in superoxide formation. *Biochemistry* 38, 8572-81.
- (200) Yin, Y., Liu, P., Anderson, R. G., and Sampson, N. S. (2002) Construction of a catalytically inactive cholesterol oxidase mutant: investigation of the interplay between active site-residues glutamate 361 and histidine 447. *Arch. Biochem. Biophys.* 402, 235-42.
- (201) Tsuge, H., Nakano, Y., Onishi, H., Futamura, Y., and Ohashi, K. (1980) A novel purification and some properties of rat liver mitochondrial choline dehydrogenase. *Biochim. Biophys. Acta* 614, 274-84.
- (202) De Ridder, J. J., and van Dam, K. (1973) The efflux of betaine from rat-liver mitochondria, a possible regulating step in choline oxidation. *Biochim. Biophys. Acta* 291, 557-63.

- (203) Peddie, B. A., Chambers, S. T., and Lever, M. (1996) Is the ability of urinary tract pathogens to accumulate glycine betaine a factor in the virulence of pathogenic strains? *J. Lab. Clin. Med.* 128, 417-22.
- (204) Peddie, B. A., Wong-She, J., Randall, K., Lever, M., and Chambers, S. T. (1998) Osmoprotective properties and accumulation of betaine analogues by *Staphylococcus aureus*. *FEMS Microbiol. Lett.* 160, 25-30.
- (205) Sleator, R. D., Wouters, J., Gahan, C. G. M., Abee, T., and Hill, C. (2001) Analysis of the role of OpuC, an osmolyte transport system, in salt tolerance and virulence potential of *Listeria monocytogenes*. *Appl. Environ. Microbiol.* 67, 2692-8.
- (206) Barrett, M. C., and Dawson, A. P. (1975) The reaction of choline dehydrogenase with some electron acceptors. *Biochem. J.* 151, 677-83.
- (207) Kempf, B., and Bremer, E. (1998) Uptake and synthesis of compatible solutes as microbial stress responses to high-osmolality environments. *Arch. Microbiol.* 170, 319-30.
- (208) Landfald, B., and Strom, A. R. (1986) Choline-glycine betaine pathway confers a high level of osmotic tolerance in *Escherichia coli*. *J. Bacteriol.* 165, 849-55.
- (209) Burg, M. B., Kwon, E. D., and Kultz, D. (1997) Regulation of gene expression by hypertonicity. *Annu. Rev. Physiol.* 59, 437-55.
- (210) Rhodes, D., and Hanson, A. D. (1993) Quaternary ammonium and tertiary sulfonium compounds in higher plants. *Annu. Rev. Plant Physiol. Plant Mol. Biol.* 115, 1541-8.
- (211) Record, M. T., Jr., Courtenay, E. S., Cayley, D. S., and Guttman, H. J. (1998) Responses of *E. coli* to osmotic stress: large changes in amounts of cytoplasmic solutes and water. *Trends Biochem. Sci.* 23, 143-8.
- (212) Gorham, J. (1995) Betaines in Higher Plants - Biosynthesis and Role in Stress Metabolism, in *Amino Acids and their Derivatives in Higher Plants* (Wallsgrave, R. M., Ed.) pp 171-203, Cambridge University Press, Cambridge.
- (213) Pratt, L. A., Hsing, W., Gibson, K. E., and Silhavy, T. J. (1996) From acids to *osmZ*: multiple factors influence synthesis of the OmpF and OmpC porins in *Escherichia coli*. *Mol. Microbiol.* 20, 911-7.
- (214) Lamark, T., Kaasen, I., Eshoo, M. W., Falkenberg, P., McDougall, J., and Strom, A. R. (1991) DNA sequence and analysis of the *bet* genes encoding the osmoregulatory choline-glycine betaine pathway of *Escherichia coli*. *Mol. Microbiol.* 5, 1049-64.
- (215) Velasco-Garcia, R., Chacon-Aguilar, V. M., Hervet-Hernandez, D., and Munoz-Clares, R. A. (2003) Inactivation of betaine aldehyde dehydrogenase from *Pseudomonas aeruginosa* and *Amaranthus hypochondriacus* L. leaves by disulfiram. *Chem. Biol. Interact.* 143, 149-58.

- (216) Sakamoto, A., and Murata, N. (2001) The use of bacterial choline oxidase, a glycinebetaine-synthesizing enzyme, to create stress-resistant transgenic plants. *Plant Physiol.* 125, 180-8.
- (217) Le Rudulier, D., Strom, A. R., Dandekar, A. M., Smith, L. T., and Valentine, R. C. (1984) Molecular biology of osmoregulation. *Science* 224, 1064-8.
- (218) Cayley, S., and Record, M. T. J. (2003) Roles of cytoplasmic osmolytes, water, and crowding in the response of *Escherichia coli* to osmotic stress: Biophysical basis of osmoprotection by glycine betaine. *Biochemistry* 42, 12596-609.
- (219) Canovas, D., Vargas, C., Kneip, S., Moron, M. J., Ventosa, A., Bremer, E., and Nieto, J. J. (2000) Genes for the synthesis of the osmoprotectant glycine betaine from choline in the moderately halophilic bacterium *Halomonas elongata* DSM 3043, USA. *Microbiology* 146 ( Pt 2), 455-63.
- (220) Houssin, C., Eynard, N., Shechter, E., and Ghazi, A. (1991) Effect of osmotic pressure on membrane energy-linked functions in *Escherichia coli*. . *Biochim. Biophys. Acta.* 1056.
- (221) Bremer, E., and Kramer, R. (2000) Coping with osmotic challenges: osmoregulation through accumulation and release of compatible solutes in bacteria, in *Bacterial stress responses*, (Storz, G., and Hengge-Aronis, R., Eds.), ASM Press, Washington, D. C.
- (222) Galinski, E. A. (1995) Osmoadaptation in bacteria. *Adv. Microb. Physiol.* 37, 273-328.
- (223) McNeil, S. D., Nuccio, M. L., and Hanson, A. D. (1999) Betaine and related osmoprotectants. Targets for metabolic engineering of stress resistance. . *Plant Physiol.* 120, 945-9.
- (224) Holmstrom, K. O., Somersalo, S., Mandal, A., Palva, T. E., and Welin, B. (2000) Improved tolerance to salinity and low temperature in transgenic tobacco producing glycine betaine. *J. Exp. Bot.* 51, 177-85.
- (225) Sakamoto, A., Alia, Murata, N., and Murata, A. (1998) Metabolic engineering of rice leading to biosynthesis of glycinebetaine and tolerance to salt and cold. *Plant Mol. Biol.* 38, 1011-9.
- (226) Sakamoto, A., Valverde, R., Alia, Chen, T. H., and Murata, N. (2000) Transformation of *Arabidopsis* with the *codA* gene for choline oxidase enhances freezing tolerance of plants. *Plant J.* 22, 449-53.
- (227) Mohanty, A., Kathuria, H., Ferjani, A., Sakamoto, A., Mohanty, P., Murata, N., and Tyagi, A. K. (2002) Transgenics of an elite indica rice variety *Pusa Basmati 1* harbouring the *codA* gene are highly tolerant to salt stress. *Theor. Appl. Genet.* 106, 51-57.
- (228) Park, E. J., Jeknic, Z., Sakamoto, A., DeNoma, J., Yuwansiri, R., Murata, N., and Chen, T. H. (2004) Genetic engineering of glycinebetaine synthesis in tomato protects seeds, plants, and flowers from chilling damage. *Plant J* 40, 474-87.

- (229) Kilbourne, J. P. (1978) Bacterial content and ionic composition of sputum in cystic fibrosis. *Lancet* *i*, 334.
- (230) Pesin, S. R., and Candia, O. A. (1982) Acetylcholine concentration and its role in ionic transport by the corneal epithelium. *Invest. Ophthalmol. Vis. Sci.* *22*, 651-9.
- (231) Rennick, B. R. (1981) Renal tubule transport of organic ions. *Am. J. Physiol.* *240*, F83-9.
- (232) Wright, J. R., and Clements, J. A. (1987) Metabolism and turnover of lung surfactant. *Am. Rev. Respir. Dis.* *136*, 426-44.
- (233) Ko, R., Smith, L. T., and Smith, G. M. (1994) Glycine betaine confers enhanced osmotolerance and cryotolerance on *Listeria monocytogenes*. *J. Bacteriol.* *176*, 426-31.
- (234) Patchett, R. A., Kelly, A. F., and Kroll, R. G. (1994) Effect of sodium chloride on the intracellular solute pools of *Listeria monocytogenes*. *Appl. Environ. Microbiol.* *58*, 3959-63.
- (235) Kunin, C. M., and Chambers, S. T. (1989) Osmoprotective properties for bacteria of renal papilla and urine: role of betaines as osmoprotectant molecules., in *Host-parasite interactions in urinary tract infections*. (Kass, E., and Svanborg Eden, C., Eds.) pp 327-32, University of Chicago Press, Chicago, IL.
- (236) Ross, D. L., and Neely, A. E. (1983) *Textbook of urinalysis and bodily fluids*, Appleton-Century-Crofts, Corwalk, CN.
- (237) Graham, J. E., and Wilkinson, B. J. (1992) *Staphylococcus aureus* Osmoregulation: Role for choline, glycine betaine, proline, and taurin. *J. Bacteriol.* *174*, 2711-6.
- (238) Pichereau, V., Bourot, S., Flahaut, S., Blanco, C., Auffray, Y., and Bernard, T. (1999) The osmoprotectant glycine betaine inhibits salt-induced cross- tolerance towards lethal treatment in *Enterococcus faecalis*. *Microbiology* *145*, 427-35.
- (239) Müh, U., Massey, V., and Williams, C. H., Jr. (1994) Lactate monooxygenase. I. Expression of the mycobacterial gene in *Escherichia coli* and site-directed mutagenesis of lysine 266. *J. Biol. Chem.* *269*, 7982-8.

## CHAPTER II

### Material and Methods

#### Materials

*Escherichia coli* strain JM109 harboring plasmid pGAH/*codA* was a kind gift from Dr. Murata, National Institute for Basic Biology, Okazaki, Japan (1, 2). A freeze-dried culture of *Arthrobacter globiformis* (ATCC 8010) was obtained from American Type Culture Collection. Restriction endonucleases *Nde* I and *EcoR* I, calf intestinal alkaline phosphatase, T4 DNA ligase, *Taq* DNA polymerase, deoxynucleotide triphosphates, and bovine serum albumin were purchased from Promega. Cloned *Pfu* DNA polymerase, *DpnI*, and *E. coli* strain XL1-Blue were obtained from Stratagene (La Jolla, CA). *Bgl* II, *BamH* I, and *Hind* III were from New England Biolab. Luria-Bertani agar, Luria-Bertani broth, chloramphenicol, tetracycline, kanamycin, isopropyl- $\beta$ -D-thiogalactopyranoside (IPTG), lysozyme, sodium hydrosulfite (dithionite), sodium sulfite, phenylmethylsulfonyl fluoride (PMSF), and betaine aldehyde bromide were obtained from Sigma-Aldrich (St. Louis, MO). Carbenicillin, ampicillin, choline chloride, and electrophoresis-grade agar were purchased from ICN Biomedicals (Aurora, OH). Nutrient Broth and Nutrient Agar #3 were from Difco. 1,2- $^2\text{H}_4$ -Choline bromide was from Isotec Inc. (Miamisburg, OH). Deuterium oxide ( $\text{D}_2\text{O}$ ) was from Cambridge Isotope Laboratories Inc. (Andover, MA). All other reagents were of the highest purity commercially available. Oligonucleotides were custom synthesized on a Beckman Oligo model 1000 M by the DNA Core Facility of the Biology Department of Georgia State University, or by Sigma Genosys (The Woodlands, TX).

*A. globiformis* genomic DNA was purified using the DNeasy midi-kit from Qiagen (Valencia, CA). Plasmids and products deriving from primer extension reaction and PCR were

purified by using QIAprep Spin Miniprep kit from Qiagen. *E. coli* strains Novablue and Rosetta(DE3)pLysS were from Novagen (Madison, WI). *E. coli* strain Novablue cells harboring plasmid pET/*codA1* or pET/*codA2*, strain XL1-Blue cells harboring plasmid pET/*codA3*, and strain Rosetta(DE3)pLysS cells harboring plasmid pET/*codA1* or pET/*codA3* were stored at  $-80^{\circ}\text{C}$  as 7% DMSO suspensions. *E. coli* MKH13 harboring pJB004 was a kind gift from Dr. Erhard Bremer (Philipps Universität, Marburg, Germany). DNA sequencing was carried out with an Applied Biosystems Big Dye kit on an Applied Biosystems model ABI 377 DNA sequencer by the DNA Core Facility of the Biology Department of Georgia State University.

### **Instruments**

UV-visible absorbance spectra were recorded using an Agilent Technologies diode-array spectrophotometer model HP 8453 equipped with a thermostated water bath. Fluorescence emission spectra were recorded with a Shimadzu Spectrofluorometer model RF-5301 PC thermostated at  $15^{\circ}\text{C}$ . Circular dichroism spectra were acquired using a Jasco J-810 spectropolarimeter at  $5^{\circ}\text{C}$ . Enzyme activity was measured polarographically by monitoring the rate of oxygen consumption with a Hansatech oxygen electrode (HansaTech Oxy-32) thermostated at  $25^{\circ}\text{C}$ . Rapid kinetics was carried out on a Hi-Tech 61 SF-DX2 Double mixing stopped-flow spectrophotometer thermostated at  $25^{\circ}\text{C}$ .

### **Subcloning and cloning of *codA***

*E. coli* strain JM109 harboring plasmid pGAH/*codA* was grown on Luria-Bertani agar medium containing kanamycin at a final concentration of  $15\text{ }\mu\text{g/ml}$  for 16 h at  $37^{\circ}\text{C}$ . Single colonies were used to inoculate 2 ml of Luria-Bertani broth medium containing kanamycin ( $15\text{ }\mu\text{g/ml}$ ) and the resulting liquid cultures were grown at  $37^{\circ}\text{C}$  for 7 h. After harvesting the cells by centrifugation at  $14,000 \times g$  for 10 min, the plasmid vector was isolated by using a QIAquick

Spin Miniprep kit (Qiagen) following the manufacturer's protocol. The isolated plasmid DNA was then used for primer extension reaction of the *codA* gene encoding for choline oxidase by using the oligonucleotide primers Chox-for A and Chox-rev containing *NdeI* and *EcoR* I restriction endonuclease sites designed to anneal to the 5' and 3' ends of the gene, respectively (Table 2.1). The *NdeI* and *EcoR* I restriction sites introduced at the 5' ends of the sense and antisense primers allowed cloning of *codA* into the corresponding sites of pET20b(+). Primer extension reaction was performed in the presence of DMSO at a final concentration of 2% for 1 min at 95 °C, followed by 31 three-step cycles of 0.5 min at 95 °C, 1 min at 55 °C, 4.5 min at 68 °C, with a final 5-min step at 68 °C, in a total volume of 50 µl by using ~15 ng of template DNA, 2.5 U of *Pfu* DNA polymerase, and the manufacturer's suggested protocol. The resulting amplicons were purified by agarose gel electrophoresis using the QIAquick Gel Extraction kit (Qiagen) following the manufacturer's protocol.

**Table 2.1.** Oligonucleotide primers used for primer extension amplification and PCR of *codA*, as well as the mutagenesis for pET/*codA*

Primer	Nucleotide sequence	Purpose
ChoxforA	CGGCAAGGAGAACC <u>C</u> ATATGCACATCGACAACATCTG	Cloning
Choxrev	CCCCGGAATTCGCCGCTCCCGCTTAGG	Cloning
PET-for a	CACTATAGGGAGACCACAACG	Sequencing
PET-revA	GCTTATGCTAGTTATTGCTCAGC	Sequencing
Choxag 3	CAATGAAGTCGTGCTCTCC	Sequencing
Choxag 5	CGAAGTTCAACACC	Sequencing
Choxag 7	CGATGCAGGAGTTGTGG	Sequencing
Cho-H466Af	CAACACCGTCTACG <u>C</u> CCCCGTGGGCACCGTGC	Mutagenesis
Cho-H466Ar	CACGGTGCCACGCGGGG <u>C</u> GTAGACGGTGTTGTGC	Mutagenesis
Cho-H466Df	CAACACCGTCTACG <u>A</u> CCCCGTGGGCACCGTGC	Mutagenesis
Cho-H466Dr	CACGGTGCCACGCGGGT <u>C</u> GTAGACGGTGTTGTGC	Mutagenesis
Cho-H310Af	CGAGCACCTGCAGGACG <u>C</u> CCCCGGAAGGCGTGG	Mutagenesis
Cho-H310Ar	GCACCACGCCTTCCGGGG <u>G</u> CGTCCTGCAGGTGCTCGCC	Mutagenesis
Cho-H310Df	GGGCGAGCACCTGCAGGACG <u>A</u> CCCCGGAAGGCGTGGTGC	Mutagenesis
Cho-H310Dr	GCACCACGCCTTCCGGGT <u>C</u> GTCTGCAGGTGCTCGCC	Mutagenesis
Cho-H310Nf	GGGCGAGCACCTGCAGGACA <u>A</u> CCCCGGAAGGCGTGGTGC	Mutagenesis
Cho-H310Nr	GCACCACGCCTTCCGGGT <u>T</u> GTCTGCAGGTGCTCGCC	Mutagenesis
Cho-E370Af	CGGCTACCCCAACCACGGC <u>G</u> AACGGCTTCAGCC	Mutagenesis
Cho-E370Ar	GAGGCTGAAGCCGTTTCG <u>C</u> CGTGTTGGGGTAGCC	Mutagenesis
Cho-H87Af	GCAACTCCTTCATGCGC <u>G</u> CTGCCCGTGCCAAGGTC	Mutagenesis
Cho-H87Ar	CCTTGGCACGGGCAGC <u>G</u> CGCATGAAGGAGTTGC	Mutagenesis
Cho-H87Cf	GCAACTCCTTCATGCGC <u>T</u> GTGCCCGTGCCAAGGTC	Mutagenesis
Cho-H87Cr	CCTTGGCACGGGCAC <u>A</u> GCGCATGAAGGAGTTGC	Mutagenesis
Cho-Y465Af	CACAACACCGTCC <u>C</u> CCACCCCGTGGGCACCGTGC	Mutagenesis
Cho-Y465Ar	CACGGTGCCACGCGGGTGGG <u>C</u> GACGGTGTTGTGC	Mutagenesis
Cho-Y465Hf	CACAACACCGTCC <u>A</u> CCACCCCGTGGGCACCGTGC	Mutagenesis
Cho-Y465Hr	CACGGTGCCACGCGGGTGGT <u>G</u> GACGGTGTTGTGC	Mutagenesis

Underlined nucleotides indicate endonuclease restriction sites for *Nde*I and *Eco*R I enzymes in cloning primers and mismatches sites in mutagenesis primers.



Cloning was performed from *A. globiformis* strain ATCC 8010, which was grown on Difco #3 Nutrient Agar medium for 48 h at 26 °C. Single colonies were used to inoculate eight 5 ml of Difco #3 Nutrient Broth and the resulting liquid cultures were grown overnight at 26 °C. The cells were harvested by centrifugation at 14,000 x g for 10 min, and the genomic DNA was isolated using the DNeasy Midi-kit (Qiagen) according to the manufacturer's instructions. The isolated genomic DNA was then used for PCR of the *codA* gene with the oligonucleotide primers described above. PCR was carried out with an Eppendorf Mastercycler in the presence of 4% DMSO for 1 min at 95 °C, followed by 31 cycles of 1 min at 95 °C, 1 min at 50 °C, 2 min at 72 °C, and a final 5-min step at 72 °C in a total volume of 50 µl by using ~200 ng of template DNA, 5 U of *Taq* DNA polymerase, 3 mM magnesium chloride, and the polymerase manufacturer's suggested protocol. The resulting amplicons were purified by agarose gel electrophoresis using the QIAquick Gel Extraction kit (Qiagen) following the manufacturer's protocol.

Endonuclease digestion of both the amplified *codA* from *A. globiformis* and pET20b(+) with *Nde*I and *Eco*R I, dephosphorylation of the plasmid with calf intestine alkaline phosphatase, and ligation were carried out as described above, and 1 µl of the ligation reaction mixture was used directly to transform by electroporation 100 µl of *E. coli* strain Novablue competent cells. The resulting transformant colonies obtained by plating on Luria-Bertani agar plates containing 50 µg/ml ampicillin and 12.5 µg/ml tetracycline were screened for the presence of *codA* by colony PCR. PCR was performed with 5 U of *Taq* DNA polymerase in the presence of 2% DMSO for 1 min at 95 °C followed by 31 three-step cycles of 1 min at 95 °C, 2 min at 55 °C, 2 min at 72 °C, and a 5-min final step at 72 °C, using sense and antisense oligonucleotide primers designed to bind to DNA regions of pET20b(+) flanking the inserted gene. The correct constructs, pET/*codA*1 and pET/*codA*2, were sequenced in both directions as described above. *E.*

*coli* strain Rosetta(DE3)pLysS competent cells were transformed with plasmid pET/*codA1* for protein expression.

### **Enzyme preparation**

Permanent frozen stocks of *E. coli* cells Rosetta(DE3)pLysS harboring plasmid pET/*codA1* were used to inoculate 50 ml of Luria-Bertani broth medium containing ampicillin (or carbenicillin) and chloramphenicol at final concentrations of 50 and 34 µg/ml, respectively, at 37 °C. After 9 h, 1 ml of the starter culture was used to inoculate 3 x 1.5 liters of the same liquid culture medium at 30 °C. When the culture reached an optical density at 600 nm between 0.8 and 1.4, typically after 16 h, IPTG was added to a final concentration of 50 µM and the temperature of the culture was lowered between 21 and 25 °C. Cells were harvested by centrifugation at 20,000 x *g* for 20 min at 4 °C and stored at -20 °C. Typically, ~8 g of wet cell paste were obtained from 1.5 liters of cells culture.

Unless otherwise stated, all the purification steps were carried out at 4 °C. The cell paste, typically 25 g, was suspended in 6 volumes of a solution of 0.1 mM PMSF, 0.2 mg/ml lysozyme, 1 mM EDTA, and 50 mM potassium phosphate at pH 7 and allowed to incubate with stirring for 30 min on ice. The resulting slurry was passed three times through an SLM Aminco French pressure cell at 20,000 lb/in<sup>2</sup> and then centrifuged at 20,000 x *g* for 20 min. The supernatant was collected, incubated with stirring for 30 min on ice with 20 µg/ml RNase and 50 µg/ml DNase in the presence of 10 mM magnesium chloride, and centrifuged as described above. The soluble fraction was brought to 30% ammonium sulfate saturation, incubated for 30 min on ice, and separated from the insoluble fraction by centrifugation as described above. Choline oxidase was then collected in the pellet fraction by treatment with ammonium sulfate at a final saturation of 65%, followed by centrifugation as described above. The resulting pellet was suspended in 25 ml

of 200 mM Tris-Cl, pH 8, and dialyzed against three 1-liter changes of the same buffer over 20 h. After dialysis, precipitated proteins were removed by centrifugation at 18,700 x g for 20 min and the resulting supernatant was loaded onto a DEAE-Sepharose Fast Flow column (3 x 28 cm) connected to an *Äktaprime* Amersham Pharmacia Biotech system equilibrated with 200 mM Tris-Cl at pH 8. The column was eluted with 2 volumes of the same buffer, followed by a linear gradient from 0 to 0.5 M NaCl developed over 5 volumes at a flow rate of 2 ml/min. The fractions with the highest purity as judged by enzymatic activity and UV-visible absorbance spectroscopy were pooled together and concentrated with the addition of 65% ammonium sulfate saturation followed by centrifugation. Oxidized FAD-containing choline oxidase was prepared at 4 °C by dialysis against three 1-liter changes of 20 mM sodium phosphate, 20 mM sodium pyrophosphate, pH 6, over 24 hours, followed by two 1-liter changes of 20-200 mM Tris-Cl, pH 8 over five hours. This enzyme could be stored at -20 °C for at least 7 months without losses in enzymatic activity.

### Site-directed mutagenesis

A QuikChange kit was used to prepare the mutant enzymes choline oxidase-H466A (CHO-H466A), choline oxidase-H466D (CHO-H466D), choline oxidase-H310A (CHO-H310A), choline oxidase-H310D<sup>1</sup> (CHO-H310D), choline oxidase-H310N<sup>2</sup> (CHO-H310N), choline oxidase-E370A<sup>3</sup> (CHO-E370A), choline oxidase-H87A (CHO-H87A), choline oxidase-H87C (CHO-H87C), choline oxidase-Y465A (CHO-Y465A), and choline oxidase-Y465H (CHO-Y465H). The method used was essentially according to the manufacturer's instructions, using

---

<sup>1</sup> Ongoing project.

<sup>2</sup> Ongoing project.

<sup>3</sup> E370A mutant form of choline oxidase has been expressed and purified. The biochemical and the kinetic characterization of that mutant form showed that there is no significant different between that mutant and the wild-type enzyme. Furthermore, the recently solved X-ray crystallographic structure of choline oxidase showed that this residue is located at the surface of protein, consistent with its similarity to the wild-type enzyme.

pET/*codA1* plasmid (3) as a template and the corresponding forward and reverse primers (Table 3.1). DNA was sequenced at the DNA Core Facility at Georgia State University using an Applied Biosystems Big Dye Kit on an Applied Biosystems model ABI 377 DNA sequencer. Sequencing confirmed the presence of the mutant genes in the correct orientation. *E. coli* strain Rosetta(DE3)pLysS competent cells were transformed with the mutated plasmid by electroporation.

### **Expression and purification of the mutated enzymes**

Permanent frozen stocks of *E. coli* cells Rosetta(DE3)pLysS harboring the mutated plasmid were used to inoculate 4.5 liters of Luria-Bertani broth medium containing 50 µg/ml ampicillin and 34 µg/ml chloramphenicol, and liquid cultures were grown overnight at 37 °C. The cultures were induced for protein expression by adding 0.05 mM IPTG and then incubated for an additional 5 h at 22 °C. 100 µl aliquots was taken 5 h after induction with IPTG to be used for visualization of the expressed proteins using sodium dodecyl sulfate polyacrylamide gel electrophoresis following the Laemmli method (4). The gel was stained with Commassie Brilliant Blue G-250. The mutant enzymes (CHO-H466A, CHO-H466D, CHO-H310A, and CHO-E370A) were purified to homogeneity using the same procedure used previously for the purification of the wild-type enzyme (3).

### **Enzyme assays**

The concentration of choline oxidase was determined with the method of Bradford (5), by using the Bio-Rad protein assay kit with bovine serum albumin as the standard. The oxidized flavin content of choline oxidase as purified was determined from the  $\Delta A_{452}$  after treatment of the enzyme with 5 mM dithionite in air-saturated 200 mM Tris-Cl, pH 8, using an  $\epsilon_{452}$  value of  $8.4 \text{ mM}^{-1}\text{cm}^{-1}$ , which corresponds to the difference between the extinction coefficients for the

enzyme-bound oxidized flavin ( $\epsilon_{452} = 8.4 \text{ mM}^{-1} \text{ cm}^{-1}$ ) and semiquinone flavin ( $\epsilon_{452} = 3 \text{ mM}^{-1} \text{ cm}^{-1}$ )

(6). Enzyme activity was measured with the method of the initial rates (7) in air-saturated 50 mM potassium phosphate at pH 7 by monitoring the rate of oxygen consumption with a computer-interfaced Oxy-32 oxygen-monitoring system (Hansatech Instrument Ltd.) thermostated at 25 °C. The reactions were started by the addition of choline oxidase to a 1 ml reaction mixture, with the final concentration of enzyme in the 0.1 to 0.5  $\mu\text{M}$  range; the concentration of choline or betaine aldehyde was between 0.02 and 35 mM. The effect of pH on the kinetic parameters of CHO-H466A were determined over a pH range from 5.5 to 11 by a series of enzyme activity assays at varying choline concentrations ranging from 0.025 to 45 mM in air-saturated 50 mM sodium pyrophosphate at 25 °C. The kinetic isotope effects of CHO-H466A were obtained by determining the kinetic parameters of the enzyme using either choline or 1,2- $[\text{}^2\text{H}_4]$ -choline as substrate in either aqueous or deuterated solvent, in air-saturated 50 mM sodium pyrophosphate at 25 °C and pL 10. For the determinations of solvent isotope effects, buffers were prepared using 99.9% deuterium oxide by adjusting the pD value with NaOD. The pD values were determined by adding 0.4 to the pH electrode readings (8). For all steady state kinetic isotope effects, activity assays were carried out by alternating substrate or solvent isoptomers. Product inhibition studies were carried out by varying the concentrations of both glycine betaine, in the range between zero and 60 mM, and choline, in the range between 0.02 and 20 mM, in air-saturated 50 mM sodium pyrophosphate at 25 °C, over a pH range from 7 to 11. The effect of imidazole on the turnover number of CHO-H466A was determined by measuring the enzymatic activity with 10 mM choline as substrate for the enzyme in the presence of varying concentrations of imidazole in the range from 0 to 250 mM in air-saturated 50 mM potassium phosphate, pH 7, or 50 mM sodium pyrophosphate for other pH values.

## Spectral studies

The UV-visible absorbance and fluorescence emission or excitation spectra of CHO-H466D, CHO-WT and CHO-H466A, were acquired in 20 mM sodium phosphate, 20 mM sodium pyrophosphate and 10% glycerol, pH 6<sup>4</sup> at 15 °C. The UV-visible absorbance spectra of the reduced form of enzymes were acquired using an anaerobic cuvette in 50 mM sodium phosphate, 50 mM sodium pyrophosphate and 10% glycerol, pH 6 at 15 °C. The cuvette contained one ml final volume of enzyme at a final concentration between 20 and 30  $\mu$ M, 300  $\mu$ M xanthine, and 10  $\mu$ M methyl viologen. A sidearm attached to the cuvette contained xanthine oxidase at a final concentration of  $\sim$ 0.5  $\mu$ M. The cuvette and contents were made anaerobic by at least 15 cycles of alternate degassing under vacuum and flushing with O<sub>2</sub>-free argon. The enzyme solution was then mixed with xanthine oxidase in the side arm, and the reduction of the enzyme-bound flavin was monitored spectrophotometrically. The extinction coefficient of the wild-type or mutant forms of choline oxidase were determined in Tris-Cl, pH 8, after denaturation of the enzymes either by incubation at 40 °C for one hour in the presence of urea at a final concentration of 4 M or 0.1% SDS at 100 °C for 5 min, based upon the  $\epsilon_{450}$  value of 11.3 mM<sup>-1</sup> cm<sup>-1</sup> for free FAD (9). The spectral properties of CHO-WT and CHO-H466A before and after the addition of 200 mM of glycine betaine were determined at 15 °C in 100 mM sodium pyrophosphate buffer, pH 6.5. All spectra were normalized to the molar extinction of the uncomplexed enzyme and corrected for dilution. For reactions with sodium sulfite, the reagent was prepared freshly as 1 M stock solution in 100 mM sodium pyrophosphate, pH 6.5. Different amounts of sodium sulfite at final concentrations ranging from 25 to 100 mM were added to the

---

<sup>4</sup> The spectral properties of the oxidized forms of CHO-WT, CHO-H466A, and CHO-H466D, were compared at pH 6 to avoid artifactual contributions on the UV-visible absorbance spectra due to pH, since the three enzyme variants showed pH effects on the UV-visible absorbance spectra of the oxidized enzymes with  $pK_a \geq 8.2$ .

enzyme solution in 100 mM sodium pyrophosphate, pH 6.5, at 15 °C, and the UV-visible absorbance spectra were recorded at different times. The pH dependences of the UV-visible absorbance spectra of oxidized enzymes were determined in 20 mM sodium phosphate, 20 mM sodium pyrophosphate, 10% glycerol, at 15 °C, by titrating sodium hydroxide into the enzyme solution at pH 6. The pH dependences of the UV-visible absorbance spectra of the reduced enzymes were determined in an all-glass spectrophotometer custom made anaerobic cuvette (Lillie Glassblowers, Smyrna, GA) that was fitted with a pH micro-electrode through a glass joint and an anaerobic syringe containing sodium hydroxide. The cuvette contained 3 ml of enzyme at a final concentration between 20 and 30  $\mu$ M in 50 mM sodium phosphate, 50 mM sodium pyrophosphate, and 10 % glycerol, pH 6. A sidearm attached to the cuvette was loaded with choline at a final concentration of 150 mM. The cuvette and contents were made anaerobic by at least 15 cycles of alternate degassing under vacuum and flushing with O<sub>2</sub>-free argon. The enzyme solution was then mixed with choline in the side arm in order to reduce the enzyme-bound flavin. With CHO-H466D, which could not be reduced anaerobically with choline, a syringe filled with anaerobic ~2 mM dithionite was inserted firstly into the cuvette under positive argon pressure, and the reduction of the enzyme-bound flavin was monitored spectrophotometrically until completion. In all the cases, once the UV-visible absorbance spectrum of the hydroquinone species was observed, a pH micro-electrode and a syringe containing anaerobic 3 M sodium hydroxide were mounted onto the anaerobic cuvette under positive argon pressure. The pH of the anaerobic enzyme solution was then changed stepwise by addition of the base, and both the pH and the UV-visible absorbance spectra were recorded after each step.

The CD spectra of CHO-WT and mutant enzymes were recorded at 5 °C in 20 mM Tris-Cl, pH 8, at concentrations of enzyme of 5 and 15  $\mu\text{M}$  for the far and the near UV, respectively. The fluorescence emission spectra of CHO-WT and mutant enzymes were acquired in 20 mM sodium phosphate, 20 mM sodium pyrophosphate and 10% glycerol, pH 6 at 15 °C.

For the quantitation of the ratio of the covalently to the uncovalently bound flavin to the enzymes,  $\sim 20 \mu\text{M}$  of enzymes were incubated on ice for 30 min after the addition of 10 % trichloroacetate, followed by removal of precipitated protein by centrifugation, and the determination of the concentration of FAD in both the supernatant and the dissolved pellet in 4 M urea solution using an  $\epsilon_{450 \text{ nm}}$  value of  $12 \text{ mM}^{-1} \text{ cm}^{-1}$ . The nature of the flavin cofactor of CHO-H466D was also verified through MALDI-TOF mass spectrometry in both the positive and negative ion mode using a 50:50 methanol/acetonitrile matrix.

### Potentiometric titrations

Potentiometric redox titrations were carried out to either the unliganded (CHO-WT, CHO-H466A and CHO-H466D) or the glycine betaine-liganded enzymes (CHO-WT and CHO-H466A) at 15 °C in a cell similar to the one described by Edmondson (1985). Potentials were measured by using a Pt electrode relative to an Ag/AgCl double junction reference electrode with an Orion Model 701A pH/mV meter (10). The reference electrode was calibrated prior to each titration as described by Edmondson (10), using a deoxygenated, saturated quinhydrone solution in 0.09 M KCl and 0.01 M HCl at 25 °C. In a typical titration, 2.5 ml of  $\sim 20\text{--}30 \mu\text{M}$  of either free or glycine betaine-liganded choline oxidase (at a final concentration of 1.5 M) in 20 mM Tris-Cl, pH 7, was scrubbed free of oxygen by at least 15 cycles of alternate degassing under vacuum and flushing with  $\text{O}_2$ -free argon. The following redox mediators were added to ensure complete redox equilibration: 2  $\mu\text{M}$  methyl viologen (-440 mV), 0.5  $\mu\text{M}$  dichlorophenolindophenol (+217



mV), 0.5  $\mu$ M phenazine methosulfate (+80mV), 0.5  $\mu$ M thionin (+60 mV), 0.5  $\mu$ M duroquinone (-5 to +5 mV), 0.5  $\mu$ M resorufin (-50 mV), and 0.5  $\mu$ M indigo carmine (-125 mV) (11, 12). The ligand-bound enzyme solutions were titrated electrochemically as described by Dutton (13), using freshly prepared sodium dithionite as reductant and potassium ferricyanide as oxidant in 20 mM Tris-Cl, pH 7 (13). Adequate time was permitted for electronic equilibration after each addition of sodium dithionite or potassium ferricyanide prior to the spectrum being recorded; equilibrium of the system was considered to be obtained when the measured potential drift was less than 1 mV in 5 min, which was typically achieved after 30 to 60 min. UV-visible absorbance spectra were recorded using an Agilent Technologies diode-array spectrophotometer model HP 8453 equipped with a thermostated cell holder and a magnetic stirrer beneath the cell holder. All spectra were corrected for any drift in the baseline by subtracting the absorbance at 800 nm.

### **Steady state kinetics**

Enzyme activity was measured polarographically by monitoring the rate of oxygen consumption with a Hansatech oxygen electrode thermostated at 25 °C. The determination of the steady state kinetic parameters was carried at varying concentrations of both choline (or betaine aldehyde), in the range from 0.02 to 35 mM, and oxygen, in the range from 0.04 to 1.1 mM. The reaction mixture was first equilibrated at the desired concentration of oxygen by bubbling the appropriate O<sub>2</sub>/N<sub>2</sub> gas mixture for at least 10 min. The reactions were then started by adding 5-25  $\mu$ l choline oxidase at a final concentration of ~0.1-0.5  $\mu$ M into a reaction mixture with a final volume of 0.5-1 ml. Enzyme assays were conducted in 50 mM sodium pyrophosphate, except for pH 7 and 7.5 where potassium phosphate was used. One unit of enzymatic activity corresponds to the consumption of one  $\mu$ mol of oxygen per min.

## Rapid kinetics

Rapid kinetics was carried out on a Hi-Tech SF-61 stopped-flow spectrophotometer thermostated at 25 °C. The rate of flavin reduction was measured by monitoring the decrease in absorbance at 452 nm that results from the decreasing of oxidized flavin species upon mixing the enzyme with the substrate. The enzyme solution was loaded into a tonometer and subjected to a 23-cycle degassing procedure by alternately applying vacuum and flushing with oxygen-free argon (pre-treated with an oxygen scrubbing cartridge, Agilent, Palo Alto, CA). Subsequently, the degassed enzyme solution was mounted onto the stopped-flow instrument, which had been subjected to an overnight treatment with an oxygen scrubbing system composed of 100 mM glucose and 30 units ml<sup>-1</sup> glucose oxidase. The organic substrate (~2 ml), was dissolved in desired buffer in H<sub>2</sub>O and then degassed by flushing oxygen-free argon for at least 15 min before mounting onto the stopped-flow. The enzyme was mixed anaerobically with an equal volume of substrate, yielding a reaction mixture containing ~15 - 40 μM choline oxidase and 0.05 to 10 mM choline.

## Data analysis

Data were fit with KaleidaGraph software (Synergy Software, Reading, PA) and Enzfitter software (Biosoft, Cambridge, UK). The steady state kinetic parameters for choline oxidase at atmospheric oxygen were determined by fitting the data to the Michaelis-Menten equation for one substrate (eq 1), where  $k_a$  represents the Michaelis-Menten constant for choline (or betaine aldehyde) ( $A$ ) and  $k_{cat}$  is the turnover number of the enzyme ( $e$ ). The steady state kinetic parameters at varying concentrations of both choline and oxygen were determined by fitting the initial rate data to eqs 2 and 3, which describe ternary complex mechanisms with reversible and irreversible catalytic steps, respectively. Data with betaine aldehyde were fit into eq 4, which

describes a ternary complex mechanism with negligible  $K_a$  value. In these equations,  $e$  represents the concentration of enzyme,  $k_{cat}$  is the turnover number of the enzyme at infinite substrates concentrations,  $K_a$  and  $K_b$  represent the Michaelis constants for the organic substrate ( $A$ ) and oxygen ( $B$ ), respectively. For the kinetic isotope effects of wild-type choline oxidase with choline as substrate, data obtained were divided into two sets, one with unlabeled substrate or solvent, and one with isotopically labeled substrate or solvent. The steady state kinetic parameters of the two sets were determined independently with eq 2 or 3, and the kinetic isotope effects were determined by taking the ratios of the steady state kinetic parameters of interest. For CHO-H466A, under atmospheric oxygen conditions at 25 °C (i.e., with a concentration of dissolved oxygen of 0.25 mM), due to the low  $K_m$  value for oxygen with a value of  $5 \pm 2 \mu\text{M}$  at pH 10 (Ghanem, M., and Gadda, G.; unpublished data), CHO-H466A is > 97% saturated with oxygen. Therefore, with CHO-H466A the true kinetic isotope effect could be determined from the  $^Dk_{cat}/K_m$  value under atmospheric conditions.

$$\frac{v}{e} = \frac{k_{cat}A}{K_a + A} \quad (1)$$

$$\frac{v}{e} = \frac{k_{cat}AB}{K_aB + K_bA + AB + K_{ia}K_b} \quad (2)$$

$$\frac{v}{e} = \frac{k_{cat}AB}{K_aB + K_bA + AB} \quad (3)$$

$$\frac{v}{e} = \frac{k_{cat}AB}{K_bA + AB + K_{ia}K_b} \quad (4)$$

The pH dependencies of steady-state kinetic parameters were determined by fitting initial rate data to eq 5, which describes a curve with a slope of +1 and a plateau region at high pH. The pH dependence of inhibition by glycine betaine was determined by fitting the initial rate data to eq 6, which describes a curve with a slope of -1 and a plateau region at low pH.  $C$  is the pH-

independent value of the kinetic parameter of interest. Data of the pH dependencies of the absorbance spectra for both the oxidized wild-type and mutant enzymes were fit to eq 7, which describes a curve with a slope of -1 and plateau regions at low and high pH, where  $A$  and  $B$  represent the absorbance values at 500 nm at low and high pH, respectively.

$$\log Y = \log \left( \frac{C}{1 + \frac{10^{-\text{pH}}}{10^{-\text{p}K_a}}} \right) \quad (5)$$

$$\log Y = \log \left( \frac{C}{1 + \frac{10^{-\text{p}K_a}}{10^{-\text{pH}}}} \right) \quad (6)$$

$$Y = \frac{A \times 10^{-\text{pH}} + B \times 10^{-\text{p}K_a}}{10^{-\text{pH}} + 10^{-\text{p}K_a}} \quad (7)$$

Product inhibition studies were performed by varying the concentrations of both glycine betaine and choline at a fixed concentration of oxygen. The data were fit to eqs 8 to 10, which describe competitive, uncompetitive, and noncompetitive inhibition patterns of the product and the organic substrate, respectively.  $P$  is the concentration of glycine betaine,  $K_{is}$  and  $K_{ii}$  are the inhibition constants for the slope and intercept term, respectively.

$$\frac{v}{e} = \frac{k_{cat} A}{K_a \left[ 1 + \left( \frac{P}{K_{is}} \right) \right] + A} \quad (8)$$

$$\frac{v}{e} = \frac{k_{cat} A}{K_a + A \left[ 1 + \left( \frac{P}{K_{ii}} \right) \right]} \quad (9)$$

$$\frac{v}{e} = \frac{k_{cat}A}{K_a \left[ 1 + \left( \frac{P}{K_{is}} \right) \right] + A \left[ 1 + \left( \frac{P}{K_{ii}} \right) \right]} \quad (10)$$

Data of the spectrophotometric titrations for complex formation between choline oxidase and various ligands were fit to eq 11, where  $Y$  and  $A$  are the observed and maximal absorbance changes at the selected wavelength, respectively,  $X$  is the concentration of the varied ligand, and  $K$  is the complex dissociation constant. Data of the pH dependencies of the absorbance spectra of the oxidized CHO-H466D were fit to eq 2, which describes a curve with a slope of +1 and plateau regions at low and high pH, where  $A$  and  $B$  represent the absorbance values at 500 nm at low and high pH, respectively. The midpoint reduction-oxidation potentials of the enzymes were determined by fitting the data to eq 13, where  $E_h$  is the observed electrode potential at equilibrium at each point in the titration,  $E'_m$  is the midpoint reduction-oxidation potential,  $R$  is the gas constant, with a value of  $8.31 \text{ J mol}^{-1} \text{ K}^{-1}$  at  $15^\circ \text{C}$ ,  $T$  is the temperature in Kelvin,  $n$  is the number of electrons transferred, and  $F$  is Faraday's constant, with a value of  $96.48 \text{ kJ V}^{-1} \text{ mol}^{-1}$ .

$$Y = \frac{AX}{X + K} \quad (11)$$

$$Y = \frac{A \times 10^{-\text{pH}} + B \times 10^{-\text{pK}_a}}{10^{-\text{pH}} + 10^{-\text{pK}_a}} \quad (12)$$

$$E_h = E'_m + \frac{2.303}{nF} \frac{RT}{\log} \frac{[\text{FAD}_{\text{Ox or Sq}}]}{[\text{FAD}_{\text{Sq or Red}}]} \quad (13)$$

## References

- (1) Deshnum, P., Los, D. A., Hayashi, H., Mustardy, L., and Murata, N. (1995) Transformation of *Synechococcus* with a gene for choline oxidase enhances tolerance to salt stress. *Plant Mol. Biol.* 29, 897-907.
- (2) Hayashi, H., Alia, Mustardy, L., Deshnum, P., Ida, M., and Murata, N. (1997) Transformation of *Arabidopsis thaliana* with the *codA* gene for choline oxidase; accumulation of glycinebetaine and enhanced tolerance to salt and cold stress. *Plant J.* 12, 133-42.
- (3) Fan, F., Ghanem, M., and Gadda, G. (2004) Cloning, sequence analysis, and purification of choline oxidase from *Arthrobacter globiformis*: a bacterial enzyme involved in osmotic stress tolerance. *Arch. Biochem. Biophys.* 421, 149-58.
- (4) Laemmli, U. K. (1970) Cleavage of structural proteins during the assembly of the head of bacteriophage T4. *Nature* 227, 680-5.
- (5) Bradford, M. M. (1976) A rapid and sensitive method for the quantitation of microgram quantities of protein utilizing the principle of protein-dye binding. *Anal. Biochem.* 72, 248-54.
- (6) Ghanem, M., Fan, F., Francis, K., and Gadda, G. (2003) Spectroscopic and kinetic properties of recombinant choline oxidase from *Arthrobacter globiformis*. *Biochemistry* 42, 15179-88.
- (7) Allison, D. R., and Purich, D. L. (1979) Practical considerations in the design of initial velocity enzyme rate, in *Methods Enzymol.* (Purich, D. L., Ed., Ed.) pp 3-19, Academic Press, New York.
- (8) Schowen, K. B., and Schowen, R. L. (1982) Solvent isotope effects of enzyme systems. *Methods Enzymol.* 87, 551-606.
- (9) Whitby, L. G. (1953) A new method for preparing flavin-adenine dinucleotide. *Biochem. J.* 54, 437-42.
- (10) Williamson, G., and Edmondson, D. E. (1985) Effect of pH on oxidation-reduction potentials of 8 alpha-N-imidazole-substituted flavins. *Biochemistry* 24, 7790-7.
- (11) Ma, Y. C., Funk, M., Dunham, W. R., and Komuniecki, R. (1993) Purification and characterization of electron-transfer flavoprotein: rhodoquinone oxidoreductase from anaerobic mitochondria of the adult parasitic nematode, *Ascaris suum*. *J. Biol. Chem.* 268, 20360-5.
- (12) Mohsen, A. W., Rigby, S. E., Jensen, K. F., Munro, A. W., and Scrutton, N. S. (2004) Thermodynamic Basis of Electron Transfer in Dihydroorotate Dehydrogenase B from *Lactococcus lactis*: Analysis by Potentiometry, EPR Spectroscopy, and ENDOR Spectroscopy. *Biochemistry* 43, 6498-6510.

- (13) Dutton, P. L. (1978) Redox potentiometry: determination of midpoint potentials of oxidation-reduction components of biological electron-transfer systems. *Methods Enzymol.* 54, 411-35.

## CHAPTER III

### Cloning, Sequence Analysis, and Purification of Choline Oxidase From *Arthrobacter*

#### *globiformis*: a Bacterial Enzyme Involved in Osmotic Stress Tolerance

(This chapter has been published verbatim in Ghanem, M., Fan, F., and Gadda, G., (2004), *Arch. Biochem. Biophys.* 142, 149-58. © 2003 Elsevier Inc. All rights reserved. The first two authors share equal contribution to the publication. The sequence reported in this paper has been deposited in the GenBank database with accession no. [AY304485](#). In particular, my contribution to this study pertains the cloning and sequencing the *codA* gene from the bacterial genome, expression and purification of the recombinant enzyme, and the preliminary biophysical and spectroscopic characterization of the recombinant enzyme).

#### Abstract

Choline oxidase catalyzes the four-electron oxidation of choline to glycine betaine, one of a limited number of compounds that accumulate to high levels in the cytoplasm of cells to prevent dehydration and plasmolysis in adverse hyperosmotic environments. In the present study, the highly GC rich *codA* gene encoding for choline oxidase was cloned from genomic DNA of *Arthrobacter globiformis* strain ATCC 8010 and expressed to high yields in *Escherichia coli* strain Rosetta(DE3)pLysS. The resulting enzyme was purified to high levels in a single chromatographic step using DEAE-Sepharose, as shown by SDS-PAGE analysis. Denaturation and mass spectroscopic analyses showed that the covalent linkage between the FAD cofactor and the protein is preserved in recombinant choline oxidase, consistent with protein flavinylation being a self-catalytic process. The enzyme was shown to be a homodimer of 120,000 Da by size-exclusion chromatography and to be active with both choline and betaine aldehyde as substrate. Sequencing analysis indicated that the nucleotide sequence of *codA* originally reported in GenBank contains seven flaws, resulting in a translated protein with a significantly altered amino acid sequence between position 298 and 410.

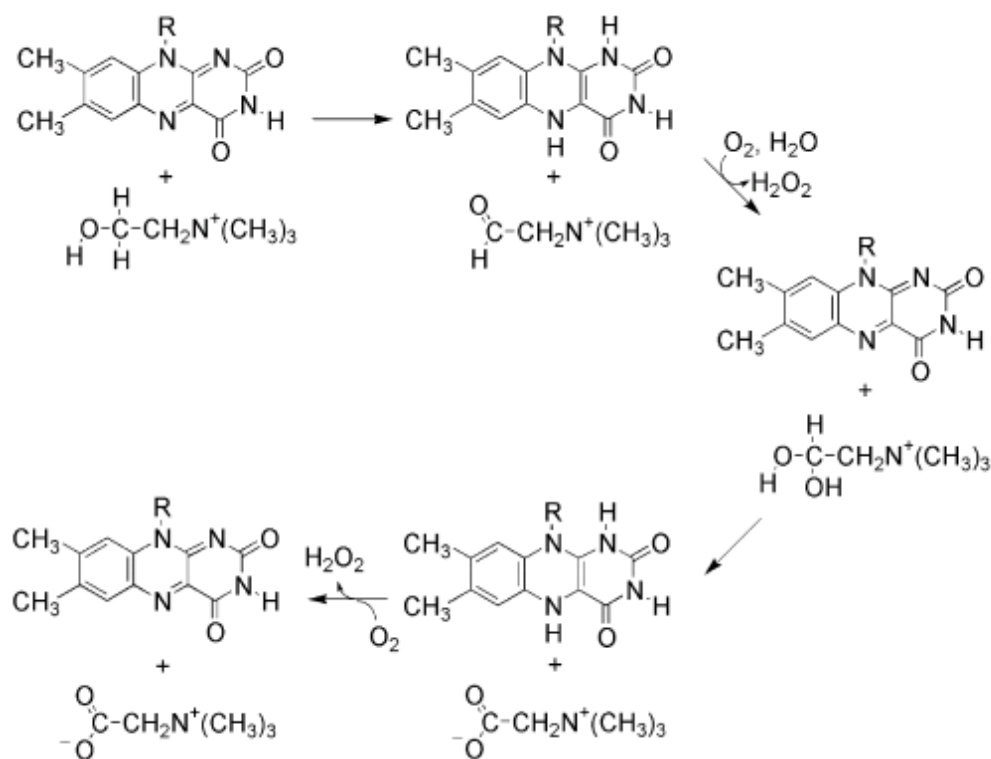


## Introduction

Choline oxidase (E.C. 1.1.3.17) catalyzes the four-electron oxidation of choline to glycine betaine (*N,N,N*-trimethylglycine; betaine) via betaine aldehyde as intermediate. Molecular oxygen acts as primary electron acceptor in the reaction (Scheme 3.1) (1). The enzyme is of importance because glycine betaine is one of a limited number of compatible solutes that accumulate to high levels in the cytoplasm of cells to prevent dehydration and plasmolysis in adverse hyperosmotic environments (2-6). Regulation of intracellular osmolality to hyperosmotic environments is also intimately connected to a number of physiological responses, such as increased heat and cold tolerance, as well as regulation of the internal pH and ionic strength (7-12). Hyperosmolarity is often encountered at human infection sites (13), where choline and its precursors are very abundant (14-16), and is a major environmental signal controlling the expression of genes associated with cellular invasion and virulence in a number of human pathogens (17-24). For these reasons, the study of choline oxidase is of considerable interest both for genetically engineering water and osmotic stress resistance in economically relevant crop plants lacking efficient glycine betaine biosynthetic systems (10, 11, 25-29), and for the potential development of therapeutic agents that inhibit the biosynthesis of glycine betaine thereby making bacteria more susceptible to conventional treatments.

Choline oxidase has been purified from *Cylindrocapsa didymum* M-1 (30), *Alcaligenes* sp. (31), and *Arthrobacter globiformis* (1). Based on amino acid sequence comparisons, the enzyme can be grouped in the GMC oxidoreductase enzyme superfamily (32), which comprises enzymes like glucose oxidase, cholesterol oxidase, or cellobiose dehydrogenase, that utilize FAD as cofactor for catalysis and nonactivated primary alcohols as substrate. Despite a wealth of studies on the biotechnological applications of the enzyme, minimal biochemical and

mechanistic investigations of choline oxidase have been reported to date. In this respect, our group has recently reported the analyses of the steady state kinetic mechanism and of the pH and deuterium kinetic isotope effects on the oxidation of choline to betaine aldehyde catalyzed by choline oxidase from *A. globiformis* (33, 34). One of the most critical impediments to future studies is the obtainment of large quantities of choline oxidase for detailed biophysical, mechanistic, and structural investigations. In the present study, we have cloned from *A. globiformis* genomic DNA the *codA* gene encoding for choline oxidase and heterogously expressed it in *Escherichia coli*. The resulting recombinant enzyme has been purified to homogeneity in a single chromatographic step and characterized for its flavin content, catalytic activity, and oligomerization state.



**Scheme 3.1.** Reaction catalyzed by choline oxidase.

## Materials and Methods

**Materials.** *E. coli* strain JM109 harboring plasmid pGAH/*codA* was a kind gift from Dr. Murata, National Institute for Basic Biology, Okazaki, Japan (27, 28). A freeze-dried culture of *A. globiformis* (ATCC 8010) was obtained from American Type Culture Collection. Restriction endonucleases *Nde*I and *Eco*R I, calf intestinal alkaline phosphatase, T4 DNA ligase, *Taq* DNA polymerase, deoxynucleotide triphosphates, and bovine serum albumin were purchased from Promega. *Pfu* DNA polymerase was obtained from Stratagene or Roche Molecular Biomedicals. Luria-Bertani agar, Luria-Bertani broth, chloramphenicol, tetracycline, kanamycin, isopropyl- $\beta$ -D-thiogalactopyranoside (IPTG), lysozyme, phenylmethylsulfonyl fluoride (PMSF), and betaine aldehyde bromide were obtained from Sigma-Aldrich. Carbenicillin, ampicillin, choline chloride, and electrophoresis-grade agar were purchased from ICN Biomedicals. Nutrient Broth and Nutrient Agar #3 were from Difco. All other reagents were of the highest purity commercially available. Oligonucleotides were custom synthesized on a Beckman Oligo model 1000 M by the DNA Core Facility of the Biology Department of Georgia State University. *A. globiformis* genomic DNA was purified using the DNeasy midi-kit from Qiagen. Plasmids and products deriving from primer extension reaction and PCR were purified by using mini-kits from Qiagen. *E. coli* strains Novablue (Novagen) and XL1-Blue (Stratagene) were used during cloning procedures, whereas strain Rosetta(DE3)pLysS (Novagen) was used for protein expression. *E. coli* strain Novablue cells harboring plasmid pET/*codA1* or pET/*codA2*, strain XL1-Blue cells harboring plasmid pET/*codA3*, and strain Rosetta(DE3)pLysS cells harboring plasmid pET/*codA1* or pET/*codA3* were stored at  $-80^{\circ}\text{C}$  as 7% DMSO suspensions. DNA sequencing was carried out with an Applied Biosystems Big Dye kit on an Applied Biosystems model ABI

377 DNA sequencer by the DNA Core Facility of the Biology Department of Georgia State University.

***Sub-Cloning of codA into the Expression Vector pET20b(+).*** *E. coli* strain JM109 harboring plasmid pGAH/*codA* was grown on Luria-Bertani agar medium containing kanamycin at a final concentration of 15 µg/ml for 16 h at 37 °C. Single colonies were used to inoculate 2 ml of Luria-Bertani broth medium containing kanamycin (15 µg/ml) and the resulting liquid cultures were grown at 37 °C for 7 h. After harvesting the cells by centrifugation at 14,000 x g for 10 min, the plasmid vector was isolated by using a QIAquick Spin Miniprep kit (Qiagen) following the manufacturer's protocol. The isolated plasmid DNA was then used for primer extension reaction of the *codA* gene encoding for choline oxidase by using the oligonucleotide primers Chox-for A and Chox-rev containing *Nde*I and *Eco*R I restriction endonuclease sites designed to anneal to the 5' and 3' ends of the gene, respectively (Table 3.1). The *Nde*I and *Eco*R I restriction sites introduced at the 5' ends of the sense and antisense primers allowed cloning of *codA* into the corresponding sites of pET20b(+). Primer extension reaction was performed in the presence of DMSO at a final concentration of 2% for 1 min at 95 °C, followed by 31 three-step cycles of 0.5 min at 95 °C, 1 min at 55 °C, 4.5 min at 68 °C, with a final 5-min step at 68 °C, in a total volume of 50 µl by using ~15 ng of template DNA, 2.5 U of *Pfu* DNA polymerase, and the manufacturer's suggested protocol. The resulting amplicons were purified by agarose gel electrophoresis using the QIAquick Gel Extraction kit (Qiagen) following the manufacturer's protocol.

**Table 3.1.** Oligonucleotide Primers Used for Primer Extension Amplification and PCR of *codA*.

Primer	Nucleotide sequence	Purpose
Chox-for A	CGGCAAGGAGAACC <u>CATATG</u> CACATCGACAACATCTG	Cloning
Chox-rev	CCCCGGAATT <u>CGCCGCT</u> CCCGCTTAGG	Cloning
PET-for A	CACTATAGGGAGACCACAACG	Sequencing
PET-rev A	GCTTATGCTAGTTATTGCTCAGC	Sequencing
Choxag 3	CAATGAAGTCGTGCTCTCC	Sequencing
Choxag 5	CGAAGTTCAACACC	Sequencing
Choxag 7	CGATGCAGGAGTTGTGG	Sequencing

Endonuclease restriction sites for *Nde*I and *Eco*R I enzymes are underline.

The pET20b(+) plasmid vector was isolated from an *E. coli* strain XL1-Blue grown for 16 h at 37 °C in 4 ml of Luria-Bertani broth containing ampicillin at a final concentration of 50 µg/ml by using the QIAprep Spin Miniprep kit from Qiagen, following the manufacturer's instructions.

Both the amplified *codA* and pET20b(+) vector were digested for 3 h at 37 °C with 30 U of *Nde*I and 36 U of *Eco*R I in a total volume of 60 µl of 10 mg/ml bovine serum albumin, 0.15 mM sodium chloride, 6 mM magnesium chloride, 1 mM dithiothreitol, and 6 mM Tris-Cl at pH 7.9, followed by purification of the DNA by agarose gel electrophoresis using the QIAquick Gel Extraction kit. To ensure minimal self-ligation of the plasmid, pET20b(+) was further treated with 3 U of calf intestine alkaline phosphatase for 3 h at 37 °C, followed by purification of the DNA by gel electrophoresis extraction. The *codA* gene (160 ng) was then ligated into the pET20b(+) (120 ng) plasmid in the presence of 2% DMSO by incubation for 16 h at 4 °C with 3 U of T4 DNA ligase in a total volume of 60 µl, and 5 µl of the ligation reaction mixture were used to transform directly 100 µl of *E. coli* strain XL1-Blue competent cells by using the electroporation method. The resulting transformant colonies obtained by plating on Luria-Bertani agar plates containing ampicillin (or carbenicillin) at a final concentration of 50 µg/ml were screened for the presence of *codA* by colony primer extension amplification with 2.5 U of *Pfu*

DNA polymerase in the presence of 2% DMSO using the protocol described above. Sense and antisense oligonucleotide primers designed to bind to the DNA regions of pET flanking the inserted gene were used in the screening (Table 3.1). The correct construct, pET/*codA3*, was sequenced in both directions by using the oligonucleotide primers shown in Table 3.1, and *E. coli* strain Rosetta(DE3)pLysS competent cells were then transformed with plasmid pET/*codA3* following the procedures described above.

***Cloning of codA from A. globiformis Genome into the Expression Vector pET20b(+).***

*A. globiformis* strain ATCC 8010 was grown on Difco #3 Nutrient Agar medium for 48 h at 26 °C. Single colonies were used to inoculate eight 5 ml of Difco #3 Nutrient Broth and the resulting liquid cultures were grown overnight at 26 °C. The cells were harvested by centrifugation at 14,000 x *g* for 10 min, and the genomic DNA was isolated using the DNeasy Midi-kit (Qiagen) according to the manufacturer's instructions. The isolated genomic DNA was then used for PCR of the *codA* gene with the oligonucleotide primers described above. PCR was carried out with an Eppendorf Mastercycler in the presence of 4% DMSO for 1 min at 95 °C, followed by 31 cycles of 1 min at 95 °C, 1 min at 50 °C, 2 min at 72 °C, and a final 5-min step at 72 °C in a total volume of 50 µl by using ~200 ng of template DNA, 5 U of *Taq* DNA polymerase, 3 mM magnesium chloride, and the polymerase manufacturer's suggested protocol. The resulting amplicons were purified by agarose gel electrophoresis using the QIAquick Gel Extraction kit (Qiagen) following the manufacturer's protocol.

Endonuclease digestion of both the amplified *codA* and pET20b(+) with *Nde*I and *Eco*R I, dephosphorylation of the plasmid with calf intestine alkaline phosphatase, and ligation were carried out as described above, and 1 µl of the ligation reaction mixture was used directly to transform by electroporation 100 µl of *E. coli* strain Novablue competent cells. The resulting

transformant colonies obtained by plating on Luria-Bertani agar plates containing 50 µg/ml ampicillin and 12.5 µg/ml tetracycline were screened for the presence of *codA* by colony PCR. PCR was performed with 5 U of *Taq* DNA polymerase in the presence of 2% DMSO for 1 min at 95 °C followed by 31 three-step cycles of 1 min at 95 °C, 2 min at 55 °C, 2 min at 72 °C, and a 5-min final step at 72 °C, using sense and antisense oligonucleotide primers designed to bind to DNA regions of pET20b(+) flanking the inserted gene. The correct constructs, pET/*codA1* and pET/*codA2*, were sequenced in both directions as described above. *E. coli* strain Rosetta(DE3)pLysS competent cells were transformed with plasmid pET/*codA1* for protein expression.

***Expression of Choline Oxidase in E. coli.*** Permanent frozen stocks of *E. coli* cells Rosetta(DE3)pLysS harboring plasmid pET/*codA1* were used to inoculate 50 ml of Luria-Bertani broth medium containing ampicillin (or carbenicillin) and chloramphenicol at final concentrations of 50 and 34 µg/ml, respectively, at 37 °C. After 9 h, 1 ml of the starter culture was used to inoculate 3 x 1.5 liters of the same liquid culture medium at 30 °C. When the culture reached an optical density at 600 nm between 0.8 and 1.4, typically after 16 h, IPTG was added to a final concentration of 50 µM and the temperature of the culture was lowered between 21 and 25 °C. Cells were harvested by centrifugation at 20,000 x g for 20 min at 4 °C and stored at -20 °C. Typically, ~8 g of wet cell paste were obtained from 1.5 liters of cells culture.

***Purification of Recombinant Choline Oxidase.*** Unless otherwise stated, all the purification steps were carried out at 4 °C. The cell paste, typically 25 g, was suspended in 6 volumes of a solution of 0.1 mM PMSF, 0.2 mg/ml lysozyme, 1 mM EDTA, and 50 mM potassium phosphate at pH 7 and allowed to incubate with stirring for 30 min on ice. The resulting slurry was passed three times through an SLM Aminco French pressure cell at 20,000

lb/in<sup>2</sup> and then centrifuged at 20,000 x g for 20 min. The supernatant was collected, incubated with stirring for 30 min on ice with 20 µg/ml RNase and 50 µg/ml DNase in the presence of 10 mM magnesium chloride, and centrifuged as described above. The soluble fraction was brought to 30% ammonium sulfate saturation, incubated for 30 min on ice, and separated from the insoluble fraction by centrifugation as described above. Choline oxidase was then collected in the pellet fraction by treatment with ammonium sulfate at a final saturation of 65%, followed by centrifugation as described above. The resulting pellet was suspended in 25 ml of 200 mM Tris-Cl, pH 8, and dialyzed against three 1-liter changes of the same buffer over 20 h. After dialysis, precipitated proteins were removed by centrifugation at 18,700 x g for 20 min and the resulting supernatant was loaded onto a DEAE-Sepharose Fast Flow column (3 x 28 cm) connected to an *Åktaprime* Amersham Pharmacia Biotech system equilibrated with 200 mM Tris-Cl at pH 8. The column was eluted with 2 volumes of the same buffer, followed by a linear gradient from 0 to 0.5 M NaCl developed over 5 volumes at a flow rate of 2 ml/min. The fractions with the highest purity as judged by enzymatic activity and UV-visible absorbance spectroscopy were pooled together and concentrated with the addition of 65% ammonium sulfate saturation followed by centrifugation. The resulting pellet was resuspended in 10 ml of 200 mM Tris-Cl, pH 8, and dialyzed against three 250-ml changes of the same buffer over 20 h. After removal of the precipitated protein by centrifugation, the enzyme stored at -20 °C was stable for at least six months.

**Enzyme Assays.** The concentration of choline oxidase was determined with the method of Bradford (35), by using the Bio-Rad protein assay kit with bovine serum albumin as the standard. The oxidized flavin content per enzyme active site was determined as described in (36). Enzyme activity was measured with the method of the initial rates (37) in air-saturated 50 mM



potassium phosphate at pH 7 by monitoring the rate of oxygen consumption with a computer-interfaced Oxy-32 oxygen-monitoring system (Hansatech Instrument Ltd.) thermostated at 25 °C. The reactions were started by the addition of choline oxidase to a 1 ml reaction mixture, with the final concentration of enzyme in the 0.1 to 0.5  $\mu$ M range; the concentration of choline or betaine aldehyde was between 0.02 and 10 mM. UV-Visible absorbance spectra were recorded using an Agilent Technologies diode-array spectrophotometer Model HP 8453 equipped with a thermostated water bath. Fluorescence emission spectra were recorded with a Shimadzu Spectrofluorometer Model RF-5301 PC thermostated at 15 °C.

**Methods.** The molecular mass of the enzyme was determined by MALDI-TOF mass spectrometry on a Micromass ToFSpec 2E at the Mass Spectrometry Laboratory of the Georgia Institute of Technology, Atlanta. Samples were prepared for MALDI-TOF analysis by gel filtration using a Sephadex G-25 column (PD-10, Amersham Pharmacia Biotech) equilibrated with 5 mM Tris-Cl, pH 8. MALDI-TOF spectra were acquired in the positive ion mode using sinapinic acid as the matrix, with an acceleration voltage of -20 kV and a pulse voltage of -16 kV. Cytochrome c [12,400], myoglobin [17,000], trypsinogen [24,000], and bovine serum albumin [66,000] were used as standards for mass calibration. The molecular weight of the enzyme under non-denaturing conditions was determined by size exclusion chromatography through a Sephacryl S-400 column (1 x 50 cm) connected to an Äktaprime Amersham Pharmacia Biotech system equilibrated with 300 mM KCl in 20 mM potassium phosphate, pH 7, at a flow rate of 0.5 ml/min. The following proteins were used as standards: horse heart cytochrome c [12,400], bovine serum albumin [66,000], yeast alcohol dehydrogenase [150,000], sweet potato  $\alpha$ -amylase [200,000], and horse spleen apoferritin [443,000]. SDS-PAGE according to the method of Laemmli (38) and PAGE under non-denaturing conditions were performed in 12%

polyacrylamide slab gels, with visualization of the proteins by staining with Coomassie brilliant blue G-250.

For denaturation experiments, choline oxidase was incubated at 40 °C for 1 h in the presence of urea at a final concentration of 4 M in 100 mM Tris-Cl, pH 8, before recording the UV-visible absorbance spectrum. The flavin content per monomer of enzyme was calculated from the ratio of the concentration of flavin in the denatured enzyme using an  $\epsilon_{450 \text{ nm}}$  value of  $11.3 \text{ mM}^{-1}\text{cm}^{-1}$  (39) to the concentration of protein determined using the Bradford assay (35). To establish whether the flavin is covalently bound to recombinant choline oxidase, the enzyme was incubated with trichloroacetic acid at a final concentration of 10% for 5 min at 100 °C, followed by removal of denatured protein by centrifugation at  $14,000 \times g$  for 10 min before measuring the UV-visible absorbance spectrum of the resulting supernatant.

**Data Analysis.** Kinetic data were fit with the KaleidaGraph software (Adalbeck Software, Reading, PA). Apparent kinetic parameters in atmospheric oxygen were determined by fitting initial reaction rates at different substrate concentrations to the Michaelis-Menten equation (eq. 1), where  $K_a$  represents the Michaelis constant for choline (or betaine aldehyde) ( $A$ ) and  $k_{cat}$  is the turnover number of the enzyme ( $e$ ).

$$\frac{v}{e} = \frac{k_{cat}A}{K_a + A} \quad (1)$$

## Results

**Cloning of *codA*.** The *codA* gene from *A. globiformis* encoding for choline oxidase was previously cloned in the binary vector plasmid pGAH for *in vivo* experiments aimed at conferring tolerance to salt stress in cyanobacteria and plants (10, 11, 25-28, 40, 41). In this study, *codA* was amplified from pGAH/*codA* by primer extension reaction by using *Pfu* DNA polymerase in the presence of 2% DMSO. Addition of DMSO was required to ensure complete denaturation of the highly GC rich DNA template in the primer extension reaction. Directional cloning of *codA* into pET20b(+) to construct plasmid pET/*codA3* was achieved by inserting *NdeI* and *EcoR* I endonuclease restriction sites at the 5' and 3' terminal ends of the gene, respectively. Plasmid pET/*codA3* was then used to transform *E. coli* competent cells strain XL1-Blue. Successful construction of plasmid pET/*codA3* was confirmed by nucleotide sequence analysis. However, seven differences were found in the nucleotide sequence of *codA* with respect to the sequence of the gene deposited in GenBank (accession no. **X84895**). Of the observed discrepancies, three accounted for missing nucleotides at position 891, 1117, and 1232, resulting in a translated sequence of 113 amino acid residues in the central portion of the protein being different from the published sequence (GenBank accession no. **S52489**). Surprisingly, no internal stop codons were created by the three single-point deletions, resulting in a translated protein of 546 amino acid residues. Two other differences were observed at position 764 and 1496, which resulted in the substitution of an arginine with a histidine residue and of a glycine with an alanine residue, respectively. Finally, two silent nucleotide substitutions that resulted in no change at the amino acid level were observed at position 832 and 846. The nucleotide sequence of *codA* was found to contain the same seven discrepancies when the gene was sequenced directly from pGAH/*codA*, suggesting that the differences did not originate in the sub-cloning procedure.

To further verify that the nucleotide differences were not introduced in the sub-cloning process from pGAH/*codA*, genomic DNA from *A. globiformis* strain ATCC 8010 was used as template to amplify the *codA* gene by using PCR with *Taq* DNA polymerase. The rationale for this strategy was that possible misincorporations of nucleotides occurring in the gene amplification procedure most likely would occur at different positions in the nucleotide sequence of the gene by using different DNA template, DNA polymerase, and PCR protocol. As a further control, *codA* was cloned from genomic DNA in two independent experiments to produce the constructs pET/*codA1* and pET/*codA2*. The nucleotide sequence of the *codA* gene cloned from genomic DNA was the same as that determined using pGAH/*codA*.

***Heterologous Expression of codA in E. coli.*** Heterologous expression of soluble choline oxidase from pET/*codA1* was achieved within 5 h of induction with 50  $\mu$ M IPTG at 25 °C in *E. coli* strain Rosetta(DE3)pLysS, which supplies tRNAs for codons that are rarely used in *E. coli*. The choice of such a bacterial host strain for protein expression was dictated by the observation that, due to its high GC content, *codA* contains 27 of such rare codons. Recombinant choline oxidase was purified to homogeneity, as judged by SDS-PAGE analysis (Figure 3.1), using 30 to 65% ammonium sulfate saturation followed by anion exchange chromatography onto a DEAE-Sepharose Fast Flow column equilibrated in 200 mM Tris-Cl at pH 8. Typically, between 150 and 200 mg of pure choline oxidase could be obtained from 4.5 liters of liquid Luria-Bertani culture medium (Table 3.2).

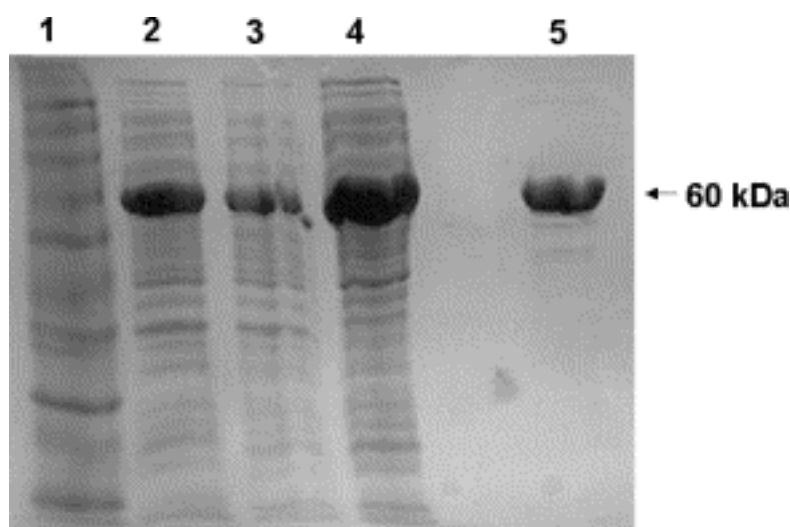


**Figure 3.1.** Purification of recombinant *A. globiformis* choline oxidase heterogously expressed in *E. coli*.

*Lane 1*, marker proteins; *lane 2*, cell-free extract of *E. coli* strain Rosetta(DE3)pLysS harboring plasmid pET/*codA1* induced with 0.05 mM IPTG for 5 hours at 22 °C; *lane 3*, sample treated with 20 µg/ml RNase and 50 µg/ml DNase in the presence of 10 mM MgCl<sub>2</sub>; *lane 4*, sample treated with 30 and 65% ammonium sulfate saturation; and *lane 5*, purified choline oxidase in 200 mM Tris-Cl, pH 8, after DEAE-Sephacrose column chromatography. The molecular mass of purified choline oxidase is indicated.

**Table 3.2.** Purification of Recombinant *A. globiformis* Choline Oxidase Heterogously Expressed in *E. coli*.

Step	Total protein, mg	Total activity <sup>a</sup> , µmol O <sub>2</sub> min <sup>-1</sup>	Specific activity, µmol O <sub>2</sub> min <sup>-1</sup> mg <sup>-1</sup>	Yield, %
Cell-free extract	1,830	1,080	0.59	100
Nuclease treated	1,500	1,060	0.71	98
30-65% Saturation of (NH <sub>4</sub> ) <sub>2</sub> SO <sub>4</sub>	1,240	1,040	0.84	96
DEAE-Sephacrose FF	185	940	5.3	87

<sup>a</sup>Enzymatic activity was measured with 10 mM choline as substrate in air-saturated 50 mM potassium phosphate, pH 7.0 and 25 °C, by monitoring the rate of oxygen consumption with a Clark-type oxygen electrode.

***Physical Properties of Recombinant Choline Oxidase.*** The molecular weight of recombinant choline oxidase was determined by MALDI-TOF mass spectrometry. Two peaks with  $m/z^+$  values of 30,307.5 and 60,618.3 were observed using the positive ion mode, corresponding to the doubly and singly protonated species of the protein, respectively (Figure 3.2). A molecular weight of  $60,614 \pm 5$  was calculated from the mass spectroscopic data, in agreement with the expected value of 60,612 calculated from the amino acid composition of the protein with one linked FAD moiety [31,43,44].

The oligomerization state of choline oxidase was determined by size exclusion chromatography onto a Sephacryl S-400 column under non-denaturing conditions. The results indicated that at concentrations of 10 or 100  $\mu\text{M}$  the enzyme has apparent molecular weights of 117,000 and 122,000, respectively (data not shown), indicating that the enzyme exists in solution as a dimer. Non-denaturing PAGE conditions of the enzyme at concentrations in the range between 2 and 48  $\mu\text{M}$  yielded single bands with similar relative migration, suggesting that the oligomerization state of choline oxidase is not dependent on the concentration of the enzyme (data not shown).

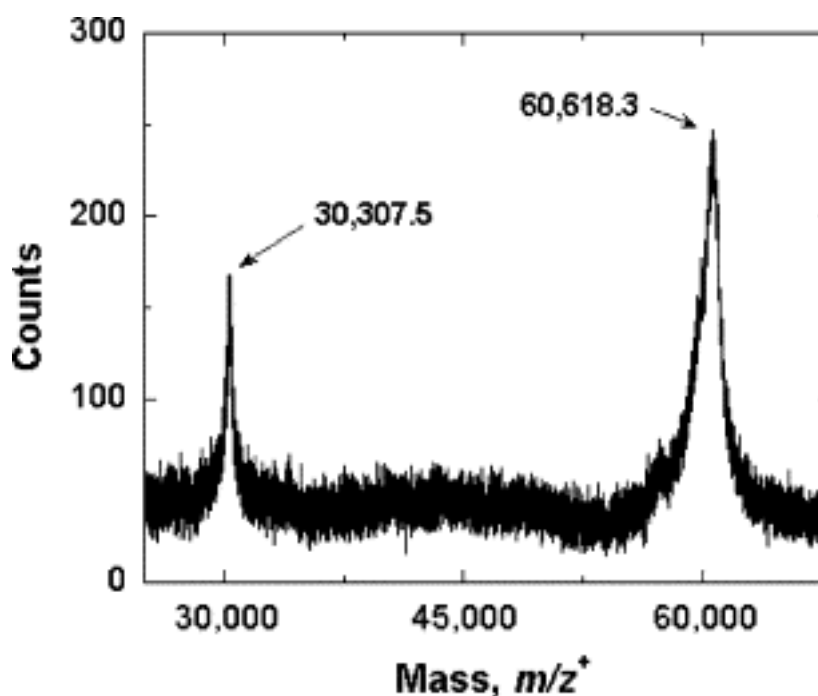


**Figure 3.2.** MALDI-TOF mass spectrometric analysis of recombinant choline oxidase. Choline oxidase at a concentration of 46  $\mu\text{M}$  was prepared as described in Experimental Procedures. Peaks with  $m/z^+$  values of 60,618.3 and 30,307.5 represent the singly and doubly protonated species of the protein.

**Flavin Content of Recombinant Choline Oxidase.** The UV-visible absorbance spectrum of the enzyme as purified is shown in Figure 3.3. Absorbance maxima were observed at 272, 373, and 454 nm, as expected for a flavin-containing enzyme but with relative intensities of the peaks in the near UV and visible regions of the spectrum suggesting that the bound flavin was present as a mixture of oxidized and anionic semiquinone states <sup>1</sup> (42). Significant variability in the relative intensities of the absorbance maxima in the near UV and visible regions of the spectrum was observed among different preparations of enzyme, with  $A_{454}/A_{373}$  ratios ranging from 0.4 to 0.7 (data not shown). Upon denaturation of the enzyme by treatment with urea, a

<sup>1</sup> A spectroscopic investigation of recombinant choline oxidase by using UV-visible and fluorescence spectroscopy, electron spin resonance, and circular dichroism, is consistent with the presence of an anionic semiquinone flavin in the enzyme as purified (36). Steady state kinetic data on the enzyme as purified suggest that the semiquinone flavin of choline oxidase is not catalytically relevant (36).

decrease in the 373 nm peak with concomitant increase in the absorbance in the 450 nm region were observed (Figure 3.3), consistent with oxidation of the semiquinone to form fully oxidized FAD in the denatured enzyme. This enzyme was devoid of enzymatic activity using 10 mM choline as substrate at pH 7, suggesting that the treatment with urea completely denatured the enzyme. No significant changes in the UV-visible absorbance spectrum of the denatured enzyme were seen after dialysis with decreasing amounts of urea, consistent with FAD being covalently bound to the enzyme (data not shown). Also, the UV-visible spectrum of a soluble fraction prepared upon treatment of choline oxidase with 10% trichloroacetic acid followed by centrifugation to remove the denatured protein was devoid of absorbance (Figure 3.3), further consistent with FAD being covalently bound to the protein. A stoichiometry of  $0.88 \pm 0.12$  FAD/monomer of enzyme could be calculated from the results of six independent experiments. The visible fluorescence emission spectrum of purified choline oxidase showed a maximum in the 525 to 530 nm region (with  $\lambda_{ex}$  at 454 nm), with about 6% the intensity of an equimolar solution of free FAD (Figure 3.3).

***Kinetic Properties of Recombinant Choline Oxidase.*** The steady state kinetic parameters for choline and betaine aldehyde as substrate for the enzyme as purified were determined in air-saturated 50 mM potassium phosphate at pH 7 and 25 °C. Apparent  $k_{cat}$  values of  $13.4 \pm 0.5$  and  $11.6 \pm 0.3 \text{ s}^{-1}$  per active site oxidized flavin and  $K_m$  values of  $0.6 \pm 0.1$  and  $2.3 \pm 0.2 \text{ mM}$  were determined with choline and betaine aldehyde, respectively. While the  $K_m$  values for recombinant choline oxidase compared well with the values of 0.6 and 2.4 mM previously reported for choline and betaine aldehyde as substrates for the native enzyme from *A. globiformis*, the  $k_{cat}$  values were between 3- and 6-fold larger, suggesting a higher purity of our enzyme preparation as compared to that of the commercially available enzyme (33).



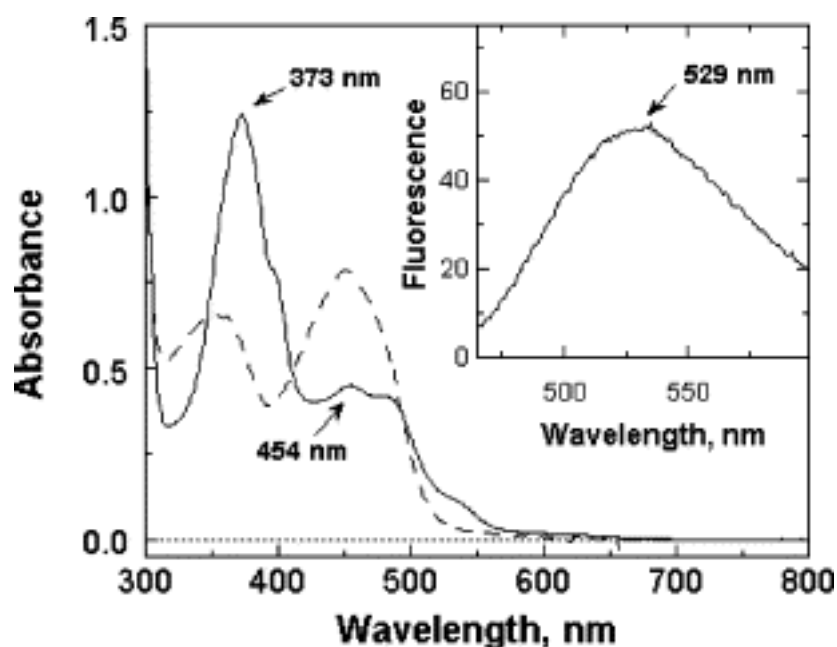


**Figure 3.3.** UV-Visible absorbance spectrum of recombinant choline oxidase.

*Solid line*, choline oxidase as purified at a concentration of 112  $\mu\text{M}$  in 200 mM Tris-Cl, pH 8; *dashed line*, after treatment with 4 M urea at 40  $^{\circ}\text{C}$  for 40 min; *dotted line*, soluble fraction after treatment of choline oxidase with 10% trichloroacetic acid for 5 min at 100  $^{\circ}\text{C}$  and centrifugation to remove denatured protein. *Inset*, fluorescence emission spectrum of choline oxidase as purified at a concentration of 28  $\mu\text{M}$  in 200 mM Tris-Cl, pH 8 and 15  $^{\circ}\text{C}$ . The excitation wavelength was at 454 nm.

## Discussion

Our group recently reported studies on the steady state kinetic mechanism, pH and substrate kinetic isotope effects on choline oxidase from *A. globiformis* (33, 34). Those studies define a framework for advanced biophysical and mechanistic studies on choline oxidase, for which large amounts of enzyme are required. To date, the enzyme from *A. globiformis* is the only choline oxidase for which the nucleotide sequence of the full gene has been reported (27). In the present study, we have cloned and heterogously expressed in *E. coli* the gene encoding for choline oxidase from *A. globiformis* genomic DNA, and purified to homogeneity the resulting protein.

Purified choline oxidase expressed in *E. coli* contains covalently bound FAD, as indicated by the mass spectroscopic analysis of the purified enzyme. Thus, the covalent linkage between His-87 and the 8 $\alpha$  position of the flavin ring is preserved in the recombinant enzyme (43), consistent with flavinylation of the protein being a self-catalytic process. In this respect, self-flavinylation of histidyl, tyrosyl, and cysteinyl residues to the 8 $\alpha$  position of the flavin ring was previously proposed to occur through initial flavin tautomerization to yield an electrophilic iminoquinone methide, which is stabilized by the presence of a positive charge located near the N(1)-C(2)=O(2) position of the flavin (43-46). Consistent with such a proposed mechanism for protein flavinylation, the presence of a weak positive charge in proximity of the flavin N(1)-C(2)=O(2) locus of choline oxidase is suggested by both stabilization of the anionic flavin semiquinone and formation of a complex with sulfite (36,47).

Under non-denaturing conditions, choline oxidase is a dimer of identical subunits with each subunit containing FAD in a 1:1 stoichiometry per monomer of protein. The oligomerization state of the recombinant enzyme determined in this study does not agree with

earlier results on native choline oxidase from *A. globiformis* and *Alcaligenes* sp., showing masses of 83,000 and 72,000 Da, respectively (1, 31). In this respect, lower native masses were reported for cholesterol oxidase from *Schizophyllum commune* (48) and *Streptomyces hygroscopicus* (49), for which interactions of the enzyme with the matrix of the resins used for the size exclusion chromatography experiments were proposed. In contrast, a dimeric oligomerization state was determined in previous studies for the enzyme from *Cylindrocarpon didymum* M-1 (30).

Choline oxidase does not contain dissociable flavins, as suggested by acid treatment of the enzyme followed by centrifugation to remove the precipitated protein. In this respect, the enzyme is different from sarcosine oxidase, a well-characterized enzyme containing both  $8\alpha$ -*N*(3)-histidyl-FMN and non-covalently bound FAD (50, 51). The mechanistic implication of choline oxidase containing only one type of flavin,  $8\alpha$ -*N*(1)-histidyl-FAD (43), is that a possible catalytic mechanism in which one flavin in the dimeric protein is responsible for choline oxidation while the second flavin carries out the oxidation of betaine aldehyde seems unlikely<sup>2</sup>. These observations are consistent with oxidation of choline to betaine aldehyde and of the aldehyde intermediate to glycine betaine occurring at the same enzyme active site in two subsequent catalytic steps (Scheme 3.1).

Our studies show that the *A. globiformis* genomic sequence originally reported in GenBank for the gene encoding for choline oxidase contains seven flaws, resulting in an amino acid sequence of the translated protein that is significantly different from the previously reported one. Mass spectrometric analysis of the resulting enzyme expressed in *E. coli* confirmed the

---

<sup>2</sup> The presence of a single type of flavin in choline oxidase also suggests that a catalytic mechanism in which one flavin in the dimeric enzyme dehydrogenates the substrate whereas a second flavin is responsible for oxygen reduction is also unlikely.

validity of the sequencing results<sup>3</sup>. Furthermore, the protein homology between choline oxidase and other members of the GMC oxidoreductase superfamily increased significantly when the newly determined amino acid sequence was used instead of the previously determined one (Figure 3.4). For example, the identities and similarities between choline oxidase and choline dehydrogenase increased from 28 to 34% and from 57 to 63%, respectively. The errors in the nucleotide sequence of the *codA* gene previously reported using the pGAH/*codA* construct likely arose from the high GC content of the *codA* gene, which could affect the fidelity of DNA polymerase in the sequencing reaction.

In summary, choline oxidase was cloned from genomic DNA of *A. globiformis* and heterologously expressed to high yields in *E. coli*. The resulting recombinant enzyme was highly purified and showed to be a dimer of identical subunits containing covalently bound FAD. To our knowledge, this study represents the first instance in which recombinant choline oxidase has been overexpressed and obtained in pure form. The availability of large quantities of recombinant choline oxidase will prove an invaluable tool for detailed mechanistic and structural studies aimed at a better understanding of four-electron oxidations of unactivated alcohols and of the mechanism of CH bond cleavage of alcohols and aldehydes catalyzed by the same flavin-linked active site. Finally, the determination of the correct nucleotide sequence of the gene encoding for choline oxidase will provide the basis for performing site-directed mutagenesis studies in this enzyme of biotechnological and medical interest.

---

<sup>3</sup> The mass of the enzyme with one linked FAD moiety is 60,612 Da when calculated by using the newly determined amino acid sequence, and 59,648 Da by using the previously reported amino acid sequence. Therefore, the experimentally determined mass of 60,614 Da for the enzyme as purified is in good agreement with the sequencing results.

CHO	-----	-----	-----MH	IDNIENLSDR	<b>EF</b> DyIv <b>GgG</b>	SA <b>GAAV</b> A <b>RL</b>	32
CHD	-----	-----	-----	-----MSQAT	<b>EF</b> DyI <b>I</b> <b>GAG</b>	SA <b>G</b> NV <b>L</b> A <b>RL</b>	25
AO	-----	-----	-----	-----MAIPE	<b>EF</b> DyIv <b>GgG</b>	ST <b>G</b> CV <b>I</b> A <b>RL</b>	25
GO	MQTL <b>LLV</b> SSLV	VSLAAALPHY	IRSN <b>G</b> IEASL	LTDPKDVSGR	<b>TV</b> DyI <b>I</b> A <b>GgG</b>	LT <b>G</b> LT <b>A</b> A <b>RL</b>	60
CHO	S-EDPA <b>V</b> S <b>V</b> A	<b>LV</b> E <b>A</b> G <b>P</b> DDR-	GVPEVLQ <b>L</b> DR	WMELLES <b>G</b> --	YDWD <b>Y</b> PIEPQ	-ENGNS <b>F</b> MRH	87
CHD	T-EDSD <b>V</b> S <b>V</b> L	<b>LLE</b> A <b>G</b> SPDY-	RFDFRTQ <b>M</b> PA	ALAYPLQ <b>G</b> KR	YNWA <b>F</b> ETDPE	PHMDNR <b>R</b> MEC	83
AO	ANVDEN <b>L</b> K <b>V</b> L	<b>LI</b> EN <b>G</b> NNL-	NNPWVYL <b>P</b> GI	YPRN <b>M</b> RLDSK	TAT <b>F</b> YNSRPS	KHLNG <b>R</b> RAIV	84
GO	T-ENPN <b>I</b> S <b>V</b> L	<b>VIE</b> S <b>G</b> SYESD	RGPIED <b>L</b> NA	YGDIF <b>G</b> SS--	VDHA <b>Y</b> ETVEL	-ATNN <b>Q</b> TALI	116
CHO	ARAK <b>V</b> M <b>G</b> G <b>C</b> S	SH <b>N</b> SCIA <b>F</b> WA	PRED <b>L</b> DE <b>W</b> EA	KYGAT <b>W</b> NAE	AAW <b>P</b> LYK <b>R</b> L <b>E</b>	TN-----	139
CHD	GRG <b>K</b> L <b>G</b> G <b>S</b> S	LI <b>N</b> GM <b>C</b> YIRG	NALD <b>Y</b> D <b>H</b> WAK	QPGLEE <b>W</b> DYL	SCL <b>P</b> Y <b>F</b> K <b>K</b> S <b>E</b>	T-----	134
AO	PQAN <b>L</b> L <b>G</b> G <b>S</b> S	SI <b>N</b> FM <b>Y</b> TRA	SASD <b>Y</b> D <b>W</b> ES	---EG <b>W</b> TTD	ELL <b>P</b> L <b>M</b> K <b>K</b> F <b>E</b>	TY-----	132
GO	RS <b>G</b> N <b>L</b> L <b>G</b> G <b>S</b> T	LV <b>N</b> GGT <b>W</b> TRP	HKAQ <b>V</b> D <b>S</b> WET	VFGNE <b>W</b> NWD	NVA <b>A</b> Y <b>S</b> LQ <b>A</b> E	RARAP <b>N</b> AQ <b>I</b>	176
CHO	-EDAG <b>P</b> DAPH	H <b>G</b> DS <b>G</b> PV <b>H</b> LM	NVPP--- <b>KD</b> P	TGVALL <b>D</b> ACE	QA <b>G</b> I <b>P</b> RAK <b>F</b> N	TGTT <b>V</b> VN- <b>G</b> A	194
CHD	-RDIG <b>P</b> NDYH	G <b>G</b> DGPV <b>S</b> VTT	PKAG--- <b>NN</b> P	LYRT <b>F</b> IE <b>A</b> GK	QA <b>G</b> Y <b>P</b> ETED <b>V</b>	NGYQ <b>E</b> -- <b>G</b> F	188
AO	-QRPC <b>N</b> NRDV	H <b>G</b> FDG <b>P</b> IK <b>V</b> S	FGNY--- <b>TY</b> P	QCQD <b>F</b> LR <b>A</b> CE	TQ <b>G</b> I <b>P</b> YVDD <b>L</b>	EDLKT <b>S</b> HG <b>A</b> E	188
GO	AAGHY <b>F</b> NASC	H <b>G</b> VNGT <b>V</b> HAG	PRDTGDD <b>S</b> P	IVKAL <b>M</b> S <b>A</b> VE	DR <b>G</b> V <b>P</b> TK <b>K</b> DF	GCGDP <b>H</b> -- <b>G</b> V	234
CHO	N <b>F</b> FQINRRAD	GT <b>R</b> SSSS <b>S</b> V <b>Y</b>	IHPIVE-Q <b>E</b> N	<b>F</b> TL <b>L</b> TGLRAR	QL <b>V</b> FDAD <b>R</b> RC	T-GVD <b>I</b> VDSA	252
CHD	GP <b>M</b> DRFVTPK	GR <b>R</b> ASTAR <b>G</b> Y	LDTAKQ-R <b>S</b> N	<b>L</b> T <b>I</b> E <b>T</b> RAVTD	V <b>I</b> E <b>F</b> EGKR--	--AV <b>G</b> V <b>R</b> YEQ	243
AO	QWLK <b>I</b> NRDF	GR <b>R</b> SDTA <b>H</b> A <b>F</b>	IHSTM <b>R</b> N <b>K</b> EN	<b>L</b> FL <b>M</b> TNTK <b>V</b> D	K <b>V</b> I <b>I</b> EDGRA <b>V</b>	A-VRT <b>V</b> PS <b>K</b> P	247
GO	SM <b>F</b> PNTLHED	Q <b>V</b> RSDAARE <b>W</b>	LLPNYQ-R <b>P</b> N	<b>L</b> QVL <b>T</b> GQY <b>V</b> G	K <b>V</b> LL <b>S</b> QNG <b>T</b> T	PRAVG <b>V</b> E <b>F</b> GT	293
CHO	FGHT--- <b>H</b> RL	T <b>A</b> RNEV <b>V</b> LST	<b>G</b> AID <b>T</b> P <b>K</b> LL <b>M</b>	<b>L</b> SG <b>I</b> G <b>P</b> AA <b>H</b> L	AEH <b>G</b> IEV <b>L</b> VD	<b>S</b> P <b>G</b> V <b>G</b> EHL <b>Q</b> D	309
CHD	KGQP--- <b>K</b> QA	R <b>A</b> RREV <b>L</b> LCG	<b>G</b> AIAS <b>P</b> Q <b>I</b> L <b>Q</b>	<b>R</b> SG <b>V</b> G <b>N</b> PE <b>W</b> L	KEL <b>G</b> IPV <b>V</b> HE	<b>L</b> P <b>G</b> V <b>G</b> EN <b>L</b> Q <b>D</b>	300
AO	IGDSK <b>V</b> S <b>R</b> TF	K <b>A</b> RKQ <b>I</b> V <b>V</b> SC	<b>G</b> T <b>V</b> SS <b>P</b> M <b>V</b> L <b>Q</b>	<b>R</b> SG <b>I</b> G <b>E</b> PS <b>K</b> L	RAA <b>G</b> V <b>K</b> E <b>I</b> VE	<b>L</b> P <b>G</b> V <b>G</b> EN <b>F</b> Q <b>D</b>	307
GO	HKG <b>N</b> -- <b>T</b> HNV	<b>Y</b> AKHEV <b>L</b> LAA	<b>G</b> S <b>A</b> V <b>S</b> P <b>T</b> IL <b>E</b>	<b>Y</b> SG <b>I</b> G <b>M</b> K <b>S</b> IL	EPL <b>G</b> ID <b>T</b> V <b>V</b> D	<b>L</b> P-V <b>G</b> LN <b>L</b> Q <b>D</b>	350
CHO	H <b>P</b> EGV <b>V</b> QFEA	KQPMVAESTQ	WW-----	E <b>I</b> G-----	-----	--IFT <b>P</b> TED <b>G</b>	342
CHD	H <b>L</b> EMY <b>I</b> QYEC	KEPISLYPAL	KWYNQ---P	K <b>I</b> GAE <b>W</b> L <b>F</b> K <b>G</b>	TGVGAS <b>N</b> Q <b>F</b> E	SCGP <b>I</b> RS <b>R</b> DD	356
AO	H <b>F</b> CY <b>F</b> V <b>P</b> YRI	KQDSSE <b>F</b> DA <b>F</b>	VSGDK <b>E</b> AQ <b>K</b> S	A <b>F</b> DQWYAT <b>G</b> A	GPLAT <b>N</b> GIEA	GVK <b>I</b> R <b>P</b> TE <b>A</b> E	367
GO	QTTAT <b>V</b> RSRI	TSAGAGQ <b>G</b> QA	AWFAT <b>P</b> N--E	T <b>F</b> G-----D	YSEKA <b>H</b> ELLN	TKLEQ <b>W</b> ABEA	402
CHO	LDRPDLMMHY	GSVP <b>F</b> DM <b>N</b> TL	RH---GYPTT	ENG <b>F</b> SLTP <b>N</b> V	THAR-----	----- <b>S</b> R <b>G</b> T	387
CHD	EEWP <b>N</b> LQYHF	LP <b>I</b> AIS <b>Y</b> N <b>G</b> K	-----SAVQ	ANG <b>F</b> QAHV <b>G</b> S	MRSE-----	----- <b>S</b> R <b>G</b> R	398
AO	LATADKAP <b>Q</b> Q	GWESY <b>F</b> E <b>N</b> K <b>P</b>	DKPLM <b>H</b> YS <b>V</b> I	SG <b>F</b> GD <b>H</b> TRL	PPGKY <b>M</b> TM <b>F</b> H	PLEY <b>P</b> FS <b>R</b> G <b>W</b>	427
GO	VARGGFHNTT	ALLIQ <b>Y</b> E <b>N</b> YR	DWIVN <b>H</b> NVAY	SEL <b>F</b> LDTAG <b>V</b>	ASFDV <b>V</b> NDLL <b>F</b>	-----FD <b>R</b> G <b>Y</b>	457
CHO	<b>V</b> RLRSR <b>D</b> FRD	KP-MVD <b>P</b> RY <b>F</b>	TDPEGHDMRV	MVAGIRKARE	IAAQ <b>P</b> AMA <b>E</b> W	TGRELS <b>P</b> G <b>V</b> E	446
CHD	<b>I</b> RLTSK <b>D</b> PHA	AP-SIL <b>F</b> NY <b>M</b>	AKEK--DWEE	FRDAIRLTRE	IIAQ <b>P</b> AFDRY	RGREIS <b>P</b> GP <b>D</b>	455
AO	LHIS <b>S</b> D <b>P</b> YA	AP-DFD <b>P</b> G <b>F</b> M	NDDR--DMWP	MVWAF <b>K</b> KSRE	TARRME <b>C</b> FAG	EPTAF <b>H</b> PHY <b>X</b>	484
GO	<b>V</b> HILDK <b>D</b> PYL	HHFAYD <b>P</b> Q <b>Y</b> F	LNEQ---LA	RNTISN----	---SGAMQ <b>T</b> Y	PAGEIL <b>P</b> G <b>D</b> N	505
CHO	AQT-----	-----	-----	-----	-----	-----	449
CHD	VQS-----	-----	-----	-----	-----	-----	458
AO	VDS <b>P</b> ARALEQ	SAEDTK <b>R</b> VAG	PLHLTANLYH	GSWST <b>P</b> IGEA	DKHDP <b>N</b> HVTS	SHIN <b>V</b> YSKDI	544
GO	LAYD-----	-----	-----	-----	-----A	D-----	511
CHO	-----DEEL	QDYIRK <b>T</b> HNT	<b>V</b> YH <b>P</b> V <b>G</b> T <b>V</b> R <b>M</b>	GAV----ED	EMS <b>P</b> L <b>D</b> PELR	<b>V</b> K <b>G</b> V <b>T</b> GL <b>R</b> V <b>A</b>	498
CHD	-----DEEL	DN <b>F</b> V <b>K</b> QHAET	<b>A</b> YH <b>P</b> C <b>G</b> SC <b>R</b> M	G-----EG	DMAV <b>T</b> DAQGR	<b>V</b> H <b>G</b> L <b>E</b> GL <b>R</b> V <b>V</b>	505
AO	QYTKEDDEAI	ENY <b>I</b> KEHAET	<b>T</b> WH <b>C</b> L <b>G</b> T <b>N</b> S <b>M</b>	APREGNKNAP	EGGV <b>L</b> D <b>P</b> RLN	<b>V</b> H <b>G</b> V <b>K</b> GL <b>K</b> V <b>A</b>	604
GO	-----LSAN	TEYIPYHFRP	<b>N</b> YH <b>D</b> V <b>G</b> T <b>C</b> S <b>M</b>	MP-----KE	MGSV <b>V</b> DNAAR	<b>V</b> Y <b>G</b> V <b>R</b> GL <b>R</b> V <b>I</b>	559
CHO	<b>D</b> AS <b>V</b> M <b>P</b> EHVT	V <b>N</b> PNIT <b>V</b> MM <b>I</b>	<b>G</b> ERCAD <b>L</b> IRS	ARAGETTTAD	AELSAALA--	-----	546
CHD	<b>D</b> AS <b>L</b> F <b>P</b> VIPT	G <b>N</b> L <b>N</b> APT <b>I</b> ML	<b>A</b> E <b>K</b> IAD <b>R</b> IRG	REPLPRASVD	YYVANGAPAK	QAS-----	558
AO	<b>D</b> LS <b>V</b> C <b>P</b> DNVG	CNT <b>F</b> STAL <b>T</b> I	<b>G</b> E <b>K</b> AAV <b>L</b> VAE	DLGYS <b>G</b> SELD	MEVPQ <b>H</b> KLKT	YEQ <b>T</b> GAARY	663
GO	<b>D</b> G <b>S</b> I <b>P</b> PTQMS	SHVMT <b>V</b> FYAM	<b>A</b> LKIS <b>D</b> AILE	DYAS <b>M</b> Q----	-----	-----	595

**Figure 3. 4.** Alignment of choline oxidase with selected members of the GMC oxidoreductase enzyme superfamily.

CHO, choline oxidase from *A. globiformis* (GenBank accession no. [AAP68832](#)); CHD, choline dehydrogenase from *Halomonas elongata* (GenBank accession no. [CAB77176](#)); AO, alcohol oxidase from *Candida bodinii* (GenBank accession no. [JC1117](#)); and GO, glucose oxidase from *Aspergillus niger* (GenBank accession no. [AF234246.2](#)).

### Acknowledgments

The authors thank Dr. Norio Murata at the National Institute for Basic Biology, Okazaki, Japan, for the kind gift of *E. coli* strain JM109 cells harboring the plasmid pGAH/*codA*; Ms. Ping Yiang at the DNA Core Facility of the Biology Department of Georgia State University for preparation of the oligonucleotide primers and for DNA sequencing; and Dr. David Bostwick at the Georgia Institute of Technology for the MALDI-TOF mass spectrometric analyses. This work was supported in part by Grant PRF #37351-G4 from the American Chemical Society (G.G.), a Research Initiation Grant and a Quality Improvement Fund from Georgia State University (G.G.).

## References

- (1) Ikuta, S., Imamura, S., Misaki, H., and Horiuti, Y. (1977) Purification and characterization of choline oxidase from *Arthrobacter globiformis*, *J. Biochem. (Tokyo)* 82, 1741-9.
- (2) Burg, M. B., Kwon, E. D., and Kultz, D. (1997) Regulation of gene expression by hypertonicity, *Annu. Rev. Physiol.* 59, 437-55.
- (3) Csonka, L. N., and Epstein, W. (1996) Osmoregulation, in *Escherichia coli and Salmonella: Cellular and Molecular Biology* (Neidhardt, F. C., Curtiss III, R., Ingraham, J. L., Lin, E. C. C., Low, K. B., Magasanik, B., Reznikoff, W. S., Riley, M., Schaechter, M., and Umberger, H. E., Eds.) pp 1210-1223, ASM Press, Washington, D.C.
- (4) Kempf, B., and Bremer, E. (1998) Uptake and synthesis of compatible solutes as microbial stress responses to high-osmolality environments, *Arch. Microbiol.* 170, 319-30.
- (5) McNeil, S. D., Nuccio, M. L., and Hanson, A. D. (1999) Betaines and related osmoprotectants. Targets for metabolic engineering of stress resistance, *Plant Physiol.* 120, 945-50.
- (6) Bremer, E., and Kramer, R. (2000) Coping with Osmotic Challenges: Osmoregulation through Accumulation and Release of Compatible Solutes in Bacteria., in *Bacterial Stress Response* (Storz, G., and Hengge-Areonis, R., Eds.) pp 79-97, ASM Press, Washington, D.C.
- (7) Ko, R., Smith, L. T., and Smith, G. M. (1994) Glycine betaine confers enhanced osmotolerance and cryotolerance on *Listeria monocytogenes*, *J. Bacteriol.* 176, 426-31.
- (8) Smith, L. T. (1996) Role of osmolytes in adaptation of osmotically stressed and chill-stressed *Listeria monocytogenes* grown in liquid media and on processed meat surfaces, *Appl. Environ. Microbiol.* 62, 3088-93.
- (9) Bayles, D. O., and Wilkinson, B. J. (2000) Osmoprotectants and cryoprotectants for *Listeria monocytogenes*, *Lett. Appl. Microbiol.* 30, 23-7.
- (10) Sakamoto, A., Alia, Murata, N., and Murata, A. (1998) Metabolic engineering of rice leading to biosynthesis of glycinebetaine and tolerance to salt and cold, *Plant Mol. Biol.* 38, 1011-9.
- (11) Sakamoto, A., Valverde, R., Alia, Chen, T. H., and Murata, N. (2000) Transformation of *Arabidopsis* with the *codA* gene for choline oxidase enhances freezing tolerance of plants, *Plant J.* 22, 449-53.
- (12) Sakamoto, A., and Murata, N. (2001) The use of bacterial choline oxidase, a glycinebetaine-synthesizing enzyme, to create stress-resistant transgenic plants, *Plant Physiol.* 125, 180-8.

- (13) Kilbourne, J. P. (1978) Bacterial content and ionic composition of sputum in cystic fibrosis, *Lancet* *i*, 334.
- (14) Lisa, T. A., Casale, C. H., and Domenech, C. E. (1994) Cholinesterase, acid phosphatase, and phospholipase C of *Pseudomonas aeruginosa* under hyperosmotic conditions in a high-phosphate medium, *Curr. Microbiol.* *28*, 71-76.
- (15) Pesin, S. R., and Candia, O. A. (1982) Acetylcholine concentration and its role in ionic transport by the corneal epithelium, *Invest. Ophthalmol. Vis. Sci.* *22*, 651-9.
- (16) Wright, J. R., and Clements, J. A. (1987) Metabolism and turnover of lung surfactant, *Am. Rev. Respir. Dis.* *136*, 426-44.
- (17) Aguilar, A., Merino, S., Rubires, X., and Tomas, J. M. (1997) Influence of osmolarity on lipopolysaccharides and virulence of *Aeromonas hydrophila* serotype O:34 strains grown at 37 degrees C, *Infect. Immun.* *65*, 1245-50.
- (18) Leclerc, G. J., Tartera, C., and Metcalf, E. S. (1998) Environmental regulation of *Salmonella typhi* invasion-defective mutants, *Infect. Immun.* *66*, 682-91.
- (19) Tartera, C., and Metcalf, E. S. (1993) Osmolarity and growth phase overlap in regulation of *Salmonella typhi* adherence to and invasion of human intestinal cells, *Infect. Immun.* *61*, 3084-9.
- (20) Badger, J. L., and Kim, K. S. (1998) Environmental growth conditions influence the ability of *Escherichia coli* K1 to invade brain microvascular endothelial cells and confer serum resistance, *Infect Immun* *66*, 5692-7.
- (21) Bajaj, V., Lucas, R. L., Hwang, C., and Lee, C. A. (1996) Co-ordinate regulation of *Salmonella typhimurium* invasion genes by environmental and regulatory factors is mediated by control of *hlyA* expression, *Mol. Microbiol.* *22*, 703-14.
- (22) Bermudez, L. E., Petrofsky, M., and Goodman, J. (1997) Exposure to low oxygen tension and increased osmolarity enhance the ability of *Mycobacterium avium* to enter intestinal epithelial (HT-29) cells, *Infect. Immun.* *65*, 3768-73.
- (23) Sage, A. E., and Vasil, M. L. (1997) Osmoprotectant-dependent expression of *plcH*, encoding the hemolytic phospholipase C, is subject to novel catabolite repression control in *Pseudomonas aeruginosa* PAO1, *J. Bacteriol.* *179*, 4874-81.
- (24) Schwan, W. R., Lee, J. L., Lenard, F. A., Matthews, B. T., and Beck, M. T. (2002) Osmolarity and pH growth conditions regulate *fim* gene transcription and type 1 pilus expression in uropathogenic *Escherichia coli*, *Infect. Immun.* *70*, 1391-402.
- (25) Alia, Hayashi, H., Chen, T. H. H., and Murata, N. (1998) Transformation with a gene for choline oxidase enhances cold tolerance of *Arabidopsis* during germination and early growth, *Plant, Cell and Environment* *21*, 232-239.



- (26) Alia, Hayashi, H., Sakamoto, A., and Murata, N. (1998) Enhancement of the tolerance of Arabidopsis to high temperatures by genetic engineering of the synthesis of glycinebetaine, *Plant J.* 16, 155-61.
- (27) Deshnum, P., Los, D. A., Hayashi, H., Mustardy, L., and Murata, N. (1995) Transformation of Synechococcus with a gene for choline oxidase enhances tolerance to salt stress, *Plant Mol. Biol.* 29, 897-907.
- (28) Hayashi, H., Alia, Mustardy, L., Deshnum, P., Ida, M., and Murata, N. (1997) Transformation of Arabidopsis thaliana with the codA gene for choline oxidase; accumulation of glycinebetaine and enhanced tolerance to salt and cold stress, *Plant J.* 12, 133-42.
- (29) Holmstrom, K. O., Somersalo, S., Mandal, A., Palva, T. E., and Welin, B. (2000) Improved tolerance to salinity and low temperature in transgenic tobacco producing glycine betaine, *J. Exp. Bot.* 51, 177-85.
- (30) Yamada, H., Mori, N., and Tani, Y. (1979) properties of choline oxidase of Cylyndrocarpon didymum M-1, *Agric. Biol. Chem.* 43, 2173-2177.
- (31) Ohta-Fukuyama, M., Miyake, Y., Emi, S., and Yamano, T. (1980) Identification and properties of the prosthetic group of choline oxidase from Alcaligenes sp, *J. Biochem. (Tokyo)* 88, 197-203.
- (32) Cavener, D. R. (1992) GMC oxidoreductases. A newly defined family of homologous proteins with diverse catalytic activities, *J. Mol. Biol.* 223, 811-4.
- (33) Gadda, G. (2003) Kinetic mechanism of choline oxidase from Arthrobacter globiformis, *Biochim. Biophys. Acta.* 1646, 112-8.
- (34) Gadda, G. (2003) pH and deuterium kinetic isotope effects studies on the oxidation of choline to betaine-aldehyde catalyzed by choline oxidase, *Biochim. Biophys. Acta.* 1650, 4-9.
- (35) Bradford, M. M. (1976) A rapid and sensitive method for the quantitation of microgram quantities of protein utilizing the principle of protein-dye binding, *Anal. Biochem.* 72, 248-54.
- (36) Ghanem, M., Fan, F., Francis, K., and Gadda, G. (2003) Spectroscopic and kinetic properties of recombinant choline oxidase from Arthrobacter globiformis, *Biochemistry* 42, 15179-15188.
- (37) Allison, D. R., and Purich, D. L. (1979) Practical considerations in the design of initial velocity enzyme rate assays, in *Methods Enzymol.* (Purich, D. L., Ed.) pp 3-19, Academic Press, New York.
- (38) Laemmli, U. K. (1970) Cleavage of structural proteins during the assembly of the head of bacteriophage T4, *Nature* 227, 680-5.

- (39) Whitby, L. G. (1953) *Biochem. J.* 54, 437-442.
- (40) Hayashi, H., Alia, Sakamoto, A., Nonaka, H., Chen, T. H. H., and Murata, N. (1998) Enhances germination under high-salt conditions of seeds of transgenic arabidopsis with a bacterial gene (codA) for choline oxidase, *J. Plant Res.* 111, 357-362.
- (41) Alia, Kondo, Y., Sakamoto, A., Nonaka, H., Hayashi, H., Saradhi, P. P., Chen, T. H., and Murata, N. (1999) Enhanced tolerance to light stress of transgenic Arabidopsis plants that express the codA gene for a bacterial choline oxidase, *Plant Mol. Biol.* 40, 279-88.
- (42) Massey, V., and Palmer, G. (1966) On the existence of spectrally distinct classes of flavoprotein semiquinones. A new method for the quantitative production of flavoprotein semiquinones, *Biochemistry* 5, 3181-9.
- (43) Trickey, P., Wagner, M. A., Jorns, M. S., and Mathews, F. S. (1999) Monomeric sarcosine oxidase: structure of a covalently flavinylated amine oxidizing enzyme, *Structure Fold Des.* 7, 331-45.
- (44) Khanna, P., and Jorns, M. S. (2003) Tautomeric rearrangement of a dihydroflavin bound to monomeric sarcosine oxidase or N-methyltryptophan oxidase, *Biochemistry* 42, 864-9.
- (45) Brandsch, R., and Bichler, V. (1991) Autoflavinylation of apo6-hydroxy-D-nicotine oxidase, *J Biol. Chem.* 266, 19056-62.
- (46) Kim, J., Fuller, J. H., Kuusk, V., Cunane, L., Chen, Z. W., Mathews, F. S., and McIntire, W. S. (1995) The cytochrome subunit is necessary for covalent FAD attachment to the flavoprotein subunit of p-cresol methylhydroxylase, *J Biol Chem* 270, 31202-9.
- (47) Massey, V., and Hemmerich, P. (1980) Active-site probes of flavoproteins, *Biochem. Soc. Trans.* 8, 246-57.
- (48) Fukuyama, M., and Miyake, Y. (1979) Purification and some properties of cholesterol oxidase from Schizophyllum commune with covalently bound flavin, *J. Biochem. (Tokyo)* 85, 1183-93.
- (49) Gadda, G., Wels, G., Pollegioni, L., Zucchelli, S., Ambrosius, D., Pilone, M. S., and Ghisla, S. (1997) Characterization of cholesterol oxidase from Streptomyces hygroscopicus and Brevibacterium sterolicum, *Eur. J. Biochem.* 250, 369-76.
- (50) Jorns, M. S. (1985) Properties and catalytic function of the two nonequivalent flavins in sarcosine oxidase, *Biochemistry* 24, 3189-94.
- (51) Willie, A., Edmondson, D. E., and Jorns, M. S. (1996) Sarcosine oxidase contains a novel covalently bound FMN, *Biochemistry* 35, 5292-9.

## CHAPTER IV

### **Spectroscopic and Kinetic Properties of Recombinant Choline Oxidase from *Arthrobacter globiformis***

(This chapter was published verbatim in Ghanem, M., Fan, F., Francis, K., and Gadda, G., (2003), *Biochemistry* 42, 15179-88. © 2003 American Chemical Society. All rights reserved. The first two authors share equal contribution to the publication. In particular, my contribution to this study pertains the spectrophotometric characterization of the enzyme bound flavin (E-FAD<sub>Ox</sub>/ E-FAD<sub>Sq</sub>), the reaction of choline oxidase with sulfite, and the enzymatic turnover with choline.)

#### **Abstract**

Choline oxidase catalyzes the four-electron oxidation of choline to glycine betaine, with molecular oxygen acting as primary electron acceptor. Recently, the recombinant enzyme expressed in *Escherichia coli* was purified to homogeneity and shown to contain FAD in a mixture of oxidized and anionic semiquinone redox states [Fan et al. (2004) *Arch. Biochem. Biophys.*, 421, 149-58]. In this study, methods have been devised to convert the enzyme-bound flavin semiquinone to oxidized FAD and vice versa, allowing characterization of the resulting forms of choline oxidase. The enzyme-bound oxidized flavin showed typical UV-visible absorbance peaks at 359 and 452 nm (with  $\epsilon_{452} = 11.4 \text{ M}^{-1}\text{cm}^{-1}$ ), and emitted light at 530 nm (with  $\lambda_{\text{ex}}$  at 452 nm). The affinity of the enzyme for sulfite was high (with a  $K_d$  value of  $\sim 50 \text{ }\mu\text{M}$  at pH 7 and 15 °C), suggesting the presence of a positive charge near the N(1)C(2)=O locus of the flavin. The enzyme-bound anionic flavin semiquinone was unusually insensitive to oxygen or ferricyanide at pH 8, and showed absorbance peaks at 372 and 495 nm ( $\epsilon_{372} = 19.95 \text{ M}^{-1}\text{cm}^{-1}$ ), maximal fluorescence emission at 454 nm (with  $\lambda_{\text{ex}}$  at 372 nm), circular dichroic signals at 370 and 406 nm, and an ESR peak-to-peak linewidth of 13.9 G. Both UV-visible absorbance studies on the enzyme under turnover with choline and steady state kinetic data with either choline or

betaine aldehyde were consistent with the flavin semiquinone being not involved in catalysis. The pH dependence of the kinetic parameters at varying concentrations of both choline and oxygen indicated that a catalytic base is required for choline oxidation but not for oxygen reduction and that the order of the kinetic steps involving substrate binding and product release is not affected by pH.

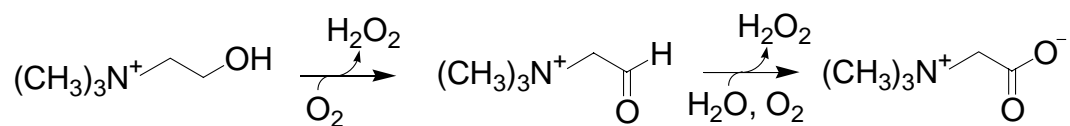
## Introduction

Choline oxidase (E.C. 1.1.3.17) catalyzes the four-electron oxidation of choline to glycine betaine (*N,N,N*-trimethylglycine; betaine) via betaine aldehyde as intermediate (Scheme 4.1) (1). The enzyme contains covalently bound FAD and utilizes molecular oxygen as primary electron acceptor (2-4). Among the members of the GMC oxidoreductase superfamily within which the enzyme can be grouped (5, 6), choline oxidase is unique in that it catalyzes the oxidation of a substrate primary alcohol to a carboxylic acid via an aldehyde intermediate. A similar oxidation reaction of an alcohol to a carboxylic acid is catalyzed by histidinol dehydrogenase (E.C. 1.1.1.23), a pyridine nucleotide-dependent enzyme well-characterized in its mechanistic and biochemical properties (7-17). In contrast, limited kinetic information is available on choline oxidase (18, 19). Consequently, the study of the mechanistic properties of choline oxidase provides the opportunity to compare the biochemical and mechanistic properties of the flavin-dependent oxidoreductases with those of the pyridine nucleotide-dependent reductases able to carry out a four-electron oxidation of a substrate alcohol. The study of an enzyme involved in glycine betaine biosynthesis is also of considerable interest for both biotechnological and biomedical applications, because recent studies have shown that accumulation of glycine betaine in the cytoplasm of cells allows growth in hyperosmotic environments of transgenic plants lacking efficient glycine betaine biosynthetic systems (20-26) and of clinical isolates of a number of human pathogens (27-34).

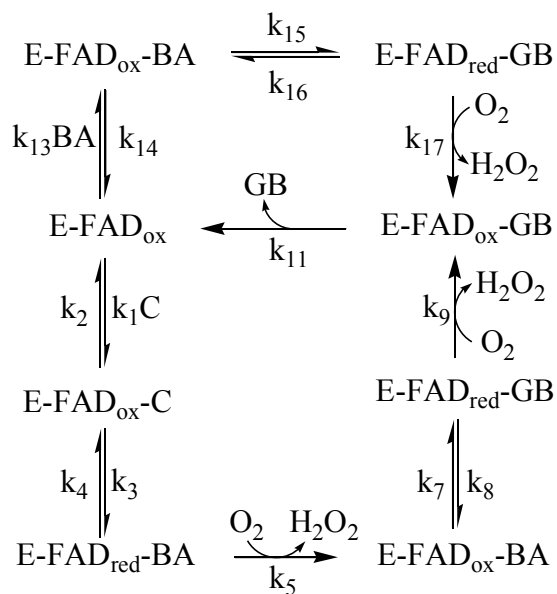
The analyses of the steady state kinetic mechanism and of the pH and deuterium kinetic isotope effects on the oxidation of choline to betaine aldehyde catalyzed by *Arthrobacter globiformis* choline oxidase were recently reported (18, 19). Briefly, with choline as substrate (lower loop in Scheme 4.2), after formation of the E-FAD<sub>ox</sub>-C complex and oxidation of choline

to yield betaine aldehyde bound to the reduced enzyme, oxygen reacts with the E-FAD<sub>red</sub>-BA complex. The catalytically competent E-FAD<sub>ox</sub>-BA species undergoes a second oxidation reaction in which glycine betaine is formed. Finally, the E-FAD<sub>red</sub>-GB complex reacts with oxygen before release of glycine betaine from the oxidized enzyme. With betaine aldehyde as substrate (upper loop in Scheme 4.2), after formation of the E-FAD<sub>ox</sub>-BA complex, betaine aldehyde is oxidized to yield glycine betaine bound to the reduced enzyme. Turnover is completed with reaction of the E-FAD<sub>red</sub>-GB complex with molecular oxygen and the final release of the product glycine betaine. A catalytic base with  $pK_a$  7.5 was proposed to participate in catalysis based on pH and substrate kinetic isotope effect studies on the enzyme (19).

Our group recently cloned the gene encoding for choline oxidase from genomic DNA of *A. globiformis* strain ATCC 8010 and expressed it to high yields in *Escherichia coli* (6). The resulting protein was purified to homogeneity and shown to be a homodimer of 120,000 Da with each subunit containing covalently-linked FAD in a mixture of semiquinone and oxidized redox states (6). In the present study, we have devised methods to obtain homogeneous preparations of recombinant choline oxidase with the flavin cofactor either in the oxidized or semiquinone state, and have characterized the biochemical and kinetic properties of the resulting forms of enzyme.



**Scheme 4.1.** Reaction catalyzed by choline oxidase.



**Scheme 4.2.** Steady state kinetics for choline oxidase.

## Experimental Procedures

**Materials.** Choline chloride was from ICN Pharmaceutical, Inc. Betaine aldehyde and glycine betaine were from Sigma-Aldrich. Recombinant choline oxidase from *A. globiformis* strain ATCC 8010 was expressed from plasmid pET/*codA1* and purified to homogeneity as described in (6). Choline oxidase as purified was stored at -20 °C in 200 mM Tris-Cl, pH 8, and found to be stable for at least six months. All other reagents were of the highest purity commercially available.

**Enzyme Assays.** The concentration of choline oxidase was determined with the method of Bradford (35), by using the Bio-Rad protein assay kit with bovine serum albumin as the standard. Enzyme activity was measured with the method of the initial rates (36) in air-saturated 50 mM potassium phosphate at pH 7 by monitoring the rate of oxygen consumption with a computer-interfaced Oxy-32 oxygen-monitoring system (Hansatech Instrument Ltd.) thermostated at 25 °C. The reactions were started by the addition of choline oxidase to a 1 ml reaction mixture, with the final concentration of enzyme in the 0.2 to 0.6  $\mu$ M range; the concentration of choline or betaine aldehyde was between 0.02 and 15 mM. When both choline (or betaine aldehyde) and oxygen concentrations were varied, the assay reaction mixture was equilibrated at the concentration of oxygen by bubbling the appropriate O<sub>2</sub>/N<sub>2</sub> gas mixture for 10 min before the reaction was started by the addition of the enzyme. When the pH was varied, 50 mM potassium phosphate was used between pH 6 and 8, and 50 mM sodium pyrophosphate was used in the pH ranges 5 to 6 and 8 to 10. Product inhibition studies were carried out by varying the concentrations of both glycine betaine and choline (or betaine aldehyde) in air-saturated 50 mM potassium phosphate, pH 6.75. One unit of enzymatic activity corresponds to the consumption of one  $\mu$ mol of oxygen per min.



UV-Visible absorbance spectra were recorded using an Agilent Technologies diode-array spectrophotometer Model HP 8453 equipped with a thermostated water bath. Fluorescence emission spectra were recorded with a Shimadzu Spectrofluorometer Model RF-5301 PC thermostated at 15 °C. Circular dichroism spectra were acquired using a Jasco J-810 spectropolarimeter at 22 °C.

**Methods.** Oxidized FAD-containing choline oxidase was prepared at 4 °C by dialysis against three 1-liter changes of 20 mM potassium phosphate, 20 mM sodium pyrophosphate, pH 6, over 24 hours, followed by two 1-liter changes of 200 mM Tris-Cl, pH 8 over five hours. This enzyme could be stored at -20 °C for at least 7 months without losses in enzymatic activity. The oxidized flavin content of choline oxidase as purified was determined from the  $\Delta A_{452}$  after treatment of the enzyme with 5 mM dithionite in air-saturated 200 mM Tris-Cl, pH 8, using an  $\epsilon_{452}$  value of  $8.4 \text{ mM}^{-1}\text{cm}^{-1}$ , which corresponds to the difference between the extinction coefficients for the enzyme-bound oxidized flavin ( $\epsilon_{452} = 8.4 \text{ mM}^{-1}\text{cm}^{-1}$ ) and semiquinone flavin ( $\epsilon_{452} = 3 \text{ mM}^{-1}\text{cm}^{-1}$ ). Reduction of choline oxidase with sodium dithionite was conducted aerobically in 200 mM Tris-Cl, pH 8, at 15 °C. Dithionite was either prepared just before use in the same buffer or added to the enzyme solution as a powder. For reactions with sodium sulfite, the reagent was prepared just prior to use as 1 M stock solution in 200 mM Tris-Cl, pH 8. Different amounts of sodium sulfite ranging from 0.5 to 25 mM were added to the enzyme solution in 200 mM Tris-Cl, pH 8, at 15 °C, and UV-visible absorbance spectra were recorded at different interval periods. Reversibility of the flavin-sulfite complex was determined by following the increase in absorbance at 452 nm following removal of the unbound sulfite by gel filtration using a Sephadex G-25 column (PD-10 column, Amersham-Pharmacia Biotech) equilibrated with 200 mM Tris-Cl, pH 8. For treatment of choline oxidase with an oxidizing

agent under non-denaturing conditions, the enzyme was incubated with 10 mM potassium ferricyanide for 30 min on ice in 10% glycerol, 1 mM EDTA, 20 mM Tris-Cl, pH 8, before removing ferricyanide by gel filtration using a Sephadex G-25 column equilibrated with 20 mM Tris-Cl, pH 8.

ESR spectral data were recorded in 3-mm quartz tubes at 141 K using a Bruker ER200D spectrophotometer equipped with an Oxford cryostat. Samples were prepared for ESR analysis by gel filtration through a Sephadex G-25 column equilibrated in 50 mM HEPES, pH 8, followed by freezing in liquid nitrogen. The following conditions and instruments settings were used: microwave power, 2 mW; modulation amplitude, 2 G; and microwave frequency, 9.4 GHz.

**Data Analysis.** Kinetic data were fit with the KaleidaGraph software (Adalbeck Software, Reading, PA) and the Enzfitter software (Biosoft, Cambridge, UK). Apparent kinetic parameters in atmospheric oxygen were determined by fitting initial reaction rates at different substrate concentrations to the Michaelis-Menten equation for one substrate. Initial rates determined by varying the concentration of both choline or betaine aldehyde and oxygen were fit to equations 1 and 2, respectively. Equation 1 describes a sequential steady state kinetic mechanism, whereas equation 2 describes a sequential mechanism in which  $K_a \ll K_{ia}$  (37).  $K_a$  and  $K_b$  are the Michaelis constants for choline (or betaine aldehyde) ( $A$ ) and oxygen ( $B$ ), respectively, and  $k_{cat}$  is the turnover number of the enzyme ( $e$ ).

$$\frac{v}{e} = \frac{k_{cat}AB}{K_aB + K_bA + AB + K_{ia}K_b} \quad (1)$$

$$\frac{v}{e} = \frac{k_{cat}AB}{K_bA + AB + K_{ia}K_b} \quad (2)$$

The pH dependences of steady state kinetic parameters were determined by fitting initial rate data to equation 3, which describes a curve with slope of +1 and a plateau region at high pH.

The pH dependence of inhibition by glycine betaine was determined by fitting the initial rate data to equation 4, which describes a curve with slope of -1 and a plateau region at low pH.  $C$  is the pH-independent value of the kinetic parameter of interest.

$$\log Y = \log \left( \frac{C}{1 + \frac{10^{-pH}}{10^{-pK_a}}} \right) \quad (3)$$

$$\log Y = \log \left( \frac{C}{1 + \frac{10^{-pK_a}}{10^{-pH}}} \right) \quad (4)$$

Product inhibition studies were performed by varying the concentrations of both glycine betaine and choline (or betaine aldehyde) at a fixed concentration of oxygen. The data were fit to equations 5 to 7, which describe competitive, uncompetitive, and noncompetitive inhibition patterns of the product and the organic substrate, respectively.  $P$  is the concentration of glycine betaine,  $K_{is}$  and  $K_{ii}$  are the inhibition constants for the slope and intercept term, respectively.

$$\frac{v}{e} = \frac{k_{cat}A}{K_a \left[ 1 + \left( \frac{P}{K_{is}} \right) \right] + A} \quad (5)$$

$$\frac{v}{e} = \frac{k_{cat}A}{K_a + A \left[ 1 + \left( \frac{P}{K_{ii}} \right) \right]} \quad (6)$$

$$\frac{v}{e} = \frac{k_{cat}A}{K_a \left[ 1 + \left( \frac{P}{K_{is}} \right) \right] + A \left[ 1 + \left( \frac{P}{K_{ii}} \right) \right]} \quad (7)$$

## Results

**Choline Oxidase as Purified (*E-FAD<sub>ox/sq</sub>*).** As shown in Figure 4.1, the UV-visible absorbance spectrum of recombinant choline oxidase as purified at pH 8 suggests that the enzyme-bound FAD is present as a mixture of oxidized and anionic semiquinone states (*E-FAD<sub>ox/sq</sub>*) (6). Upon treatment of the enzyme with 10 mM potassium ferricyanide at pH 8 followed by gel filtration to remove the oxidizing agent, no significant spectral changes in the near-UV and visible regions of the absorbance spectrum were observed (data not shown). These results indicate that the addition of an oxidant under non-denaturing conditions had no effect on the enzyme-bound flavin semiquinone.

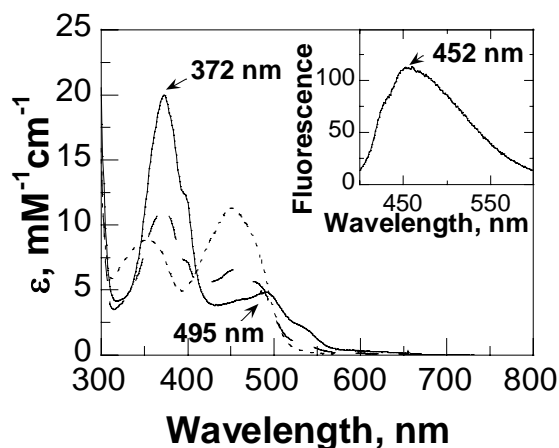


**Figure 4.1.** Reaction of recombinant choline oxidase with sodium dithionite.

*Dashed line*, the UV-visible absorbance spectrum of choline oxidase as purified was recorded at a concentration of 60  $\mu\text{M}$  in 200 mM Tris-Cl, pH 8; *solid line*, air-stable flavin semiquinone-containing enzyme prepared by treatment with 5 mM sodium dithionite in aerobiosis and gel filtration onto a Sephadex G-25 column equilibrated with the same buffer; *dotted line*, after treatment of the flavin semiquinone-containing enzyme with 4 M urea at 40  $^{\circ}\text{C}$  for 40 min. *Inset*, fluorescence emission spectrum of flavin semiquinone-containing choline oxidase at a concentration of 8  $\mu\text{M}$  in 200 mM Tris-Cl, pH 8 and 15  $^{\circ}\text{C}$ . The excitation wavelength was at 372 nm.

***Spectral Properties of Flavin Semiquinone-Containing Choline Oxidase (E-FAD<sub>sq</sub>).***

When the enzyme was incubated aerobically with 5 mM dithionite, a bleaching of the peak at 454 nm was observed in the visible absorbance spectrum of the enzyme and a spectrum with maxima at 372 and 495 nm was obtained (data not shown). The  $\Delta A_{452}$  was used to determine the FAD<sub>ox</sub> content per enzyme active site, by using the  $\epsilon_{452}$  values determined for the enzyme-bound flavin in the oxidized and semiquinone states (*see below*). Typically, the enzyme as purified contained variable amounts of flavin in the oxidized state, ranging from 15 to 55% of the total flavin content (data not shown). Removal of excess dithionite by gel filtration yielded a similar absorbance spectrum (Figure 4.1), indicating that the enzyme is capable of stabilizing the anionic semiquinone species of the flavin (FAD<sub>sq</sub>) in the presence of molecular oxygen. Upon incubation of the FAD<sub>sq</sub>-containing choline oxidase in the presence of 4 M urea, the visible absorbance spectrum of oxidized FAD with the typical peaks centered at 350 and 452 nm was observed (Figure 4.1), consistent with the FAD<sub>sq</sub> being stabilized by the protein microenvironment and the cofactor becoming fully oxidized by molecular oxygen upon unfolding the protein. An extinction coefficient of  $19.95 \text{ mM}^{-1}\text{cm}^{-1}$  was calculated at 372 nm for the enzyme-bound semiquinone of choline oxidase based upon the  $\epsilon_{450 \text{ nm}}$  value of  $11.3 \text{ mM}^{-1}\text{cm}^{-1}$  for FAD<sup>1</sup> after denaturation of the enzyme by treatment with urea (38). At pH 8 and 15 °C, the enzyme-bound anionic semiquinone emitted light at 454 nm upon excitation at 372 nm (Figure 4.1). As for the case of the visible absorbance spectrum, the typical fluorescence properties of oxidized FAD with maximal emission at 530 nm (with  $\lambda_{\text{max}}$  at 450 nm) were observed upon denaturation of the FAD<sub>sq</sub>-containing enzyme by treatment with urea (data not shown). The

---

<sup>1</sup> It is assumed here that the  $\epsilon_{450 \text{ nm}}$  for 8 $\alpha$ -N(1)-histidyl FAD is the same as that for free FAD in solution, with a value of  $11.3 \text{ mM}^{-1}\text{cm}^{-1}$ .

circular dichroism spectrum of the E-FAD<sub>sq</sub> form of choline oxidase showed a negative band at 370 nm, a sharp positive band at 406 nm, and a broad negative dichroic signal spanning from 450 to 650 nm (Figure 4.2). Such a spectrum is in agreement with previously reported circular dichroic spectra of enzyme-bound anionic flavin semiquinones (39, 40).

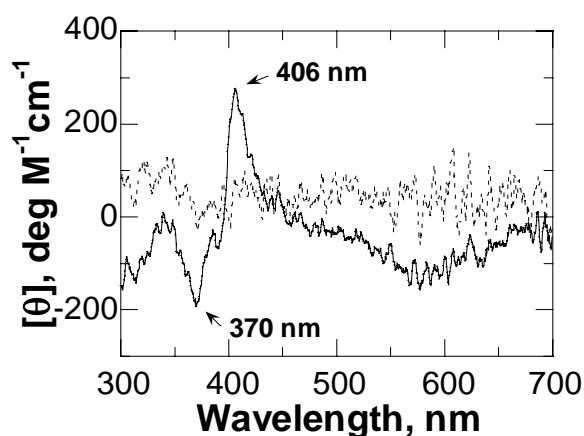


**Figure 4.2.** Circular dichroism spectrum of flavin semiquinone-containing choline oxidase. *Solid line*, choline oxidase after treatment with 5 mM sodium dithionite in aerobiosis followed by gel filtration onto a Sephadex G-25 column equilibrated with 200 mM Tris-Cl, pH 8; *dotted line*, after treatment of the flavin semiquinone-containing enzyme with 4 M urea at 40 °C for 30 min. Spectra were recorded at 22 °C.

As an independent approach to characterizing the enzyme-bound semiquinone flavin of choline oxidase, ESR spectra of the enzyme as purified and of the semiquinone-containing enzyme were determined. As shown in Figure 4.3, E-FAD<sub>ox/sq</sub> yielded an ESR signal at 2 G with a peak-to-peak linewidth of 15.4 G, providing further evidence for the presence of an anionic flavin semiquinone in the enzyme (41). A similar ESR spectrum with peak linewidth of 13.9 G was observed when the enzyme was analyzed after treatment with dithionite and gel filtration to remove the excess dithionite, further consistent with the formation of an air-stable anionic semiquinone upon reduction of the enzyme by dithionite.

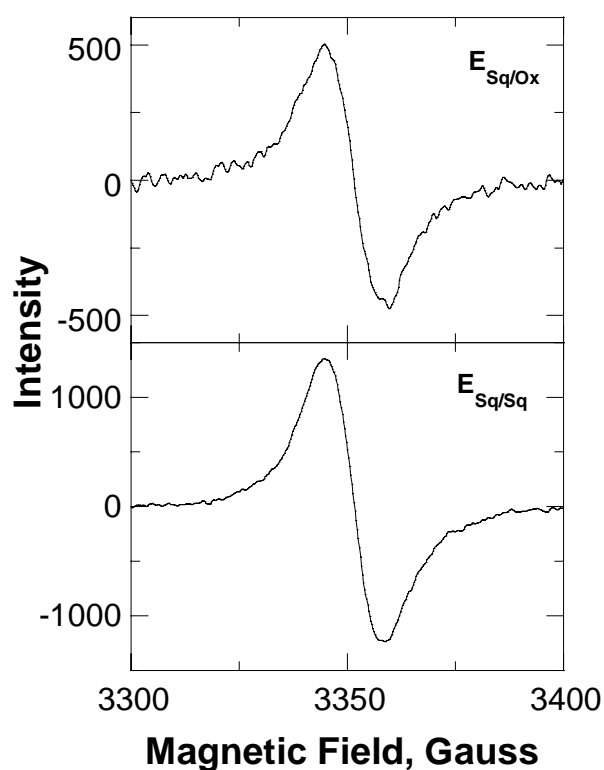


**Figure 4.3.** Electron spin resonance spectrum of recombinant choline oxidase. Spectra of choline oxidase were acquired at a concentration of 60  $\mu$ M in 50 mM HEPES, pH 8. The following spectral conditions were used: microwave power, 2 mW; modulation amplitude, 2 G; gain,  $6.3 \times 10^5$ ; temperature, 141 K. *Panel A*, choline oxidase as purified; *panel B*, flavin semiquinone-containing choline oxidase prepared freshly by addition of sodium dithionite and gel filtration onto a Sephadex G-25 column.

*Spectral Properties of Oxidized FAD-Containing Choline Oxidase (E-FAD<sub>ox</sub>).*

Treatment of choline oxidase at pH 6 and 15 °C resulted in the slow bleaching of the near-UV band centered at 373 nm and concomitant increase of absorbance at 452 nm (Figure 4.4). The resulting enzyme species showed absorbance maxima in the near-UV and visible regions centered at 359 and 452 nm, as expected for an enzyme with the bound flavin in the oxidized state (E-FAD<sub>ox</sub>). At 15 °C, a  $k_{obs}$  value of  $219 \pm 1 \times 10^{-6} \text{ s}^{-1}$  was determined from the absorbance changes at 452 nm for the complete conversion of E-FAD<sub>ox/sq</sub> to E-FAD<sub>ox</sub> (Figure 4.4, *inset*). To minimize possible protein losses due to the prolonged incubation of the enzyme at pH 6, E-FAD<sub>ox</sub> was also prepared by dialysis at 4 °C. When 1,300 units of choline oxidase as purified were dialyzed at pH 6 for 24 hours 4,100 units of E-FAD<sub>ox</sub> were recovered, consistent with formation of E-FAD<sub>ox</sub> being due to oxidation rather than denaturation of E-FAD<sub>sq</sub>. As shown in Figure 4.5, an extinction coefficient at 452 nm of  $11.4 \pm 0.6 \text{ mM}^{-1}\text{cm}^{-1}$  was calculated for E-FAD<sub>ox</sub> from six independent experiments after denaturation of the enzyme by treatment with urea. A fluorescence emission spectrum with a maximum at 530 nm (with  $\lambda_{ex}$  at 452 nm) was observed for E-FAD<sub>ox</sub>, providing further evidence for the presence of oxidized FAD. As for the case of the E-FAD<sub>ox/sq</sub> species, a UV-visible absorbance spectrum identical to that of E-FAD<sub>sq</sub> was obtained upon aerobic addition of dithionite to E-FAD<sub>ox</sub> (data not shown).

Formation of a covalent *N*(5)-flavin adduct with sulfite is a feature that distinguishes flavoprotein oxidases from dehydrogenases (42, 43). As shown in Figure 4.6, treatment of FAD<sub>ox</sub>-containing choline oxidase with sodium sulfite resulted in the bleaching of the peak at 452 nm with the concomitant appearance of a peak centered at 320 nm, consistent with formation of a sulfite *N*(5)-flavin adduct. At pH 7 and 15 °C, complex formation was slow and required several hours for completion at concentrations of sulfite as high as 25 mM. Values for the rate of



complex formation ( $k_{on}$ ) and dissociation ( $k_{off}$ ) of  $0.035 \pm 0.001 \text{ M}^{-1}\text{s}^{-1}$  and  $4.9 \pm 8.4 \times 10^{-6} \text{ s}^{-1}$  were calculated from a plot of  $k_{obs}$  versus sulfite concentration, respectively (Figure 4.6, *inset*). Although a  $k_{off}$  value not significantly different from zero was observed, by using the upper limiting  $k_{off}$  value of  $1.33 \times 10^{-5} \text{ s}^{-1}$  calculated from the sum of the y-intercept value in Figure 4.5 and the standard deviation associated with the measurement, an upper  $K_d$  value of  $\sim 40 \text{ }\mu\text{M}$  could be estimated from the ratio of the  $k_{off}$  to  $k_{on}$  values. From a plot of  $\Delta A_{452}$  versus [sulfite], a  $K_d$  value of  $51 \pm 10 \text{ }\mu\text{M}$  was determined from the reaction at various concentrations of sulfite (data not shown), in fairly good agreement with the value determined kinetically. Reversibility of the flavin-sulfite adduct was established by following the increase in absorbance at 452 nm after removing the excess sulfite by gel filtration (data not shown). However, an accurate determination of the  $k_{off}$  value could not be carried out due to instability of the enzyme over the prolonged incubation times required for complete sulfite dissociation. Although the slow rates of sulfite complex formation and dissociation observed with choline oxidase are atypical for flavoprotein oxidases, similar results were recently observed for another flavin-linked enzyme, *N*-methyltryptophan oxidase (44).

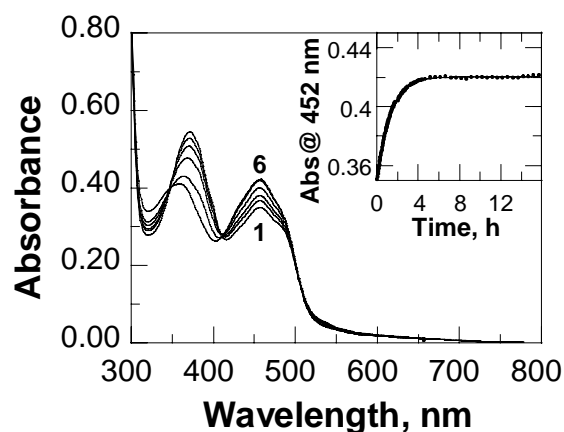


**Figure 4. 4.** Conversion of E-FAD<sub>ox/sq</sub> to E-FAD<sub>ox</sub>.

Choline oxidase as purified at a concentration of 33  $\mu$ M was incubated in air-saturated buffer at pH 6 and 15 °C. Absorbance spectra were recorded at different times of incubation until no further spectral changes were observed. Only selected spectra are shown: *curve 1*, absorbance spectrum of choline oxidase recorded 1 min after gel filtration of the enzyme through a Sephadex G-25 column equilibrated with 20  $\mu$ M potassium phosphate, 20 mM sodium pyrophosphate, pH 6; *curve 6*, same sample after 15 h of incubation. *Inset*, time course of absorbance changes at 452 nm. The curve is a fit of the data to  $y = 0.420 - 0.071 * e^{(0.79x)}$  ( $R^2 = 0.9997$ ).

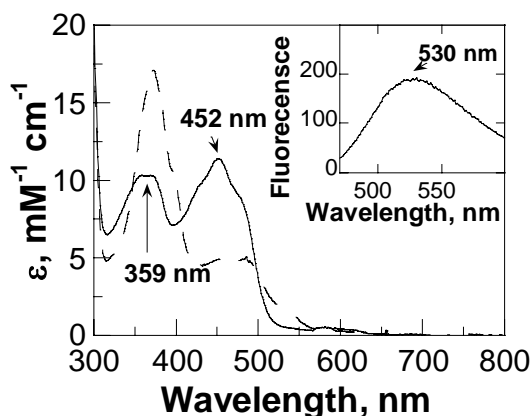


**Figure 4. 5.** Reaction of FAD<sub>ox</sub>-containing choline oxidase with sodium dithionite.

*Solid line*, the UV-visible absorbance spectrum of FAD<sub>ox</sub>-containing choline oxidase was recorded at a concentration of 75  $\mu$ M in 200 mM Tris-Cl, pH 8; *Dashed line*, air-stable semiquinone-containing enzyme prepared by treatment with 5 mM sodium dithionite in aerobiosis and gel filtration onto a sephadex G-25 column equilibrated with the same buffer. *Inset*, fluorescence emission spectrum of FAD<sub>ox</sub>-containing choline oxidase at a concentration of 15  $\mu$ M in 200 mM Tris-Cl, pH 8 and 15 °C. The excitation wavelength was at 453 nm.

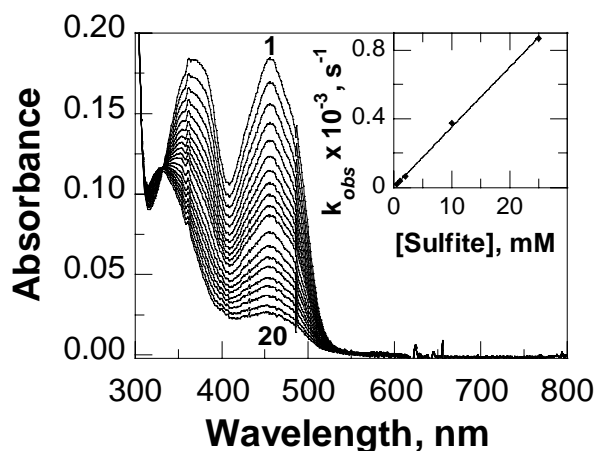


**Figure 4.6.** Reaction of choline oxidase with sulfite.

FAD<sub>ox</sub>-containing choline oxidase at a concentration of 15  $\mu$ M was incubated with 25 mM sodium sulfite in air-saturated 100 mM potassium phosphate, pH 7 and 15  $^{\circ}$ C. Absorbance spectra were recorded at different times of incubation until no further spectral changes were observed. Only selected spectra are shown: *curve 1*, absorbance spectrum of choline oxidase recorded 10 s after addition of sulfite; *curve 20*, same sample after 2 h of incubation. *Inset*, plot of the observed rate of decrease in absorbance at 452 nm versus the concentration of sulfite. The line is a fit of the data to  $y = 0.035x + 0.0000049$  ( $R^2 = 0.999$ ).

**Enzymatic Turnover of E-FAD<sub>ox/sq</sub>, E-FAD<sub>sq</sub> and E-FAD<sub>ox</sub> with Choline.** To determine whether the flavin semiquinone of choline oxidase participates in catalysis, choline oxidase containing either FAD<sub>ox/sq</sub>, FAD<sub>sq</sub>, or FAD<sub>ox</sub>, was incubated with 4 mM choline in air-saturated 200 mM Tris-Cl, at pH 8 and 15 °C. As shown in Figure 4.7, a UV-visible absorbance spectrum with maxima at 372 and 495 nm was observed with the FAD<sub>ox/sq</sub>-containing enzyme, suggesting that the enzyme-bound oxidized flavin was fully reduced in the presence of the substrate, and that the flavin semiquinone did not react with choline or oxygen under enzyme turnover. After removal of the excess choline by gel filtration, a UV-visible absorbance spectrum substantially identical to that of the resting state of E-FAD<sub>ox/sq</sub> was observed (Figure 4.7), further consistent with the flavin semiquinone not participating in catalysis. When a freshly prepared sample of the E-FAD<sub>sq</sub> form of choline oxidase was subjected to the same treatment, no changes were observed in the UV-visible absorbance spectra of both the enzyme under turnover and in the resting state after removal of excess choline by gel filtration (Figure 4.7), in good agreement with the results observed with the enzyme containing a mixture of oxidized and semiquinone flavins. Finally, a peak centered at 356 nm was observed in the UV-visible absorbance spectrum of the FAD<sub>ox</sub>-containing enzyme in the presence of choline and oxygen, suggesting that this species of enzyme was fully reduced under these conditions (Figure 4.7). After removing the excess choline by gel filtration, an absorbance spectrum substantially identical to that of the initial E-FAD<sub>ox</sub> species in the resting state was observed (Figure 4.7). Altogether, the results of these experiments are consistent with the flavin semiquinone of choline oxidase being not catalytically competent and with the enzyme-bound flavin cycling between fully oxidized and reduced states during catalytic turnover of the enzyme with the substrates.

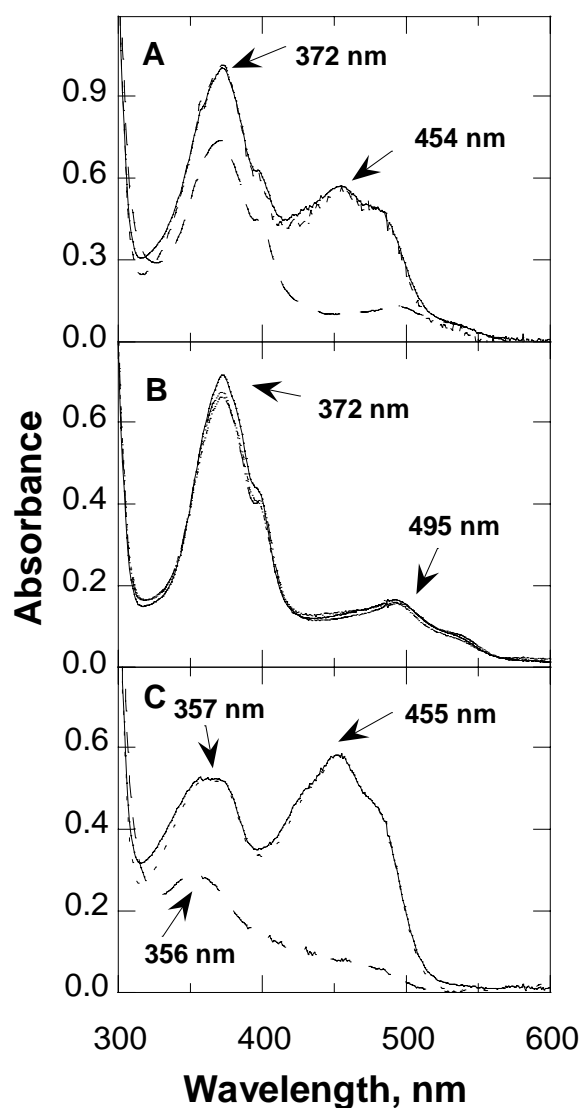


**Figure 4.7.** UV-Visible absorbance spectra of choline oxidase during turnover with choline. Choline oxidase containing different relative amounts of flavin semiquinone and oxidized flavin was incubated for 30 min with 4 mM choline in air-saturated 100 mM potassium phosphate, pH 7 and 15 °C, before stopping the reaction by gel filtration onto a Sephadex G-25 column equilibrated with the same buffer. UV-Visible absorbance spectra were recorded for the enzyme in the resting state before turnover (*solid curve*), under turnover (*dashed curve*), and in the resting state after turnover (*dotted curve*). *Panel A*, 95  $\mu\text{M}$  choline oxidase containing  $\text{FAD}_{\text{ox/sq}}$ ; *panel B*, 50  $\mu\text{M}$  choline oxidase containing  $\text{FAD}_{\text{sq}}$ ; and *panel C*, 79  $\mu\text{M}$  choline oxidase containing  $\text{FAD}_{\text{ox}}$ . Spectra for the resting enzyme after turnover were normalized to those of the resting enzyme before turnover.

**Steady State Kinetics.** The steady state kinetic parameters for recombinant choline oxidase were determined for both the E-FAD<sub>ox</sub> and E-FAD<sub>ox/sq</sub> forms of choline oxidase, by measuring the rate of oxygen consumption at varying concentrations of both the organic substrate and oxygen at pH 7 and 25 °C. As expected based on previous studies on *A. globiformis* choline oxidase (18), the kinetic data with choline and betaine aldehyde were fit best by equations 1 and 2, which describe sequential kinetic mechanisms with finite and negligible  $K_a$  values, respectively (37). As shown in Table 4.1, when the kinetic parameters were expressed per active site oxidized flavin content, no significant differences were observed in the  $k_{cat}$  and  $k_{cat}/K_m$  values when enzyme forms with different FAD<sub>ox</sub>/FAD<sub>total</sub> ratios were compared, providing independent evidence that the flavin semiquinone of choline oxidase does not participate in catalysis<sup>2</sup>.

**Product Inhibition Studies.** As an independent approach to examining the steady state kinetic mechanism of recombinant choline oxidase, the inhibition patterns of the product glycine betaine with respect to either choline or betaine aldehyde were determined in air-saturated buffer at pH 6.75. As shown in Table 4.2, the results were best fit by equation 5, consistent with glycine betaine being competitive versus either choline or betaine aldehyde. Moreover, similar kinetic parameters were obtained irrespective of the use of E-FAD<sub>ox/sq</sub> or E-FAD<sub>ox</sub> when the initial rates were expressed per active site oxidized flavin (Table 4.2).

---

<sup>2</sup> If the flavin semiquinone were as catalytically competent as the oxidized flavin in the reaction catalyzed by choline oxidase, similar  $k_{cat}$  and  $k_{cat}/K_m$  values should have been obtained by expressing the enzymatic activity per active site total flavin content. Alternatively, if the flavin semiquinone were either less or more catalytically competent than the oxidized flavin, due to the kinetic complexity of the reaction catalyzed by choline oxidase, significantly different  $k_{cat}$ ,  $K_m$ ,  $K_{ia}$ , and  $k_{cat}/K_m$  values should have been observed irrespective of whether the enzymatic activity is expressed per active site oxidized flavin content or total flavin content. Within experimental error, the kinetic results observed with enzyme forms containing different relative amounts of flavin semiquinone and oxidized flavin are therefore consistent with the conclusion that the oxidized flavin is solely responsible for catalytic activity.

**Table 4.1.** Steady-State Kinetic Parameters for Recombinant Choline Oxidase with Choline or Betaine Aldehyde as Substrate at pH 7<sup>a</sup>

Substrate	FAD <sub>OX</sub> /FAD <sub>total</sub> <sup>b</sup>	$k_{cat}$ , s <sup>-1</sup> <sup>c</sup>	$K_a$ , mM <sup>d</sup>	$k_{cat}/K_a$ , M <sup>-1</sup> s <sup>-1</sup> <sup>e</sup>	$K_{O_2}$ , $\mu$ M	$k_{cat}/K_{O_2}$ , M <sup>-1</sup> s <sup>-1</sup>	$K_{ia}$ , mM	eq.	$R^2$
Choline	1.00	61 $\pm$ 6	1.7 $\pm$ 0.3	36,000 $\pm$ 6,400	703 $\pm$ 102	87,100 $\pm$ 15,300	0.2 $\pm$ 0.05	1	0.998
Choline	0.37	60 $\pm$ 5	2.9 $\pm$ 0.3	21,000 $\pm$ 3,000	830 $\pm$ 90	72,400 $\pm$ 9,900	0.2 $\pm$ 0.03	1	0.999
betaine aldehyde	1.00	69 $\pm$ 1			1090 $\pm$ 30	64,000 $\pm$ 2,100	2.2 $\pm$ 0.09	2	0.998
betaine aldehyde	0.37	67 $\pm$ 1			970 $\pm$ 1	69,000 $\pm$ 100	2.3 $\pm$ 0.01	2	1.000

<sup>a</sup> Enzyme activity was measured at varying concentrations of both organic substrate and oxygen in 50 mM potassium phosphate, pH 7 and 25°C. <sup>b</sup> Oxidized flavin content per total enzyme-bound flavin. <sup>c</sup> Rates are expressed per active site oxidized flavin content. <sup>d</sup>  $K_a$  is the  $K_m$  value for either choline or betaine aldehyde as substrate. <sup>e</sup>  $k_{cat}/K_a$  is the  $k_{cat}/K_m$  value for either choline or betaine aldehyde as substrate.

Substrate	FAD <sub>ox</sub> / FAD <sub>total</sub> <sup>b</sup>	type of inhibition <sup>c</sup>	$k_{cat}$ , s <sup>-1</sup> <sup>d</sup>	$K_m$ , mM	$K_{is}$ , mM	$K_{ii}$ , mM	eq	$R^2$
Choline	1.00	C	10.6 ± 0.2	0.8 ± 0.1	15 ± 1		5	0.999
		UC	11.3 ± 0.2	1.1 ± 0.1		27 ± 1	6	0.929
		NC	9.3 ± 0.4	0.6 ± 0.1	12 ± 2	10 <sup>8</sup> ± 10 <sup>14</sup>	7	0.995
	0.37	C	9.7 ± 0.1	0.8 ± 0.1	12 ± 0.3		5	0.993
		UC	9.4 ± 0.1	0.7 ± 0.1		21 ± 0.1	6	0.941
		NC	9.7 ± 0.1	0.8 ± 0.1	12 ± 0.1	10 <sup>8</sup> ± 10 <sup>11</sup>	7	0.993
betaine aldehyde	1.00	C	6.1 ± 0.1	2.0 ± 0.1	56 ± 2		5	0.991
		UC	10.0 ± 0.1	5.0 ± 0.1		41 ± 2	6	0.971
		NC	7.6 ± 0.7	2.8 ± 0.7	51 ± 26	10 <sup>3</sup> ± 10 <sup>4</sup>	7	0.960
	0.37	C	5.9 ± 0.1	2.6 ± 0.1	48 ± 4		5	0.996
		UC	7.8 ± 0.1	4.0 ± 0.1		29 ± 1	6	0.982
		NC	7.2 ± 0.3	3.3 ± 0.4	49 ± 11	755 ± 926	7	0.993

<sup>a</sup> Enzyme activity was measured at varying concentrations of organic substrate and glycine betaine in air-saturated 50 mM potassium phosphate, pH 6.75 and 25 °C. <sup>b</sup> Oxidized flavin content per total enzyme-bound flavin. <sup>c</sup> C, competitive; UC, uncompetitive, NC, noncompetitive. <sup>d</sup> Rates are expressed per active site oxidized flavin content.



***pH Dependence of the  $k_{cat}$  and  $k_{cat}/K_m$  Values.*** The pH-dependence of the kinetic parameters with choline as substrate was determined at varying concentrations of both choline and oxygen in the pH range 6 to 10. As shown in Figure 4.8, both the  $k_{cat}/K_m$  and  $k_{cat}$  values for choline increased with increasing pH, reaching limiting values above pH 8. Apparent  $pK_a$  values of  $7.6 \pm 0.2$  and  $7.1 \pm 0.2$  were determined for a group that must be unprotonated for catalysis from the  $k_{cat}/K_m$  and  $k_{cat}$  pH-profiles, respectively. In contrast, the  $k_{cat}/K_m$  values for oxygen were independent of pH, with values in the  $10^4 \text{ M}^{-1}\text{s}^{-1}$  range (Figure 4.9).

To establish whether a measurable  $K_m$  value could be determined with betaine aldehyde as substrate for the enzyme, initial rates of reaction were measured at pH 6.5 and 10 by varying the concentrations of both betaine aldehyde and oxygen. At both pH values the data were fit best to equation 2 (data not shown), consistent with  $k_{cat}$  being independent of the concentration of betaine aldehyde (37). The  $k_{cat}$  values with betaine aldehyde were  $42 \pm 2$  at pH 6.5 and  $70 \pm 1 \text{ s}^{-1}$  at pH 10. As for the case of choline, the  $k_{cat}/K_m$  values for oxygen determined with betaine aldehyde as the organic substrate were independent of the pH (Figure 4.9).

As an approach to establishing whether some changes in the kinetic properties of the enzyme take place in the conversion of E-FAD<sub>ox/sq</sub> to E-FAD<sub>ox</sub>, the pH dependences of the kinetic parameters with choline as substrate for both enzyme species were determined in air-saturated buffer in the pH range from 5 to 10. As shown in Figure 4.10, both the  $k_{cat}/K_m$  and  $k_{cat}$  values yielded similar pH profiles irrespective of whether the E-FAD<sub>ox</sub> or the E-FAD<sub>ox/sq</sub> species was used, indicating that no changes other than oxidation of E-FAD<sub>sq</sub> occur in the preparation of E-FAD<sub>ox</sub> by treatment at pH 6. The  $pK_a$  values were  $7.4 \pm 0.1$  and  $7.3 \pm 0.1$  in the  $k_{cat}/K_m$  pH profiles, and  $6.4 \pm 0.1$  and  $6.6 \pm 0.1$  in the  $k_{cat}$  pH profiles with E-FAD<sub>ox</sub> and E-FAD<sub>ox/sq</sub>,

respectively, in agreement with the values of  $7.2 \pm 0.2$  and  $6.4 \pm 0.1$  recently determined for choline oxidase from *A. globiformis* (19).

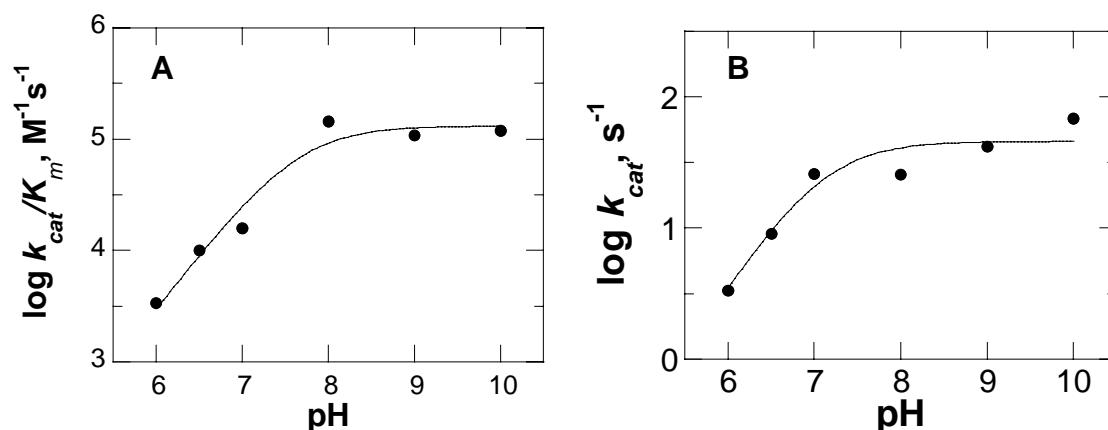


**Figure 4.8.** pH Dependence of the  $k_{cat}/K_m$  and  $k_{cat}$  values for choline as substrate for recombinant choline oxidase.

Choline oxidase activity was measured at varying concentration of both choline and oxygen at 25 °C as described in the Experimental Procedures section. The lines are fits of the data to equation 3. *Panel A*, pH dependence of the  $k_{cat}/K_m$  values; *panel B*, pH dependence of the  $k_{cat}$  values.

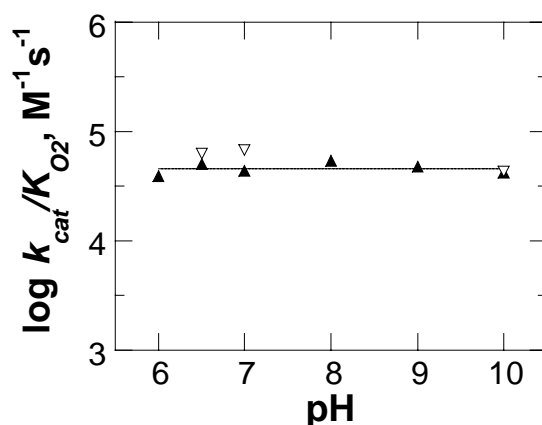


**Figure 4.9.** pH Dependence of the  $k_{cat}/K_m$  values for oxygen with choline or betaine aldehyde as substrate for recombinant choline oxidase.

Choline oxidase activity was measured at varying concentration of both choline (or betaine aldehyde) and oxygen at 25 °C as described in the Experimental Procedures section. (▼) Values determined with choline; (△) values determined with betaine aldehyde. The line represents the average pH-independent  $k_{cat}/K_m$  value with choline as substrate.

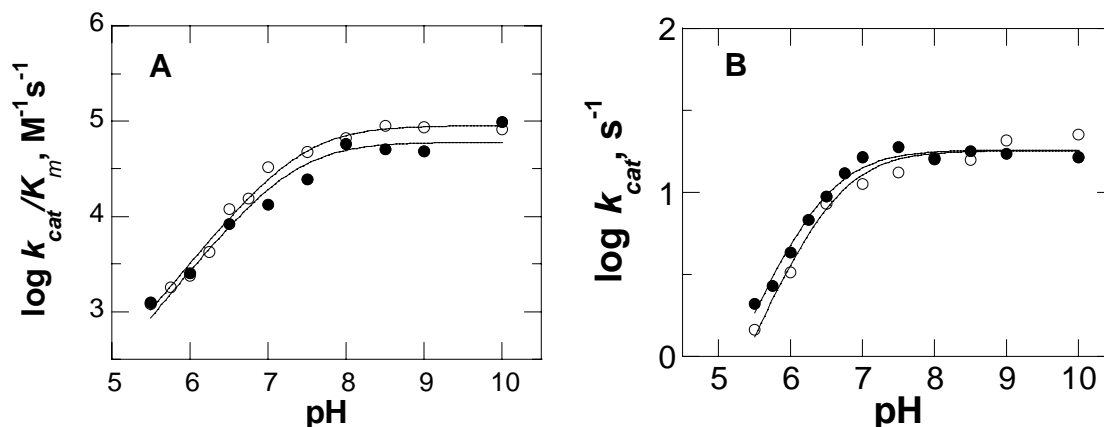


**Figure 4.10.** pH Dependence of the apparent kinetic parameters of E-FAD<sub>ox/sq</sub> and E-FAD<sub>ox</sub> with choline as substrate.

Choline oxidase activity was measured in air-saturated buffer at 25 °C. (●) Values determined with E-FAD<sub>ox</sub>; (○) values determined with E-FAD<sub>ox/sq</sub>. The lines are fits of the data to equation 3. *Panel A*, pH dependence of the  $k_{cat}/K_m$  values; *panel B*, pH dependence of the  $k_{cat}$  values.

**pH Dependence of Inhibition by Glycine Betaine.** The pH dependence of the inhibition by glycine betaine was determined in atmospheric oxygen using choline as substrate for E-FAD<sub>ox</sub>. As shown in Figure 4.11, the data were fit best by equation 4, consistent with a single ionizable group with a  $pK_a$  value of  $7.5 \pm 0.1$  that must be protonated for inhibition.

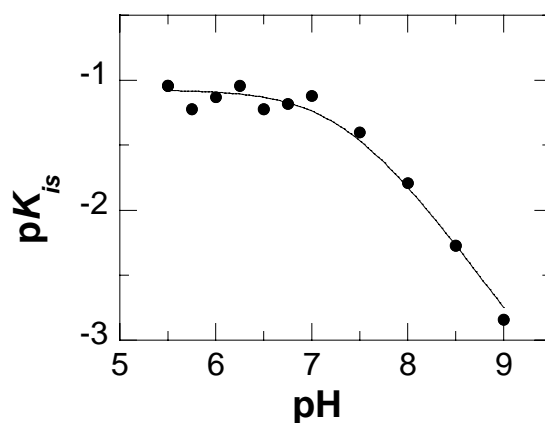


**Figure 4.11.** pH Dependence of inhibition by glycine betaine.

At each pH value, choline oxidase activity was measured at varying concentrations of both choline and glycine betaine in air-saturated buffer at 25 °C. The  $K_{is}$  values for glycine betaine were determined by fitting the initial rate data to equation 5. The line is a fit of the data to equation 4.

## Discussion

Recombinant choline oxidase expressed in *E. coli* cells contains between 35 and 85% of bound flavin in an anionic semiquinone form that requires the protein microenvironment to be stabilized. At pH 8, this enzyme-bound flavosemiquinone is unusually insensitive to both molecular oxygen<sup>3</sup> and the oxidizing agent ferricyanide, suggesting that the unpaired electron is localized in a region of the flavin that is not accessible for reaction. Earlier studies on native choline oxidase from *Alcaligenes* sp. showed that an anionic semiquinone that was poorly reactive towards oxygen is stabilized by the enzyme (45), suggesting that this property does not arise from the expression of the recombinant enzyme in the heterologous system used in our study. A rationale for the unusual air-stability of the flavin semiquinone can be proposed based on recent *ab initio* theoretical calculations, showing that most of the spin density in anionic flavin semiquinones is distributed on either the benzene ring or the *N*(5) position of the flavin (46, 47). The flavin *N*(5) locus is expected to be freely accessible to oxygen, because of the role it plays in catalysis by accepting the hydride equivalent generated in the oxidation of the substrate. In contrast, the benzene ring of FAD is involved in a 8 $\alpha$ -*N*(1)-histidyl linkage with the protein (4) and is likely to be hindered by the protein moiety. Stabilization of the spin density on the benzene ring of the anionic semiquinone might further be contributed by the inductive effect of the flavin 8 $\alpha$ -*N*(1)-histidyl linkage with the protein moiety.

The choline oxidase-bound semiquinone undergoes a slow conversion to the fully oxidized state at pH 6, indicating that a hundred fold increase in proton concentration significantly destabilizes the flavin radical. Although not investigated further in this study, a

---

<sup>3</sup> The rate of reaction with oxygen of anionic flavin semiquinones in solution is almost diffusion-controlled, with second order rate constant values of 10<sup>8</sup> M<sup>-1</sup>s<sup>-1</sup> (69, 70). That for enzyme-bound anionic semiquinones has been reported for glucose oxidase to be in the 10<sup>4</sup> M<sup>-1</sup>s<sup>-1</sup> range (49).

possible rationale for the oxidation of the flavin semiquinone in choline oxidase is that at low pH a limited fraction of the enzyme-bound semiquinone becomes protonated to yield the neutral species of the semiquinone, which would be readily oxidized by molecular oxygen because of localization of the unpaired electron on the highly oxygen-reactive C(4a) locus of the flavin (43). pH-Dependent stabilization of both anionic and neutral flavin semiquinones by the same enzyme was previously shown in another member of the GMC oxidoreductase superfamily, glucose oxidase (42, 48), for which it was shown that the neutral semiquinone reacts with oxygen with a second order rate constant of  $1.4 \times 10^4 \text{ M}^{-1}\text{s}^{-1}$  at 25 °C (49). Unusual stabilization of neutral semiquinones by flavoprotein oxidases was also reported for nitroalkane oxidase (50) and D-amino acid oxidase in the presence of benzoic acid (51).

The spectral studies of the enzyme under turnover establish that the flavin semiquinone of choline oxidase is not catalytically relevant and that the enzyme under turnover cycles between its fully oxidized and fully reduced states. This conclusion is further supported by kinetic data, showing a good correlation between the turnover numbers of the enzyme with choline and betaine aldehyde as substrate and the content of oxidized flavin per active site. Consistent with the lack of catalytic role for the flavin semiquinone, variable  $\text{FAD}_{\text{ox}}/\text{FAD}_{\text{sq}}$  ratios for the enzyme-bound flavin are observed among different preparations of enzyme (6). Thus, choline oxidase appears to be similar to methanol oxidase, which was shown in earlier studies to contain a mixture of oxidized FAD and an air-stable anionic semiquinone that is not required for catalysis (52). In contrast, air-stable flavin semiquinones for which a catalytic role of the flavin radical was proposed (53, 54) were reported in the resting state of monoamine oxidase B (55-57) and *E. coli* DNA photolyase (58, 59).

A weak positive charge is located in the active site of choline oxidase in proximity of the N(1)-C(2)=O locus of FAD, as suggested by both the stabilization of the anionic semiquinone and the high affinity of the enzyme for sulfite (43). By analogy with other members of the GMC oxidoreductase superfamily whose three-dimensional structure is available, such as glucose oxidase (60, 61), cholesterol oxidase (62, 63), and cellobiose dehydrogenase (64), it is likely that the positive charge in choline oxidase is provided by the dipole of an  $\alpha$ -helix.

A steady state kinetic analysis of choline oxidase from *A. globiformis* was recently reported at pH 7 (18). The results of the kinetic studies reported here indicate that recombinant and native choline oxidase share identical steady state sequential mechanisms in which the products are released from the oxidized enzyme (Scheme 4.2) and, most importantly, that the order of the kinetic steps involving substrate binding and product release is not affected by pH. Independent evidence for product release occurring after reaction of the reduced enzyme with oxygen is provided by the competitive inhibition patterns observed with glycine betaine versus both choline and betaine aldehyde. The product inhibition patterns observed in this study also rule out possible kinetically relevant conformational changes occurring after release of the product from the enzyme active site, such as those observed with nitroalkane oxidase (65).

His-466 with a  $pK_a$  value of 7.5 was recently proposed to participate in catalysis by accepting the hydroxyl proton of choline, based on pH dependence studies in atmospheric oxygen with choline oxidase from *A. globiformis* and sequence alignment comparison with other members of the GMC enzyme superfamily (19). Consistent with those results, an amino acid residue with  $pK_a$  value of 7.6 is seen in the  $k_{cat}/K_m$  pH-profile of recombinant choline oxidase determined at varying concentrations of choline and oxygen. In the kinetic mechanism of Scheme 4.2, the  $k_{cat}/K_m$  value for choline is a combination of rate constants reflecting substrate

binding,  $k_1$  and  $k_2$ , the catalytic step in which choline is oxidized to betaine aldehyde,  $k_3$  and  $k_4$ , and the kinetic step in which the reduced enzyme-product complex is oxidized by oxygen,  $k_5$ , as illustrated by equation 8. This raises the possibility that the catalytic base may be involved in oxygen reduction rather than in substrate oxidation. However, the observation that the  $k_{cat}/K_m$  values for oxygen are independent of pH unequivocally establishes the involvement of the catalytic base in the oxidation of choline to betaine aldehyde.

$$\frac{k_{cat}}{K_m} = \frac{k_1 k_3 k_5 [O_2]}{k_2 k_4 + k_2 k_5 [O_2] + k_3 k_5 [O_2]} \quad (8)$$

The  $pK_a$  value of 7.5 seen in the pH profile of glycine betaine inhibition is due to an amino acid residue that must be protonated for product binding, as expected if this residue is involved in binding the caboxylate moiety of glycine betaine. This amino acid group is likely to be the same histidine residue that must be unprotonated for catalysis and is responsible for the  $pK_a$  value of 7.6 observed in the  $k_{cat}/K_m$  pH profile. Since  $pK_a$  values determined with competitive inhibitors are expected to reflect true equilibrium dissociation constants, these results establish choline as a slow substrate with little if any external forward commitment to catalysis (66). This conclusion does not agree with that recently reported for choline oxidase from *A. globiformis* based on pH and kinetic isotope effects studies using  $[1,2-^2H_4]$ -choline in atmospheric oxygen, showing a decrease in the  $^Dk_{cat}/K_m$  values with increasing pH (19). A reasonable explanation that accounts for all the available data is that the decrease in the apparent  $^Dk_{cat}/K_m$  values with increasing pH when the concentration of oxygen is well below saturation is not due to choline being a fast substrate for the enzyme as originally proposed (19), but to the

reverse catalytic step ( $k_4$  in Scheme 4.2) becoming significantly fast as compared to the kinetic step in which the enzyme-bound reduced flavin is oxidized ( $k_5$  in Scheme 4.2)<sup>4</sup>.

No ionizable groups with  $pK_a$  value in the pH range from 6 to 10 are required for oxygen reduction in the betaine aldehyde- or glycine betaine-choline oxidase complexes, as suggested by the pH independence of the  $k_{cat}/K_m$  values for oxygen with either choline or betaine aldehyde as substrate. These data are consistent with a hydrophobic environment being required for flavin activation in the reduced enzyme-product complexes. In this respect, a hydrophobic channel that may serve as an entrance for oxygen to the active site was recently proposed for another member of the GMC oxidoreductase superfamily, cholesterol oxidase (67). Oxygen reactivity in choline oxidase therefore appears to be different from that of glucose oxidase, for which protonation of the active site His-516 residue was recently shown to increase the reactivity of the reduced enzyme towards oxygen by about 4 orders of magnitude (68).

In summary, the results of the studies on choline oxidase presented herein have established that the enzyme is a typical flavoprotein oxidase, showing formation of an anionic flavin semiquinone and reactivity with sulfite. However, stabilization of the flavin semiquinone by the enzyme is unusual in that it occurs in the presence of molecular oxygen. Such a lack of

---

<sup>4</sup> In the kinetic mechanism of Scheme 4.2, the observed isotope effect on the  $k_{cat}/K_m$  value is given by

$$\frac{{}^D k_{cat}}{K_m} = \frac{{}^D k_3 + \frac{k_3}{k_2} + 1.24 \frac{k_4}{k_5 [O_2]}}{1 + \frac{k_3}{k_2} + \frac{k_4}{k_5 [O_2]}} \quad (66), \text{ where 1.24 is the value for the equilibrium kinetic isotope effect for the}$$

conversion of an alcohol to an aldehyde (71). If the forward commitment to catalysis  $k_3/k_2$  is negligible, any decrease in the observed kinetic isotope effect must be due to the reverse commitment to catalysis  $k_4/k_5 [O_2]$ , which depends on the concentration of oxygen. Since choline oxidase from *A. globiformis* has a  $K_m$  value for oxygen of 0.6 mM at pH 7 and 19 °C (18), and the concentration of oxygen in air-saturated buffers at 19 °C is ~0.3 mM, it follows that under these conditions the rate of oxidation of the enzyme-bound reduced flavin becomes significantly slow. Consequently, a significant increase in the reverse commitment to catalysis is expected at concentrations of oxygen well below saturation in the enzyme-catalyzed oxidation of choline.



reactivity towards oxygen has allowed a spectroscopic characterization of the enzyme-bound anionic flavin semiquinone and to establish that the flavin semiquinone does not participate in catalysis. From a mechanistic standpoint, the kinetic data presented here have indicated that the recently proposed catalytic base of choline oxidase, His-466, participates in the oxidation of the organic substrate but not in the reduction of molecular oxygen.

### **Acknowledgment**

The authors thank Dr. Dale E. Edmondson and Ms. Manuela Trani at the Department of Biochemistry of Emory University, Atlanta, for the electron spin resonance spectral analyses; Dr. Yiming Ye for his assistance in the circular dichroism spectral analyses; and the reviewers for their insightful suggestions.

## References

- (1) Ikuta, S., Imamura, S., Misaki, H., and Horiuti, Y. (1977) Purification and characterization of choline oxidase from *Arthrobacter globiformis*, *J. Biochem. (Tokyo)* 82, 1741-9.
- (2) Ohishi, N., and Yagi, K. (1979) Covalently bound flavin as prosthetic group of choline oxidase, *Biochem. Biophys. Res. Commun.* 86, 1084-8.
- (3) Ohta-Fukuyama, M., Miyake, Y., Emi, S., and Yamano, T. (1980) Identification and properties of the prosthetic group of choline oxidase from *Alcaligenes sp*, *J. Biochem. (Tokyo)* 88, 197-203.
- (4) Rand, T., Halkier, T., and Hansen, O. C. (2003) Structural characterization and mapping of the covalently linked FAD cofactor in choline oxidase from *Arthrobacter globiformis*, *Biochemistry* 42, 7188-94.
- (5) Cavener, D. R. (1992) GMC oxidoreductases. A newly defined family of homologous proteins with diverse catalytic activities, *J. Mol. Biol.* 223, 811-4.
- (6) Fan, F., Ghanem, M., and Gadda, G. (2004) Cloning, sequence analysis, and purification of choline oxidase from *Arthrobacter globiformis*: a bacterial enzyme involved in osmotic stress tolerance, *Arch. Biochem. Biophys.* 421, 149-158.
- (7) Eccleston, E. D., Thayer, M. L., and Kirkwood, S. (1979) Mechanisms of action of histidinol dehydrogenase and UDP-Glc dehydrogenase. Evidence that the half-reactions proceed on separate subunits, *J. Biol. Chem.* 254, 11399-404.
- (8) Gorisch, H. (1979) Steady-state investigations of the mechanism of histidinol dehydrogenase, *Biochem. J.* 181, 153-7.
- (9) Burger, E., and Gorisch, H. (1981) Evidence for an essential lysine at the active site of L-histidinol:NAD<sup>+</sup> oxidoreductase; a bifunctional dehydrogenase, *Eur. J. Biochem.* 118, 125-30.
- (10) Burger, E., and Gorisch, H. (1981) Patterns of product inhibition of a bifunctional dehydrogenase; L- histidinol:NAD<sup>+</sup> oxidoreductase, *Eur. J. Biochem.* 116, 137-42.
- (11) Grubmeyer, C. T., Chu, K. W., and Insinga, S. (1987) Kinetic mechanism of histidinol dehydrogenase: histidinol binding and exchange reactions, *Biochemistry* 26, 3369-73.
- (12) Grubmeyer, C. (1991) A paradigm for aldehyde oxidation: histidinol dehydrogenase, *Adv. Exp. Med. Biol.* 284, 105-12.
- (13) Kheirulomoom, A., Mano, J., Nagai, A., Ogawa, A., Iwasaki, G., and Ohta, D. (1994) Steady-state kinetics of cabbage histidinol dehydrogenase, *Arch. Biochem. Biophys.* 312, 493-500.

- (14) Nagai, A., and Ohta, D. (1994) Histidinol dehydrogenase loses its catalytic function through the mutation of His261-->Asn due to its inability to ligate the essential Zn, *J. Biochem. (Tokyo)* 115, 22-5.
- (15) Grubmeyer, C., and Teng, H. (1999) Mechanism of *Salmonella typhimurium* histidinol dehydrogenase: kinetic isotope effects and pH profiles, *Biochemistry* 38, 7355-62.
- (16) Teng, H., and Grubmeyer, C. (1999) Mutagenesis of histidinol dehydrogenase reveals roles for conserved histidine residues, *Biochemistry* 38, 7363-71.
- (17) Barbosa, J. A., Sivaraman, J., Li, Y., Larocque, R., Matte, A., Schrag, J. D., and Cygler, M. (2002) Mechanism of action and NAD<sup>+</sup>-binding mode revealed by the crystal structure of L-histidinol dehydrogenase, *Proc. Natl. Acad. Sci. U. S. A.* 99, 1859-64.
- (18) Gadda, G. (2003) Kinetic mechanism of choline oxidase from *Arthrobacter globiformis*, *Biochim. Biophys. Acta.* 1646, 112-8.
- (19) Gadda, G. (2003) pH and deuterium kinetic isotope effects studies on the oxidation of choline to betaine-aldehyde catalyzed by choline oxidase, *Biochim. Biophys. Acta.* 1650, 4-9.
- (20) Sakamoto, A., Alia, Murata, N., and Murata, A. (1998) Metabolic engineering of rice leading to biosynthesis of glycinebetaine and tolerance to salt and cold, *Plant Mol Biol* 38, 1011-9.
- (21) Sakamoto, A., Valverde, R., Alia, Chen, T. H., and Murata, N. (2000) Transformation of *Arabidopsis* with the *codA* gene for choline oxidase enhances freezing tolerance of plants, *Plant J.* 22, 449-53.
- (22) Alia, Kondo, Y., Sakamoto, A., Nonaka, H., Hayashi, H., Saradhi, P. P., Chen, T. H., and Murata, N. (1999) Enhanced tolerance to light stress of transgenic *Arabidopsis* plants that express the *codA* gene for a bacterial choline oxidase, *Plant Mol. Biol.* 40, 279-88.
- (23) Holmstrom, K. O., Somersalo, S., Mandal, A., Palva, T. E., and Welin, B. (2000) Improved tolerance to salinity and low temperature in transgenic tobacco producing glycine betaine, *J. Exp. Bot.* 51, 177-85.
- (24) Alia, Hayashi, H., Sakamoto, A., and Murata, N. (1998) Enhancement of the tolerance of *Arabidopsis* to high temperatures by genetic engineering of the synthesis of glycinebetaine, *Plant J.* 16, 155-61.
- (25) Deshnum, P., Gombos, Z., Nishiyama, Y., and Murata, N. (1997) The action in vivo of glycine betaine in enhancement of tolerance of *Synechococcus* sp. strain PCC 7942 to low temperature, *J. Bacteriol.* 179, 339-44.
- (26) Deshnum, P., Los, D. A., Hayashi, H., Mustardy, L., and Murata, N. (1995) Transformation of *Synechococcus* with a gene for choline oxidase enhances tolerance to salt stress, *Plant Mol. Biol.* 29, 897-907.

- (27) Bae, J. H., Anderson, S. H., and Miller, K. J. (1993) Identification of a high-affinity glycine betaine transport system in *Staphylococcus aureus*, *Appl Environ Microbiol* 59, 2734-6.
- (28) Culham, D. E., Emmerson, K. S., Lasby, B., Mamelak, D., Steer, B. A., Gyles, C. L., Villarejo, M., and Wood, J. M. (1994) Genes encoding osmoregulatory proline/glycine betaine transporters and the proline catabolic system are present and expressed in diverse clinical *Escherichia coli* isolates, *Can. J. Microbiol.* 40, 397-402.
- (29) Graham, J. E., and Wilkinson, B. J. (1992) *Staphylococcus aureus* osmoregulation: roles for choline, glycine betaine, proline, and taurine, *J. Bacteriol.* 174, 2711-6.
- (30) Kaenjak, A., Graham, J. E., and Wilkinson, B. J. (1993) Choline transport activity in *Staphylococcus aureus* induced by osmotic stress and low phosphate concentrations, *J. Bacteriol.* 175, 2400-6.
- (31) Le Rudulier, D., and Bouillard, L. (1983) Glycine betaine, an osmotic effector in *Klebsiella pneumoniae* and other members of the *Enterobacteriaceae*, *Appl. Environ. Microbiol.* 46, 152-9.
- (32) Le Rudulier, D., Bernard, T., Goas, G., and Hamelin, J. (1984) Osmoregulation in *Klebsiella pneumoniae*: enhancement of anaerobic growth and nitrogen fixation under stress by proline betaine, gamma- butyrobetaine, and other related compounds, *Can. J. Microbiol.* 30, 299-305.
- (33) Pichereau, V., Bourot, S., Flahaut, S., Blanco, C., Auffray, Y., and Bernard, T. (1999) The osmoprotectant glycine betaine inhibits salt-induced cross- tolerance towards lethal treatment in *Enterococcus faecalis*, *Microbiology* 145, 427-35.
- (34) Peddie, B. A., Wong-She, J., Randall, K., Lever, M., and Chambers, S. T. (1998) Osmoprotective properties and accumulation of betaine analogues by *Staphylococcus aureus*, *FEMS Microbiol Lett* 160, 25-30.
- (35) Bradford, M. M. (1976) A rapid and sensitive method for the quantitation of microgram quantities of protein utilizing the principle of protein-dye binding, *Anal. Biochem.* 72, 248-54.
- (36) Allison, D. R., and Purich, D. L. (1979) Practical considerations in the design of initial velocity enzyme rate assays, in *Methods Enzymol.* (Purich, D. L., Ed.) pp 3-19, Academic Press, New York.
- (37) Segel, I. H. (1975) *Enzyme Kinetics*, John Wiley & Sons, Inc., New York.
- (38) Whitby, L. G. (1953) *Biochem. J.* 54, 437-442.
- (39) Edmondson, D. E., and Tollin, G. (1971) Circular dichroism studies of the flavin chromophore and of the relation between redox properties and flavin environment in oxidases and dehydrogenases, *Biochemistry* 10, 113-24.

- (40) Ohta-Fukuyama, M., Miyake, Y., Shiga, K., Nishina, Y., Watari, H., and Yamano, T. (1980) Circular dichroism studies on flavoproteins containing covalently bound coenzymes, *J. Biochem. (Tokyo)* 88, 205-9.
- (41) Edmondson, D. E., Ackrell, B. A., and Kearney, E. B. (1981) Identification of neutral and anionic 8 alpha-substituted flavin semiquinones in flavoproteins by electron spin resonance spectroscopy, *Arch. Biochem. Biophys.* 208, 69-74.
- (42) Massey, V., Brumby, P. E., and Komai, H. (1969) Studies on milk xanthine oxidase. Some spectral and kinetic properties, *J. Biol. Chem.* 244, 1682-91.
- (43) Massey, V., and Hemmerich, P. (1980) Active-site probes of flavoproteins, *Biochem. Soc. Trans.* 8, 246-57.
- (44) Khanna, P., and Schuman Jorns, M. (2001) N-methyltryptophan oxidase from *Escherichia coli*: reaction kinetics with N-methyl amino acid and carbinolamine substrates, *Biochemistry* 40, 1451-9.
- (45) Ohta, M., Miura, R., Yamano, T., and Miyake, Y. (1983) Spectroscopic studies on the photoreaction of choline oxidase, a flavoprotein, with covalently bound flavin, *J. Biochem. (Tokyo)* 94, 879-92.
- (46) Garcia, J. I., Medina, M., Sancho, J., Alonso, P. J., Gomez-Moreno, C., Mayoral, J. A., and Martinez, J. I. (2002) Theoretical analysis of the electron spin density distribution of the flavin semiquinone isoalloxazine ring within model protein environments, *J. Phys. Chem.* 106, 4729-35.
- (47) Zheng, Y. J., and Ornstein, R. L. (1996) A theoretical study of the structures of flavin in different oxidation and protonation states, *J Am Chem Soc* 118, 9402-8.
- (48) Massey, V., and Palmer, G. (1966) On the existence of spectrally distinct classes of flavoprotein semiquinones. A new method for the quantitative production of flavoprotein semiquinones, *Biochemistry* 5, 3181-9.
- (49) Stankovich, M. T., Schopfer, L. M., and Massey, V. (1978) Determination of glucose oxidase oxidation-reduction potentials and the oxygen reactivity of fully reduced and semiquinoid forms, *J. Biol. Chem.* 253, 4971-9.
- (50) Gadda, G., and Fitzpatrick, P. F. (1998) Biochemical and physical characterization of the active FAD-containing form of nitroalkane oxidase from *Fusarium oxysporum*, *Biochemistry* 37, 6154-64.
- (51) Yagi, K., Takai, A., and Oishi, N. (1972) Conversion of the red semiquinone of D-amino acid oxidase to the blue semiquinone by complex formation, *Biochim. Biophys. Acta.* 289, 37-43.
- (52) Mincey, T., Tayrien, G., Mildvan, A. S., and Abeles, R. H. (1980) Presence of a flavin semiquinone in methanol oxidase, *Proc. Natl. Acad. Sci. U. S. A.* 77, 7099-101.

- (53) Silverman, R. B. (1995) Radical ideas about monoamine oxidase, *Acc. Chem. Res.* 28, 335-342.
- (54) Jorns, M. S., Wang, B., and Jordan, S. P. (1987) DNA repair catalyzed by *Escherichia coli* DNA photolyase containing only reduced flavin: elimination of the enzyme's second chromophore by reduction with sodium borohydride, *Biochemistry* 26, 6810-6.
- (55) Yue, K. T., Bhattacharyya, A. K., Zhelyaskov, V. R., and Edmondson, D. E. (1993) Resonance Raman spectroscopic evidence for an anionic flavin semiquinone in bovine liver monoamine oxidase, *Arch. Biochem. Biophys.* 300, 178-85.
- (56) Woo, J. C., and Silverman, R. B. (1994) Observation of two different chromophores in the resting state of monoamine oxidase B by fluorescence spectroscopy, *Biochem. Biophys. Res. Commun.* 202, 1574-8.
- (57) DeRose, V. J., Woo, J. C., Hawe, W. P., Hoffman, B. M., Silverman, R. B., and Yelekci, K. (1996) Observation of a flavin semiquinone in the resting state of monoamine oxidase B by electron paramagnetic resonance and electron nuclear double resonance spectroscopy, *Biochemistry* 35, 11085-91.
- (58) Kay, C. W., Feicht, R., Schulz, K., Sadewater, P., Sancar, A., Bacher, A., Mobius, K., Richter, G., and Weber, S. (1999) EPR, ENDOR, and TRIPLE resonance spectroscopy on the neutral flavin radical in *Escherichia coli* DNA photolyase, *Biochemistry* 38, 16740-8.
- (59) Payne, G., Heelis, P. F., Rohrs, B. R., and Sancar, A. (1987) The active form of *Escherichia coli* DNA photolyase contains a fully reduced flavin and not a flavin radical, both *in vivo* and *in vitro*, *Biochemistry* 26, 7121-7.
- (60) Hecht, H. J., Kalisz, H. M., Hendle, J., Schmid, R. D., and Schomburg, D. (1993) Crystal structure of glucose oxidase from *Aspergillus niger* refined at 2.3 Å resolution, *J. Mol. Biol.* 229, 153-72.
- (61) Wohlfahrt, G., Witt, S., Hendle, J., Schomburg, D., Kalisz, H. M., and Hecht, H. J. (1999) 1.8 and 1.9 Å resolution structures of the *Penicillium amagasakiense* and *Aspergillus niger* glucose oxidases as a basis for modelling substrate complexes, *Acta Crystallogr. D. Biol. Crystallogr.* 55, 969-77.
- (62) Vrieling, A., Lloyd, L. F., and Blow, D. M. (1991) Crystal structure of cholesterol oxidase from *Brevibacterium sterolicum* refined at 1.8 Å resolution, *J. Mol. Biol.* 219, 533-54.
- (63) Li, J., Vrieling, A., Brick, P., and Blow, D. M. (1993) Crystal structure of cholesterol oxidase complexed with a steroid substrate: implications for flavin adenine dinucleotide dependent alcohol oxidases, *Biochemistry* 32, 11507-15.

- (64) Hallberg, B. M., Henriksson, G., Pettersson, G., and Divne, C. (2002) Crystal structure of the flavoprotein domain of the extracellular flavocytochrome cellobiose dehydrogenase, *J. Mol. Biol.* 315, 421-34.
- (65) Gadda, G., and Fitzpatrick, P. F. (2000) Iso-mechanism of nitroalkane oxidase: 1. Inhibition studies and activation by imidazole, *Biochemistry* 39, 1400-5.
- (66) Cook, P. F., and Cleland, W. W. (1981) pH variation of isotope effects in enzyme-catalyzed reactions. 1. Isotope- and pH-dependent steps the same., *Biochemistry* 20, 1797-1805.
- (67) Coulombe, R., Yue, K. Q., Ghisla, S., and Vrielink, A. (2001) Oxygen access to the active site of cholesterol oxidase through a narrow channel is gated by an Arg-Glu pair, *J. Biol. Chem.* 276, 30435-41.
- (68) Roth, J. P., and Klinman, J. P. (2003) Catalysis of electron transfer during activation of O<sub>2</sub> by the flavoprotein glucose oxidase, *Proc. Natl. Acad. Sci. U. S. A.* 100, 62-7.
- (69) Vaish, S. P. (1971) Flash photolysis of flavines. V. Oxidation and disproportionation of flavine radicals, *J. Bioenergetics* 2, 61-72.
- (70) Faraggi, M., Hemmerich, P., and Pecht, I. (1975) O<sub>2</sub>-affinity of flavin radical species as studied by pulse radiolysis, *FEBS Lett.* 51, 47-51.
- (71) Cleland, W. W. (1980) *Methods Enzymol.* 64, 104-25.

## CHAPTER V

### On the Catalytic Role of the Conserved Active Site Residue His<sub>466</sub> of Choline Oxidase

(This chapter was published in verbatim in Ghanem, M., and Gadda, G., (2005), *Biochemistry* 44, 893-904. © 2005 American Chemical Society. All rights reserved.)

#### Abstract

The oxidation of alcohols to aldehydes is catalyzed by a number of flavin-dependent enzymes, which have been grouped in the Glucose-Methanol-Choline oxidoreductase enzyme superfamily. These enzymes exhibit little sequence similarity in their substrates binding domains, but share a highly conserved catalytic site, suggesting a similar activation mechanism for the oxidation of their substrates. In this study, the fully conserved histidine residue at position 466 of choline oxidase was replaced with an alanine residue by site-directed mutagenesis and the biochemical, spectroscopic, and mechanistic properties of the resulting CHO-H466A mutant enzyme were characterized. CHO-H466A showed  $k_{\text{cat}}$  and  $k_{\text{cat}}/K_{\text{m}}$  values with choline as substrate that were 60- and 1000-fold lower than the wild-type enzyme, while the  $k_{\text{cat}}/K_{\text{m}}$  value for oxygen was unaffected, suggesting the involvement of His<sub>466</sub> in the oxidation of the alcohol substrate but not in the reduction of oxygen. Replacement of His<sub>466</sub> with alanine significantly affected the microenvironment of the flavin, as indicated by the altered behavior of CHO-H466A with sulfite and dithionite. In agreement with this conclusion, a midpoint reduction potential of +106 mV for the two-electron transfer in the catalytically competent enzyme-product complex was determined at pH 7 for CHO-H466A, which was ~25 mV more negative than that of the wild-type enzyme. Enzymatic activity in CHO-H466A could be partially rescued with exogenous imidazolium, but not imidazole, consistent with the protonated form of histidine exerting a catalytic role. pH profiles for glycine betaine inhibition, the deprotonation of the N(3)-flavin



locus, and the  $k_{\text{cat}}/K_{\text{m}}$  value for choline all showed a significant shift upward in their  $\text{p}K_{\text{a}}$  values, consistent with a change in the polarity of the active site. Finally, kinetic isotope effects with isotopically labeled substrate and solvent indicated that the histidine to alanine substitution affected the timing of substrate OH and CH bond cleavages, consistent with removal of the hydroxyl proton being concerted with hydride transfer in the mutant enzyme. All taken together, the results presented in this study suggest that in choline oxidase, His<sub>466</sub> modulates the electrophilicity of the enzyme-bound flavin and the polarity of the active site, and contributes to the stabilization of the transition state for the oxidation of choline to betaine aldehyde.

## Introduction

The oxidation of alcohols to aldehydes is catalyzed by a number of flavin-dependent enzymes, among which are choline oxidase (1, 2), choline dehydrogenase (3), glucose oxidase (4, 5), cholesterol oxidase (6), and cellobiose dehydrogenase (7). These enzymes all utilize FAD as a cofactor for catalysis and have been grouped in the Glucose-Methanol-Choline (GMC<sup>1</sup>) oxidoreductase enzyme superfamily (8). Although GMC enzymes exhibit little sequence similarity in their substrate binding domains, the crystal structure of glucose oxidase (9, 10), cholesterol oxidase (11-13), and the flavin domain of cellobiose dehydrogenase (14), show that they all share a highly conserved catalytic site (Figure 5.1), suggesting a similar activation mechanism for the oxidation of their substrates. Recent mechanistic studies on choline oxidase with the use of isotopically labeled substrate and solvent indicated that alcohol oxidation occurs through a base-catalyzed formation of an alkoxide species that precedes the transfer of a hydride from the substrate  $\alpha$ -carbon to the isoalloxazine system of the FAD cofactor (Scheme 5.1) (15). To date, the nature of both the catalytic base that abstracts the hydroxyl proton from the substrate and the amino acid residue(s) that provide the necessary stabilization of the ensuing alkoxide species in catalysis remains elusive. Earlier mechanistic studies on cholesterol oxidase (16, 17), cellobiose dehydrogenase (18), and glucose oxidase (10, 19, 20), suggested that an histidine residue, which is fully conserved within the GMC family and corresponds to His<sub>466</sub> of choline oxidase, might act as the specific base that participates in the oxidation of the alcohol substrate

---

<sup>1</sup> Abbreviations: CHO-H466A, mutant form of choline oxidase with His<sub>466</sub> replaced with Ala; CHO-WT, wild-type choline oxidase; GMC, Glucose-Methanol-Choline oxidoreductase enzyme superfamily;  $^Dk_{\text{cat}}/K_m$  and  $^Dk_{\text{cat}}/K_{m(D_2O)}$  indicate substrate kinetic isotope effects determined with 1,2-[<sup>2</sup>H<sub>4</sub>]-choline in aqueous and deuterated solvent, respectively;  $^{D_2O}k_{\text{cat}}/K_m$  and  $^{D_2O}k_{\text{cat}}/K_{m(D)}$  represent solvent kinetic isotope effects determined with choline and deuterated choline, respectively;  $^{D,D_2O}k_{\text{cat}}/K_m$  is multiple kinetic isotope effect determined with choline in H<sub>2</sub>O and deuterated choline in D<sub>2</sub>O.

(Figure 5.1). However, the recent availability of a crystal structure of an unliganded form of cholesterol oxidase at sub-atomic resolution, in which it was shown that the Ne2 position of the active site His<sub>447</sub> residue pointing at the substrate hydroxyl group is protonated (13), clearly does not support this histidine residue acting as a specific base in catalysis. These structural observations prompted the authors to suggest that the conserved histidine residue might act as a hydrogen bond donor to the hydroxyl oxygen of the substrate, which would assist in positioning the substrate with respect to the flavin for efficient catalysis (13).

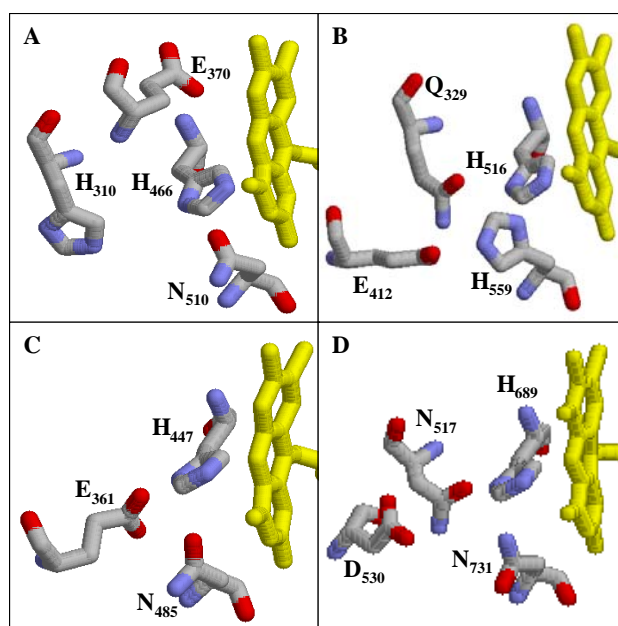
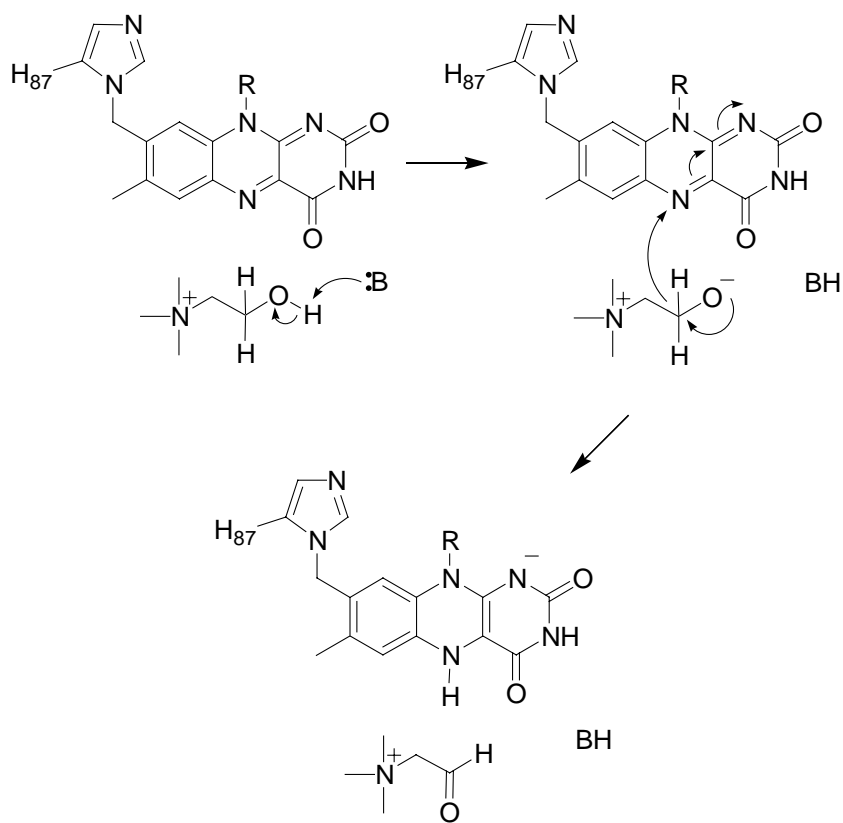
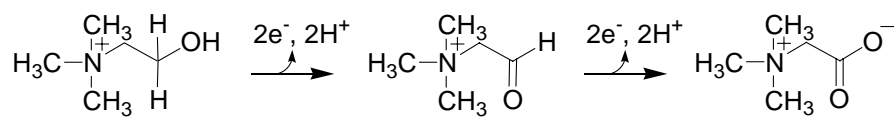


**Figure 5.1.** The conserved active site residues in the GMC oxidoreductase superfamily. *Panel A*, hypothetical structure of choline oxidase generated by using SWISS-MODEL software and energy minimization by using SYBIL 6.9 software and the structure of glucose oxidase as template; *panel B*, glucose oxidase (PDB code 1CF3); *panel C*, cholesterol oxidase (PDB code 1COY); *panel D*, cellobiose dehydrogenase (PDB code 1NAA).



**Scheme 5.1.** Chemical mechanism for choline oxidation catalyzed by choline oxidase.



**Scheme 5.2.** Chemical reaction catalyzed by choline oxidase.

Our group recently cloned and overexpressed the gene coding for choline oxidase (E.C. 1.1.3.17) from *Arthrobacter globiformis* strain ATCC 8010 (21), and showed that the resulting enzyme maintains biochemical and kinetic properties similar to those of the native choline oxidase (21-23). The enzyme is a homodimer of 120 kDa, with each subunit containing covalently bound FAD in a 8 $\alpha$ -N(1)-histidyl linkage (21, 23, 24), and it catalyzes the oxidation of choline to glycine betaine through two sequential flavin-linked hydride transfers from choline and the ensuing betaine aldehyde intermediate to molecular oxygen (Scheme 5.2) (21-23). This reaction is of considerable interest for medical and biotechnological applications, since accumulation of glycine betaine in many pathogens and plants enables their stress-resistance towards hyperosmotic environments (25, 26). Consequently, the study of choline oxidase has potential for the development of therapeutic agents that inhibit the biosynthesis of glycine betaine and render pathogenic bacteria susceptible to either conventional treatments or the innate immune system, and for the improvement of water stress resistance in genetically engineered crops lacking efficient glycine betaine biosynthetic systems.

In the present study, a mutant choline oxidase in which the active site residue His<sub>466</sub> was replaced with alanine was prepared by site-directed mutagenesis and the biochemical, spectroscopic, and mechanistic properties of the resulting CHO-H466A mutant enzyme were characterized in order to obtain insights on the catalytic role played by this conserved histidine residue. The results of the studies presented herein provide new insights into the chemical mechanism of choline oxidase and, by extension, of the GMC oxidoreductase enzyme superfamily.

## Experimental Procedures

**Materials.** *Escherichia coli* strain Rosetta(DE3)pLysS were from Novagen (Madison, WI). The QuikChange Site-Directed Mutagenesis kit was from Stratagene (La Jolla, CA). The QIAprep Spin Miniprep kit was from Qiagen (Valencia, CA). Oligonucleotides used for site-directed mutagenesis and for sequencing of the mutant gene were custom synthesized by the DNA Core Facility of the Department of Biology of Georgia State University or by Sigma Genosys (The Woodlands, TX). Oligonucleotides, bovine serum albumin, chloramphenicol, tetracycline, isopropyl- $\beta$ -D-thiogalactopyranoside (IPTG), lysozyme, sodium hydrosulfite (dithionite), sodium sulfite, betaine aldehyde, glycine betaine, Luria-Bertani agar and broth, and PMSF were from Sigma (St. Louis, MO). Choline chloride and ampicillin were from ICN (Aurora, OH). 1,2-[ $^2\text{H}_4$ ]-Choline bromide was from Isotec Inc. (Miamisburg, OH). Deuterium oxide ( $\text{D}_2\text{O}$ ) was from Cambridge Isotope Laboratories Inc. (Andover, MA). Wild-type choline oxidase (CHO-WT) from *Arthrobacter globiformis* strain ATCC 8010 was expressed from pET/*codA1* and purified to homogeneity as previously described (21). The fully oxidized FAD-containing CHO-WT was prepared as described in ref. (27). All other reagents were of the highest purity commercially available.

**Instruments.** UV-visible absorbance spectra were recorded using an Agilent Technologies diode-array spectrophotometer model HP 8453 equipped with a thermostated water bath. Fluorescence emission spectra were recorded with a Shimadzu Spectrofluorometer model RF-5301 PC thermostated at 15 °C. Circular dichroism spectra were acquired using a Jasco J-810 spectropolarimeter at 5 °C.

**Site-Directed Mutagenesis.** A QuikChange kit was used to prepare the mutant enzyme choline oxidase-H466A (CHO-H466A). The method used was essentially according to the

manufacturer's instructions, using pET/*codA1* plasmid (21) as a template and Cho-H466Af (5'CAACACCGTCTACGCCCCCGTGGGCACCGTGC 3') and Cho-H466Ar (5'CACGGTGCCACGGGGGCGTAGACGGTGTTGTGC 3') oligonucleotides as forward and reverse primers (underlined letters indicate mismatches), respectively. DNA was sequenced at the DNA Core Facility at Georgia State University using an Applied Biosystems Big Dye Kit on an Applied Biosystems model ABI 377 DNA sequencer. Sequencing confirmed the presence of the mutant gene in the correct orientation. *E. coli* strain Rosetta(DE3)pLysS competent cells were transformed with plasmid pET/*codA1*-H466A by electroporation.

**Expression and Purification of CHO-H466A.** Permanent frozen stocks of *E. coli* cells Rosetta(DE3)pLysS harboring plasmid pET/*codA1*-H466A were used to inoculate 4.5 liters of Luria-Bertani broth medium containing 50 µg/ml ampicillin and 34 µg/ml chloramphenicol, and liquid cultures were grown overnight at 37 °C. The cultures were induced for protein expression by adding 0.1 mM IPTG and then incubated for an additional 5 h at 22 °C. A 100 µl aliquot was taken 5 h after induction with IPTG to be used for visualization of the expressed protein using sodium dodecyl sulfate polyacrylamide gel electrophoresis following the Laemmli method (28). The gel was stained with Commassie Brilliant Blue G-250. The mutant enzyme CHO-H466A was purified to homogeneity using the same procedure used previously for the purification of the wild-type enzyme (21).

**Spectral Studies.** The extinction coefficient of CHO-H466A was determined in Tris-Cl, pH 8, after denaturation of the enzyme by treatment with 0.1% SDS at 100 °C for 5 min, based upon the  $\epsilon_{450}$  value of 11.3 mM<sup>-1</sup> cm<sup>-1</sup> for free FAD (29). The spectral properties of CHO-WT and CHO-H466A before and after the addition of 200 mM of glycine betaine were determined at 15 °C in 100 mM sodium pyrophosphate buffer, pH 6.5. All spectra were normalized to the

molar extinction of the uncomplexed enzyme and corrected for dilution. For reactions with sodium sulfite, the reagent was prepared freshly as 1 M stock solution in 100 mM sodium pyrophosphate, pH 6.5. Different amounts of sodium sulfite at final concentrations ranging from 25 to 100 mM were added to the enzyme solution in 100 mM sodium pyrophosphate, pH 6.5, at 15 °C, and the UV-visible absorbance spectra were recorded at different times. Since previous studies on wild type choline oxidase showed that the enzyme is reduced by treatment with dithionite in the presence of oxygen (23), reduction of CHO-H466A with dithionite was carried out aerobically in 20 mM Tris-Cl, pH 8, at 15 °C, by adding dithionite to the enzyme solution as a powder. The excess amount of dithionite was removed by gel filtration using a Sephadex G-25 column equilibrated with 20 mM Tris-Cl, pH 8. The pH dependence of the absorbance spectra for both wild-type and mutant enzymes at concentrations of ~20 µM in 20 mM sodium phosphate, 20 mM sodium pyrophosphate, pH 6, and 15 °C, were determined by titrating with sodium hydroxide.

The CD spectra of CHO-WT and CHO-H466A were recorded at 5 °C in 20 mM Tris-Cl, pH 8, at concentrations of enzyme of 5 and 15 µM for the far and the near UV, respectively. The fluorescence emission spectra of CHO-WT and CHO-H466A were acquired in 20 mM Tris-Cl buffer, pH 8 at 15 °C. The excitation wavelengths for CHO-WT and CHO-H466A were 453 nm and 458 nm, respectively.

**Enzyme Assays.** The enzymatic activity of CHO-H466A was measured by the method of initial rates as described for the wild-type enzyme (21, 23) using a computer-interfaced Oxy-32 oxygen-monitoring system (Hansatech Instrument Ltd.). The kinetic parameters of CHO-H466A were determined by varying the concentrations of both choline, in the range between 2.5 and 35 mM, and oxygen, in the range between 24 and 460 µM, as substrates, in 50 mM potassium



phosphate, pH 7, at 25 °C. The effect of pH on the kinetic parameters of CHO-H466A were determined over a pH range from 5.5 to 11 by a series of enzyme activity assays at varying choline concentrations ranging from 0.025 to 45 mM in air-saturated 50 mM sodium pyrophosphate at 25 °C. The kinetic isotope effects of CHO-H466A were obtained by determining the kinetic parameters of the enzyme using either choline or 1,2- $^{2}\text{H}_4$ -choline as substrate in either aqueous or deuterated solvent, in air-saturated 50 mM sodium pyrophosphate at 25 °C and pL 10. For the determinations of solvent isotope effects, buffers were prepared using 99.9% deuterium oxide by adjusting the pD value with NaOD. The pD values were determined by adding 0.4 to the pH electrode readings (30). For all steady state kinetic isotope effects, activity assays were carried out by alternating substrate or solvent isoptomers. Product inhibition studies were carried out by varying the concentrations of both glycine betaine, in the range between zero and 60 mM, and choline, in the range between 0.02 and 20 mM, in air-saturated 50 mM sodium pyrophosphate at 25 °C, over a pH range from 7 to 11. The effect of imidazole on the turnover number of CHO-H466A was determined by measuring the enzymatic activity with 10 mM choline as substrate for the enzyme in the presence of varying concentrations of imidazole in the range from 0 to 250 mM in air-saturated 50 mM potassium phosphate, pH 7, or 50 mM sodium pyrophosphate for other pH values.

**Potentiometric Titrations.** All redox titrations of wild-type and H466A CHO were carried out on the glycine betaine-liganded enzyme at 15 °C in a cell similar to the one described by Edmondson (1985). Potentials were measured by using a Pt electrode relative to an Ag/AgCl double junction reference electrode with an Orion Model 701A pH/mV meter (31). The reference electrode was calibrated prior to each titration as described by Edmondson (31), using a deoxygenated, saturated quinhydrone solution in 0.09 M KCl and 0.01 M HCl at 25 °C. In a

typical titration, 2.5 ml of ~20-30  $\mu\text{M}$  choline oxidase containing glycine betaine at a concentration of 1.5 M in 20 mM Tris-Cl, pH 7, was scrubbed free of oxygen by at least 15 cycles of alternate degassing under vacuum and flushing with  $\text{O}_2$ -free argon. The following redox mediators were added to ensure complete redox equilibration: 2  $\mu\text{M}$  methyl viologen (-440 mV), 0.5  $\mu\text{M}$  dichlorophenolindophenol (+217 mV), 0.5  $\mu\text{M}$  phenazine methosulfate (+80mV), 0.5  $\mu\text{M}$  thionin (+60 mV), 0.5  $\mu\text{M}$  duroquinone (-5 to +5 mV), 0.5  $\mu\text{M}$  resorufin (-50 mV), and 0.5  $\mu\text{M}$  indigo carmine (-125 mV) (32, 33). The ligand-bound enzyme solutions were titrated electrochemically as described by Dutton (34), using freshly prepared sodium dithionite as reductant and potassium ferricyanide as oxidant in 20 mM Tris-Cl, pH 7 (34). Adequate time was permitted for electronic equilibration after each addition of sodium dithionite or potassium ferricyanide prior to the spectrum being recorded; equilibrium of the system was considered to be obtained when the measured potential drift was less than 1 mV in 5 min, which was typically achieved after 30 to 60 min. UV-visible absorbance spectra were recorded using an Agilent Technologies diode-array spectrophotometer model HP 8453 equipped with a thermostated cell holder and a magnetic stirrer beneath the cell holder. All spectra were corrected for any drift in the baseline by subtracting the absorbance at 800 nm.

**Data Analysis.** Kinetic data were fit with the KaleidaGraph software (Synergy Software, Reading, PA) and the Enzfitter software (Biosoft, Cambridge, UK). Apparent kinetic parameters in atmospheric oxygen were determined by fitting initial reaction rates at different substrate concentrations to the Michaelis-Menten equation for one substrate. Initial rates determined by varying the concentration of both choline and oxygen were fit to eq 1, which describes a sequential steady-state kinetic mechanism.  $K_a$  and  $K_b$  are the Michaelis constants for choline ( $A$ ) and oxygen ( $B$ ), respectively, and  $k_{\text{cat}}$  is the turnover number of the enzyme ( $e$ ). Product

inhibition studies data were fit to eq 2, which describes competitive inhibition pattern of the product and the organic substrate.  $P$  is the concentration of glycine betaine, and  $K_{is}$  is the inhibition constant for the slope effect. The pH dependencies of steady-state kinetic parameters were determined by fitting initial rate data to eq 3, which describes a curve with a slope of +1 and a plateau region at high pH. The pH dependence of inhibition by glycine betaine was determined by fitting the initial rate data to eq 4, which describes a curve with a slope of -1 and a plateau region at low pH.  $C$  is the pH-independent value of the kinetic parameter of interest. Data of the pH dependencies of the absorbance spectra for both wild-type and mutant enzymes were fit to eq 5, which describes a curve with a slope of -1 and plateau regions at low and high pH, where  $A$  and  $B$  represent the absorbance values at 500 nm at low and high pH, respectively. The mid-point reduction potentials of the enzymes were determined by fitting the data to the Nernst equation (eq 6), where  $Eh$  is the measured electrode potential at equilibrium at each point in the titration;  $E_m$  is the mid-point redox potential;  $R$  is the gas constant, with a value of  $8.31 \text{ J mol}^{-1}$  at  $15^\circ\text{C}$ ;  $T$  is the temperature in Kelvin;  $n$  is the number of electron transferred;  $F$  is Faraday's constant, with a value of  $96.48 \text{ kJ V}^{-1} \text{ mol}^{-1}$ .

$$\frac{v}{e} = \frac{k_{\text{cat}} AB}{K_a B + K_b A + AB + K_{ia} K_b} \quad (1)$$

$$\frac{v}{e} = \frac{k_{\text{cat}} A}{K_a \left[ 1 + \left( \frac{P}{K_{is}} \right) \right] + A} \quad (2)$$

$$\log Y = \log \left( \frac{C}{1 + \frac{10^{-\text{pH}}}{10^{-\text{p}K_a}}} \right) \quad (3)$$

$$\log Y = \log \left( \frac{C}{1 + \frac{10^{-pK_a}}{10^{-pH}}} \right) \quad (4)$$

$$Y = \frac{A10^{-pH} + B10^{-pK_a}}{10^{-pH} + 10^{-pK_a}} \quad (5)$$

$$Eh = E_m + \frac{2.303}{nF} RT \log \frac{[FAD_{ox}]}{[FAD_{red}]} \quad (6)$$

## Results

***Expression and Purification of CHO-H466A.*** CHO-H466A was expressed and purified to homogeneity as judged by SDS-PAGE using the same protocol developed for the wild-type enzyme (data not shown). As for the case of the wild-type enzyme, about 150 mg of pure mutant enzyme could be typically obtained from 4.5 liters of Luria-Bertani culture medium. The specific activity of the H466A form of choline oxidase was ~45-times lower than that of the wild-type enzyme [0.12 vs. 5.3  $\mu\text{mol O}_2 \text{ min}^{-1} \text{ mg}^{-1}$  (21)], suggesting that His<sub>466</sub> plays a role in catalysis in choline oxidase.

***Spectral Properties.*** In order to verify that the mutant enzyme maintains an overall fold similar to that of the wild-type enzyme, the structural properties of CHO-H466A were examined using CD and fluorescence spectroscopy. The near- and the far-UV CD spectra of CHO-H466A were found to be similar to those of the wild-type enzyme (Figure 5.2), suggesting an overall fold of the mutant enzyme similar to that of the wild-type enzyme. As shown in Figure 5.2, the protein fluorescence emission spectrum of CHO-H466A obtained upon excitation at 285 nm yielded a peak at 340 nm, as for the case of the wild-type enzyme, but with increased intensity. Such an increase in fluorescence intensity is consistent with either a decrease in the polarity of the microenvironment surrounding nearby aromatic residues (35) or the removal of a quenching effect upon substituting the active site histidine with an alanine residue, both effects attributable to the presence of a tyrosine residue, Tyr<sub>465</sub>, adjacent to the site of mutation in the amino acid sequence of the enzyme (21).

The UV-visible absorbance spectrum of CHO-H466A at pH 8 showed the typical flavin peaks in the near-UV and visible region of the absorbance spectrum (Figure 5.2), indicating that the enzyme-bound flavin cofactor in the mutant enzyme as purified is in the oxidized state. As

expected for an enzyme containing covalently bound FAD, the soluble fraction prepared upon treatment of CHO-H466A with 10% trichloroacetic acid followed by centrifugation to remove the denatured protein was devoid of absorbance (data not shown). A stoichiometry of  $0.32 \pm 0.05$  FAD per monomer of protein was calculated for CHO-H466A, indicating that the flavin content of the mutant enzyme was significantly less than that of the wild-type choline oxidase, for which a stoichiometry close to unity was previously reported<sup>2</sup> (21). The enzyme-bound flavin of CHO-H466A showed an extinction coefficient at 458 nm of  $12 \text{ mM}^{-1} \text{ cm}^{-1}$ , in agreement with the value of  $11.4 \text{ mM}^{-1} \text{ cm}^{-1}$  at 452 nm previously determined with the wild-type form of the enzyme (23). The flavin fluorescence emission spectrum of CHO-H466A had a maximum at  $\sim 530$  ( $\lambda_{\text{ex}}$  at 458 nm), with a relative intensity of  $\sim 50\%$  of that seen for the wild-type enzyme (Figure 5.2), consistent with an altered flavin microenvironment in the mutant protein.

The absence of a flavin semiquinone in the UV-visible absorbance spectrum of CHO-H466A as purified (Figure 5.2) is in stark contrast to the observation recently reported for the wild-type form of choline oxidase, for which the enzyme-bound cofactor was found as a mixture of oxidized and air-stable anionic semiquinone flavin species (21, 23). Treatment of the mutant enzyme under aerobic conditions with dithionite at pH 8 resulted in the rapid bleaching of the peak at 458 nm and the appearance of a spectrum with maxima at 372 and 495 nm (data not shown), consistent with reduction of the enzyme-bound flavin to the semiquinone state, as for the case of wild-type enzyme (23).

---

<sup>2</sup> A lower flavin to protein stoichiometry was reported in earlier studies on mutant forms of trimethylamine dehydrogenase and *p*-cresol methylhydroxylase, in which a positively charged arginine residue in the proximity of the N(1)-C(2)=O locus of the flavin cofactor was selectively replaced (36, 37). Although the low degree of enzyme flavinylation in CHO-H466A was not investigated further in this study, it is reasonable that the low flavin content in the mutated enzyme might be due to the removal of the positively charged His<sub>466</sub> (*vide infra*) from the active site of the enzyme, which results in an altered flavin microenvironment in CHO-H466A. In this context, an effect of the alanine replacement of His<sub>466</sub> on the flavin microenvironment of choline oxidase is supported by several observations presented herein.

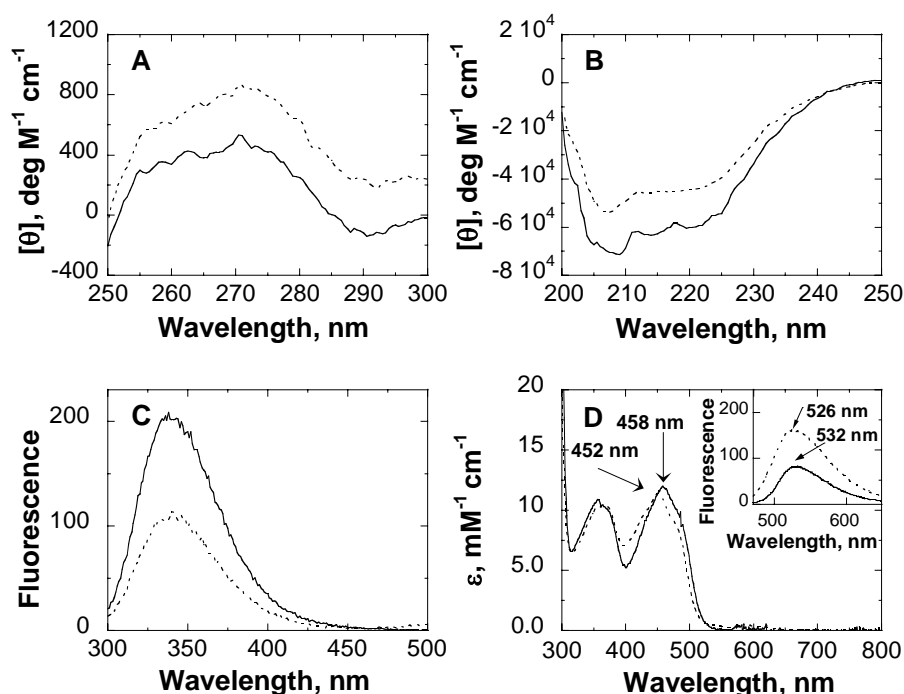


**Figure 5.2.** Comparison of the spectral properties of CHO-H466A (solid curves) and CHO-WT (dotted curves).

*Panels A and B*, circular dichroism spectra of CHO-H466A and CHO-WT in 20 mM Tris-Cl, pH 8, at 5 °C. Enzyme concentrations were 15 and 5  $\mu$ M for the near-UV and far-UV determinations, respectively; *panel C*, protein fluorescence emission spectra of CHO-H466A and CHO-WT in 20 mM Tris-Cl, pH 8, at 15 °C, the excitation wavelength was 285 nm for both enzymes; *panel D*, UV-visible absorbance and fluorescence emission spectra of CHO-H466A and CHO-WT in 20 mM Tris-Cl, pH 8, at 15 °C, the excitation wavelengths for CHO-WT and CHO-H466A were 453 nm and 458 nm, respectively.

However, while no spectral changes were observed with the wild-type enzyme upon aerobic incubation at pH 8 of the semiquinone-containing enzyme after removal of the excess dithionite by gel filtration (23), complete reoxidation of the enzyme-bound anionic flavin semiquinone was observed with CHO-H466A as indicated by the increase in absorbance at 458 nm (data not shown). These data clearly indicate that the lack of flavin semiquinone in the CHO-H466A protein as purified is due to an impaired ability of this mutant enzyme to stabilize the

anionic flavin semiquinone rather than to promote its formation. In contrast to wild type choline oxidase, which was recently shown to form a tight reversible N(5)-flavin sulfite adduct with a  $K_d$  value of  $\sim 50 \mu\text{M}$  at  $15^\circ\text{C}$  (23), no significant absorbance changes were observed upon treatment of CHO-H466A with either 25 or 100 mM sodium sulfite at pH 6.5 over 3.5 h of incubation (Figure 5.3). All taken together, these data further suggest a change in the flavin microenvironment upon replacing His<sub>466</sub> with alanine.

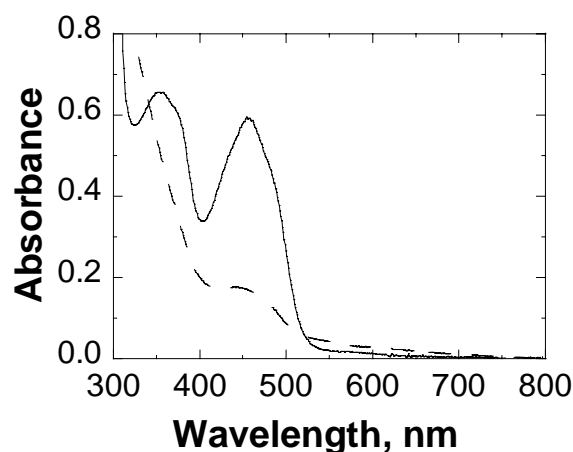


**Figure 5.3.** Reaction of CHO-H466A with sulfite.

UV-visible absorbance spectra of CHO-H466A after 3.5 hours of incubation with 100 mM sodium sulfite in the absence (solid curve) or the presence (dotted curve) of 100 mM imidazole. Enzyme concentrations were  $50 \mu\text{M}$  in 100 mM sodium pyrophosphate, pH 6.5, at  $15^\circ\text{C}$ .

***Effect of pH on the Spectral Properties of CHO-H466A and Wild-type Choline Oxidase.*** The effect of pH on the spectral properties of the histidine mutant was determined and compared to that of wild-type enzyme. At pH 6, CHO-H466A exhibited absorbance maxima at 458 and 369 nm, whereas the wild-type enzyme showed maxima at 455 and 357 nm (data not shown). As the pH is increased, a decrease in absorbance in the near-UV and visible regions of the spectra associated with increased resolution in the 430-500 nm region were observed with



both CHO-H466A and the wild-type enzymes (Figure 5.4). Such spectral perturbations are consistent with deprotonation of the FAD at the N(3)-H position occurring as the pH is increased (38). From the spectral changes at 500 nm, a  $pK_a$  value of  $9.3 \pm 0.2$  was determined for the ionization of the N(3)-H locus of the enzyme-bound  $8\alpha$ -N(1)-histidyl-FAD in CHO-H466A (Figure 5.4). Such a value compares well with the value of 9.7 that is observed for  $8\alpha$ -N-imidazolyl-riboflavin in solution (31). In contrast, a  $pK_a$  value of  $8.2 \pm 0.1$  was determined for the wild-type enzyme (Figure 5.4). These data are consistent with His<sub>466</sub> significantly affecting the ionization of the oxidized flavin at the N(3)-H locus in choline oxidase, and with a change in the flavin microenvironment upon replacing His<sub>466</sub> with alanine.

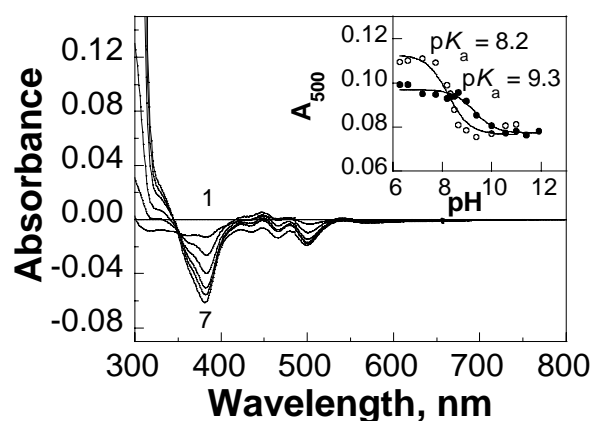


**Figure 5.4.** Effect of pH on the spectral properties of CHO-H466A and CHO-WT.

Absorbance spectra were recorded at an enzyme concentration of 21  $\mu$ M in 20 mM sodium phosphate, 20 mM sodium pyrophosphate, at 15  $^{\circ}$ C. Only selected difference absorbance spectra in the pH range between 6 (curve 1) to 12 (curve 7) are shown for CHO-H466A. Insets, UV-visible absorbance values at 500 nm of CHO-H466A ( $\bullet$ ) and CHO-WT ( $\circ$ ) as a function of pH; the curves are fits of the data to eq (5).

**Redox Potentiometry.** The mid-point reduction-oxidation potential of CHO-H466A in complex with glycine betaine was determined through the reductive titration of the enzyme with sodium dithionite as a reductant, and was compared to that for the wild-type form of the enzyme. This determination was carried out on the glycine betaine-enzyme complex rather than the unliganded enzyme because the catalytic transfers of hydride equivalents from choline and the aldehyde intermediate to molecular oxygen via the flavin cofactor occur when the active site of the enzyme is occupied by either the substrate or the product of the reaction (22, 23). As shown in Figure 5.5, the oxidized flavin bound to CHO-H466A was reduced to the hydroquinone with no significant formation of semiquinone species, as expected based on previous data indicating that the enzyme under turnover cycles between the oxidized and reduced states<sup>3</sup> (23). At pH 7, a mid-point reduction-oxidation potential ( $E_{m,7}$ ) of  $+106 \pm 0.5$  mV was determined in two independent experiments for CHO-H466A by fitting the data to Nernst equation (eq 6). A value of 24 mV was calculated from the slope in a plot of the reduction-oxidation potential as a function of the logarithm of [oxidized]/[reduced] flavin (Figure 5.5), in good agreement with the theoretical value of 28.5 mV for a two-electron transfer reaction at 15 °C. A similar analysis of the wild-type enzyme yielded an  $E_{m,7}$  value of  $+132 \pm 1$  mV for the two-electron transfer in the glycine betaine-enzyme complex (data not shown), a value that is in keeping with previously reported values for other flavoenzymes whose cofactor is covalently linked to the protein, such

---

<sup>3</sup> Attempts to determine the  $E_{m,7}$  through the oxidative titration of the enzyme using potassium ferricyanide as an oxidant failed with both the mutant and wild-type enzymes, mainly due to instability of the enzyme in the reduced state over the prolonged times required for equilibration of the system after each addition of oxidant. Nonetheless, we are confident of the quality of the data reported herein since with both the mutant and wild-type enzymes the  $E_{m,7}$  values determined in two independent experiments were in excellent agreement with each other. Furthermore, the  $E_{m,7}$  values for both enzymes differed by less than 2% when the data were analyzed by using

$$A_{458} = \frac{a + b \times 10^{(E_{m,7} - E)/28.5}}{1 + 10^{(E_{m,7} - E)/28.5}}, \text{ where } a \text{ and } b \text{ are component absorbance values contributed by the flavin in}$$

the oxidized and reduced states, respectively, and  $E$  and  $E_{m,7}$  are the electrode potential and the midpoint reduction-oxidation potential for a two-electron transfer process, respectively (34, 39).

as *p*-cresol methylhydroxylase ( $E_{m,7} = 84$  mV) (40) or vanillyl alcohol oxidase ( $E_{m,7} = 55$  mV) (41). Consequently, a  $\sim 25$  mV decrease in the reduction-oxidation potential of the enzyme-bound flavin is effected by the replacement of the active site histidine with an alanine residue.

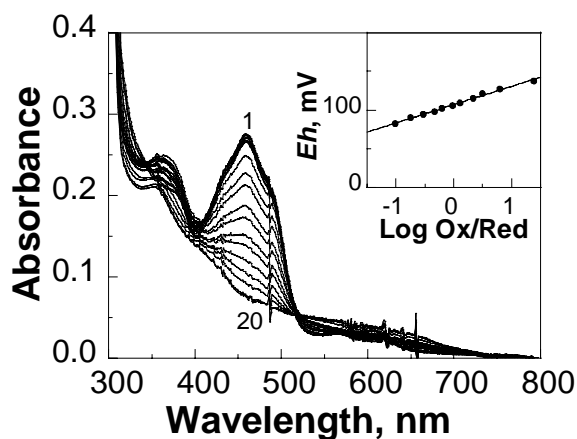


**Figure 5.5.** Potentiometric redox titration of CHO-H466A in complex with glycine betaine. *Curve 1*, UV-absorbance spectrum of the fully oxidized CHO-H466A at a concentration of  $\sim 23$   $\mu$ M in the presence of 1.5 M glycine betaine, in 20 mM Tris-Cl, pH 7 at 15  $^{\circ}$ C; *curves 2-19*, are selected intermediate spectra recorded during the reduction of the ligand bound CHO-H466A after each addition of sodium dithionite; *curve 20*, UV-absorbance spectrum of the fully reduced ligand bound CHO-H466A. *Inset*, Nernst plot of the potentiometric data for the reduction of the enzyme-bound flavin in CHO-H466A. The line is a fit of the data to eq 6.

**Steady-State Kinetics.** The steady-state kinetic parameters for wild-type choline oxidase with choline as substrate were recently reported (23). Here, the steady-state kinetic parameters of CHO-H466A were determined by monitoring the rate of oxygen consumption at varying concentrations of both choline and oxygen at pH 7 and 25  $^{\circ}$ C. As expected from previous data with the wild-type enzyme, the best fit of the data was observed to a sequential steady-state kinetic mechanism (eq 1), consistent with the order of the kinetic steps involving substrate binding and product release being not changed by the substitution of His<sub>466</sub> with alanine. When the kinetic parameters for CHO-H466A were compared to those of the wild-type enzyme (Table

5.1), a 60- and 1000-fold decrease in both the  $k_{\text{cat}}$  and  $k_{\text{cat}}/K_{\text{m}}$  values for choline were observed, respectively, indicating a direct participation of His<sub>466</sub> in the oxidation of choline. In contrast, the  $k_{\text{cat}}/K_{\text{m}}$  value for oxygen was only 1.5-times lower in CHO-H466A as compared to the wild-type enzyme (Table 5.1), suggesting a minimal involvement of the histidine residue in the oxidation of the enzyme-bound reduced flavin by molecular oxygen.

***Rescuing Effects of Imidazole.*** From a structural standpoint, the histidine to alanine mutation in the active site of choline oxidase is equivalent to the removal of an imidazole moiety from the side chain of the amino acid residue at position 466. In principle, both the kinetic and biochemical properties that have been affected by such a mutation should be at least partially restored in the enzyme in the presence of exogenous imidazole. At pH 7, the  $k_{\text{cat}}$  value with choline as substrate increased in a concentration-dependent pattern with increasing amounts of exogenous imidazole in the assay reaction mixture (Table 5.2), indicating that CHO-H466A activity can be rescued by imidazole. In contrast, no significant effect was observed with the wild-type enzyme under the same conditions. Although the effect of imidazole accounted for only a limited rescue of the enzymatic activity of CHO-H466A when compared to that of the wild-type enzyme, i.e., less than 10% at pH 7, it was nonetheless significant and allowed the determination of the effect of pH on the imidazole effect in order to establish whether the protonated or the unprotonated form of imidazole is responsible for the effect.

**Table 5.1.** Steady State Kinetic Parameters of CHO-H466A and CHO-WT with Choline as Substrate at pH 7<sup>a</sup>

kinetic parameters	CHO-H466A	CHO-WT <sup>b</sup>
$k_{\text{cat}}$ , s <sup>-1</sup>	1.1 ± 0.1	61 ± 6
$K_{\text{a}}$ , mM <sup>c</sup>	29 ± 1	1.7 ± 0.3
$k_{\text{cat}}/K_{\text{a}}$ , M <sup>-1</sup> s <sup>-1</sup> <sup>c</sup>	38 ± 2	36000 ± 6400
$K_{\text{O}_2}$ , μM	21 ± 2	703 ± 102
$k_{\text{cat}}/K_{\text{O}_2}$ , M <sup>-1</sup> s <sup>-1</sup>	55000 ± 5000	87100 ± 15300
$K_{\text{ia}}$ , mM	8.5 ± 2.9	0.20 ± 0.05
$R^2$	0.997	0.998

<sup>a</sup> Enzymatic activity was measured by varying the concentrations of both choline and oxygen in 50 mM potassium phosphate, pH 7, at 25 °C.

<sup>b</sup> From ref. (23).

<sup>c</sup>  $K_{\text{a}}$  and  $k_{\text{cat}}/K_{\text{a}}$  are the  $K_{\text{m}}$  and  $k_{\text{cat}}/K_{\text{m}}$  values for choline, respectively.

**Table 5.2.** The Effect of Imidazole on the Turnover Number of CHO-H466A at Different pH Values <sup>a</sup>

PH	$k_{\text{cat}}$ , s <sup>-1b</sup>	$k_{\text{cat}}$ (Imidazole), s <sup>-1b</sup>	$K_{\text{Imidazole}}$ , mM <sup>c</sup>	$R^2$
5.5	0.03	0.21 ± 0.05	52 ± 6	0.998
6	0.07	0.32 ± 0.02	71 ± 15	0.985
7	0.37	0.52 ± 0.06	18 ± 3	0.992
8	0.72	0.67 <sup>d</sup>	nd <sup>f</sup>	Nd
10	0.73	0.70 <sup>e</sup>	nd	Nd

<sup>a</sup> Enzymatic activity was measured in the presence of imidazole (0-250 mM) with 10 mM choline as a substrate in 50 mM air-saturated buffer at 25 °C.

<sup>b</sup>  $k_{\text{cat}}$  and  $k_{\text{cat}}$  (Imidazole) are the turnover numbers of the enzyme in the absence and the presence of saturated imidazole, respectively.

<sup>c</sup>  $K_{\text{Imidazole}}$  is the concentration of imidazole at which half the maximal turnover number is observed.

<sup>d,e</sup> Turnover number in the presence of 80 mM and 100 mM imidazole, respectively.

<sup>f</sup> nd, not determined.

As summarized in Table 5.2, no changes on  $k_{\text{cat}}$  with choline were observed in the presence of imidazole at both pH 8 and 10, whereas 5- and 10-fold increases in the  $k_{\text{cat}}$  values were seen at pH 6 and 5.5, respectively. When the relative increase in the  $k_{\text{cat}}$  values due to exogenous imidazole was analyzed as a function of pH (Figure 5.6), the data could be fit to a curve with a slope of -1 (eq 5), indicating a pH effect on the rescuing of the enzymatic activity of CHO-H466A. These results clearly indicate that the protonated form of imidazole is the catalytically relevant species responsible for the partial rescue of enzymatic activity in CHO-H466A, thereby providing strong evidence against His<sub>466</sub> acting as a the specific base in choline oxidase.

Addition of exogenous imidazole was also effective in restoring the ability of CHO-H466A to stabilize an N(5)-flavin adduct with sulfite, as indicated by the bleaching of the flavin peak at 458 nm upon incubating the enzyme with 100 mM sodium sulfite at pH 6.5 in the presence of 100 mM imidazole (Figure 5.3).

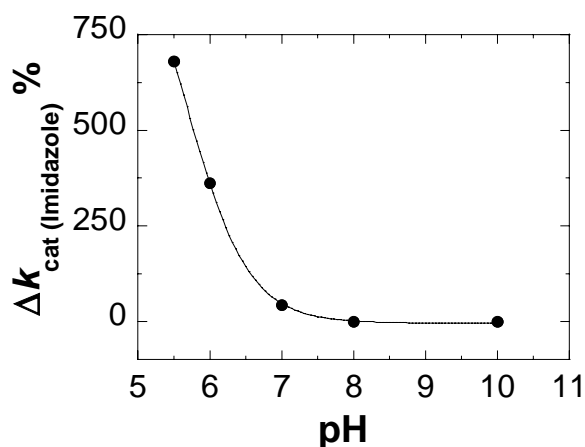


**Figure 5.6.** pH dependence of the imidazole-rescued activity of CHO-H466A.

The percentage of increase in  $k_{\text{cat}}$  values of CHO-H466A as a function of pH, calculated from the ratio of the  $k_{\text{cat}}$  value with choline measured in the presence of saturating imidazole to the  $k_{\text{cat}}$  value measured in the absence of imidazole. The curve is a fit of the data to eq 5.

***pH Dependence of the  $k_{\text{cat}}$  and  $k_{\text{cat}}/K_{\text{m}}$  Values.*** Previous pH dependence studies with choline oxidase established the requirement of a catalytic base with  $\text{p}K_{\text{a}}$  value of  $\sim 7.5$  in the oxidation of choline but not in the subsequent oxidation of the reduced enzyme-bound flavin (23). Here, the kinetic parameters of CHO-H466A were measured as a function of pH by varying the concentration of choline in air-saturated buffer since, as previously shown, with wild-type choline oxidase the  $\text{p}K_{\text{a}}$  value determined in the  $k_{\text{cat}}/K_{\text{m}}$  pH profile for the organic substrate is independent of the concentration of oxygen (21, 23, 27). With CHO-H466A, both the  $k_{\text{cat}}/K_{\text{m}}$  and  $k_{\text{cat}}$  values for choline increased with increasing pH and reached limiting values at high pH (Figure 5.7), consistent with the requirement for an unprotonated group in catalysis with the mutant enzyme. A  $\text{p}K_{\text{a}}$  value of  $9.0 \pm 0.1$  was determined in the pH profile for the  $k_{\text{cat}}/K_{\text{m}}$  value, consistent with replacement of the histidine with an alanine at position 466 affecting the electrostatic properties of the active site and with His<sub>466</sub> not being the active site catalytic base in choline oxidase<sup>4</sup>. A  $\text{p}K_{\text{a}}$  value of  $6.0 \pm 0.1$  was also determined in the pH profile of the  $k_{\text{cat}}$  value for CHO-H466A.

***Substrate and Solvent Kinetic Isotope Effects.*** Substrate and solvent kinetic isotope effects on the  $k_{\text{cat}}/K_{\text{m}}$  value with 1,2- $[\text{}^2\text{H}_4]$ -choline as substrate for wild-type choline oxidase were recently reported and are summarized in Table 5.3 (21). With that enzyme, the observed  $^{\text{D}}k_{\text{cat}}/K_{\text{m}}$  value corresponds to the true kinetic isotope effect and can be used to probe the status of the CH bond in catalysis, since at saturating oxygen concentrations both the forward and reverse

---

<sup>4</sup> In principle, the results of the pH dependence studies of CHO-H466A are also consistent with the histidine residue being the catalytic base in the wild-type enzyme, and with some amino acid residues other than His<sub>466</sub> becoming the catalytic base in the mutant enzyme devoid of histidine, as originally suggested for H<sub>447</sub> of cholesterol oxidase (17). If this were the case, the increase in the enzymatic activity of the CHO-H466A mutant protein in the presence of imidazole should show pH dependence with maximal effects above pH 7, i.e., above the  $\text{p}K_{\text{a}}$  value of imidazole, at which the fraction of unprotonated imidazole that might act as a base is higher. The data presented in Figure 6 clearly do not support this alternative interpretation of the pH profile data.

commitments to catalysis are negligible (21). Here, the effect of isotopically substituted choline on the  $k_{\text{cat}}/K_m$  value with CHO-H466A was determined in air-saturated 50 mM sodium pyrophosphate at pH 10 and 25 °C, at which the true kinetic isotope effects could be measured<sup>5</sup>. With CHO-H466A there was a significant decrease in the  $^{\text{D}}k_{\text{cat}}/K_m$  value with respect to the wild-type enzyme (Table 5.3), consistent with either a nonlinear transition state in which the stretching vibration of the hydride in motion is not completely lost in the transition state (42-44), or with the kinetic step in which the substrate CH bond is cleaved becoming partially masked by some other slow kinetic steps in the mutant enzyme. The effect of deuterated solvent, which was previously used to establish that OH bond cleavage of the choline substrate is kinetically fast in the reaction catalyzed by the wild-type enzyme (21), was also determined at a pL value of 10. As shown in Table 5.3, a significant  $^{\text{D}_2\text{O}}k_{\text{cat}}/K_m$  value was observed with CHO-H466A, suggesting that OH bond cleavage has become partially rate-limiting in the mutant enzyme. No significant changes in the  $^{\text{D}}k_{\text{cat}}/K_m$  value were observed upon substituting H<sub>2</sub>O with D<sub>2</sub>O. Similarly, the  $^{\text{D}_2\text{O}}k_{\text{cat}}/K_m$  value was the same irrespective of the isotopic composition of the substrate. Finally, a multiple kinetic isotope effect on the  $k_{\text{cat}}/K_m$  value that was equal to the product of the substrate and the solvent isotope effects was determined. These kinetic data are consistent with removal of the hydroxyl proton being concerted with hydride transfer to the flavin in CHO-H466A (45). From a mechanistic standpoint, these data indicate that in choline oxidase the replacement of the histidine at position 466 with an alanine residue results in a significant perturbation of the timing of substrate bond cleavage in the oxidation of the choline substrate.

---

<sup>5</sup> Under atmospheric oxygen conditions at 25 °C (i.e., with a concentration of dissolved oxygen of 0.25 mM), due to the low  $K_m$  value for oxygen with a value of  $5 \pm 2$   $\mu\text{M}$  at pH 10 (Ghanem, M., and Gadda, G.; unpublished data), CHO-H466A is > 97% saturated with oxygen. Therefore, with CHO-H466A the true kinetic isotope effect could be determined from the  $^{\text{D}}k_{\text{cat}}/K_m$  value under atmospheric conditions.



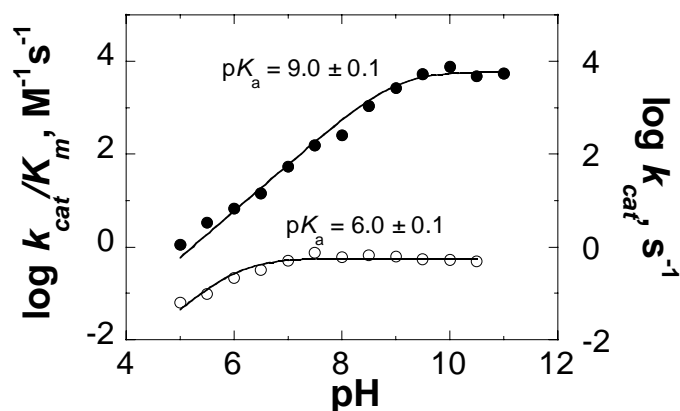


**Figure 5.7.** pH dependence of  $k_{\text{cat}}/K_{\text{m}}$  (●) and  $k_{\text{cat}}$  (○) values of CHO-H466A for choline as substrate.

Enzymatic activity was measured at varying concentrations of choline in air-saturated buffer between pH 5.5 and 11, at 25 °C. The curves are fits of the data to eq 3.

<b>Table 5.3.</b> Substrate and Solvent Isotope Effects on the Oxidation of Choline Catalyzed by CHO-H466A		
kinetic parameters	CHO-H466A <sup>a</sup>	CHO-WT <sup>b</sup>
$^{\text{D}}k_{\text{cat}}/K_{\text{m}}$	$6.3 \pm 0.8$	$10.7 \pm 2.6$
$^{\text{D}}k_{\text{cat}}/K_{\text{m}(\text{D}_2\text{O})}$	$6.0 \pm 0.7$	nd <sup>c</sup>
$^{\text{D}_2\text{O}}k_{\text{cat}}/K_{\text{m}}$	$2.2 \pm 0.3$	$1.1 \pm 0.2$
$^{\text{D}_2\text{O}}k_{\text{cat}}/K_{\text{m}(\text{D})}$	$2.0 \pm 0.2$	nd
$^{\text{D}, \text{D}_2\text{O}}k_{\text{cat}}/K_{\text{m}}$	$13.2 \pm 1.3$	$10.4 \pm 1.8$
<sup>a</sup> Enzymatic activity was measured by varying the concentrations of either choline or 1,2-[ <sup>2</sup> H <sub>4</sub> ]-choline in air-saturated 50 mM sodium pyrophosphate, pL 10, at 25 °C. Values shown are the average of two independent experiments.		
<sup>b</sup> From ref. (21).		
<sup>c</sup> nd, not determined.		

***Binding of Glycine Betaine.*** Recent kinetic data showed that glycine betaine inhibits choline oxidase by binding at the active site of the enzyme, resulting in spectral perturbations of the UV-visible absorbance spectrum (23, 27). Here, the effect of glycine betaine binding on the spectral properties of CHO-H466A was determined and compared to that of the wild-type enzyme by recording the absorbance spectrum for the enzyme before and after the addition of 200 mM glycine betaine, at pH 6.5 and 15 °C. As shown in Figure 5.8, binding of the inhibitor to the enzyme resulted in significant spectral perturbations in the 300 to 500 nm region of the absorbance spectrum, with a maximal increase in absorbance at ~496 nm. In contrast, the wild-type enzyme produced a maximal increase in absorbance at ~450 nm upon binding glycine betaine (Figure 5.8). The pH dependence of the inhibition by glycine betaine was determined in atmospheric oxygen using choline as substrate for CHO-H466A. As shown in Figure 8, the data were consistent with a single ionizable group that must be protonated for inhibition, as expected from previous studies on the wild-type enzyme (23). Although the  $pK_a$  value for such a protonated group was poorly defined due to instability of the CHO-H466A enzyme at high pH values, a  $pK_a$  value  $\geq 9$  could be estimated from the visual inspection of the data in Figure 8. Such a value is at least 1.5 pH units higher than the value of 7.5 previously determined for wild-type choline oxidase (23, 27, 46). Interestingly, glycine betaine binding was slightly tighter with CHO-H466A than with the wild-type enzyme, as suggested by the limiting  $K_{is}$  values of  $5.2 \pm 0.5$  and  $12.5 \pm 1.1$  determined at low pH for the two enzymes (Figure 5.8), suggesting that His<sub>466</sub> does not directly participate in product binding.

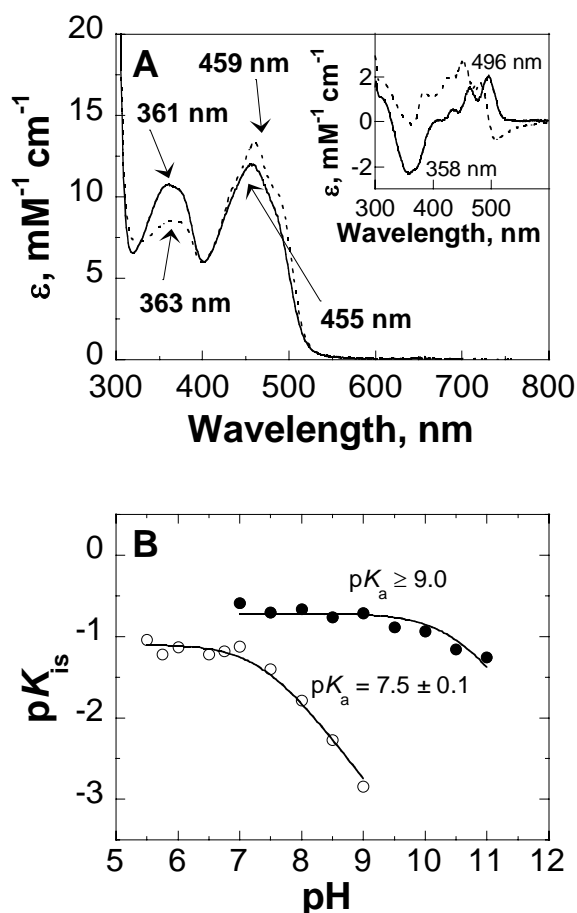


**Figure 5.8.** Binding of glycine betaine to CHO-H466A.

*Panel A*, the UV-visible absorbance spectra of CHO-H466A at a concentration of 51  $\mu\text{M}$  were recorded in 100 mM sodium pyrophosphate, pH 6.5 and 15  $^{\circ}\text{C}$ , before (solid curve) and after (dotted curve) the addition of 200 mM glycine betaine. *Inset*, comparison of the difference spectrum of CHO-H466A (solid curve) with that of CHO-WT (dotted curve) under the same conditions. *Panel B*, comparison between the pH dependence of the product inhibition of CHO-H466A ( $\bullet$ ) and wild-type enzyme ( $\circ$ ) from ref. (23), using glycine betaine. Enzymatic activity was measured at varying concentrations of choline and glycine betaine in air-saturated buffer between pH 7 and 11 for CHO-H466A, and between pH 5.5 to 9 for wild-type enzyme, at 25  $^{\circ}\text{C}$ . The lines are fits of the data to eq 4. The  $K_{\text{is}}$  values for glycine betaine were determined by fitting the initial rate data to eq 2.

## Discussion

The mutant form of choline oxidase in which the active site histidine at position 466 was replaced by an alanine residue maintains structural and kinetic properties that are similar to those of the wild-type enzyme, as indicated by both the spectroscopic and the steady-state kinetics data presented in this study. Consequently, the mechanistic properties that allow the elucidation of the role this amino acid residue plays in the reaction catalyzed by choline oxidase could be investigated by using a combination of biochemical, spectroscopic, and mechanistic probes.

The active site residue His<sub>466</sub> is involved in the oxidation of the choline substrate, but not in the following reduction of molecular oxygen catalyzed by choline oxidase. Evidence supporting this conclusion comes from the steady-state kinetic data with CHO-H466A as compared to those with the wild-type enzyme, showing that the  $k_{\text{cat}}/K_{\text{m}}$  value for choline decreases by three orders of magnitude whereas that for oxygen is not significantly changed in the mutant enzyme. The lack of involvement of His<sub>466</sub> in the oxidative half-reaction agrees well with previous kinetic data on choline oxidase as a function of pH, showing that no ionizable groups with  $\text{p}K_{\text{a}}$  values between 6 and 10 are required for oxidation of the enzyme-bound reduced flavin in catalysis (23).

His<sub>466</sub> is likely not the specific base with  $\text{p}K_{\text{a}}$  of  $\sim 7.5$  that abstracts the hydroxyl proton of the substrate in the reductive half-reaction in which choline is oxidized to betaine aldehyde. Strong evidence supporting this conclusion comes from the pH dependence of the imidazole effect with CHO-H466A, showing that imidazolium, but not imidazole, is the catalytically relevant species responsible for the partial rescue of the enzymatic activity of the mutant enzyme. These data are clearly difficult to reconcile with the assumption that His<sub>466</sub> is the catalytic base participating in the oxidation of choline since, if that were the case, maximal

rescue of the enzymatic activity of the mutant enzyme would have been observed at increasing pH. Consistent with His<sub>466</sub> not being the catalytic base in choline oxidase, the limiting  $k_{\text{cat}}/K_{\text{m}}$  value with choline at high pH is only ~20-fold lower in CHO-H466A as compared to the wild-type enzyme (23). In this respect, recent structural data at sub-atomic resolution showed that the N $\epsilon$ 2 atom of the equivalent histidine residue in the active site of cholesterol oxidase, His<sub>447</sub>, is protonated, suggesting that this conserved residue in the GMC oxidoreductase superfamily may play a role other than acting as a specific base in catalysis (13). In this context, a number of observations presented in this study suggest that in choline oxidase His<sub>466</sub> contributes to catalysis by modulating the electrophilicity of the flavin cofactor and the polarity of the active site, and by stabilizing the negative charge that is formed in the transition state for the oxidation of choline to betaine aldehyde.

A significant contribution to the electrophilicity of the FAD cofactor, which accounts for a fraction of the decreased rate of choline oxidation, is provided by the side chain of His<sub>466</sub>, as indicated by the decrease of ~25 mV in the midpoint reduction potential of the enzyme-bound flavin in CHO-H466A with respect to the wild-type choline oxidase. A direct electrostatic interaction of the imidazole side chain, through its N $\epsilon$ 2 locus, and the N(1)-locus of the flavin cofactor was previously proposed in glucose oxidase based on X-ray crystallographic data (9), suggesting that an analogous interaction might occur in choline oxidase (Figure 5.9). Evidence supporting the presence of such an interaction in choline oxidase is provided by the lack of stabilization of the anionic flavin semiquinone and of the sulfite N(5)-flavin adduct that were observed with CHO-H466A, which is consistent with a change in the protein microenvironment surrounding the N(1)-C(2)=O region of the flavin (36, 47-52). From the  $\Delta E_{m,7}$  value of -25 mV determined upon replacing H<sub>466</sub> with alanine in choline oxidase one can calculate an energetic

contribution of  $\sim 4.2 \text{ kJ mol}^{-1}$ , which accounts for a five-fold decrease in the rate of hydride transfer to the flavin in the mutant enzyme as compared to the wild-type form of choline oxidase. Since mechanistic investigations on wild-type choline oxidase are consistent with the  $k_{\text{cat}}/K_{\text{m}}$  value for choline reflecting the kinetic step of choline oxidation (21), a  $\sim 20$ -fold decrease in the rate of choline oxidation can be estimated from the ratio of the limiting  $k_{\text{cat}}/K_{\text{m}}$  values for choline at high pH determined in this study with CHO-H466A and the wild-type enzyme (23). Consequently, while His<sub>466</sub> contributes to the electrophilicity of the enzyme-bound flavin for efficient substrate oxidation, such an effect cannot fully explain the decreased catalytic activity observed with the mutant enzyme, consistent with His<sub>466</sub> contributing to catalysis by using also other strategies (*vide infra*). The modulation of the redox potential of the flavin does not appear to correlate with the rate of electron transfer from the reduced flavin to molecular oxygen, as indicated by the similar  $k_{\text{cat}}/K_{\text{m}}$  values for oxygen of CHO-H466A and the wild-type enzyme. Thus, it is likely that other factors, such as steric or solvation effects, are important in the activation of the reduced flavin for reaction with molecular oxygen.

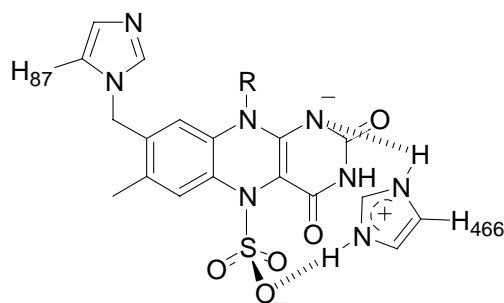


**Figure 5.9.** Proposed interaction of His<sub>466</sub> with the flavin N(5)-sulfite adduct.

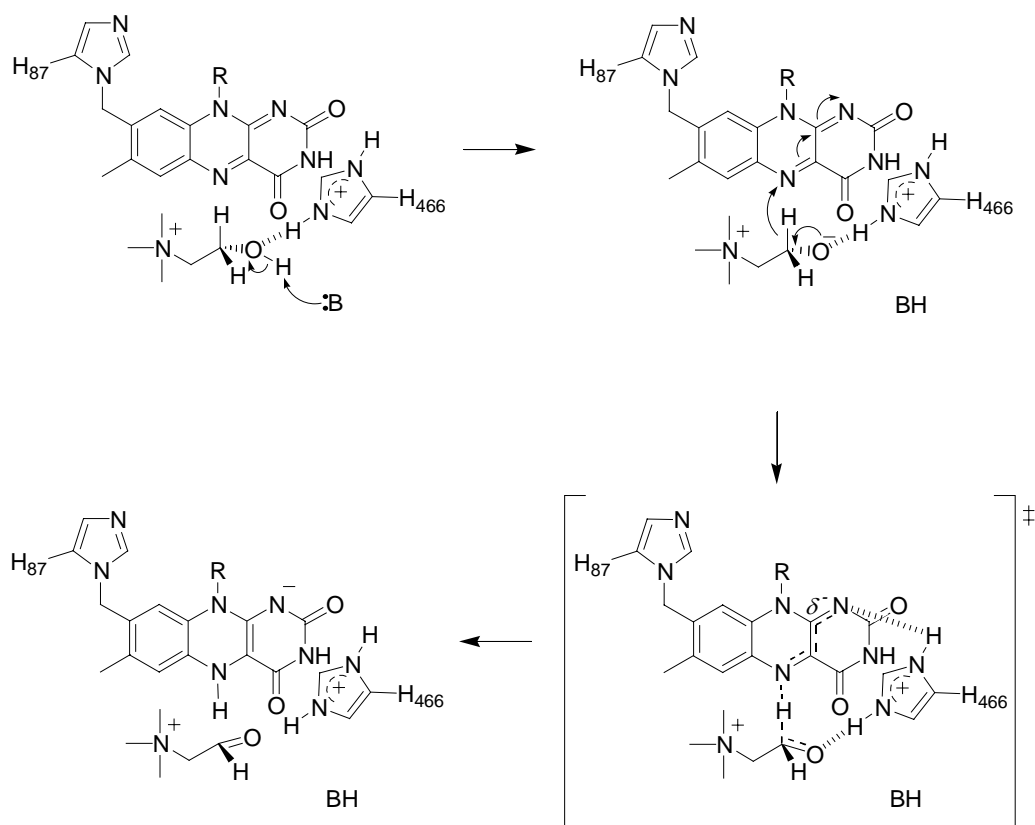
His<sub>466</sub> provides stabilization to the transition state that is formed in the oxidation of choline to betaine aldehyde, thereby facilitating the activation of the alcohol substrate for facile hydride transfer to the flavin cofactor (Scheme 5.3). Such a transition state in the mechanism of choline oxidase is supported by mechanistic studies on the wild-type form of choline oxidase using substrate and solvent deuterium kinetic isotope effects. (21) Evidence for stabilization of the alkoxide species by His<sub>466</sub> comes from the effects of histidine replacement on the relative timing for bond cleavage in the mutant enzyme, showing that the hydroxyl proton is in flight in the transition state for CH bond cleavage. Indeed, the loss of stabilization of the alkoxide species would make its formation energetically unfavorable, resulting in the loss of the "chelating effect" provided by the electrostatic interaction in the wild-type enzyme. In the absence of such a "chelating effect" catalysis would still occur, but it would be significantly slower because it requires that the vibrational motions of the pairs of atoms involved in bond breaking and making, i.e., the hydroxyl proton and the catalytic base along with the flavin N(5) and the  $\alpha$ -carbon hydrogen, be in phase to allow both proton and hydride transfer to occur. Alternatively, initiation of the hydride transfer would decrease the  $pK_a$  of the oxygen sufficiently for proton transfer to the catalytic base. In either case, removal of the hydroxyl proton would be concerted with hydride transfer, as was observed with CHO-H466A. Independent evidence for stabilization of the alkoxide species comes from the complete loss of the ability of CHO-H466A to form an N(5)-flavin adduct with sulfite, which is restored in the presence of exogenous imidazole. Although following the seminal work of Massey (49-51), the ability of flavoenzymes to stabilize a tight flavin adduct with sulfite has been mainly used as a probe of the electrophilicity of the flavin, N(5)-flavin adducts with sulfite depend also on steric factors as well as stabilizing interactions in the active site. With choline oxidase, it is likely that the negatively charged

oxygen atom of the sulfite N(5)-flavin adduct is stabilized by a direct interaction with the side chain of His<sub>466</sub> (Figure 5.9). In the absence of this interaction, such as in the case of CHO-H466A, the N(5)-flavin adduct with sulfite would not be stabilized; exogenous imidazole would restore such an interaction in the mutant enzyme by bridging the methyl side chain of the alanine residue at position 466 to the oxygen atom of the sulfite-flavin adduct. Such a direct interaction between the sulfite oxygen and an active site amino acid residue was previously observed in the three-dimensional structures of flavocytochrome *b*<sub>2</sub> (53) and glycolate oxidase (52), providing direct structural support for an analogous interaction in choline oxidase. The stabilization of the transition state is likely provided by the protonated form of His<sub>466</sub>, as suggested by the pH studies on the rescuing effect of the activity of CHO-H466A by exogenous imidazole, showing that the enzymatic activity of the mutant enzyme can be partially restored by imidazolium, but not imidazole. A stabilization of an alkoxide species by an active site tyrosine residue similar to that proposed here for His<sub>466</sub> of choline oxidase was recently proposed in flavocytochrome *b*<sub>2</sub> (54), suggesting that this might be a common strategy utilized by flavin-dependent enzymes for the oxidation of inactivated as well activated alcohols, such as  $\alpha$ -hydroxy acids.

The polarity of the active site, which is essential for efficient proton transfer of the hydroxyl proton from the alcohol substrate to the active site proton acceptor, is modulated by His<sub>466</sub>. Evidence supporting this conclusion comes from the pH profiles of the absorbance spectra of CHO-H466A and the wild-type enzyme, showing that the  $pK_a$  value for the ionization of the N(3) locus of FAD increases by one pH unit upon substituting His<sub>466</sub> with alanine. Such an increase in the  $pK_a$  value is consistent with a decreased polarity in the protein microenvironment surrounding the flavin N(3) locus (38). Consistent with a less polar active site, an increase in both the protein fluorescence of the unliganded enzyme and the absorbance at 496 nm of the



enzyme in complex with glycine betaine is seen with CHO-H466A with respect to the wild-type enzyme (35, 38). The decrease in polarity of the active site of CHO-H466A results in the perturbation of equilibria for ionization of groups that participate in catalysis, among which the amino acid group that accepts the hydroxyl proton from the substrate. Indeed, in CHO-H466A the  $pK_a$  value for the catalytic base in the active site is raised from 7.5 to  $\sim 9$ , as indicated by the pH profile of the  $k_{\text{cat}}/K_m$  values for choline. In agreement with previous studies on wild-type choline oxidase (23), the same  $pK_a$  value of  $\sim 9$  is seen in the pH-profile of glycine betaine inhibition with CHO-H466A. Thus, His<sub>466</sub> appears to be important for regulating the reactivity of the catalytic base that accepts the hydroxyl proton of the substrate for efficient catalysis.



**Scheme 5.3.** Proposed role of His466 in stabilizing the transition state during the oxidation of choline catalyzed by choline oxidase.

On the basis of the results of the rescuing experiments with imidazole, showing that the activity of CHO-H466A can be partially rescued by imidazolium, one would expect His<sub>466</sub> to interact with the carboxylate moiety of the glycine betaine product of the reaction. This expectation would be reinforced by the proposed role for His<sub>466</sub> in the stabilization of the alkoxide intermediate, since both the alkoxide and the carboxylate bear negatively charged oxygen. If this were the case, a significant increase to the extent of 2 to 3 orders of magnitude should be observed in the inhibition constant for glycine betaine with the CHO-H466A enzyme, as in the case of mutant forms of D-amino acid oxidase (48) or sarcosine oxidase (55), where positively charged groups on the enzyme that ion pair the carboxylate moieties of the product were replaced. However, the results of the product inhibition studies show that binding of glycine betaine to CHO-H466A is unaffected, if not slightly tighter, with respect to the wild-type enzyme. In this respect, recent studies with a number of substituted product analogs indicated that in choline oxidase the acetate moiety of glycine betaine does not contribute to binding, but that the trimethylammonium headgroup is a major determinant instead (27). This apparent discrepancy of His<sub>466</sub> interacting with the negatively charged oxygen of the transient alkoxide species but not with that of the carboxylate product is readily dissipated when one considers the spatial location of their respective oxygen atoms with respect to the histidine residue. Indeed, while the positioning of both the alkoxide and the product is dictated by the interactions established in the active site by the trimethylammonium headgroup (27), the alkoxide oxygen is linked to an  $sp^3$ -hybridized carbon whereas the carboxylate oxygen is attached to an  $sp^2$ -hybridized carbon. The change from the tetrahedral configuration of the alkoxide to the planar configuration of the carboxylate-containing product results in the carboxylate oxygen moving  $\sim 1$  Å away from the side chain of His<sub>466</sub>, thereby abating the electrostatic interaction between the

two charges. Although the results presented here do not allow us to draw any conclusion concerning the binding of the substrate in choline oxidase, it is expected that due to the lack of a negatively charged oxygen, binding of choline is somewhat weaker than that of the alkoxide. A similar result where substitution of an active site histidine residue resulted in differential binding of the substrate and the transition state was recently reported for (*S*)-mandelate dehydrogenase (56).

In summary, the results presented herein using a combination of biochemical, spectroscopic, and mechanistic approaches support evidence for the conserved His<sub>466</sub> playing multiple, but equally important, roles in the oxidation of the alcohol substrate catalyzed by choline oxidase. This residue modulates the electrophilicity of the enzyme-bound FAD for efficient hydride transfer from the substrate; it contributes to the polarity of the active site for efficient proton transfer from the substrate hydroxyl oxygen; and, it stabilizes the choline alkoxide transient species to facilitate hydride transfer from the substrate to the flavin. In light of the structural similarities among the members of the GMC oxidoreductase superfamily, the present results strongly suggest that those enzymes that catalyze the oxidation of unpolarized alcohols are likely to use similar catalytic strategies. Finally, the conclusions presented herein provide an example of the difficulty in developing a comprehensive description of the role carried out by amino acid residues located at the active site of enzymes, which arises from the complex nature of enzyme function to which individual residues are likely to contribute through multiple strategies. Current studies in our laboratory are aimed at the elucidation of the nature of the catalytic base that abstracts the hydroxyl proton from the alcohol substrate in the active site of choline oxidase.

### **Acknowledgment**

The authors thank Dr. Dale E. Edmondson at the Department of Biochemistry of Emory University, Atlanta, for his assistance and guidance in the determination of the redox potentials using the potentiometric method, and Fan Fan for building the hypothetical three-dimensional model of choline oxidase and her assistance in the preparation of Figure 1. The authors also thank Dr. Thomas L. Netzel for discussions on the "chelating effect" in catalysis by choline oxidase.

## References

- (1) Ohishi, N., and Yagi, K. (1979) Covalently bound flavin as prosthetic group of choline oxidase. *Biochem. Biophys. Res. Commun.* 86, 1084-8.
- (2) Ikuta, S., Imamura, S., Misaki, H., and Horiuti, Y. (1977) Purification and characterization of choline oxidase from *Arthrobacter globiformis*. *J. Biochem. (Tokyo)* 82, 1741-9.
- (3) Tsuge, H., Nakano, Y., Onishi, H., Futamura, Y., and Ohashi, K. (1980) A novel purification and some properties of rat liver mitochondrial choline dehydrogenase. *Biochim. Biophys. Acta* 614, 274-84.
- (4) Weibel, M. K., and Bright, H. J. (1971) The glucose oxidase mechanism. Interpretation of the pH dependence. *J. Biol. Chem.* 246, 2734-44.
- (5) Gibson, Q. H., Swoboda, B. E., and Massey, V. (1964) Kinetics and Mechanism of Action of Glucose Oxidase. *J. Biol. Chem.* 239, 3927-34.
- (6) Kamei, T., Takiguchi, Y., Suzuki, H., Matsuzaki, M., and Nakamura, S. (1978) Purification of 3 $\beta$ -hydroxysteroid oxidase of *Streptomyces violascens* origin by affinity chromatography on cholesterol. *Chem. Pharm. Bull. (Tokyo)* 26, 2799-2804.
- (7) Higham, C. W., Gordon-Smith, D., Dempsey, C. E., and Wood, P. M. (1994) Direct <sup>1</sup>H NMR evidence for conversion of beta-D-cellobiose to cellobionolactone by cellobiose dehydrogenase from *Phanerochaete chrysosporium*. *FEBS Lett.* 351, 128-32.
- (8) Cavener, D. R. (1992) GMC oxidoreductases. A newly defined family of homologous proteins with diverse catalytic activities. *J. Mol. Biol.* 223, 811-4.
- (9) Hecht HJ, K. H., Hendle J, Schmid RD, Schomburg D. (1993) Crystal structure of glucose oxidase from *Aspergillus niger* refined at 2.3 Å resolution. *J. Mol. Biol.* 229, 153-172.
- (10) Wohlfahrt, G., Witt, S., Hendle, J., Schomburg, D., Kalisz, H. M., and Hecht, H. J. (1999) 1.8 and 1.9 Å resolution structures of the *Penicillium amagasakiense* and *Aspergillus niger* glucose oxidases as a basis for modelling substrate complexes. *Acta Crystallogr. D. Biol. Crystallogr.* 55, 969-77.
- (11) Vrieling, A., Lloyd, L. F., and Blow, D. M. (1991) Crystal structure of cholesterol oxidase from *Brevibacterium sterolicum* refined at 1.8 Å resolution. *J. Mol. Biol.* 219, 533-54.
- (12) Li, J., Vrieling, A., Brick, P., and Blow, D. M. (1993) Crystal structure of cholesterol oxidase complexed with a steroid substrate: implications for flavin adenine dinucleotide dependent alcohol oxidases. *Biochemistry* 32, 11507-15.

- (13) Lario, P. I., Sampson, N., and Vrielink, A. (2003) Sub-atomic resolution crystal structure of cholesterol oxidase: what atomic resolution crystallography reveals about enzyme mechanism and the role of the FAD cofactor in redox activity. *J. Mol. Biol.* 326, 1635-50.
- (14) Hallberg, B. M., Henriksson, G., Pettersson, G., and Divne, C. (2002) Crystal structure of the flavoprotein domain of the extracellular flavocytochrome cellobiose dehydrogenase. *J. Mol. Biol.* 315, 421-34.
- (15) Fan, F., and Gadda, G. (2005) On the catalytic mechanism of choline oxidase. *J. Am. Chem. Soc.* 127, 2067-74.
- (16) Yin, Y., Liu, P., Anderson, R. G., and Sampson, N. S. (2002) Construction of a catalytically inactive cholesterol oxidase mutant: investigation of the interplay between active site-residues glutamate 361 and histidine 447. *Arch. Biochem. Biophys.* 402, 235-42.
- (17) Kass, I. J., and Sampson, N. S. (1998) Evaluation of the role of His447 in the reaction catalyzed by cholesterol oxidase. *Biochemistry* 37, 17990-8000.
- (18) Rotsaert, F. A., Renganathan, V., and Gold, M. H. (2003) Role of the flavin domain residues, His689 and Asn732, in the catalytic mechanism of cellobiose dehydrogenase from *Phanerochaete chrysosporium*. *Biochemistry* 42, 4049-56.
- (19) Su, Q., and Klinman, J. P. (1999) Nature of oxygen activation in glucose oxidase from *Aspergillus niger*: the importance of electrostatic stabilization in superoxide formation. *Biochemistry* 38, 8572-81.
- (20) Roth, J. P., and Klinman, J. P. (2003) Catalysis of electron transfer during activation of O<sub>2</sub> by the flavoprotein glucose oxidase. *Proc. Natl. Acad. Sci. U S A* 100, 62-7.
- (21) Fan, F., Ghanem, M., and Gadda, G. (2004) Cloning, sequence analysis, and purification of choline oxidase from *Arthrobacter globiformis*: a bacterial enzyme involved in osmotic stress tolerance. *Arch. Biochem. Biophys.* 421, 149-58.
- (22) Gadda, G. (2003) Kinetic mechanism of choline oxidase from *Arthrobacter globiformis*. *Biochim. Biophys. Acta* 1646, 112-8.
- (23) Ghanem, M., Fan, F., Francis, K., and Gadda, G. (2003) Spectroscopic and kinetic properties of recombinant choline oxidase from *Arthrobacter globiformis*. *Biochemistry* 42, 15179-88.
- (24) Rand, T., Halkier, T., and Hansen, O. C. (2003) Structural characterization and mapping of the covalently linked FAD cofactor in choline oxidase from *Arthrobacter globiformis*. *Biochemistry* 42, 7188-94.
- (25) Burg, M. B., Kwon, E. D., and Kultz, D. (1997) Regulation of gene expression by hypertonicity. *Annu. Rev. Physiol.* 59, 437-55.

- (26) McNeil, S. D., Nuccio, M. L., and Hanson, A. D. (1999) Betaines and related osmoprotectants. Targets for metabolic engineering of stress resistance. *Plant Physiol.* 120, 945-50.
- (27) Gadda, G., Powell, N., and Menon, P. (2004) The trimethylammonium headgroup of choline is a major determinant for substrate binding and specificity in choline oxidase. *Arch. Biochem. Biophys.*, In press.
- (28) Laemmli, U. K. (1970) Cleavage of structural proteins during the assembly of the head of bacteriophage T4. *Nature* 227, 680-5.
- (29) Whitby, L. G. (1953) A new method for preparing flavin-adenine dinucleotide. *Biochem. J.* 54, 437-42.
- (30) Schowen, K. B., and Schowen, R. L. (1982) Solvent isotope effects of enzyme systems. *Methods Enzymol.* 87, 551-606.
- (31) Williamson, G., and Edmondson, D. E. (1985) Effect of pH on oxidation-reduction potentials of 8  $\alpha$ -N-imidazole-substituted flavins. *Biochemistry* 24, 7790-7.
- (32) Ma, Y. C., Funk, M., Dunham, W. R., and Komuniecki, R. (1993) Purification and characterization of electron-transfer flavoprotein: rhodoquinone oxidoreductase from anaerobic mitochondria of the adult parasitic nematode, *Ascaris suum*. *J. Biol. Chem.* 268, 20360-5.
- (33) Mohsen, A. W., Rigby, S. E., Jensen, K. F., Munro, A. W., and Scrutton, N. S. (2004) Thermodynamic Basis of Electron Transfer in Dihydroorotate Dehydrogenase B from *Lactococcus lactis*: Analysis by Potentiometry, EPR Spectroscopy, and ENDOR Spectroscopy. *Biochemistry* 43, 6498-6510.
- (34) Dutton, P. L. (1978) Redox potentiometry: determination of midpoint potentials of oxidation-reduction components of biological electron-transfer systems. *Methods Enzymol.* 54, 411-35.
- (35) Nakajou, K., Watanabe, H., Kragh-Hansen, U., Maruyama, T., and Otagiri, M. (2003) The effect of glycation on the structure, function and biological fate of human serum albumin as revealed by recombinant mutants. *Biochim. Biophys. Acta* 1623, 88-97.
- (36) Efimov, I., Cronin, C. N., Bergmann, D. J., Kuusk, V., and McIntire, W. S. (2004) Insight into covalent flavinylation and catalysis from redox, spectral, and kinetic analyses of the R474K mutant of the flavoprotein subunit of *p*-cresol methylhydroxylase. *Biochemistry* 43, 6138-48.
- (37) Mewies, M., Packman, L. C., Mathews, F. S., and Scrutton, N. S. (1996) Flavinylation in wild-type trimethylamine dehydrogenase and differentially charged mutant enzymes: a study of the protein environment around the N1 of the flavin isoalloxazine. *Biochem. J.* 317, 267-72.

- (38) Massey, V., and Ganther, H. (1965) On the interpretation of the absorption spectra of flavoproteins with special reference to D-amino acid oxidase. *Biochemistry* 4, 1161-73.
- (39) Daff, S. N., Chapman, S. K., Turner, K. L., Holt, R. A., Govindaraj, S., Poulos, T. L., and Munro, A. W. (1997) Redox control of the catalytic cycle of flavocytochrome P-450 BM3. *Biochemistry* 36, 13816-23.
- (40) Efimov, I., Cronin, C. N., and McIntire, W. S. (2001) Effects of noncovalent and covalent FAD binding on the redox and catalytic properties of *p*-cresol methylhydroxylase. *Biochemistry* 40, 2155-66.
- (41) Fraaije, M. W., van den Heuvel, R. H., van Berkel, W. J., and Mattevi, A. (1999) Covalent flavinylation is essential for efficient redox catalysis in vanillyl-alcohol oxidase. *J. Biol. Chem.* 274, 35514-20.
- (42) Winstein, S., and Takahashi, J. (1958) Neighboring hydrogen, isotope effect, and conformation in solvolysis of 3-methyl-2-butyl *p*-toluenesulfonate. *Tetrahedron* 2, 316-321.
- (43) Collins, C. J., Rainey, W. T., Smith, W. B., and Kaye, I. A. (1959) Molecular Rearrangements. XIV. The Hydrogen-Deuterium Isotope Effect in the Pinacol Rearrangement of Triarylethylene Glycols. *J. Am. Chem. Soc.* 81, 460-466.
- (44) Hawthorne, M. F., and Lewis, E. S. (1958) Amine Boranes. III. Hydrolysis of Pyridine Diphenylborane and the Mechanism of Hydride Transfer Reactions. *J. Am. Chem. Soc.* 80, 4296-4299.
- (45) Cleland, W. W. (1991) multiple isotope effects in enzyme-catalyzed reactions, in *Enzyme mechanism from isotope effects* (Cook, P. F., Ed.) pp 291-311, CRC Press, Boca Raton, FL.
- (46) Gadda, G. (2003) pH and deuterium kinetic isotope effects studies on the oxidation of choline to betaine-aldehyde catalyzed by choline oxidase. *Biochim. Biophys. Acta* 1650, 4-9.
- (47) Müh, U., Williams, C. H., Jr., and Massey, V. (1994) Lactate monooxygenase. II. Site-directed mutagenesis of the postulated active site base histidine 290. *J. Biol. Chem.* 269, 7989-93.
- (48) Molla, G., Porrini, D., Job, V., Motteran, L., Vegezzi, C., Campaner, S., Pilone, M. S., and Pollegioni, L. (2000) Role of arginine 285 in the active site of *Rhodotorula gracilis* D-amino acid oxidase. A site-directed mutagenesis study. *J. Biol. Chem.* 275, 24715-21.
- (49) Müller, F., and Massey, V. (1969) Flavin-sulfite complexes and their structures. *J. Biol. Chem.* 244, 4007-16.
- (50) Massey, V., Müller, F., Feldberg, R., Schuman, M., Sullivan, P. A., Howell, L. G., Mayhew, S. G., Matthews, R. G., and Foust, G. P. (1969) The reactivity of flavoproteins



- with sulfite. Possible relevance to the problem of oxygen reactivity. *J. Biol. Chem.* 244, 3999-4006.
- (51) Massey, V., and Hemmerich, P. (1980) Active-site probes of flavoproteins. *Biochem. Soc. Trans.* 8, 246-57.
  - (52) Stenberg, K., Clausen, T., Lindqvist, Y., and Macheroux, P. (1995) Involvement of Tyr24 and Trp108 in substrate binding and substrate specificity of glycolate oxidase. *Eur. J. Biochem.* 228, 408-16.
  - (53) Tegoni, M., and Cambillau, C. (1994) Structural studies on recombinant and point mutants of flavocytochrome *b*<sub>2</sub>. *Biochimie* 76, 501-14.
  - (54) Sobrado, P., and Fitzpatrick, P. F. (2003) Solvent and primary deuterium isotope effects show that lactate CH and OH bond cleavages are concerted in Y254F flavocytochrome *b*<sub>2</sub>, consistent with a hydride transfer mechanism. *Biochemistry* 42, 15208-14.
  - (55) Zhao, G., Song, H., Chen, Z. W., Mathews, F. S., and Jorns, M. S. (2002) Monomeric sarcosine oxidase: role of histidine 269 in catalysis. *Biochemistry* 41, 9751-64.
  - (56) Lehoux, I. E., and Mitra, B. (2000) Role of arginine 277 in (*S*)-mandelate dehydrogenase from *Pseudomonas putida* in substrate binding and transition state stabilization. *Biochemistry* 39, 10055-65.

## CHAPTER VI

### Effects of Reversing the Protein Positive Charge in Proximity of the N(1)-Flavin Locus of Choline Oxidase

(This chapter was published in verbatim in Ghanem, M., and Gadda, G., (2006), *Biochemistry* 45, 3437-47. © 2006 American Chemical Society. All rights reserved.)

#### Abstract

A protein positive charge near the flavin N(1) locus is a distinguishing feature in common to most flavoprotein oxidases, with mechanistic implications for the modulation of flavin reactivity. A recent study showed that in the active site of choline oxidase the protein positive charge is provided by His<sub>466</sub>. Here, we have reversed the charge by substitution with aspartate (CHO-H466D), and for the first instance characterized a flavoprotein oxidase with a negative charge near the flavin N(1) locus. CHO-H466D formed a stable complex with choline, but lost the ability to oxidize the substrate. In contrast to the wild type enzyme, which binds FAD covalently in a 1:1 ratio, CHO-H466D contained ~0.3 FAD per protein, of which 75% was not covalently bound to the enzyme. Anaerobic reduction of CHO-H466D resulted in the formation of neutral hydroquinone, with no stabilization of flavin semiquinone; in contrast, the anionic semiquinone and hydroquinone species were observed with the wild type and a H466A variant of the enzyme. The midpoint reduction potential for the oxidized/reduced couple in CHO-H466D was ~160 mV lower than that of the wild type enzyme. Finally, CHO-H466D lost the ability to form complexes with glycine betaine or sulfite. Thus, upon reversing the protein charge near the FAD N(1) locus, choline oxidase lost the ability to stabilize negative charges in the active site, irrespective of whether they develop on the flavin or are borne on ligands, resulting in defective

flavinylation of the protein, decreased electrophilicity of the flavin, and consequent loss of catalytic activity.

## Introduction

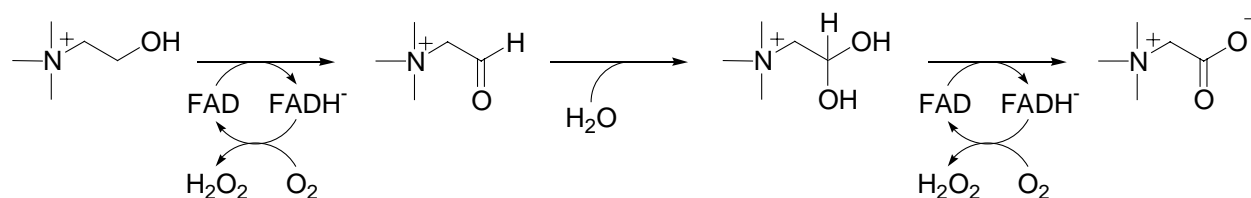
The presence of a protein positive charge proximal to the N(1) locus of the flavin has been proposed in flavoprotein oxidases long before the three dimensional structures of a number of flavin-dependent oxidases have become available (1-5). Indeed, most flavoprotein oxidases stabilize thermodynamically the anionic flavin semiquinone (6-11), form a stable reversible N(5)-flavin adduct with sulfite (1-4, 6, 7, 11-13), and stabilize the benzoquinoid anion forms of 6-hydroxy-, 8-hydroxy-, 6-mercapto-, and 8-mercapto-flavin analogs (4, 14-17), all features that require the stabilization of a negative charge localized in the N(1)-C(2)=O region of the flavin. The mechanistic implications for a protein positive charge stabilizing a negative charge on the N(1) locus of the flavin are: *i*) to render flavin reduction thermodynamically favorable by elevating the midpoint reduction-oxidation potential of the bound flavin (1, 4, 15, 17-19); *ii*) to preferentially stabilize the anionic form of the reduced flavin that readily reacts with oxygen (1-4, 18, 19); *iii*) to facilitate the flavinylation process for those enzymes in which the flavin is covalently linked to the protein moiety (20). To date, the X-ray crystallographic structures of glucose oxidase from *Aspergillus niger* (21) and *Penicillium amagasakiense* (22), cholesterol oxidase from *Brevibacterium sterolicum* (23) and *Streptomyces sp.* (24, 25), pyranose 2-oxidase from *Peniophora sp.* (26) and *Trametes multicolor* (27), cellobiose dehydrogenase from *Phanerochaete chrysosporium* (28), baker's yeast flavocytochrome  $b_2$  (29), spinach glycolate oxidase (30), pig kidney D-amino acid oxidase (31), and bacterial sarcosine oxidase (32), trimethylamine dehydrogenase (33), and dihydroorotate dehydrogenase (34), have shown that either a positively charged amino acid residue or a dipole of an  $\alpha$ -helix is oriented toward the N(1)-C(2)=O region of the enzyme-bound flavin. While the effects of replacing the positive charge with a neutral amino acid on the flavin properties have been investigated for lactate

monooxygenase (35), no studies have addressed the characterization of the flavin properties of an oxidase in which the positive charge close to the flavin N(1) was reversed.

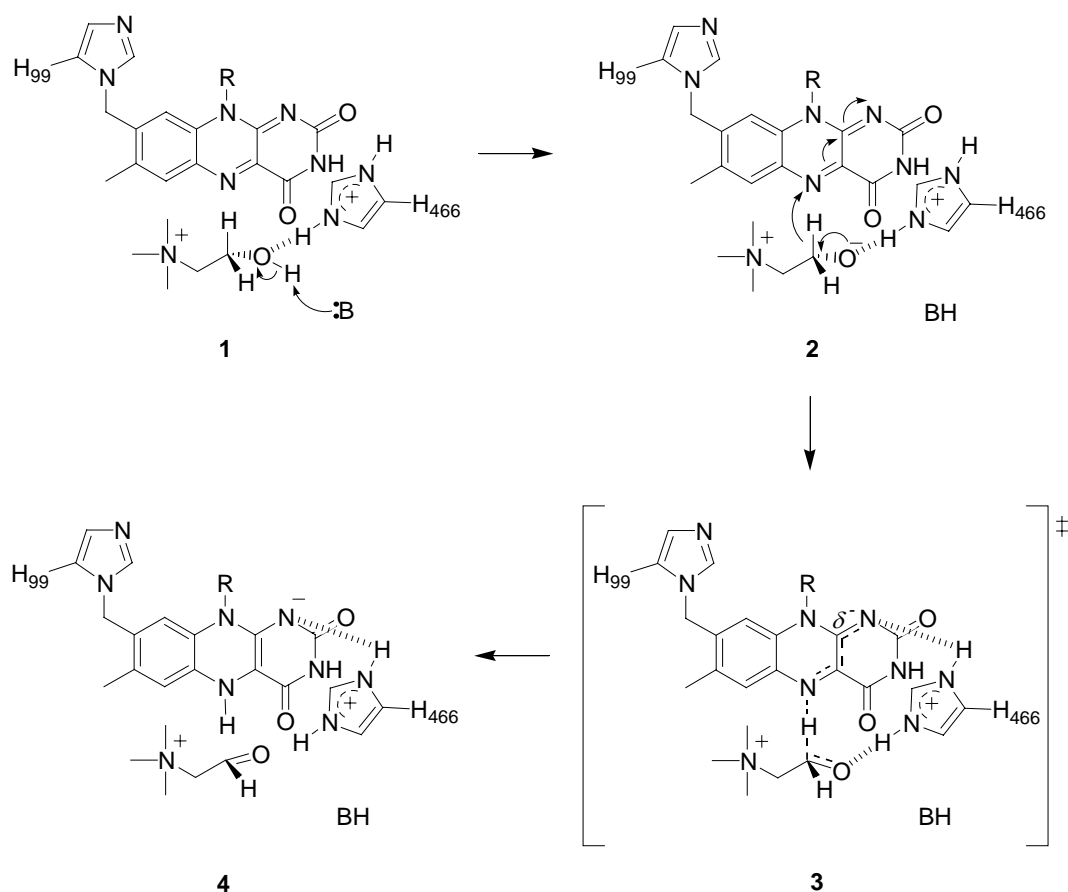
Choline oxidase (E.C. 1.1.3.17) is a flavin-dependent enzyme that oxidizes choline to glycine betaine via an enzyme-bound aldehyde intermediate (Scheme 1). This reaction is of considerable interest for medical and biotechnological applications, since accumulation of glycine betaine in many pathogens and plants enables their stress-resistance towards hyperosmotic environments (36, 37). Choline oxidase has been characterized in its biophysical, structural, and mechanistic properties. The enzyme is a homodimer with a mass of 120 kDa (38), contains covalently linked FAD in a 1:1 stoichiometry (38), and under turnover cycles between its fully oxidized and reduced states (39, 40). A detailed picture of the catalytic mechanism of choline oxidase has emerged from pH, kinetic isotope, and temperature effects studies (39-43), as well as mechanistic studies with substrate and product analogs (44) and site-directed mutants (45). Briefly, in catalysis an unidentified active site base with  $pK_a$  of 7.5 activates the alcohol substrate with formation of an alkoxide species (species 1 in Scheme 2) (39), which is transiently stabilized in the active site through electrostatic interaction with the imidazolium side chain of His<sub>466</sub> (45) (species 2 and 3 Scheme 2). Hydride transfer from the  $\alpha$ -carbon of the substrate to the enzyme-bound flavin occurs quantum mechanically from the activated choline alkoxide species (species 3 in Scheme 2) (41). Substrate binding is mainly dictated by interactions involving the trimethylammonium headgroup of the alcohol, with little participation of the ethyl moiety (44). In a recent study in which His<sub>466</sub> was replaced with alanine, our group showed that in catalysis His<sub>466</sub> is protonated and that, besides stabilizing the transient alkoxide species that is formed in catalysis, this protein group modulates the electrophilicity of the enzyme-bound FAD and the polarity of the active site (species 3 in Scheme 2) (45). Consistent with the proposed

roles, the recent determination of the X-ray structure of choline oxidase showed that His<sub>466</sub> is located at distance of  $\sim 3.3$  Å from the N(1) locus of the enzyme-bound flavin (Figure 1) (George Lountos, Fan Fan, Giovanni Gadda, and Allen M. Orville; unpublished results).

In the present study, we have prepared by site-directed mutagenesis a choline oxidase variant in which His<sub>466</sub> was replaced with aspartate, and characterized the biochemical and biophysical properties of the enzyme-bound flavin in the mutant enzyme bearing a negative charge at position 466. The results presented show that the protein positive charge proximal to the flavin N(1) locus is important for correct flavinylation of the enzyme, modulation of flavin reactivity and, consequently, the catalytic activity of the enzyme.



**Scheme 6.1.** Reaction catalyzed by choline oxidase.



**Scheme 6.2.** Chemical mechanism for choline oxidation catalyzed by choline oxidase.

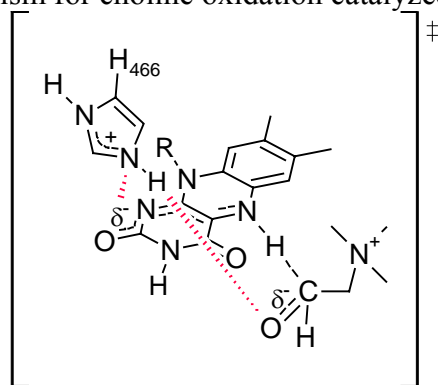


**Figure 6.1.** Line draw showing the interaction of His<sub>466</sub> with the N(1)–C(2)=O locus of FAD and the choline alkoxide species in the transition state for the oxidation of choline catalyzed by choline oxidase.

The positioning of His<sub>466</sub> relative to the flavin is from the X-ray crystallographic structure of the enzyme recently determined at 1.86 Å resolution (George Lountos, Fan Fan, Giovanni Gadda, and Allen M. Orville; unpublished results), the positioning of choline is arbitrary.

## Experimental Procedures

**Materials.** *Escherichia coli* strain Rosetta(DE3)pLysS was from Novagen (Madison, WI). The QuikChange Site-Directed Mutagenesis kit was from Stratagene (La Jolla, CA). The QIAprep Spin Miniprep kit was from Qiagen (Valencia, CA). Oligonucleotides used for site-directed mutagenesis and for sequencing of the mutant gene were custom synthesized by the DNA Core Facility of the Department of Biology of Georgia State University or by Sigma Genosys (The Woodlands, TX). Nucleotides, bovine serum albumin, chloramphenicol, tetracycline, isopropyl- $\beta$ -D-thiogalactopyranoside (IPTG), lysozyme, sodium hydrosulfite (dithionite), sodium sulfite, betaine aldehyde, glycine betaine, xanthine, xanthine oxidase, Luria-Bertani agar and broth, and PMSF were from Sigma (St. Louis, MO). Choline chloride and ampicillin were from ICN (Aurora, OH). Recombinant choline oxidase (CHO-WT)<sup>1</sup> from *Arthrobacter globiformis* strain ATCC 8010 was expressed in *E. coli* strain Rosetta(DE3)pLysS from plasmid pET/*codA1* and purified to homogeneity as previously described (38). Fully oxidized FAD-containing CHO-WT was prepared as described in ref. (44). The mutant form of choline oxidase with histidine 466 replaced with alanine (CHO-H466A) was prepared, expressed and purified to homogeneity according to ref. (45). All other reagents were of the highest purity commercially available.

**Instruments.** UV-visible absorbance spectra were recorded using an Agilent Technologies diode-array spectrophotometer model HP 8453 equipped with a thermostated water bath. Fluorescence spectra were recorded with a Shimadzu Spectrofluorometer model RF-5301

---

<sup>1</sup> CHO-WT, wild type choline oxidase; CHO-H466D, mutant form of choline oxidase with histidine 466 replaced with aspartate; CHO-H466A, mutant form of choline oxidase with histidine 466 replaced with alanine;  $E'_1$  and  $E'_2$ , midpoint reduction-oxidation potential of the oxidized/semiquinone and semiquinone/reduced FAD redox couples;  $E'_{m,7}$ , midpoint reduction-oxidation potential of the oxidized/reduced FAD redox couple determined at pH 7.



PC thermostated at 15 °C. Enzymatic activity of choline oxidase was measured polarographically using a computer-interfaced Oxy-32 oxygen-monitoring system (Hansatech Instrument Ltd.).

***Site-Directed Mutagenesis.*** A QuikChange kit was used to prepare CHO-H466D, in which histidine 466 was replaced with aspartate. The method used was essentially according to the manufacturer's instructions, using the pET/*codA1* plasmid (38) as a template and Cho-H466Df (5'-CAACACCGTCTACGACCCCGTGGGCACCGTGC-3') and Cho-H466Dr (5'-CACGGTGCCACGGGGTCGTAGACGGTGTTGTGC-3') oligonucleotides as forward and reverse primers, respectively (underlined letters indicate mismatches). DNA was sequenced at the DNA Core Facility at Georgia State University using an Applied Biosystems Big Dye Kit on an Applied Biosystems model ABI 377 DNA sequencer. Sequencing confirmed the presence of the correct mutation. *E. coli* strain Rosetta(DE3)pLysS competent cells were transformed with plasmid pET/*codA1*-H466D by electroporation.

***Expression and Purification of CHO-H466D.*** CHO-H466D was expressed and purified to homogeneity as judged by SDS-PAGE using the same procedure used previously for the purification of CHO-WT and CHO-H466A (38, 45). Glycerol at a final concentration of 10% was incorporated in the buffers throughout the purification procedure to increase the stability of the enzyme.

***Spectrophotometric Studies.*** The UV-visible absorbance and fluorescence emission or excitation spectra of CHO-H466D, CHO-WT and CHO-H466A, were acquired in 20 mM sodium phosphate, 20 mM sodium pyrophosphate and 10% glycerol, pH 6 at 15 °C. The UV-visible absorbance spectra of the reduced form of enzymes were acquired using an anaerobic cuvette in 50 mM sodium phosphate, 50 mM sodium pyrophosphate and 10% glycerol, pH 6 at 15 °C. The cuvette contained one ml final volume of enzyme at a final concentration between 20

and 30  $\mu\text{M}$ , 300  $\mu\text{M}$  xanthine, and 10  $\mu\text{M}$  methyl viologen. A sidearm attached to the cuvette contained xanthine oxidase at a final concentration of  $\sim 0.5$   $\mu\text{M}$ . The cuvette and contents were made anaerobic by at least 15 cycles of alternate degassing under vacuum and flushing with  $\text{O}_2$ -free argon. The enzyme solution was then mixed with xanthine oxidase in the side arm, and the reduction of the enzyme-bound flavin was monitored spectrophotometrically. Spectra of the reduced enzymes reported in this study were recorded prior to the accumulation of significant amounts of viologen radical.

The extinction coefficient of CHO-H466D was determined in 20 mM Tris-Cl, pH 8, after denaturation of the enzyme by incubation at 40  $^{\circ}\text{C}$  for one hour in the presence of urea at a final concentration of 4 M, based upon the  $\epsilon_{450}$  value of 11.3  $\text{mM}^{-1} \text{cm}^{-1}$  for free FAD (46). A value of 12  $\text{mM}^{-1} \text{cm}^{-1}$  was determined at 450 nm, which was similar to the values of 11.4  $\text{mM}^{-1} \text{cm}^{-1}$  at 452 nm for CHO-WT and 12  $\text{mM}^{-1} \text{cm}^{-1}$  at 458 nm for CHO-H466A (40, 45). For the quantitation of covalently bound flavin,  $\sim 20$   $\mu\text{M}$  CHO-H466D was incubated on ice for 30 min after the addition of 10 % trichloroacetic acid, followed by removal of precipitated protein by centrifugation. The concentration of FAD was then determined in both the supernatant and the pellet dissolved in 4 M urea solution as described above. Identification of the flavin cofactor released by acid treatment was carried out through MALDI-TOF mass spectrometry in both positive and negative ion modes using a 50:50 methanol/acetonitrile matrix. Anaerobic incubation of CHO-H466D with choline was carried out in 20 mM Tris-Cl, pH 8, after anaerobiosis was established by repeated cycles of alternate degassing under vacuum and flushing with ultra-pure  $\text{O}_2$ -free argon in an anaerobic cell equipped with two side arms. Choline, at a final concentration of 10 mM, was initially loaded into a side arm and subsequently mixed with CHO-H466D under anaerobiosis. Few grains of sodium dithionite were loaded into the

second side arm and mixed with CHO-H466D in complex with choline after an hour of anaerobic incubation to ensure the functionality of the enzyme-bound flavin. Binding of glycine betaine and sulfite to the enzymes was carried out as previously described (40, 45). The pH dependence of the UV-visible absorbance spectra of oxidized CHO-H466D was determined in 20 mM sodium phosphate, 20 mM sodium pyrophosphate, 10% glycerol, at 15 °C, by titrating sodium hydroxide into the enzyme solution at pH 6. The pH dependences of the UV-visible absorbance spectra of the reduced enzymes were determined in a custom made anaerobic cuvette (Lillie Glassblowers, Smyrna, GA) that was fitted with a pH micro-electrode through a glass joint and an anaerobic syringe containing sodium hydroxide. The cuvette contained 3 ml of enzyme at a final concentration between 20 and 30  $\mu$ M in 50 mM sodium phosphate, 50 mM sodium pyrophosphate, and 10 % glycerol, pH 6. A sidearm attached to the cuvette was loaded with choline at a final concentration of 150 mM. The cuvette and contents were made anaerobic by at least 15 cycles of alternate degassing under vacuum and flushing with O<sub>2</sub>-free argon. The enzyme solution was then mixed with choline in the side arm in order to reduce the enzyme-bound flavin. With CHO-H466D, which could not be reduced anaerobically with choline, a syringe filled with anaerobic ~2 mM dithionite was inserted firstly into the cuvette under positive argon pressure, and the reduction of the enzyme-bound flavin was monitored spectrophotometrically until completion. In all the cases, once the UV-visible absorbance spectrum of the hydroquinone species was observed, a pH micro-electrode and a syringe containing anaerobic 3 M sodium hydroxide were mounted onto the anaerobic cuvette under positive argon pressure. The pH of the anaerobic enzyme solution was then changed stepwise by addition of the base, and both the pH and the UV-visible absorbance spectra were recorded after each step.

**Potentiometric Titrations.** The midpoint reduction-oxidation potentials of unliganded CHO-H466D, CHO-H466A, and CHO-WT, were determined through the reductive titration of the enzyme with sodium dithionite as a reductant as previously described for CHO-WT and CHO-H466A in complex with glycine betaine (45).

**Enzyme Assays.** The enzymatic activity of CHO-H466D was measured polarographically with choline by measuring the rate of oxygen consumption as described for the wild type enzyme (38, 40).

**Data Analysis.** Data of the spectrophotometric titrations for complex formation between choline oxidase and various ligands were fit to eq 1, where  $Y$  and  $A$  are the observed and maximal absorbance changes at the selected wavelength, respectively,  $X$  is the concentration of the varied ligand, and  $K$  is the complex dissociation constant. Data of the pH dependencies of the absorbance spectra were fit to eq 2, which describes a curve with a slope of +1 and plateau regions at low and high pH, where  $A$  and  $B$  represent the absorbance values at 500 nm at low and high pH, respectively. The midpoint reduction-oxidation potentials of the enzymes were determined by fitting the data to eq 3, where  $E_h$  is the observed electrode potential at equilibrium at each point in the titration,  $E'_m$  is the midpoint reduction-oxidation potential,  $R$  is the gas constant, with a value of  $8.31 \text{ J mol}^{-1} \text{ K}^{-1}$ ,  $T$  is the temperature in Kelvin,  $n$  is the number of electrons transferred, and  $F$  is Faraday's constant, with a value of  $96.48 \text{ kJ V}^{-1} \text{ mol}^{-1}$ .

$$Y = \frac{AX}{X + K} \quad (1)$$

$$Y = \frac{A \times 10^{-\text{pH}} + B \times 10^{-\text{pK}_a}}{10^{-\text{pH}} + 10^{-\text{pK}_a}} \quad (2)$$

$$E_{\text{h}} = E'_{\text{m}} + \frac{2.303}{nF} RT \log \frac{[\text{FAD}_{\text{Ox or Sq}}]}{[\text{FAD}_{\text{Sq or Red}}]} \quad (3)$$

## Results

**Expression and Purification of CHO-H466D.** CHO-H466D was expressed and purified at pH 8 to high level as judged by SDS-PAGE using the same protocol used for the wild type enzyme (Figure 6.2). About 100-150 mg of pure CHO-H466D could be typically obtained from 4.5 liters of Luria-Bertani culture medium. In contrast to the wild type enzyme, for which 35 to 85% of the bound flavin exists at pH 8 in an air-stable anionic semiquinone state (38, 40) that can be oxidized by extended incubation at pH 6 (40), the flavin in CHO-H466D was in the oxidized state throughout the purification procedure. In this respect, CHO-H466D is similar to CHO-H466A, for which no flavin semiquinone was observed in the UV-visible absorbance spectrum of the purified enzyme (45). Purified CHO-H466D at final concentrations as high as 20  $\mu\text{M}$  showed no oxygen consumption when assayed with 30 mM choline as a substrate at pH 7 and 25  $^{\circ}\text{C}$ . In comparison, the CHO-WT at a final concentration of 0.1  $\mu\text{M}$  typically shows a catalytic activity of  $\sim 15\text{ s}^{-1}$  with 10 mM choline (38), suggesting that replacement of the histidine at position 466 with aspartate results in the complete loss of catalytic activity in choline oxidase.

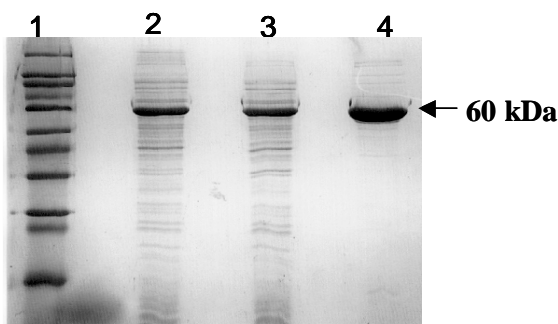


**Figure 6.2.** Purification of CHO-H466D.

Lane 1, molecular weight marker proteins; lane 2, cell-free extract of *Escherichia coli* strain Rosetta(DE3)pLysS harboring plasmid pET/*codA*-H466D induced with 0.05 mM IPTG for 5 h at 23  $^{\circ}\text{C}$ ; lane 3, sample treated with 30 and 65% ammonium sulfate saturation; lane 4, purified CHO-H466D in 20 mM Tris-Cl and 10% glycerol, pH 8, after DEAE-Sepharose column chromatography. The molecular mass of the purified CHO-H466D is indicated.

***Spectral Properties of Oxidized CHO-H466D.*** The UV-visible absorbance spectrum of oxidized CHO-H466D at pH 6<sup>2</sup> showed a 10 nm hypsochromic shift of the visible peak centered at ~450 nm and a 10% decrease in the intensity of the 372 nm peak with respect to both CHO-WT and CHO-H466A (Figure 6.3A), suggesting an altered protein microenvironment in the protein containing aspartate at position 466. Accordingly, the relative intensity of the flavin fluorescence emission at ~525 nm (with  $\lambda_{\text{ex}}$  at 447 nm) was 5 and 10 times larger than that observed with CHO-WT and CHO-H466A, respectively (Figure 6.3B). Similarly, the flavin fluorescence excitation spectrum of CHO-H466D had maxima at 376 and 460 nm (with  $\lambda_{\text{em}}$  at 530 nm), with 5- and 10-fold the intensities seen with the CHO-WT and CHO-H466A (Figure 6.3C). In contrast, no significant differences were seen in the intensities of the protein fluorescence emission peaks at 340 nm among the three different forms of enzyme (Figure 6.3D), suggesting that the overall folds of the mutant enzymes were similar to that of the wild type enzyme. The spectral properties of oxidized CHO-H466D, CHO-WT and CHO-H466A, are summarized in Table 6.1.

---

<sup>2</sup> The spectral properties of the oxidized forms of CHO-WT, CHO-H466A, and CHO-H466D, were compared at pH 6 to avoid artifactual contributions on the UV-visible absorbance spectra due to pH, since the three enzyme variants showed pH effects on the UV-visible absorbance spectra of the oxidized enzymes with  $\text{pK}_{\text{a}} \geq 8.2$  (this study and ref. (45)).

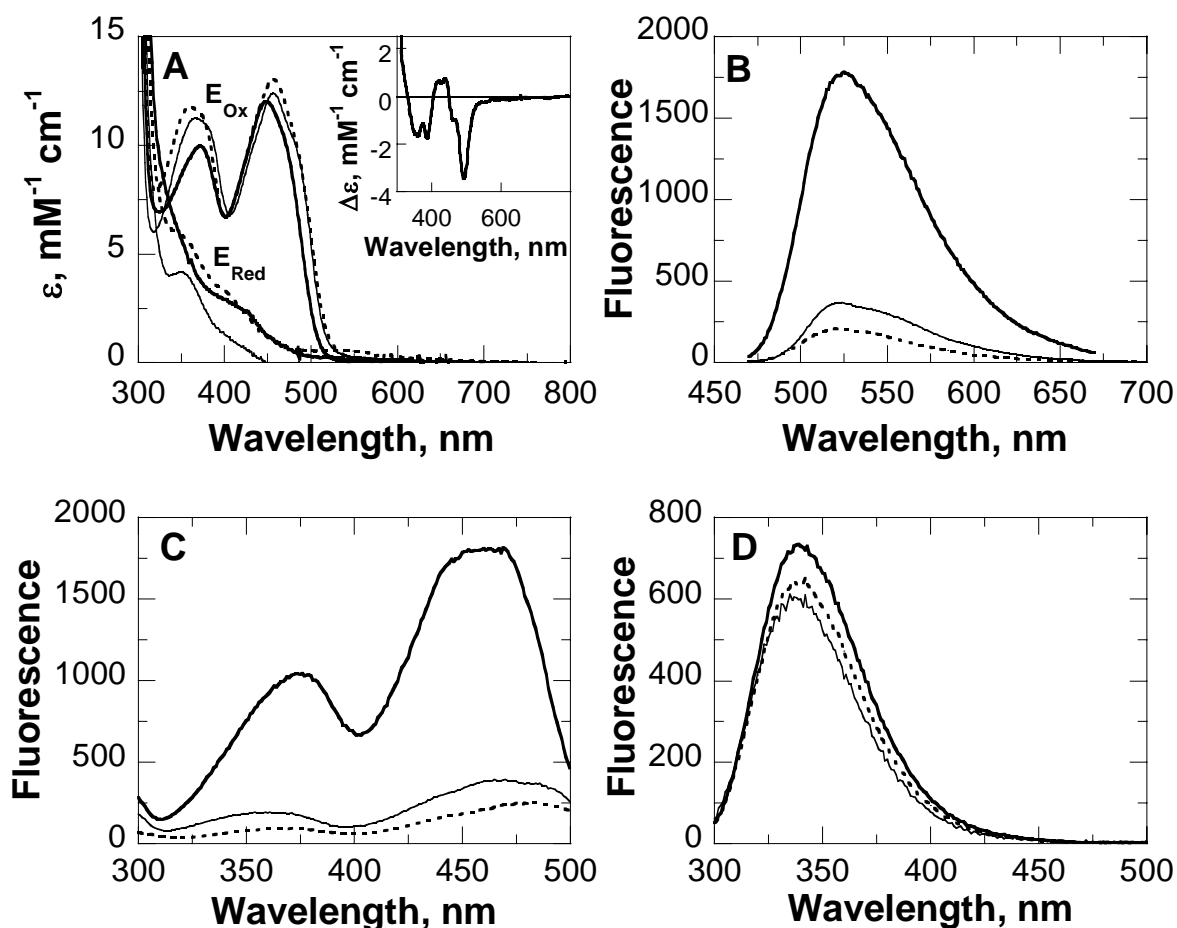


**Figure 6.3.** Comparison of the spectral properties of CHO-H466D, CHO-WT and CHO-H466A. Comparison of the spectral properties of CHO-H466D (thick solid curves), CHO-WT (thin solid curves) and CHO-H466A (dotted curves) in 20 mM sodium phosphate, 20 mM sodium pyrophosphate and 10% glycerol, pH 6 at 15 °C. Panel A, UV-visible absorbance spectra of the oxidized and reduced species of enzymes after treatment with xanthine (300  $\mu\text{M}$ ) and xanthine oxidase ( $\sim 0.5 \mu\text{M}$ ). Inset, difference absorbance spectrum of oxidized CHO-H466D (thick solid curve) minus that of CHO-WT as a reference; panel B, flavin fluorescence emission spectra, the excitation wavelengths were 447, 457 and 457 nm for CHO-H466D, CHO-WT and CHO-H466A, respectively; panel C, flavin fluorescence excitation spectra, the emission wavelength was 530 nm for all forms of enzyme; panel D, protein fluorescence emission spectra, the excitation wavelengths were 285 nm.



**Table 6.1.** Comparison of the Spectral Properties Parameters of CHO-H466D, CHO-H466A, and CHO-WT, at pH 6

	CHO-H466D	CHO-H466A	CHO-WT
<b>E-FAD<sub>Ox</sub></b>			
UV-visible absorbance ( $\lambda_{\max}$ , nm)	276, 372, 447	267, 361, 457	279, 366, 457
$\epsilon$ (mM <sup>-1</sup> cm <sup>-1</sup> )	210, 10, 12	272, 11.8, 13	154, 11.3, 12.4
Stoichiometry (FAD/protein)	0.29 $\pm$ 0.03	0.32 $\pm$ 0.05 <sup>a</sup>	0.88 $\pm$ 0.12 <sup>b</sup>
% of FAD covalently bound	~25%	100% <sup>a</sup>	100% <sup>b</sup>
Fluorescence emission ( $\lambda_{\max}$ , nm)			
$\lambda_{\text{ex}}$ = 447 or 457 nm	525	524	524
$\lambda_{\text{ex}}$ = 372, 361 or 366 nm	524	519	522
$\lambda_{\text{ex}}$ = 285 nm	339	342	335
Fluorescence excitation ( $\lambda_{\max}$ , nm)			
$\lambda_{\text{em}}$ = 530 nm	376, 460	371, 475	361, 470
pK <sub>a</sub> (N(3)-H)	10.3 $\pm$ 0.1	9.3 $\pm$ 0.2 <sup>a</sup>	8.2 $\pm$ 0.1 <sup>a</sup>
<b>E-FAD<sub>Red</sub></b>			
UV-visible absorbance ( $\lambda_{\max}$ , nm)	~340, ~400	~350, ~400	347
$\epsilon$ (mM <sup>-1</sup> cm <sup>-1</sup> )	~6.7, ~2.9	~5.8, ~3.3	4.2
<b>E-FAD<sub>Ox-glycine betaine</sub></b>			
UV-visible absorbance ( $\lambda_{\max}$ , nm)	nd <sup>c</sup>	361, 459	358, 455
K <sub>d</sub> , mM	nd	4.2 $\pm$ 0.4	15 $\pm$ 2
K <sub>is</sub> , mM <sup>d</sup>	nd	5.2 $\pm$ 0.5	13 $\pm$ 1
<sup>a</sup> From ref (45). <sup>b</sup> From ref (38). <sup>c</sup> Not determined. <sup>d</sup> Limiting inhibition constant determined kinetically with choline as substrate at low pH; from ref (45).			

**Flavin Stoichiometry and Content of CHO-H466D.** Previous studies showed that choline oxidase contains covalently linked FAD in a 1:1 stoichiometry (38). In contrast, upon denaturation of the CHO-H466D variant by treatment with urea, a stoichiometry of 0.29  $\pm$  0.03 FAD per monomer of enzyme could be determined from two independent experiments. Similar flavin content was previously reported for the CHO-H466A variant (Table 6.1) (45), suggesting that the flavin content in choline oxidase is significantly affected by replacement of the active site histidine with either a neutral or anionic amino acid residue. Interestingly, treatment of CHO-H466D with 10% cold trichloroacetic acid followed by centrifugation to remove the denatured protein yielded a UV-visible absorbance spectrum of the soluble fraction with peaks at

370 and 450 nm, suggesting that at least part of the flavin in CHO-H466D is not covalently bound (Figure 6.4). A MALDI-TOF mass spectrometric analysis of the flavin released from CHO-H466D yielded a  $m/z^-$  ratio of 784.1 (Figure 6.4), consistent with the non-covalently bound flavin in CHO-H466D being FAD. From the intensities of the peaks at 450 nm in the supernatant and pellet dissolved in 4 M urea obtained upon acid treatment of CHO-H466D, it was estimated that ~75% of the flavin in CHO-H466D is tightly but not covalently bound to the enzyme. These data clearly suggest that reversing the positive charge in proximity of the FAD N(1) locus affects not only the flavin content in the protein but also the extent of protein flavinylation.

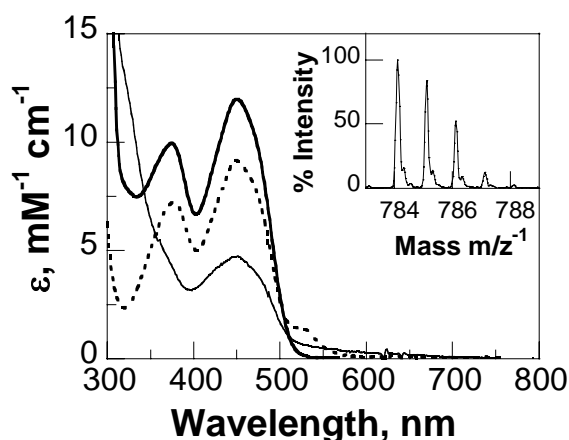


**Figure 6.4.** Stoichiometry and flavin content of CHO-H466D.

Thick solid curve, UV-visible absorbance spectrum of CHO-H466D in 20 mM Tris-Cl and 10% glycerol, pH 8; dotted curve, UV-visible absorbance spectrum of the soluble fraction after treatment of CHO-H466D with 10% of trichloroacetic acid for 30 min on ice and centrifugation to remove denatured protein; thin solid curve, UV-visible absorbance spectrum of the denatured precipitated fraction after solubilization in 4 M urea. Inset, MALDI-TOF mass spectrometric analysis of the soluble fraction after treatment of CHO-H466D with 10% of trichloroacetic acid. The spectrum was recorded in negative ion mode with a 50:50 methanol/acetonitrile matrix.

***Spectrophotometric Properties of Reduced CHO-H466D.*** The UV-visible absorbance spectrum of the fully reduced form of CHO-H466D was obtained by anaerobic incubation of the enzyme with xanthine and xanthine oxidase, at pH 6. As shown in Figure 6.3A, an indistinct shoulder with no well-defined peaks was observed in the 400 to 450 nm region of the absorbance spectrum of CHO-H466D hydroquinone, suggesting that at pH 6 the flavin hydroquinone bound to this enzyme variant was present in the neutral form (47-49). During the reduction process, no flavin semiquinone intermediate was observed (data not shown). A similar reduction of CHO-WT yielded a UV-visible absorbance spectrum with a well-defined peak at 347 nm (Figure 6.3A), consistent with previous data on anaerobic substrate reduction of the wild type enzyme that suggested the presence of the reduced flavin in the anionic state (40). In the case of CHO-H466A, anaerobic reduction of the enzyme at pH 6 resulted in a UV-visible absorbance spectrum with features that were intermediate between those of CHO-H466D and CHO-WT, i.e., both a poorly defined peak at ~350 nm and a shoulder in the 400 nm region (Figure 6.3A). Thus, at pH 6 the reduced flavin in CHO-H466A is likely present as a mixture of anionic and neutral hydroquinones. The spectral properties of the three enzyme variants in the reduced state are summarized in Table 6.1.

***Effect of pH on the Spectrophotometric Properties of CHO-H466D.*** The effects of pH on the UV-visible absorbance spectra of CHO-H466D were determined on the oxidized and reduced enzymes. As shown in Figure 6.5, the absorbance at 500 nm increased between limiting values upon increasing pH, yielding a  $pK_a$  value of  $10.3 \pm 0.1$ , which could be assigned to the ionization of the N(3) locus of the oxidized enzyme-bound FAD (50). Previous data on CHO-H466A and CHO-WT yielded  $pK_a$  values of ~9.3 and ~8.2, respectively (45), consistent with

significant changes in the microenvironment surrounding the FAD N(3) locus upon replacing His<sub>466</sub> with a neutral or anionic amino acid.

No significant spectral changes were observed in the UV-visible absorbance spectrum of CHO-H466D hydroquinone upon raising the pH from 6 to 10, consistent with the neutral species of the reduced flavin being stabilized in this pH range (data not shown). Similarly, no spectral changes were observed in the same pH range with CHO-WT hydroquinone, suggesting that ionization of the N(1) position of FAD has a  $pK_a$  significantly lower than 6 or that the N(1) position of FAD is not solvent accessible in the wild type reduced enzyme (data not shown). In contrast, the UV-visible absorbance spectrum of CHO-H466A hydroquinone at pH 8 showed features that are typically associated with the anionic reduced flavin, i.e., a distinct peak at 356 nm (Figure 6.6). Thus, in CHO-H466A the relative amount of anionic versus neutral hydroquinone increased significantly upon increasing the pH from 6 to 8, suggesting that the flavin N(1) locus in this enzyme variant is both solvent accessible and ionizable in this pH range.

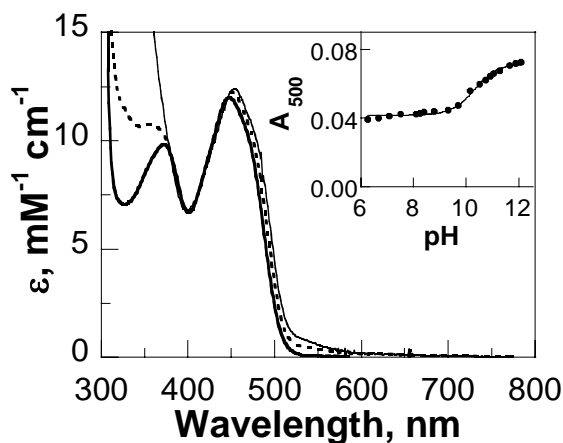


**Figure 6.5.** Effect of pH on the spectral properties of CHO-H466D.

UV-visible absorbance spectra were recorded at an enzyme concentration of  $\sim 20 \mu\text{M}$  in 20 mM sodium phosphate, 20 mM sodium pyrophosphate and 10% glycerol, at 15 °C. Only selected spectra are shown for the enzyme at pH 6 (thick solid curve), pH 10 (dotted curve), and pH 12 (thin solid curve). Inset, Absorbance values at 500 nm as a function of pH; data were fit to eq (2).

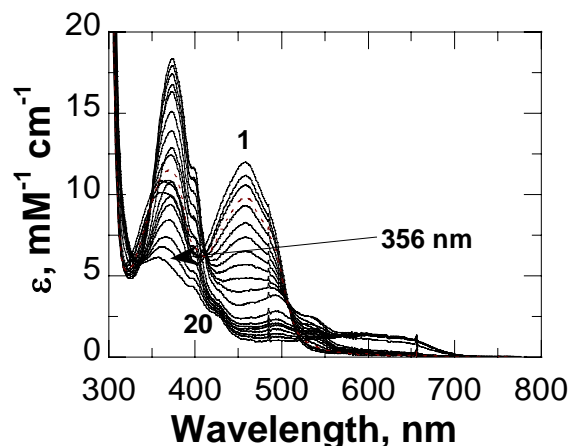


**Figure 6.6.** Anaerobic reduction of CHO-H466A using xanthine and xanthine oxidase.

Anaerobic reduction of CHO-H466A with 300  $\mu$ M xanthine and  $\sim 0.5$   $\mu$ M xanthine oxidase in 50 mM sodium phosphate, 50 mM sodium pyrophosphate and 10% glycerol, at pH 8 and 15  $^{\circ}$ C. Curve 1: UV-visible absorbance spectrum of the fully oxidized species of the enzyme. Unnumbered curves: selected intermediate spectra recorded during the reduction of the enzyme showing the formation of anionic flavin semiquinone. Curve 20: UV-visible absorbance spectrum of the hydroquinone form of enzyme.

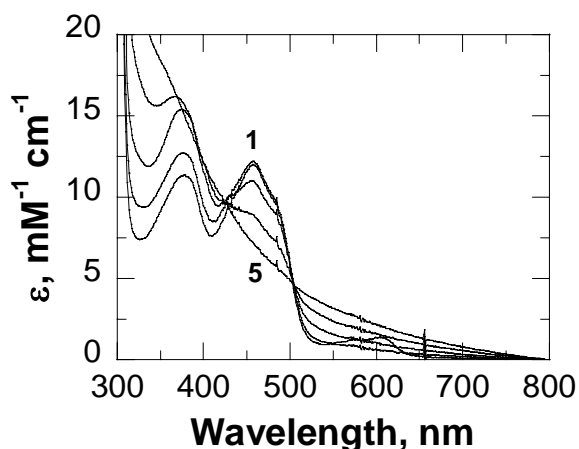


**Figure 6.7.** Potentiometric reduction titration of CHO-H466D in complex with choline.

Curve 1: UV-visible absorbance spectrum of the fully oxidized CHO-H466D at an ambient redox potential of +267 mV at a concentration of  $\sim 20$   $\mu$ M in the presence of 10 mM choline, in 20 mM Tris-Cl and 10% glycerol, pH 7, at 15  $^{\circ}$ C. Curves 2-4: selected intermediate spectra recorded during reduction of the ligand-bound CHO-H466D after each addition of sodium dithionite at ambient redox potentials of +40, -77, and -130 mV, respectively. Curve 5: UV-visible absorbance spectrum of the fully reduced ligand-bound CHO-H466D at ambient redox potential of -217 mV, showing significant turbidity of the reduced enzyme solution.

***Redox Potentiometry of Unliganded CHO-H466D, CHO-H466A, and CHO-WT.***

Previous studies established that with choline oxidase in complex with glycine betaine the replacement of His<sub>466</sub> with alanine resulted in a decrease of the midpoint reduction-oxidation potential for the oxidized-reduced flavin couple from +132 mV to +106 mV at pH 7 (45). Since CHO-H466D does not bind glycine betaine, but forms a stable complex without reacting with choline (*vide infra*), here we have attempted to determine the reduction-oxidation potential of CHO-H466D in the presence of 10 mM choline at pH 7 and 15 °C. However, significant turbidity of the enzyme solution developed during the course of the reduction (Figure 6.7), preventing the determination of the reduction-oxidation potential of CHO-H466D in complex with a ligand. Consequently, the midpoint reduction-oxidation potential of CHO-H466D, and those for CHO-WT and CHO-H466A for comparison, were determined on the free enzymes in the absence of ligands at pH 7. With both CHO-WT and CHO-H466A, the midpoint reduction-oxidation potentials for the first and second reducing equivalents were well separated, resulting in the thermodynamic stabilization of the flavin anionic semiquinone species (Figure 6.8A-D). In agreement with the observed potentials for the first and second electron transfer equilibria, 100% and 90% of flavin semiquinones were seen with CHO-WT and CHO-H466A, respectively (Figure 6.8E and Table 6.2). In contrast, with CHO-H466D no flavin semiquinone was observed during reduction of the enzyme at pH 7 resulting in the determination of the  $E'_{m,7}$  values for the oxidized-reduced enzyme couple (Figure 6.8F). In all cases, the analyses of the data according to the Nernst formalism yielded lines in plots of  $E_h$  versus  $\log ([\text{oxidized or semiquinone species}]/[\text{semiquinone or reduced species}])$  with slopes of ~59 and 35 for the one- and two-electron transfers, respectively, in agreement with the expected values of 57 and 28.5 mV at 15 °C (Figure 6.8 and Table 6.2). As illustrated in Table 6.2, the  $E'_{m,7}$  for the transfer of the two

electrons with CHO-H466D had a value that was  $\sim 130$  mV and  $\sim 160$  mV more negative than the calculated midpoint potentials for the corresponding two-electron transfers in CHO-H466A and CHO-WT. These data are consistent with a significant effect of the amino acid residue at position 466 on the electrophilicity of the enzyme-bound flavin in choline oxidase. Interestingly, the midpoint reduction-oxidation potential for the oxidized-semiquinone couple in wild type choline oxidase was  $+211$  mV, which is to our knowledge the highest value for such thermodynamic equilibrium reported for a flavoprotein oxidase (9, 11, 51-56).

**Table 6.2.** Midpoint Reduction-Oxidation Potentials for the Enzyme-FAD of Unliganded CHO-WT, CHO-H466A, and CHO-H466D, at pH 7<sup>a</sup>

Enzyme	$E'_1$ (mV) <sup>b</sup> [slope, mV]	$E'_2$ (mV) <sup>c</sup> [slope, mV]	% Sq	$E'_{m,7}$ (mV) <sup>d</sup> [slope, mV]
CHO-WT	$+211 \pm 2$ [60 $\pm$ 3]	$-65 \pm 2$ [57 $\pm$ 4]	100	$+73^e$
CHO-H466A	$+91 \pm 2$ [57 $\pm$ 3]	$-6 \pm 2$ [59 $\pm$ 3]	90	$+42.5^e$
CHO-H466D	na <sup>f</sup>	Na	0	$-89 \pm 1$ [35 $\pm$ 1]

<sup>a</sup> Conducted in 20 mM Tris-Cl, pH 7, at 15 °C. <sup>b</sup> Midpoint potential ( $n = 1$ ) of the oxidized/semiquinone FAD redox couple. <sup>c</sup> Midpoint potential ( $n = 1$ ) of the semiquinone/hydroquinone FAD redox couple. <sup>d</sup> Midpoint potential ( $n = 2$ ) of the oxidized/hydroquinone FAD redox couple. <sup>e</sup> Calculated midpoint potential for CHO-WT and CHO-H466A ( $E'_{m,7} = (E'_1 + E'_2)/2$ ; (57)). <sup>f</sup> Not available.

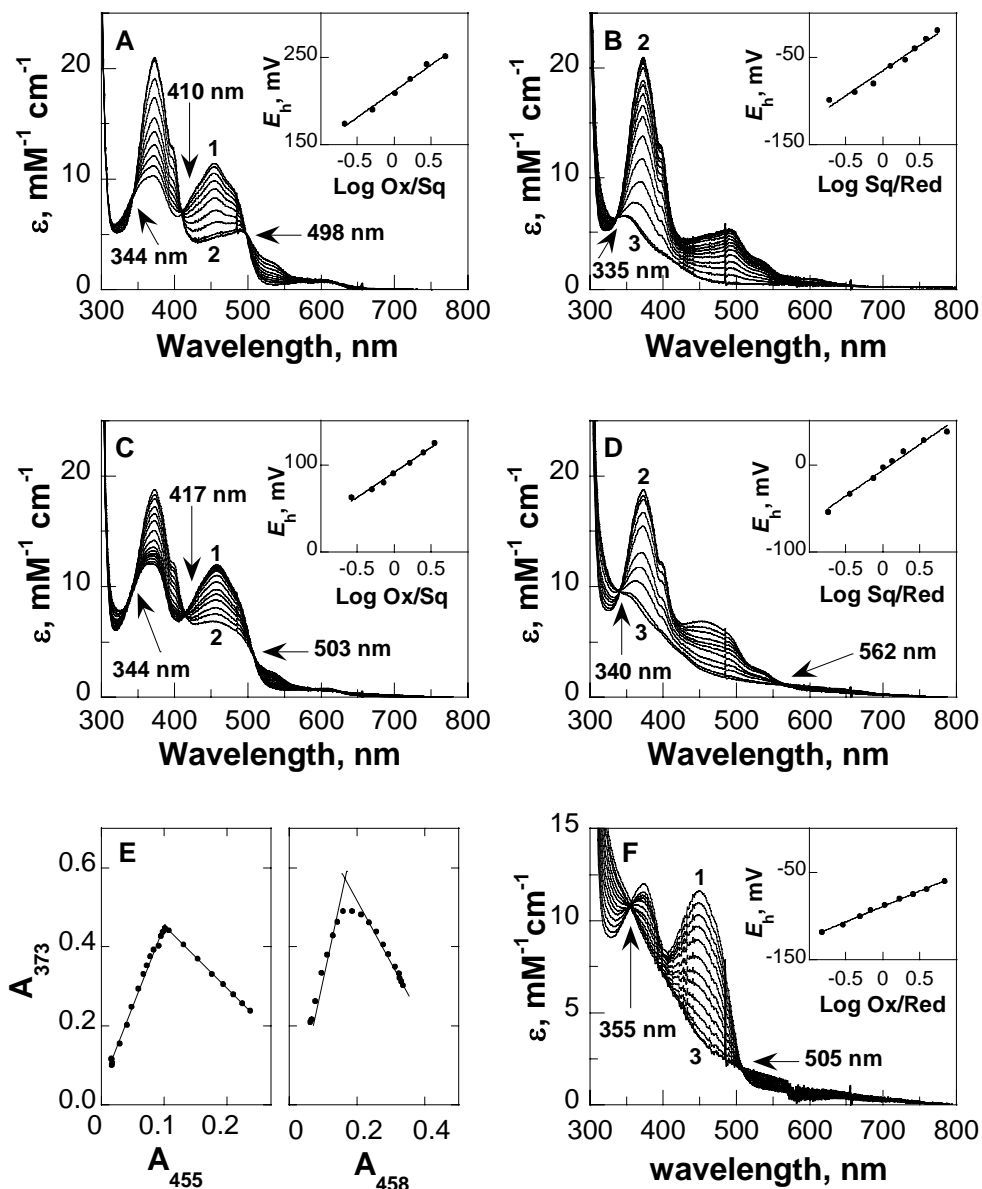


**Figure 6.8.** Potentiometric reduction-oxidation titration of CHO-WT, CHO-H466A, and CHO-H466D.

Potentiometric reduction-oxidation titration of CHO-WT (Panel A and B), CHO-H466A (Panel C and D), and CHO-H466D (Panel F) at concentrations of  $\sim 20 \mu\text{M}$ , in 20 mM Tris-Cl, pH 7 at 15 °C. Curves 1, UV-visible absorbance spectra of the oxidized species of enzymes; curves 2, UV-visible absorbance spectra of the maximum red anionic semiquinone that formed during the reductive titrations; curves 3, UV-visible absorbance spectra of the fully reduced species of enzymes. Panel E, quantitation of the amount of flavin semiquinone formed with CHO-WT (left panel) and CHO-H466A (right panel). Insets, determination of the midpoint reduction potentials: Panel A, B, C, and D Nernst plots of the potentiometric data for the reduction of the enzyme-bound flavin in CHO-WT and CHO-H466A (panel A and C:  $\text{Ox} \rightarrow \text{Sq}$ ; panel B and D:  $\text{Sq} \rightarrow \text{Red}$ ), data were fit to eq (3); panel F, Nernst plot of the potentiometric data for the reduction of the enzyme-bound flavin in CHO-H466D ( $\text{Ox} \rightarrow \text{Red}$ ), data were fit to eq (3).



***Binding of Choline, Glycine Betaine, and Sulfite to CHO-H466D.*** In agreement with the lack of oxygen consumption of CHO-H466D when assayed polarographically with choline as substrate, the anaerobic mixing of this mutant protein with 10 mM choline resulted in no bleaching of the flavin peak at ~450 nm over 60 min of incubation, as shown in Figure 6.9A. However, a 4 nm bathochromic shift associated with an increase in absorbance at 375 nm was observed in the UV-visible absorbance spectrum of CHO-H466D in the presence of choline (Figure 6.9A). These spectral changes were similar to those seen for the CHO-H466A variant in complex with glycine betaine (Figure 6.10B), suggesting that CHO-H466D retained the ability to bind choline at the active site without subsequent oxidation of the substrate. The lack of reactivity of CHO-H466D with choline was exploited for the determination of an equilibrium constant for the dissociation of choline from the enzyme ( $K_d$ ) of  $0.45 \pm 0.04$  mM at pH 8, which was carried out spectrophotometrically by following the UV-visible spectral changes of the enzyme in the visible region at increasing concentrations of choline (Figure 6.9B). Such a  $K_d$  value was four-times lower than the  $K_d$  value of ~1.8 mM that was recently determined through rapid reaction studies of CHO-WT reacting with choline at pH 8 (58), suggesting that reversing the charge at position 466 results in a slightly tighter binding of choline to the active site of the enzyme.

The lack of enzymatic activity of CHO-H466D prevented a kinetic determination of the inhibition constant for binding of glycine betaine to the enzyme, as was previously carried out for both CHO-WT (40) and CHO-H466A (45). Consequently, the determination of the dissociation constant for glycine betaine binding was carried out on the wild type and mutant forms of choline oxidase by following the spectral changes associated with mixing of the enzyme with increasing concentrations of ligand. With both CHO-WT and CHO-H466A,  $K_d$  values for

glycine betaine binding that were in good agreement with those previously determined using the kinetic approach could be determined at pH 6 (Figure 6.10A-B and Table 6.1) (40, 45). In contrast, no significant spectral changes could be observed with CHO-H466D at concentrations of glycine betaine as high as 80 mM (Figure 6.10C), suggesting that choline oxidase lost the ability to bind glycine betaine upon replacing the active site histidine with aspartate.

Wild type choline oxidase was shown previously to form a tight reversible N(5)-flavin sulfite adduct with a  $K_d$  value of  $\sim 50$   $\mu$ M at pH 7 and 15 °C (40). In contrast, with CHO-H466A an N(5)-flavin sulfite adduct could be obtained only in the presence of exogenous imidazole, while in the absence of imidazole no adduct could be formed even after 3.5 h of incubation of CHO-H466A with 100 mM sulfite (45). Similarly, no spectral changes could be detected here when CHO-H466D was incubated for 3 h at pH 6 and 15 °C in the presence of 100 mM sodium sulfite (Figure 6.11), consistent with lack of stabilization of the sulfite-flavin adduct in CHO-H466D.

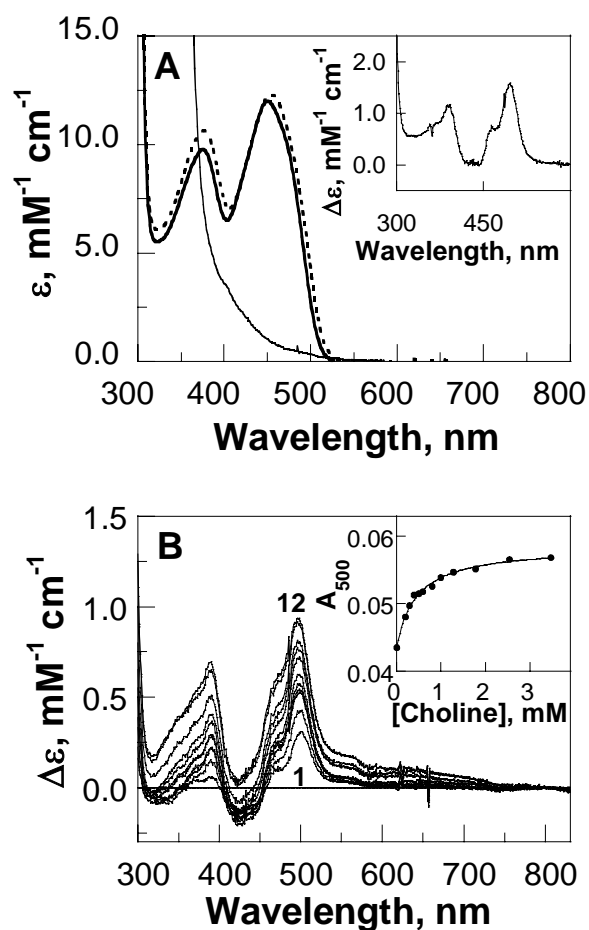


**Figure 6.9.** Binding of choline to CHO-H466D.

Panel A, UV-visible absorbance spectra of CHO-H466D were recorded at a concentration of  $\sim 30 \mu\text{M}$  in 20 mM Tris-Cl, pH 8 and  $15^\circ\text{C}$ , before (thick solid curve), after one hour of anaerobic incubation of the enzyme with 10 mM choline (dotted curve) and after the addition of dithionite powder (thin solid curve). Inset, difference spectrum of the enzyme bound choline to the free enzyme; panel B, difference absorbance spectra of CHO-H466D at a concentration of  $\sim 20 \mu\text{M}$  in 20 mM Tris-Cl, pH 8 and  $15^\circ\text{C}$ , during the aerobic titration of choline in the concentration range between zero (curve 1) and 3.5 mM (curve 12). Inset, Absorbance values at 500 nm as a function of choline concentration; data were fit to eq 1.

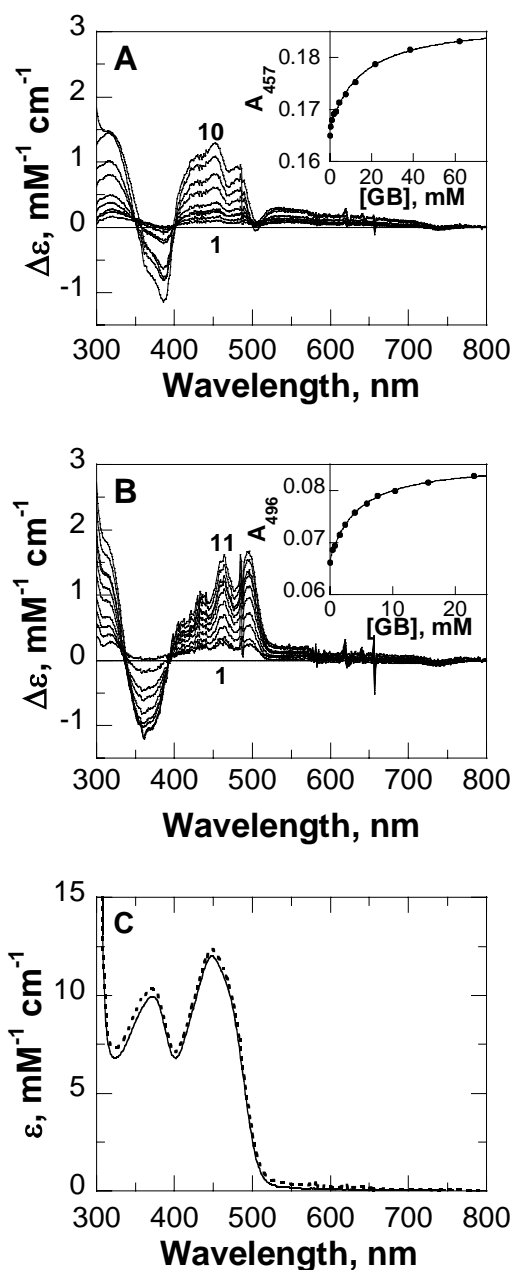


**Figure 6.10.** Binding of glycine betaine to CHO-WT, CHO-H466A and CHO-H466D. Difference spectra of CHO-WT (panel A) and CHO-H466A (panel B) during the aerobic titration of glycine betaine in a concentration range between zero (curves 1, panel A and B) and 62 mM (curve 10, panel A) or 23 mM (curve 11, panel B). Insets, Absorbance values at 457 nm (panel A) and 496 nm (panel B) as a function of glycine betaine concentration for CHO-WT and CHO-H466A; the curves are fits of the data to eq 1. Panel C, UV-visible absorbance spectra of CHO-H466D before (solid curve) and after aerobic titration of glycine betaine up to a final concentration of ~80 mM (dotted curve). Absorbance spectra were recorded at enzymes concentration of ~20  $\mu\text{M}$  in 20 mM sodium phosphate, 20 mM sodium pyrophosphate and 10% glycerol, pH 6.

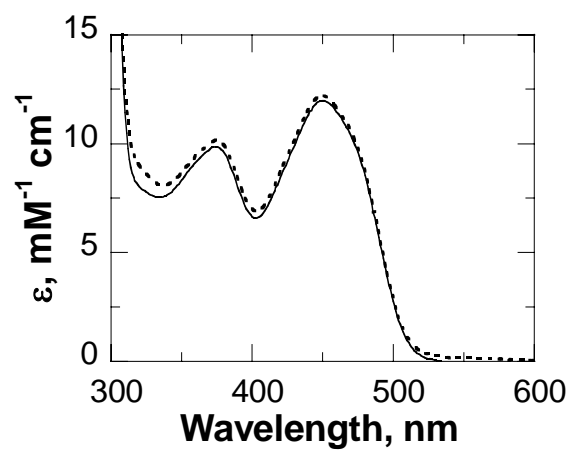


**Figure 6.11.** Reaction of CHO-H466D with sulfite.

UV-visible absorbance spectra of CHO-H466D before (solid curve) and after 3 h of aerobic incubation with 100 mM sodium sulfite (dotted curve). Enzyme concentration was 15  $\mu\text{M}$  in 100 mM sodium pyrophosphate, pH 6, at 15  $^{\circ}\text{C}$ .

## Discussion

A recent biochemical and mechanistic study on a mutant form of choline oxidase in which the active site histidine at position 466 was replaced with alanine established the involvement of His<sub>466</sub> in the reductive half-reaction in which choline is oxidized to betaine aldehyde, but not in the following oxidative half-reaction in which oxygen is reduced to hydrogen peroxide (45). Of particular interest was the finding that in catalysis His<sub>466</sub> is protonated, as suggested by the observation that the enzymatic activity of CHO-H466A could be partially rescued in the presence of exogenous imidazolium, but not imidazole (45). The positively charged His<sub>466</sub> was proposed to play multiple roles in the oxidation of choline catalyzed by choline oxidase, by contributing to the polarity of the active site, stabilizing the negatively charged transition state, and activating the flavin for the oxidation reaction (45). As illustrated in Scheme 6.2, the contribution of His<sub>466</sub> to the active site polarity would be required for the efficient removal of the substrate hydroxyl proton that results in the activation of the substrate (species 1 and 2). The stabilization of the resulting choline alkoxide species (species 2) and the activation of the enzyme-bound flavin (species 3) would correctly position and facilitate the quantum mechanical transfer of the hydride from the substrate  $\alpha$ -carbon to the N(5) flavin locus (species 3) (39, 45, 58). The recent determination of the crystal structure of choline oxidase showed that His<sub>466</sub> is located in the active site at  $\sim 3.3$  Å from the N(1) locus of the flavin (Figure 6.1) (George Lountos, Fan Fan, Giovanni Gadda, and Allen M. Orville; unpublished results), consistent with the proposed roles for this residue in catalysis. In the present study, we have prepared a second variant of choline oxidase in which His<sub>466</sub> was replaced with an aspartate residue by site-directed mutagenesis, and investigated the effects of reversing the charge in proximity of the N(1) locus of the flavin by using biochemical and biophysical approaches.

From a biophysical standpoint, reversing the protein positive charge at position 466 in choline oxidase results in the lack of stabilization of the negative charge that is produced on the N(1) locus of the enzyme-bound flavin in the one- and two-electron reduced forms of choline oxidase. Evidence for this conclusion comes primarily from the UV-visible absorbance spectrum of the two-electron reduced form of CHO-H466D at pH 6, which is consistent with the enzyme-bound flavin hydroquinone being in the neutral state (47-49). The lack of changes in the UV-visible absorbance spectrum of the reduced flavin upon raising the pH from 6 to 10 is further consistent with stabilization of the neutral flavin hydroquinone in CHO-H466D being due to the effect of the negatively charged aspartyl side chain, since such a residue is expected not to change its ionization state above pH 6. In contrast, the wild type enzyme stabilizes the anionic form of hydroquinone between pH 6 and 10, as shown by the well-resolved peak at 356 nm in the UV-visible absorbance spectrum of the two-electron reduced enzyme. These data, in turn, suggest that the histidyl side chain at position 466 either decreases the  $pK_a$  value for the ionization of the N(1) FAD locus in the reduced enzyme to values below 6 or hinders solvent accessibility to the N(1) locus, thereby preventing its protonation during flavin reduction. In agreement with these conclusions, the alanyl variant of the enzyme, which carries a small and neutral side chain proximal to the FAD N(1) position, exists as a mixture of neutral and anionic hydroquinones at pH 6 and as the anionic species at pH 8. Different stabilization of the negative charge on the N(1) locus of the flavin in the histidyl, alanyl, and aspartyl enzymes is independently suggested by the observation that the anionic flavin semiquinone was stabilized at pH 7 only in the wild type and H466A mutant enzymes, but not in CHO-H466D. These results suggest that at least in choline oxidase the removal of the positive charge in proximity of the N(1) locus of the flavin is not sufficient to destabilize the anionic flavin semiquinone, and that

such a destabilization requires the presence of a protein negative charge. Finally, the lack of changes in the UV-visible absorbance spectrum of oxidized CHO-H466D in the presence of sodium sulfite, which was previously observed to form a tight reversible N(5)-flavin adduct with the wild type enzyme (40), provides independent evidence that replacing the protein positive charge at position 466 results in lack of stabilization of the negative charge on the N(1)-C(2)=O flavin locus.

The most dramatic effect arising from the lack of stabilization of the negative charge on the pyrimidine ring of the reduced flavin in CHO-H466D is that about 75% of the enzyme-bound FAD is tightly, but not covalently, bound to the protein moiety. This conclusion is supported by the analysis of the supernatant obtained upon acid treatment of the enzyme containing aspartate at position 466 followed by centrifugation to remove the denatured protein. In contrast, both CHO-WT and CHO-H466A have been recently reported to contain only covalently bound FAD (38, 45), suggesting that replacing the protein positive charge close to the N(1) atom of the flavin with a neutral residue is not sufficient to affect the flavinylation of the enzyme. With both the aspartyl and alanyl mutant proteins the total FAD content was three- to four-fold lower than that previously observed for the wild type enzyme, in which a 1:1 stoichiometry of FAD to protein was established, further suggesting that the presence of a protein positive charge close to the N(1) position of the flavin is important for the formation of the covalent linkage between FAD and the protein in choline oxidase. These results are in keeping with other studies recently reported on trimethylamine dehydrogenase, sarcosine oxidase, *N*-methyltryptophan oxidase, and *p*-cresol methylhydroxylase (20, 59-62), suggesting that a positively charged microenvironment close to the flavin N(1)-C(2)=O locus is important for the stabilization of negatively charged



reduced flavin that is proposed to transiently form during the covalent attachment of the flavin to either the 6- or 8-position of the isoalloxazine ring (62).

From a functional standpoint, the most notable effect of reversing the protein positive charge on the side chain at position 466 in choline oxidase is a  $\sim 160$  mV decrease in the midpoint reduction-oxidation potential of the enzyme-bound flavin for the two-electron transfer occurring between the oxidized and reduced enzyme-bound flavin. Such an effect arises from both the lack of covalent linkage between the enzyme-bound flavin and the protein and the presence of the negatively charged aspartyl side chain near the flavin N(1) locus. Earlier results on a number of flavin-dependent enzymes containing covalently bound flavins, namely cholesterol oxidase (63), vanillyl-alcohol oxidase (55), and *p*-cresol methylhydroxylase (54), showed that, irrespective of the type of flavin linkage and protein, removing the covalent linkage between the flavin and the enzyme results in a decrease of the  $E'_{m,7}$  value of the bound flavin of  $\sim 100$  mV. If one assumes a similar contribution to the  $E'_{m,7}$  value of  $\sim 100$  mV from the covalent linkage in choline oxidase, the effect of the negative charge of the aspartyl side chain on the midpoint reduction-oxidation potential of the flavin in CHO-H466D can be estimated at -60 mV. Since a 30 mV decrease in the  $E'_{m,7}$  value was observed in this study upon replacing His<sub>466</sub> with alanine, it can be concluded that the electrophilicity of the enzyme-bound flavin is increased by  $\sim 6$  kJ mol<sup>-1</sup> in the presence of a positive charge and decreased by a similar extent in the presence of a negative charge near the N(1) locus of the flavin. A similar energetic contribution of a protein positive charge near the flavin N(1) locus on the electrophilicity of the flavin was previously reported for lactate monooxygenase, where substituting Lys<sub>266</sub> with a methionine residue resulted in a decrease of 30 mV in the midpoint reduction-oxidation potential of the flavin (35). Although replacement of a histidine with either an aspartate or glutamate residue was

previously reported in cholesterol oxidase from *Brevibacterium sterolicum*, no potentiometric data were reported in that study (64). Consequently, this is the first instance in which the effect of reversing the charge near the flavin N(1) locus on the electrophilicity of the enzyme-bound flavin has been investigated in a flavin-dependent oxidase.

Reversing the positive charge of His<sub>466</sub> with aspartate in choline oxidase results in the complete loss of enzymatic activity, as suggested by the lack of both oxygen consumption and bleaching of the enzyme-bound flavin upon mixing CHO-H466D with choline. The loss of enzymatic activity correlates well with the  $\Delta E'_{m,7}$  value of ~160 mV observed between CHO-H466D and CHO-WT, which accounts for a ~250,000-fold decrease in the rate of hydride transfer to the flavin in the H466D mutant enzyme as compared to the wild type enzyme<sup>3</sup>. However, the 30 mV decrease in the  $E'_{m,7}$  value observed here for CHO-H466A, which agrees well with the previously reported value of ~25 mV (45), cannot fully explain the 20-fold decrease in the rate of choline oxidation that was previously reported for CHO-H466A as compared to the wild type enzyme (45). With CHO-H466A, the decrease in catalytic activity was explained by both a decrease in the flavin electrophilicity, which is reflected in the  $E'_{m,7}$  value, and the lack of stabilization of the negatively charged alkoxide species that is transiently formed in the oxidation of choline (45). The data presented here with CHO-H466D, which could not bind glycine betaine or sulfite, suggest that also the H466D variant likely lost the ability to stabilize extra negative charges in the active site<sup>4</sup>. Similar results in which the enzyme did not

---

<sup>3</sup> A more rigorous approach for the correlation of the loss of enzymatic activity of CHO-H466D with the change in the midpoint oxidation-reduction potential of the enzyme-bound flavin would entail a study of the linear free energy relationship of the rate of flavin reduction using choline oxidase reconstituted with a number of flavin analogues. Such an analyses was beyond the purpose of the current study.

<sup>4</sup> The denaturation of the enzyme that ensues upon anaerobic reduction of CHO-H466D in complex with saturating concentrations of choline is also consistent with inability of CHO-H466D to accommodate an extra negative charge in the active site. Indeed, while the anaerobic reduction of the free unliganded enzyme results in the stabilization of the neutral hydroquinone, it is likely that the presence of choline in the active site hinders solvent access to the N(1)

show catalytic activity upon replacing the protein positive charge near the flavin N(1) locus were previously reported for active site mutant forms of cholesterol oxidase in which His<sub>447</sub>, which is the residue equivalent to His<sub>466</sub> of choline oxidase, was replaced by either a glutamate or aspartate residue. However, in that study the characterization of the enzyme-bound flavin was not reported.

Our recent study on the H466A mutant protein of choline oxidase showed that the enzymatic activity of the enzyme is only 20-times lower than that of the wild type enzyme and that, most importantly, the enzymatic activity could be partially rescued in the presence of exogenous imidazolium but not imidazole in the assay reaction mixture (45). Although these data are consistent with H<sub>466</sub> acting as an electrostatic catalyst by stabilizing the transient alkoxide species that forms in the oxidation of choline (species 2 and 3 in Scheme 6.2), they do not unequivocally rule out His<sub>466</sub> as being the general base catalyst that removes the hydroxyl proton of the substrate (species 1 in Scheme 6.2). Indeed, His<sub>466</sub> would still be able to electrostatically stabilize the anionic species of the substrate after removing the hydroxyl proton from the substrate and acquiring a positive charge. If this were the case, substitution of His<sub>466</sub> with aspartate would be expected to generate a mutant enzyme with at least partial catalytic activity, since the negatively charged aspartyl side chain at position 466 would be neutralized upon abstracting the substrate hydroxyl proton, thereby allowing the transient formation of the alkoxide species. However, the observation that CHO-H466D is completely devoid of enzymatic activity with choline is not consistent with Asp<sub>466</sub> acting as a base in the active site of the aspartyl mutant of choline oxidase.

---

position of the bound flavin, thereby preventing its protonation during reduction with the consequent unfolding of the protein due to charge repulsion between Asp<sub>466</sub> and the negatively charged reduced flavin.

In summary, the results of the biochemical and biophysical investigation of a choline oxidase variant in which the protein charge near the flavin N(1) locus was reversed by site-directed mutagenesis suggest that the enzyme has lost the ability to stabilize negative charges in the active site, irrespective of whether they develop on the flavin or are borne on active site ligands. This effect results in the defective flavinylation of the protein, decreased electrophilicity of the enzyme-bound flavin and, consequently, loss of catalytic activity in the enzyme. The latter conclusion is further consistent with His<sub>466</sub> in the wild type enzyme not acting as a general base catalyst in the reductive half-reaction in which choline is initially activated to the alkoxide species upon removal of its hydroxyl proton. Taken together, the data presented here provide further evidence for the importance of a protein positive charge close to the N(1) flavin in choline oxidase and, by extension, in flavoprotein oxidases, and indicate that the enzyme loses its functionality upon reversing, but not neutralizing, such a positive charge.

### **Acknowledgment**

This paper is dedicated to the memory of the late Professor Vincent Massey (1927-2002). The authors thank Ms. Kunchala Rungsruriyachai for kindly providing purified wild type choline oxidase for the potentiometric experiments and Dr. Siming Wang for the MALDI-TOF mass spectrometric analysis of the flavin extracted from CHO-H466D. The first author thanks the Egyptian Government for the continuous financial support.

## References

- (1) Massey, V., Ghisla, S., and Moore, E. G. (1979) 8-Mercaptoflavins as active site probes of flavoenzymes. *J. Biol. Chem.* 254, 9640-50.
- (2) Fitzpatrick, P. F., and Massey, V. (1983) The reaction of 8-mercaptoflavins and flavoproteins with sulfite. Evidence for the role of an active site arginine in D-amino acid oxidase. *J. Biol. Chem.* 258, 9700-5.
- (3) Massey, V., Müller, F., Feldberg, R., Schuman, M., Sullivan, P. A., Howell, L. G., Mayhew, S. G., Matthews, R. G., and Foust, G. P. (1969) The reactivity of flavoproteins with sulfite. Possible relevance to the problem of oxygen reactivity. *J. Biol. Chem.* 244, 3999-4006.
- (4) Müller, F. (1972) On the interaction of flavins with phosphine-derivatives. *Z. Naturforsch [B]* 27, 1023-6.
- (5) Massey, V., and Hemmerich, P. (1980) Active-site probes of flavoproteins. *Biochem. Soc. Trans.* 8, 246-57.
- (6) Macheroux, P., Kieweg, V., Massey, V., Soderlind, E., Stenberg, K., and Lindqvist, Y. (1993) Role of tyrosine 129 in the active site of spinach glycolate oxidase. *Eur. J. Biochem.* 213, 1047-54.
- (7) Wagner, M. A., Trickey, P., Chen, Z. W., Mathews, F. S., and Jorns, M. S. (2000) Monomeric sarcosine oxidase: 1. Flavin reactivity and active site binding determinants. *Biochemistry* 39, 8813-24.
- (8) Ohta-Fukuyama, M., Miyake, Y., Emi, S., and Yamano, T. (1980) Identification and properties of the prosthetic group of choline oxidase from *Alcaligenes sp.* *J. Biochem. (Tokyo)* 88, 197-203.
- (9) Gomez-Moreno, C., Choy, M., and Edmondson, D. E. (1979) Purification and properties of the bacterial flavoprotein: thiamin dehydrogenase. *J. Biol. Chem.* 254, 7630-5.
- (10) Brühmüller, M., Möhler, H., and Decker, K. (1972) Covalently bound flavin in D-6-hydroxynicotine oxidase from *Arthrobacter oxidans*. *Z. Naturforsch [B]* 27, 1073-4.
- (11) Gadda, G., Wels, G., Pollegioni, L., Zucchelli, S., Ambrosius, D., Pilone, M. S., and Ghisla, S. (1997) Characterization of cholesterol oxidase from *Streptomyces hygroscopicus* and *Brevibacterium sterolicum*. *Eur. J. Biochem.* 250, 369-76.
- (12) Müller, F., and Massey, V. (1969) Flavin-sulfite complexes and their structures. *J. Biol. Chem.* 244, 4007-16.
- (13) Gadda, G., and Fitzpatrick, P. F. (1998) Biochemical and physical characterization of the active FAD-containing form of nitroalkane oxidase from *Fusarium oxysporum*. *Biochemistry* 37, 6154-64.

- (14) Ghisla, S., Massey, V., and Yagi, K. (1986) Preparation and some properties of 6-substituted flavins as active site probes for flavin enzymes. *Biochemistry* 25, 3282-9.
- (15) Massey, V., and Ghisla, S. (1983) in *Biological Oxidations* (Sund, H., and Ullrich, V., Eds.) pp 114-139, Springer, Berlin.
- (16) Mayhew, S. G., Whitfield, C. D., Ghisla, S., and Schuman-Jorns, M. (1974) Identification and properties of new flavins in electron-transferring flavoprotein from *Peptostreptococcus elsdenii* and pig-liver glycolate oxidase. *Eur. J. Biochem.* 44, 579-91.
- (17) Müller, F., Ghisla, S., and Bacher, A. (1986) in *Wasserlösliche Vitamine* (Isler, O., Brubacher, G., and Ghisla, S., Eds.), Thieme, Stuttgart.
- (18) Fraaije, M. W., and Mattevi, A. (2000) Flavoenzymes: diverse catalysts with recurrent features. *Trends Biochem. Sci.* 25, 126-32.
- (19) Trimmer, E. E., Ballou, D. P., Galloway, L. J., Scannell, S. A., Brinker, D. R., and Casas, K. R. (2005) Aspartate 120 of *Escherichia coli* Methylenetetrahydrofolate Reductase: Evidence for Major Roles in Folate Binding and Catalysis and a Minor Role in Flavin Reactivity. *Biochemistry* 44, 6809-22.
- (20) Mewies, M., Packman, L. C., Mathews, F. S., and Scrutton, N. S. (1996) Flavinylation in wild-type trimethylamine dehydrogenase and differentially charged mutant enzymes: a study of the protein environment around the N1 of the flavin isoalloxazine. *Biochem. J.* 317, 267-72.
- (21) Hecht HJ, K. H., Hendle J, Schmid RD, Schomburg D. (1993) Crystal structure of glucose oxidase from *Aspergillus niger* refined at 2.3 Å resolution. *J. Mol. Biol.* 229, 153-172.
- (22) Wohlfahrt, G., Witt, S., Hendle, J., Schomburg, D., Kalisz, H. M., and Hecht, H. J. (1999) 1.8 and 1.9 Å resolution structures of the *Penicillium amagasakiense* and *Aspergillus niger* glucose oxidases as a basis for modelling substrate complexes. *Acta Crystallogr. D. Biol. Crystallogr.* 55, 969-77.
- (23) Vrielink, A., Lloyd, L. F., and Blow, D. M. (1991) Crystal structure of cholesterol oxidase from *Brevibacterium sterolicum* refined at 1.8 Å resolution. *J. Mol. Biol.* 219, 533-54.
- (24) Lario, P. I., Sampson, N., and Vrielink, A. (2003) Sub-atomic resolution crystal structure of cholesterol oxidase: what atomic resolution crystallography reveals about enzyme mechanism and the role of the FAD cofactor in redox activity. *J. Mol. Biol.* 326, 1635-50.
- (25) Yue, Q. K., Kass, I. J., Sampson, N. S., and Vrielink, A. (1999) Crystal structure determination of cholesterol oxidase from *Streptomyces* and structural characterization of key active site mutants. *Biochemistry* 38, 4277-86.

- (26) Bannwarth, M., Bastian, S., Heckmann-Pohl, D., Giffhorn, F., and Schulz, G. E. (2004) Crystal structure of pyranose 2-oxidase from the white-rot fungus *Peniophora* sp. *Biochemistry* 43, 11683-90.
- (27) Hallberg, B. M., Leitner, C., Haltrich, D., and Divne, C. (2004) Crystal structure of the 270 kDa homotetrameric lignin-degrading enzyme pyranose 2-oxidase. *J. Mol. Biol.* 341, 781-96.
- (28) Hallberg, B. M., Henriksson, G., Pettersson, G., and Divne, C. (2002) Crystal structure of the flavoprotein domain of the extracellular flavocytochrome cellobiose dehydrogenase. *J. Mol. Biol.* 315, 421-34.
- (29) Xia, Z. X., and Mathews, F. S. (1990) Molecular structure of flavocytochrome  $b_2$  at 2.4 Å resolution. *J. Mol. Biol.* 212, 837-63.
- (30) Lindqvist, Y., and Branden, C. I. (1989) The active site of spinach glycolate oxidase. *J. Biol. Chem.* 264, 3624-8.
- (31) Mattevi, A., Vanoni, M. A., Todone, F., Rizzi, M., Teplyakov, A., Coda, A., Bolognesi, M., and Curti, B. (1996) Crystal structure of D-amino acid oxidase: a case of active site mirror-image convergent evolution with flavocytochrome  $b_2$ . *Proc. Natl. Acad. Sci. U S A* 93, 7496-501.
- (32) Trickey, P., Wagner, M. A., Jorns, M. S., and Mathews, F. S. (1999) Monomeric sarcosine oxidase: structure of a covalently flavinylated amine oxidizing enzyme. *Structure Fold Des.* 7, 331-45.
- (33) Lim, L. W., Shamala, N., Mathews, F. S., Steenkamp, D. J., Hamlin, R., and Xuong, N. H. (1986) Three-dimensional structure of the iron-sulfur flavoprotein trimethylamine dehydrogenase at 2.4-Å resolution. *J. Biol. Chem.* 261, 15140-6.
- (34) Rowland, P., Björnberg, O., Nielsen, F. S., Jensen, K. F., and Larsen, S. (1998) The crystal structure of *Lactococcus lactis* dihydroorotate dehydrogenase A complexed with the enzyme reaction product throws light on its enzymatic function. *Protein Sci.* 7, 1269-79.
- (35) Müh, U., Massey, V., and Williams, C. H., Jr. (1994) Lactate monooxygenase. I. Expression of the mycobacterial gene in *Escherichia coli* and site-directed mutagenesis of lysine 266. *J. Biol. Chem.* 269, 7982-8.
- (36) Burg, M. B., Kwon, E. D., and Kultz, D. (1997) Regulation of gene expression by hypertonicity. *Annu. Rev. Physiol.* 59, 437-55.
- (37) McNeil, S. D., Nuccio, M. L., and Hanson, A. D. (1999) Betaines and related osmoprotectants. Targets for metabolic engineering of stress resistance. *Plant Physiol.* 120, 945-50.

- (38) Fan, F., Ghanem, M., and Gadda, G. (2004) Cloning, sequence analysis, and purification of choline oxidase from *Arthrobacter globiformis*: a bacterial enzyme involved in osmotic stress tolerance. *Arch. Biochem. Biophys.* 421, 149-58.
- (39) Fan, F., and Gadda, G. (2005) On the catalytic mechanism of choline oxidase. *J. Am. Chem. Soc.* 127, 2067-74.
- (40) Ghanem, M., Fan, F., Francis, K., and Gadda, G. (2003) Spectroscopic and kinetic properties of recombinant choline oxidase from *Arthrobacter globiformis*. *Biochemistry* 42, 15179-88.
- (41) Fan, F., and Gadda, G. (2005) Oxygen- and temperature-dependent kinetic isotope effects in choline oxidase: correlating reversible hydride transfer with environmentally enhanced tunneling. *J. Am. Chem. Soc.* 127, 17954-61.
- (42) Gadda, G. (2003) Kinetic mechanism of choline oxidase from *Arthrobacter globiformis*. *Biochim. Biophys. Acta* 1646, 112-8.
- (43) Gadda, G. (2003) pH and deuterium kinetic isotope effects studies on the oxidation of choline to betaine-aldehyde catalyzed by choline oxidase. *Biochim. Biophys. Acta* 1650, 4-9.
- (44) Gadda, G., Powell, N. L., and Menon, P. (2004) The trimethylammonium headgroup of choline is a major determinant for substrate binding and specificity in choline oxidase. *Arch. Biochem. Biophys.* 430, 264-73.
- (45) Ghanem, M., and Gadda, G. (2005) On the catalytic role of the conserved active site residue His466 of choline oxidase. *Biochemistry* 44, 893-904.
- (46) Whitby, L. G. (1953) A new method for preparing flavin-adenine dinucleotide. *Biochem. J.* 54, 437-42.
- (47) Corrado, M. E., Aliverti, A., Zanetti, G., and Mayhew, S. G. (1996) Analysis of the oxidation-reduction potentials of recombinant ferredoxin-NADP<sup>+</sup> reductase from spinach chloroplasts. *Eur J Biochem* 239, 662-7.
- (48) Ghisla, S., Massey, V., Lhoste, J. M., and Mayhew, S. G. (1974) Fluorescence and optical characteristics of reduced flavines and flavoproteins. *Biochemistry* 13, 589-97.
- (49) Yalloway, G. N., Mayhew, S. G., Malthouse, J. P., Gallagher, M. E., and Curley, G. P. (1999) pH-dependent spectroscopic changes associated with the hydroquinone of FMN in flavodoxins. *Biochemistry* 38, 3753-62.
- (50) Massey, V., and Ganther, H. (1965) On the interpretation of the absorption spectra of flavoproteins with special reference to D-amino acid oxidase. *Biochemistry* 4, 1161-73.
- (51) Ackrell, B. A., Cochran, B., and Cecchini, G. (1989) Interactions of oxaloacetate with *Escherichia coli* fumarate reductase. *Arch. Biochem. Biophys.* 268, 26-34.



- (52) Ackrell, B. A., Kearney, E. B., and Edmondson, D. (1975) Mechanism of the reductive activation of succinate dehydrogenase. *J. Biol. Chem.* 250, 7114-9.
- (53) Barber, M. J., Pollock, V., and Spence, J. T. (1988) Microcoulometric analysis of trimethylamine dehydrogenase. *Biochem. J.* 256, 657-9.
- (54) Efimov, I., Cronin, C. N., and McIntire, W. S. (2001) Effects of noncovalent and covalent FAD binding on the redox and catalytic properties of *p*-cresol methylhydroxylase. *Biochemistry* 40, 2155-66.
- (55) Fraaije, M. W., van den Heuvel, R. H., van Berkel, W. J., and Mattevi, A. (1999) Covalent flavinylation is essential for efficient redox catalysis in vanillyl-alcohol oxidase. *J. Biol. Chem.* 274, 35514-20.
- (56) Meyer, T. E., Bartsch, R. G., Caffrey, M. S., and Cusanovich, M. A. (1991) Redox potentials of flavocytochromes c from the phototrophic bacteria, *Chromatium vinosum* and *Chlorobium thiosulfatophilum*. *Arch. Biochem. Biophys.* 287, 128-34.
- (57) Clark, W. M. (1960) *Oxidation-reduction potentials of organic systems*, Williams & Wilkins, Baltimore, MD.
- (58) Fan, F., Germann, M. W., and Gadda, G. (2006) Mechanistic studies of choline oxidase with betaine aldehyde and its isosteric analogue 3,3-dimethylbutyraldehyde. *Biochemistry* 45, 1979-86.
- (59) Engst, S., Kuusk, V., Efimov, I., Cronin, C. N., and McIntire, W. S. (1999) Properties of *p*-cresol methylhydroxylase flavoprotein overproduced by *Escherichia coli*. *Biochemistry* 38, 16620-8.
- (60) Khanna, P., and Jorns, M. S. (2003) Tautomeric rearrangement of a dihydroflavin bound to monomeric sarcosine oxidase or N-methyltryptophan oxidase. *Biochemistry* 42, 864-9.
- (61) Kim, J., Fuller, J. H., Kuusk, V., Cunane, L., Chen, Z. W., Mathews, F. S., and McIntire, W. S. (1995) The cytochrome subunit is necessary for covalent FAD attachment to the flavoprotein subunit of *p*-cresol methylhydroxylase. *J. Biol. Chem.* 270, 31202-9.
- (62) Mewies, M., McIntire, W. S., and Scrutton, N. S. (1998) Covalent attachment of flavin adenine dinucleotide (FAD) and flavin mononucleotide (FMN) to enzymes: the current state of affairs. *Protein Sci.* 7, 7-20.
- (63) Motteran, L., Pilone, M. S., Molla, G., Ghisla, S., and Pollegioni, L. (2001) Cholesterol oxidase from *Brevibacterium sterolicum*. The relationship between covalent flavinylation and redox properties. *J. Biol. Chem.* 276, 18024-30.
- (64) Kass, I. J., and Sampson, N. S. (1998) Evaluation of the role of His447 in the reaction catalyzed by cholesterol oxidase. *Biochemistry* 37, 17990-8000.

## CHAPTER VII

### On the Role of the Active Site Residue His310 of Choline Oxidase

#### Abstract

Choline oxidase (E.C. 1.1.3.17) from *Arthrobacter globiformis* is a member of the Glucose-Methanol-Choline (GMC) oxidoreductase enzyme superfamily. The enzyme catalyzes the oxidation of choline to glycine betaine through two sequential flavin-linked hydride transfers from choline and the ensuing betaine aldehyde intermediate to molecular oxygen. The presence of a protein positive charge close to the N(1) locus of the bound flavin is a common characteristic feature of flavoprotein oxidases. Recent studies revealed that in the active site of choline oxidase the protein positive charge is provided by His<sub>466</sub>, which is located at a distance of ~3.3 Å from the N(1) locus of the enzyme-bound flavin (His<sub>466</sub><sup>Nε2</sup>-N(1)-FAD). The X-ray crystal structure of choline oxidase also showed that another histidine residue, His<sub>310</sub>, is located at a distance of ~2.9 Å from His<sub>466</sub> (His<sub>466</sub><sup>Nδ1</sup>-His<sub>310</sub><sup>Nδ1</sup>). To assess the contribution made by His<sub>310</sub> in catalysis, a mutant form of the enzyme was prepared in which the active site residue His<sub>310</sub> was substituted with alanine. Polarographic preliminary results on the enzyme obtained by substituting His<sub>310</sub> by an alanine residue showed that the purified mutant enzyme completely lost its catalytic activity with choline as substrate, suggesting the involvement of His<sub>310</sub> in catalysis. However, spectrophotometrically, CHO-H310A was still able to bind choline with the subsequent reduction of the enzyme-bound flavin, which happened significantly slower than with the wild-type form of choline oxidase (16 h vs 1 s) and in a biphasic way. The results obtained herein also indicated the involvement of His<sub>310</sub> in the flavinylation process and the binding of the coenzyme to the polypeptide chain of the protein as the removal of this residue resulted in a

significant alteration of the stoichiometric amount of the flavin. Therefore, these results together with the structural information suggest an important role of His<sub>310</sub> in catalysis and the modulation of the enzyme-bound flavin.

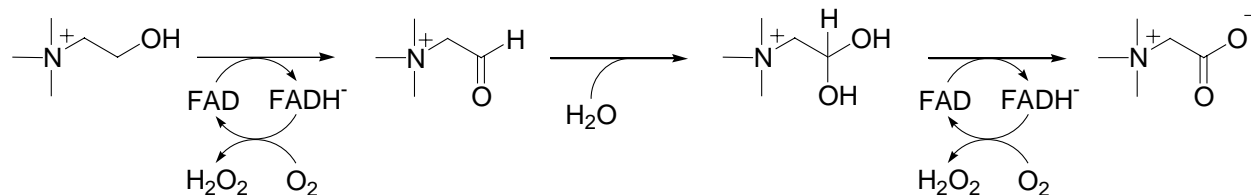
## Introduction

Choline oxidase (E.C. 1.1.3.17) is a flavin-dependent cytosolic enzyme that catalyzes the oxidation of choline to glycine betaine via an enzyme-bound aldehyde intermediate (Scheme 7.1). This reaction is of considerable interest for medical and biotechnological applications, since accumulation of glycine betaine in many pathogens and plants enables their stress-resistance towards hyperosmotic environments (1, 2). Therefore, the study of choline oxidase has potential for the development of therapeutic agents that inhibit the biosynthesis of glycine betaine and render pathogenic bacteria susceptible to either conventional treatments or the innate immune system, and for the improvement of water stress resistance in genetically engineered crops lacking efficient glycine betaine biosynthetic systems. Choline oxidase has been characterized in its biophysical, structural, and mechanistic properties. The enzyme is a homodimer with a mass of 120 kDa (3), contains covalently linked FAD in a 1:1 stoichiometry (3), and under turnover cycles between its fully oxidized and reduced states (4, 5). A detailed picture of the mechanism of the reaction catalyzed by choline oxidase was obtained from the biophysical, kinetic, structural and mechanistic studies of the wild-type *Arthrobacter globiformis* choline oxidase as well as selected mutant forms of the enzyme (4-11). In summary, during the reductive half-reaction, the alcohol substrate, choline, is activated through the proton abstraction of its hydroxyl group by an unidentified active site base with  $pK_a$  of 7.5 with the subsequent formation of an alkoxide species (4). This choline alkoxide intermediate species is transiently stabilized in the active site through an electrostatic interaction with the N(3) atom of the protonated imidazole side chain of His<sub>466</sub> (Figure 7.1) (10). Hydride transfer from the  $\alpha$ -carbon of the substrate to the N(5) locus of the isoalloxazine nucleus of the enzyme-bound FAD occurs quantum mechanically from the activated choline alkoxide species (6). The trimethylammonium headgroup of the

substrate alcohol is the major determinant for substrate binding and specificity, with little participation of the ethyl moiety (9).

The presence of a protein positive charge close to the N(1) locus of the bound flavin is a common characteristic feature of flavoprotein oxidases. In recent studies our group showed that in the active site of choline oxidase the protein positive charge is provided by His<sub>466</sub> (10, 11), which is located at a distance of  $\sim 3.3$  Å from the N(1) locus of the enzyme-bound flavin (His<sub>466</sub><sup>Nε2</sup>-N(1)-FAD) (George Lountos, Fan Fan, Giovanni Gadda, and Allen M. Orville; unpublished results). The X-ray crystal structure of choline oxidase also showed that another histidine residue, His<sub>310</sub>, is at a distance of  $\sim 2.9$  Å from His<sub>466</sub> (His<sub>466</sub><sup>Nδ1</sup>-His<sub>310</sub><sup>Nδ1</sup>) (Figure 7.2). In addition, the X-ray crystallographic data of the enzyme also showed that the N(3) atom of His<sub>310</sub> is located at a distance of  $\sim 2.8$  Å from the carbonyl main chain oxygen atoms of Thr<sub>380</sub> and Val<sub>507</sub> (Figure 7.2). These structural data, along with our previous studies on the role of the conserved active site His<sub>466</sub> residue suggest that His<sub>466</sub> is hydrogen bonded to both N(1)-FAD and His<sub>310</sub><sup>Nδ1</sup> through its N(3) and N(1) atoms, respectively. Moreover, these data also suggest that His<sub>310</sub> is hydrogen bonded to the carbonyl oxygen atoms of Thr<sub>380</sub> and Val<sub>507</sub> through its N(3) atom (Figure 7.2). Accordingly, one would expect the existence a proton-transfer network between the protonated conserved active site residue His<sub>466</sub> and His<sub>310</sub>.

In the present study, to assess the contribution made by His<sub>310</sub> in catalysis, a mutant form of choline oxidase was prepared in which His<sub>310</sub> was substituted with alanine.



**Scheme 7.1.** Reaction catalyzed by choline oxidase.

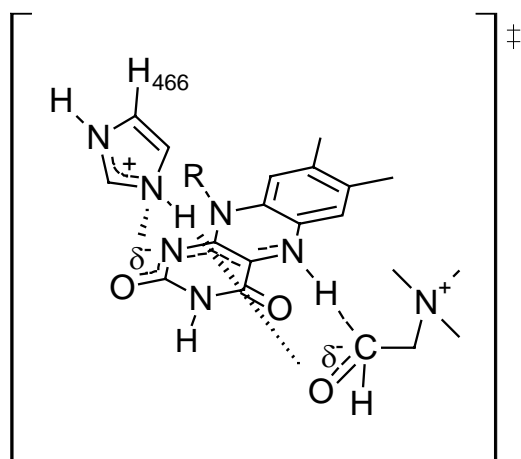


**Figure 7.1.** Line draw showing the interaction of His<sub>466</sub> with the N(1)–C(2)=O locus of FAD and the choline alkoxide species in the transition state for the oxidation of choline catalyzed by choline oxidase.

The positioning of His<sub>466</sub> relative to the flavin is from the X-ray crystallographic structure of the enzyme recently determined at 1.86 Å resolution (George Lountos, Fan Fan, Giovanni Gadda, and Allen M. Orville; unpublished results), the positioning of choline is arbitrary.

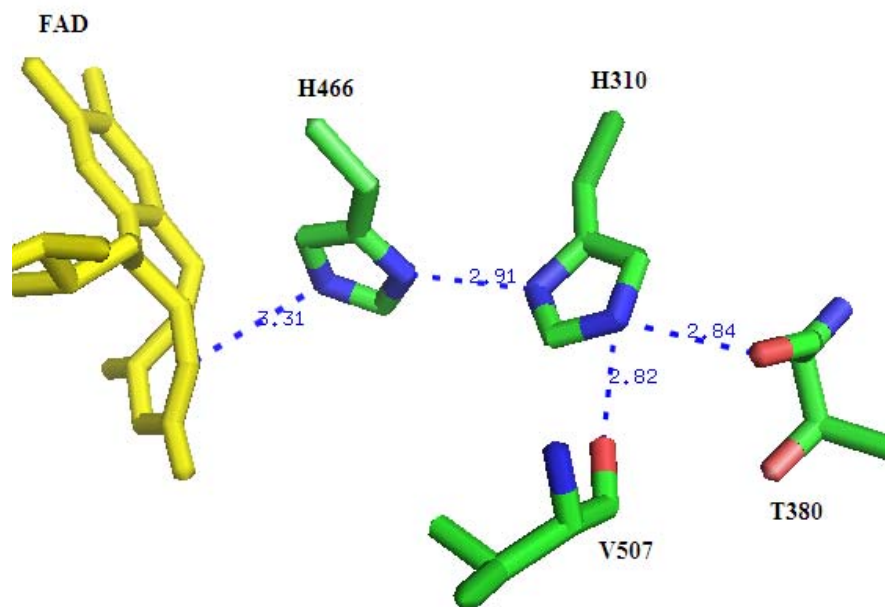


**Figure 7.2.** Crystal structure of choline oxidase.

X-ray crystallographic structure of the active site of choline oxidase determined at 1.86 Å resolution (George Lountos, Fan Fan, Giovanni Gadda, and Allen M. Orville; unpublished results).

## Experimental Procedures

**Materials.** *Escherichia coli* strain Rosetta(DE3)pLysS was from Novagen (Madison, WI). The QuikChange Site-Directed Mutagenesis kit was from Stratagene (La Jolla, CA). The QIAprep Spin Miniprep kit was from Qiagen (Valencia, CA). Oligonucleotides used for site-directed mutagenesis and for sequencing of the mutant gene were custom synthesized by the DNA Core Facility of the Department of Biology of Georgia State University or by Sigma Genosys (The Woodlands, TX). Oligonucleotides, bovine serum albumin, chloramphenicol, tetracycline, isopropyl- $\beta$ -D-thiogalactopyranoside (IPTG), lysozyme, sodium hydrosulfite (dithionite), sodium sulfite, betaine aldehyde, glycine betaine, Luria-Bertani agar and broth, and PMSF were from Sigma (St. Louis, MO). Choline chloride and ampicillin were from ICN (Aurora, OH). Wild-type choline oxidase (CHO-WT) from *Arthrobacter globiformis* strain ATCC 8010 was expressed from pET/*codA1* and purified to homogeneity as previously described (3). The fully oxidized FAD-containing CHO-WT was prepared as described in ref.(9). All other reagents were of the highest purity commercially available.

**Instruments.** UV-visible absorbance spectra were recorded using an Agilent Technologies diode-array spectrophotometer model HP 8453 equipped with a thermostated water bath. Rapid kinetics was carried out on a Hi-Tech SF-61 stopped-flow spectrophotometer thermostated at 15 °C.

**Site-Directed Mutagenesis.** A QuikChange kit was used to prepare the mutant forms of choline oxidase (CHO-H310A; CHO-H310D; and CHO-H310N). The method used was essentially according to the manufacturer's instructions, using pET/*codA1* plasmid (3) as a template and Cho-H310Af (5' CGAGCACCTGCAGGACGCCCCGGAAGGCGTG 3'); Cho-H310Df (5' GGGCGAGCACCTGCAGGACGACCCGGAAGGCGTG 3'); Cho-H310Nf



(5' GGGCGAGCACCTGCAGGACAAACCCGGAAGGCGTGGTGC 3') and Cho-H310Ar (5' GCACCACGCCTTCCGGGGGCTCCTGCAGGTGCTCGCC 3'); ChoH310Dr (5' GCACCACGCCTTCCGGGTCGCCTGCAGGTGCTCGCC 3'); Cho-H310Nr (5' GCACCACGCCTTCCGGGTTTGCCTGCAGGTGCTCGCC 3') oligonucleotides as forward and reverse primers, respectively (underlined letters indicate mismatches). DNA was sequenced at the DNA Core Facility at Georgia State University using an Applied Biosystems Big Dye Kit on an Applied Biosystems model ABI 377 DNA sequencer. Sequencing confirmed the presence of the mutant genes in the correct orientation. *E. coli* strain Rosetta(DE3)pLysS competent cells were transformed with pET plasmids harboring the mutant genes by electroporation.

***Expression and Purification of CHO-H310A.*** CHO-H310A was expressed and purified to homogeneity as judged by SDS-PAGE using the same procedure used previously for the purification of CHO-WT and CHO-H466A (3, 10). The enzyme as purified was stored at -20 °C in 20 mM Tris-Cl and 10% glycerol (to increase the solubility and stability of the purified enzyme), pH 8.

***Spectrophotometric Studies.*** The UV-visible absorbance spectra of CHO-H310A were acquired in 20 mM Tris-Cl and 10% glycerol, pH 8, at 15 °C. The extinction coefficient of CHO-H310A was determined in 20 mM Tris-Cl, pH 8, after denaturation of the enzyme by incubation at 40 °C for 3.5 h in the presence of urea at a final concentration of 4 M, based upon the  $\epsilon_{450}$  value of 11.3 mM<sup>-1</sup> cm<sup>-1</sup> for free FAD (12). For the quantitation of the ratio of the covalently to the uncovalently bound flavin to the enzyme, ~ 20 µM of enzyme was incubated on ice for 30 min after the addition of 10 % trichloroacetate, followed by removal of precipitated protein by centrifugation, and the determination of the concentration of FAD in the supernatant solution. For the anaerobic reaction of CHO-H310A with its organic substrate, choline, CHO-H310A in

20 mM Tris-Cl and 10% glycerol, pH 8, was made anaerobic by repeated cycles of alternate degassing under vacuum and flushing with ultra-pure O<sub>2</sub>-free argon in an anaerobic cell equipped with two side arms. The organic substrate, choline was loaded into one side arm and was mixed with CHO-H310A at final concentrations ranging from 0.5 to 20 mM and incubated for 16-40 h.

**Enzyme Assays.** The enzymatic activity of CHO-H310A was measured by the method of initial rates as described for the wild-type enzyme (3, 5) using a computer-interfaced Oxy-32 oxygen-monitoring system (Hansatech Instrument Ltd.). The effect of imidazole on the turnover number of CHO-H310A was determined by measuring the enzymatic activity with 10 mM choline as substrate for the enzyme in the presence of 100 mM of imidazole in air-saturated 50 mM sodium pyrophosphate, pH 6 or 10.

**Data Analysis.** Spectroscopic data points of the anaerobic incubation of CHO-H310A with its organic substrate choline were fit into eq 1 that describes a case of double-exponential decay, in which  $k_1$  and  $k_2$  represent the first-order rate constants for the fast and the slow phase of the reductive half reaction, respectively,  $t$  is time,  $A_t$  is the value of absorbance at 456 nm,  $A_1$  and  $A_2$  are the amplitude of the total change in the fast and the slow phase of the reductive half reaction, respectively, and  $A_\infty$  is the absorbance at infinite time. Data points obtained for the observe rate of the slow phase of flavin reduction were fit to eq 2, where  $k_{\text{obs}}$  is the observed rate for the reduction of enzyme bound flavin,  $k_{\text{red}}$  is the limiting rate of flavin reduction at saturated substrate concentration,  $K_d$  is the dissociation constant, and  $A$  is the substrate concentration.

$$A_t = A_1 \exp(-k_1 t) + A_2 \exp(-k_2 t) + A_\infty \quad (1)$$

$$k_{\text{obs}} = \frac{k_{\text{red}} A}{K_d + A} \quad (2)$$

## Results

**Expression and Purification of CHO-H310A.** CHO-H310A was expressed and purified to high purity and quantity using the same protocol established for the CHO-WT (Figure 7.3). Similar to wild-type enzyme, about 100-150 mg of pure CHO-H310A could be typically obtained from 4.5 liters of Luria-Bertani culture medium. Polarographically, CHO-H310A as purified at final concentrations as high as 20  $\mu\text{M}$  did not show any catalytic activity toward its organic substrate choline at final concentration of 20-30 mM at pH 7, at 25 °C. In comparison, the CHO-WT at a final concentration of 0.1  $\mu\text{M}$  typically shows a catalytic activity of  $\sim 15 \text{ s}^{-1}$  with 10 mM choline (3), suggesting that histidine at position 310 is essential for the catalytic activity in choline oxidase.

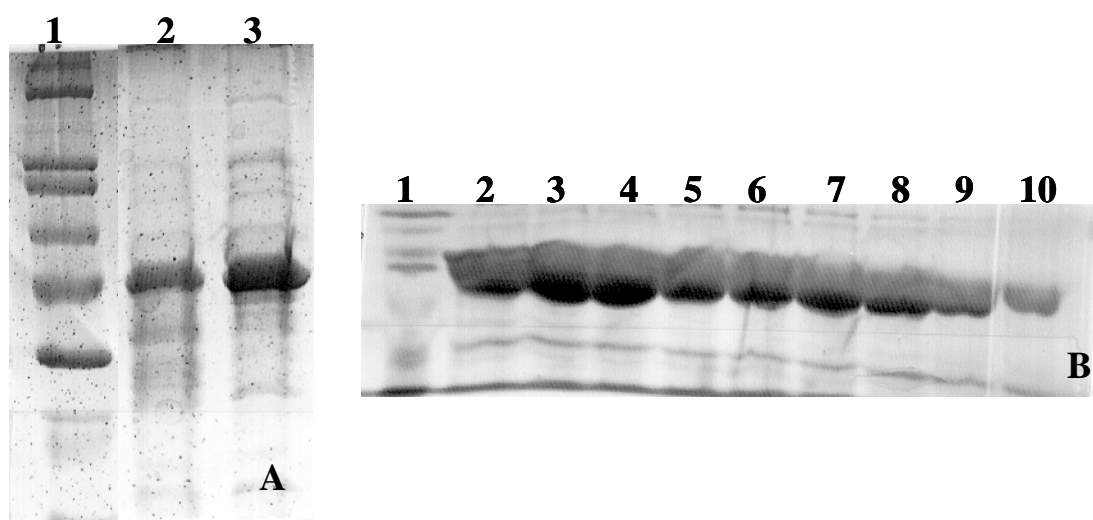


**Figure 7.3.** Expression and purification of CHO-H310A.

Figure A: *lane 1*, molecular weight marker proteins; *lane 2*, total cell proteins before induction; *lane 3*, total cell proteins after induction with 0.1 mM IPTG for 5 hours at 23 °C. Figure B: *lane 1*, molecular weight marker proteins; *lane 2-10*, pooled purified fractions of CHO-H310A in 200 mM Tris-Cl, pH 8, after DEAE column chromatography.

**Spectral Properties.** The UV-visible absorbance spectrum of oxidized CHO-H310A at pH 8 showed the typical spectrum of the oxidized flavin with peaks centered at 272, 356 and 458 nm in the near-UV and visible regions (Figure 7.4), suggesting that the enzyme-bound flavin cofactor in the mutant enzyme as purified is in the oxidized redox state. The enzyme-bound flavin of CHO-H310A showed an extinction coefficient at 458 nm of  $11.6 \text{ mM}^{-1} \text{ cm}^{-1}$  (Figure 7.4), consistent with the values of  $11.4 \text{ mM}^{-1} \text{ cm}^{-1}$  at 452 nm,  $12 \text{ mM}^{-1} \text{ cm}^{-1}$  at 458 nm, and  $12 \text{ mM}^{-1} \text{ cm}^{-1}$  at 450 nm that were previously determined for the wild-type, CHO-H466A, and CHO-H466D enzymes, respectively (5, 10, 11). Similar to wild-type or CHO-H466A forms of choline oxidase, CHO-H310A bound FAD covalently. A stoichiometry of  $\sim 0.11$  FAD per monomer of protein was calculated for CHO-H310A, indicating that the flavin content of CHO-H310A was significantly less than that of the wild-type choline oxidase, for which a stoichiometry close to unity was previously reported (3). A stoichiometry of  $\sim 0.3$  FAD per monomer of protein was previously determined for both CHO-H466A and CHO-H466D mutant forms of choline oxidase (10, 11). This result suggests that histidine residue at position 310 significantly affects the flavinylation and the coenzyme binding of choline oxidase.

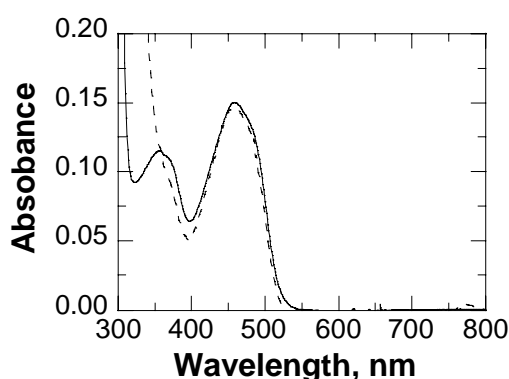


**Figure 7.4.** Spectral properties of CHO-H310A. *Solid curve*, UV-visible absorbance spectrum of CHO-H310A in 20 mM Tris-Cl and 10% glycerol, pH 8; *dashed curve*, after incubation with 4 M urea at 40 °C for 3.5 h.

**Reaction of CHO-H310A with Choline.** Purified CHO-H310A at final concentrations as high as 20  $\mu\text{M}$  showed no oxygen consumption when assayed with 20-30 mM choline as a substrate at pH 7 and 25  $^{\circ}\text{C}$ . Nevertheless, the anaerobic incubation of CHO-H310A with choline at a final concentration ranging from 0.75 to 20 mM resulted in a biphasic reduction of the oxidized enzyme-bound flavin, with a fast phase that started right after mixing the enzyme with its organic substrate and lasted for  $\sim 30$  min, and a slow phase that lasted for  $\sim 16$ -40 h until the full reduction of the bound flavin (Figure 7.5 and 7.6). This result clearly suggests that although CHO-H310A does not show any catalytic activity toward its organic substrate choline as measured polarographically, as assessed spectrophotometrically, CHO-H310A is still capable to bind and oxidize its organic substrate choline but with a significantly slower rate compared to that of CHO-WT or even CHO-H466A. The data points obtained for the observed rate of the fast phase of flavin reduction after the anaerobic incubation of CHO-H310A with different concentrations of choline (0.75-20 mM), were scattered and did not allow the determination of the  $k_{\text{red}}$  and the  $K_{\text{d}}$  for such fast phase (Figure 7.7A). However, the data points obtained for the observed rate of the slow phase of flavin reduction, with the exception of the point at the highest concentration of choline (20 mM), fit to eq 2 (data not shown). The value obtained for  $k_{\text{red}}$  by fitting those data points to eq 2 was  $\sim 200,000$ -fold lower than that for wild-type enzyme ( $4.37 \times 10^{-4} \text{ s}^{-1}$  vs  $93 \text{ s}^{-1}$ ), and the value determined for  $K_{\text{d}}$  was at least 2-fold higher than that of wild-type enzyme (0.65 mM vs 0.29 mM) (4). Alternatively, the data points for the observed rate of the slow phase of flavin reduction fit to substrate inhibition equation (Figure 7.7B). However, due to the lack of the data points at the inhibitory phase it did not allow the determination of the  $k_{\text{red}}$ ,  $K_{\text{i}}$  and  $K_{\text{m}}$ . The scattering of the data points that have been observed during the fast phase of CHO-H310A reaction with choline could be attributed either to the independence of the reaction

to the substrate concentration, or due to a conformational change of the enzyme upon the substitution of the active site residue His<sub>310</sub> to alanine. This conformational change could be studied in the future by examining the overall fold of the mutant enzyme and compare it with that of the wild type choline oxidase using either tryptophan fluorescence or CD-spectrophotometer.

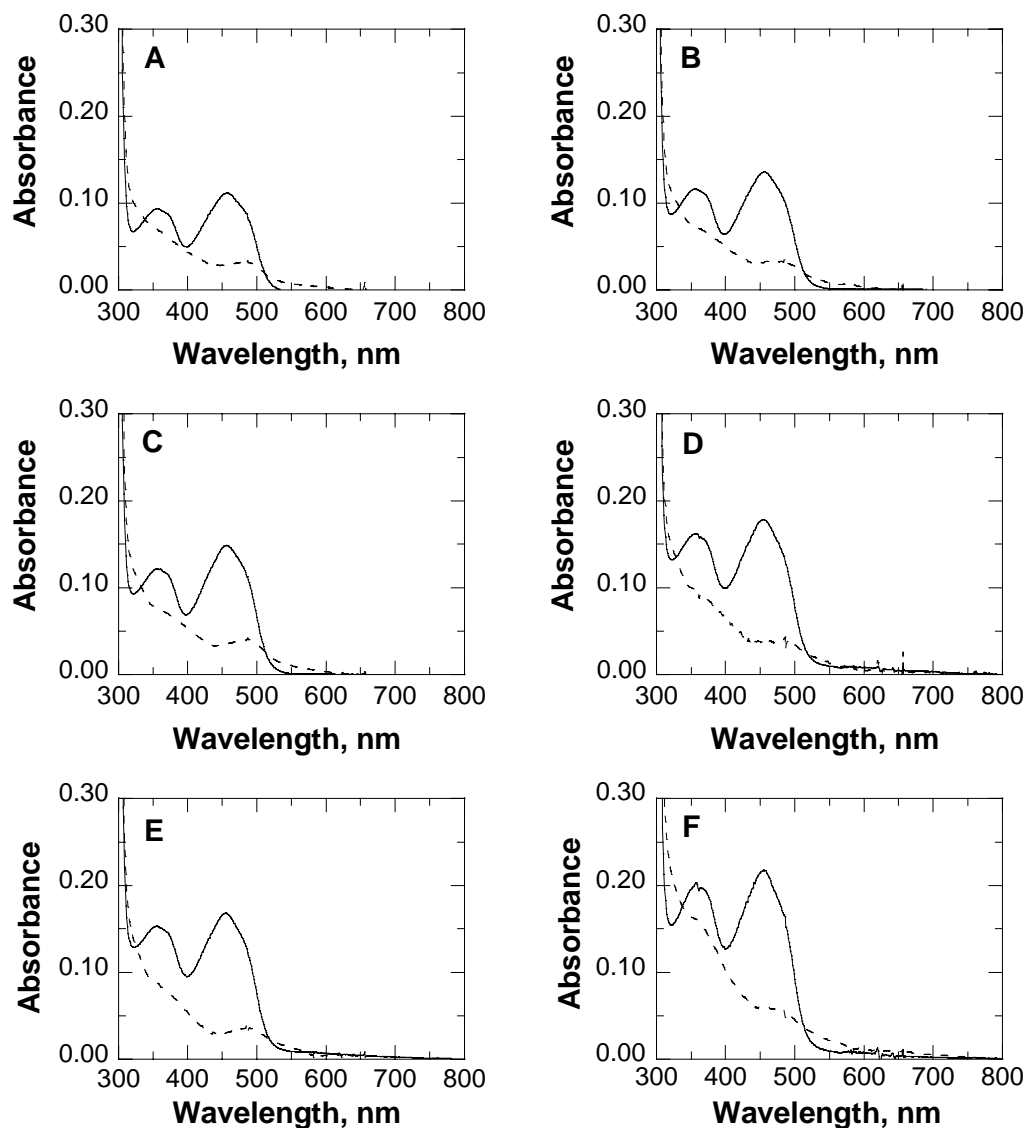


**Figure 7.5.** Anaerobic reaction of CHO-H310A with choline (1).

*Solid curves*, UV-visible absorbance spectra of CHO-H310A before incubation with choline; *dashed curves*, UV-visible absorbance spectra of CHO-H310A after anaerobic incubation with 0.75 mM of choline for 40 h (*panel A*), 1 mM choline for 16 h (*panel B*), 1.5 mM choline for 16 h (*panel C*), 2 mM choline for 16 h (*panel D*), 5 mM choline for 16 h (*panel E*), and 10 mM choline for 5.5 h (*panel F*). Enzyme concentrations were 10-20  $\mu$ M in 20 mM Tris-Cl and 10% glycerol, pH 8, at 15  $^{\circ}$ C.

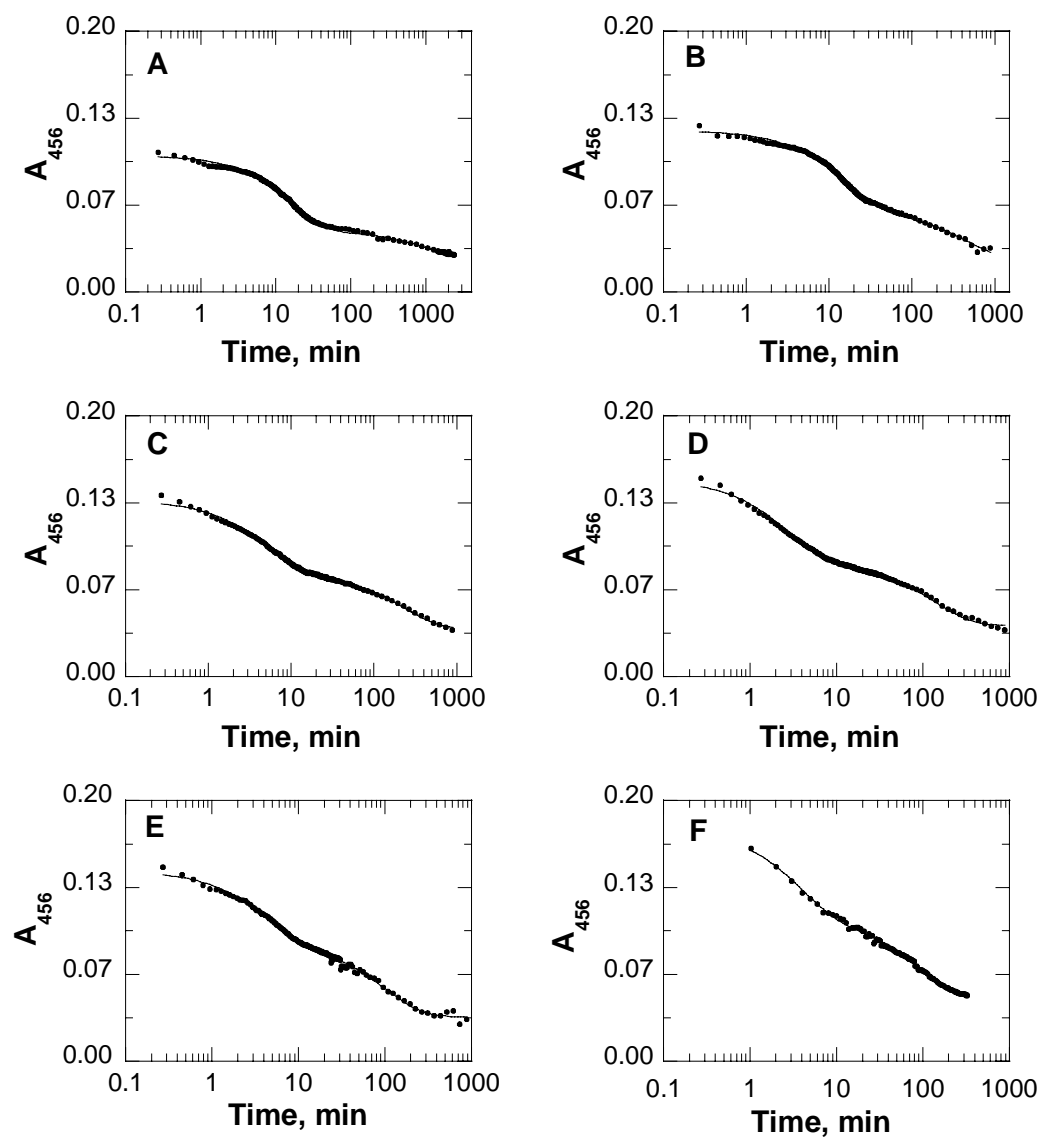


**Figure 7.6.** Anaerobic reaction of CHO-H310A with choline (2).

UV-visible absorbance values (●) at 456 nm as a function of time after the anaerobic incubation of CHO-H310A with 0.75 mM of choline for 40 h (*panel A*), 1 mM choline for 16 h (*panel B*), 1.5 mM choline for 16 h (*panel C*), 2 mM choline for 16 h (*panel D*), 5 mM choline for 16 h (*panel E*), and 10 mM choline for 5.5 h (*panel F*). The curves are fits of the data to eq 1.



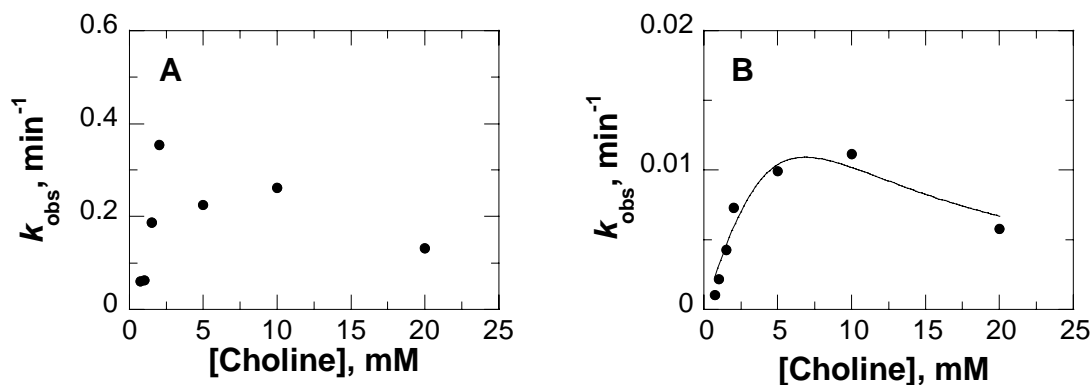


**Figure 7.7.** Anaerobic reaction of CHO-H310A with choline (3).

Observed rate (●) of the decrease of absorbance at 456 nm as a function of choline concentration for CHO-H310A during the fast phase (*panel A*) and the slow phase (*panel B*).

**Table 7.1.** Anaerobic Spectral Incubation of CHO-H310A with Choline<sup>a</sup>

[Choline], mM	Fast phase	Slow phase
	$k_{\text{obs}}$ , $\text{min}^{-1}$	$k_{\text{obs}} \times 10^3$ , $\text{min}^{-1}$
0.75	$0.061 \pm 0.001$	$1.0 \pm 0.1$
1	$0.063 \pm 0.001$	$2.0 \pm 0.3$
1.5	$0.187 \pm 0.002$	$4.0 \pm 0.1$
2	$0.35 \pm 0.005$	$7.0 \pm 0.2$
5	$0.23 \pm 0.005$	$10 \pm 0.3$
10	$0.26 \pm 0.01$	$11 \pm 0.2$
20	$0.13 \pm 0.005$	$6.0 \pm 0.5$

<sup>a</sup> Enzyme concentrations were 10–20  $\mu\text{M}$  in 20 mM Tri-Cl and 10 % glycerol, pH 8, at 15 °C.

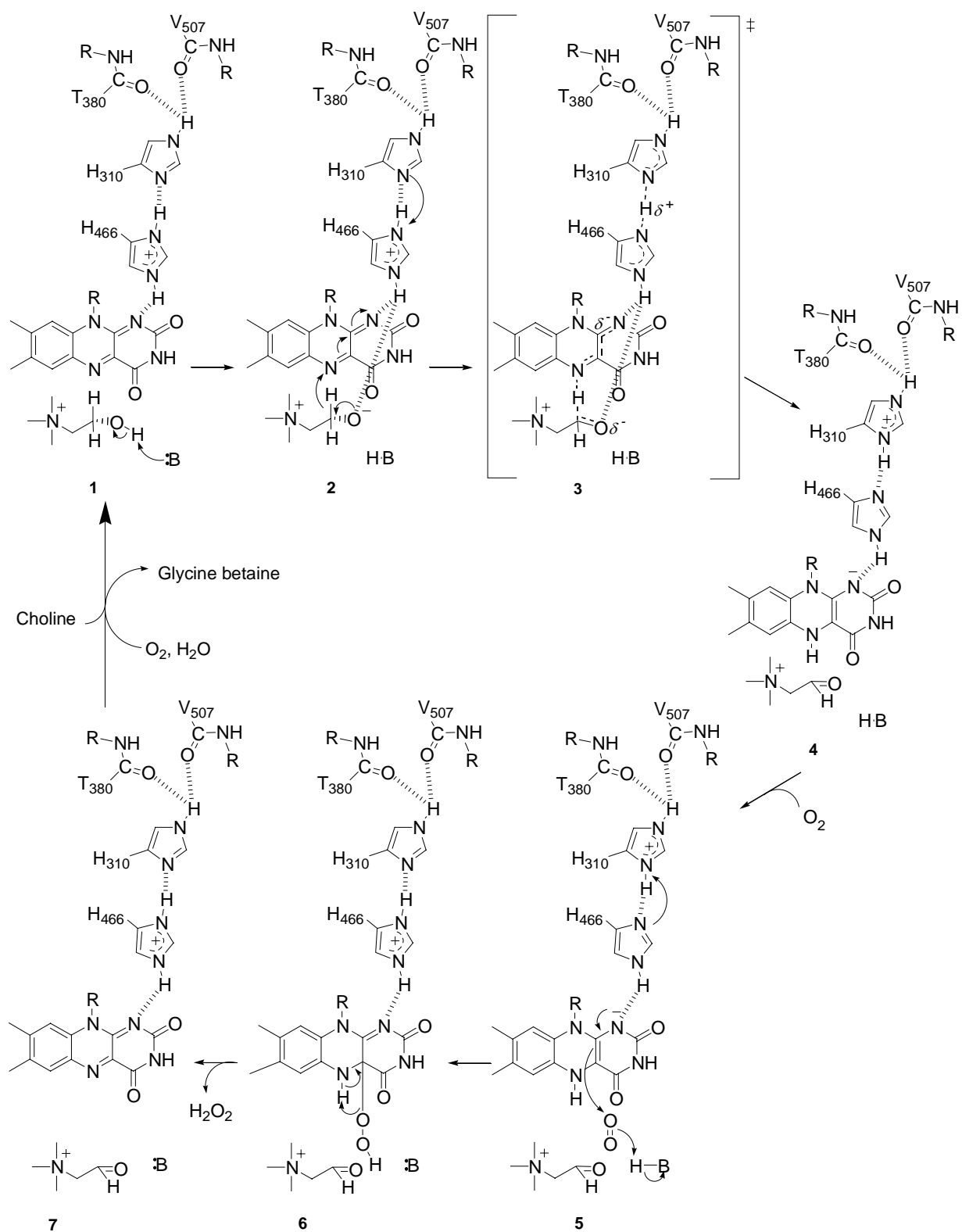
## Discussion

***A proton-transfer network in the active site of choline oxidase.*** In a recent study in which His<sub>466</sub> was replaced with alanine, our group showed that His<sub>466</sub> is protonated and that, besides stabilizing the transient alkoxide species that is formed in catalysis, this protein group modulates the electrophilicity of the enzyme-bound flavin and the polarity of the active site (species 3 in Scheme 7.2) (10). In another recent study in which His<sub>466</sub> was replaced with aspartate, our group was able to show that His<sub>466</sub>, which is located at a distance of  $\sim 3.3 \text{ \AA}$  from the N(1) locus of the bound FAD, is responsible for stabilizing the negative charge that develops in the enzyme active site (species 3,4, and 5 in Scheme 7.2) (11). The X-ray crystal structure of choline oxidase showed that His<sub>310</sub> is located at a distance of  $\sim 2.9 \text{ \AA}$  from His<sub>466</sub> (His<sub>466</sub><sup>N $\delta$ 1</sup>-His<sub>310</sub><sup>N $\delta$ 1</sup>) (Figure 7.2). The X-ray crystal structure of the enzyme along with our previous studies on the role of the conserved active site His<sub>466</sub> residue suggest the existence of a proton-transfer network between the protonated conserved active site residue His<sub>466</sub> and His<sub>310</sub>; the latter residue is hydrogen bonded to the carbonyl oxygen atoms of Thr<sub>380</sub> and Val<sub>507</sub> through its N(3) atom (Figure 7.2).

The preliminary results obtained herein by substituting the active site residue His<sub>310</sub> of choline oxidase show that the resulting enzyme is completely devoid of any catalytic activity with choline as substrate, suggesting that His<sub>310</sub> plays an essential role in the active site of choline oxidase. As shown in Scheme 7.2, our proposed model of the mechanism of reaction for the oxidation of choline catalyzed by choline oxidase in which a proton-transfer network between His<sub>466</sub> and His<sub>310</sub> is proposed can be summarized as follows. 1) During the reductive half-reaction, an unidentified active site base with a pK<sub>a</sub> of 7.5 activates the alcohol substrate with formation of an alkoxide species (species 1 and 2 in Scheme 7.2) (4, 5). 2) This alkoxide

intermediate is transiently stabilized in the active site through electrostatic interaction with the Ne2 atom of the protonated side chain of His<sub>466</sub> (species 3 in Scheme 7.2) (10). 3) The protonated His<sub>466</sub> also stabilizes electrostatically the negative charge that develops at N(1)-C(2)=O locus of the reduced flavin (anionic species) through its Ne2 atom (species 3 in Scheme 7.2) (11). 4) The hydride transfer from the  $\alpha$ -carbon of the substrate to the N(5) locus of the bound occurs quantum mechanically from the activated choline alkoxide species (species 3 in scheme 7.2) (6). 5) His<sub>466</sub> is hydrogen bonded to His<sub>310</sub> (His<sub>466</sub><sup>N $\delta$ 1</sup>-His<sub>310</sub><sup>N $\delta$ 1</sup>); the latter residue is hydrogen bonded to the main chain carbonyl oxygen atoms of Thr<sub>380</sub> and Val<sub>507</sub>. The main proposed role of such a proton-transfer network is to prevent the protonated His<sub>466</sub> from losing its proton during the oxidative half-reaction. This proton-transfer network serves to transfer this proton from His<sub>466</sub> to His<sub>310</sub> before the reaction of molecular oxygen. As a result of such proton transfer, the negative charge at the N(1)-C(2)=O locus of the anionic hydroquinone is stabilized through hydrogen bonding with Ne2 atom of the imidazole side chain of His<sub>466</sub> (species 4 in Scheme 7.2). 6) During the oxidative half-reaction, and after the transfer of the proton from His<sub>466</sub> to His<sub>310</sub>, the electron delocalization from the N(1) locus of the anionic hydroquinone along with the proton transfer from an unidentified catalytic base results in the formation of the C(4a)-hydroperoxo-flavin (species 5 in Scheme 7.2); 7) the highly unstable C(4a)-hydroperoxo-flavin abstracts the second proton from the hydride at N(5) locus of the FAD with the subsequent release of H<sub>2</sub>O<sub>2</sub> and the formation of oxidized enzyme-bound FAD (species 6 and 7 in Scheme 7.2); 8) finally, the oxidation of the hydrated betaine aldehyde occurs through a base catalyzed transfer of a hydride ion from the organic substrate to the enzyme-bound FAD, with a mechanism that is similar to that proposed for the oxidation of choline as proposed recently in a study by our group on the mechanism of aldehyde oxidation (13).

In summary, the previously obtained results on the CHO-H466A and CHO-H466D mutants (*10, 11*) suggested that His<sub>466</sub> plays an important role in the transient stabilization of choline alkoxide intermediate, in stabilization of the negative charge that develops on the N(1)-C(2)=O locus of the bound flavin, and in modulation of the electrophilicity of the bound FAD and the polarity of the active site. The preliminary results obtained herein on the CHO-H310A mutant form of choline oxidase suggested that His<sub>310</sub> plays an essential role in the active site of choline oxidase because its substitution with alanine resulted in a complete loss of its catalytic activity toward choline as a substrate. One would expect that CHO-H310A is completely devoid of activity with choline due to the fact that the substitution of His<sub>310</sub> with alanine resulted in alteration of the position of His<sub>466</sub> and in turn resulted in an completely inactive enzyme or at least 200,000-time slower than CHO-WT. In addition, the substitution of His<sub>310</sub> with alanine would disrupt the proposed proton-transfer network between His<sub>466</sub> and His<sub>310</sub>. In that sense, further site-directed mutagenesis studies (H310D and H310N) are currently underway in order to gain insights into the role played by such a proton-transfer network involving His<sub>310</sub> and His<sub>466</sub> in the reaction catalyzed by choline oxidase.



**Scheme 7.2.** Proposed role of His<sub>310</sub> in the reaction catalyzed by choline oxidase.

## References

- (1) Burg, M. B., Kwon, E. D., and Kultz, D. (1997) Regulation of gene expression by hypertonicity. *Annu. Rev. Physiol.* 59, 437-55.
- (2) McNeil, S. D., Nuccio, M. L., and Hanson, A. D. (1999) Betaines and related osmoprotectants. Targets for metabolic engineering of stress resistance. *Plant Physiol.* 120, 945-50.
- (3) Fan, F., Ghanem, M., and Gadda, G. (2004) Cloning, sequence analysis, and purification of choline oxidase from *Arthrobacter globiformis*: a bacterial enzyme involved in osmotic stress tolerance. *Arch. Biochem. Biophys.* 421, 149-58.
- (4) Fan, F., and Gadda, G. (2005) On the catalytic mechanism of choline oxidase. *J. Am. Chem. Soc.* 127, 2067-74.
- (5) Ghanem, M., Fan, F., Francis, K., and Gadda, G. (2003) Spectroscopic and kinetic properties of recombinant choline oxidase from *Arthrobacter globiformis*. *Biochemistry* 42, 15179-88.
- (6) Fan, F., and Gadda, G. (2005) Oxygen- and temperature-dependent kinetic isotope effects in choline oxidase: correlating reversible hydride transfer with environmentally enhanced tunneling. *J. Am. Chem. Soc.* 127, 17954-61.
- (7) Gadda, G. (2003) Kinetic mechanism of choline oxidase from *Arthrobacter globiformis*. *Biochim. Biophys. Acta* 1646, 112-8.
- (8) Gadda, G. (2003) pH and deuterium kinetic isotope effects studies on the oxidation of choline to betaine-aldehyde catalyzed by choline oxidase. *Biochim. Biophys. Acta* 1650, 4-9.
- (9) Gadda, G., Powell, N. L., and Menon, P. (2004) The trimethylammonium headgroup of choline is a major determinant for substrate binding and specificity in choline oxidase. *Arch. Biochem. Biophys.* 430, 264-73.
- (10) Ghanem, M., and Gadda, G. (2005) On the catalytic role of the conserved active site residue His466 of choline oxidase. *Biochemistry* 44, 893-904.
- (11) Ghanem, M., and Gadda, G. (2006) Effects of reversing the protein positive charge in proximity of the N(1)-flavin locus of choline oxidase. *Biochemistry* 45, 3437-47.
- (12) Whitby, L. G. (1953) A new method for preparing flavin-adenine dinucleotide. *Biochem. J.* 54, 437-42.
- (13) Fan, F., Germann, M. W., and Gadda, G. (2006) Mechanistic studies of choline oxidase with betaine aldehyde and its isosteric analogue 3,3-dimethylbutyraldehyde. *Biochemistry* 45, 1979-86.

## CHAPTER VIII

### General Discussion

Choline oxidase from *Arthrobacter globiformis* catalyzes the oxidation of choline to glycine betaine (1-3). This reaction is of considerable interest for biotechnological and biomedical applications. The biotechnological and biomedical importance come from the reaction product glycine betaine, which is one of the most commonly used compatible solutes that is accumulated in the cytoplasm of many plants and microorganisms to counteract hyperosmotic environments (4). The accumulation of glycine betaine was observed in many human pathogenic bacteria, allowing their growth and survival under hyperosmotic conditions that are frequently encountered at human infectious sites (5-7). The development of efficient specific inhibitors targeting glycine betaine synthetic pathway therefore has potential for the microbial treatment. Similarly, in transgenic plants, glycine betaine serves a similar function, enabling bioengineering of economically relevant crop plants with enhanced stress resistances (8-11). From a chemical standpoint, the oxidation reaction catalyzed by choline oxidase is of particular interest in that the cleavage of the substrate CH bond is energetically unfavorable due to the high  $pK_a$  value of the CH group (12). In this study, the biophysical, biochemical, structural, and mechanistic properties of wild-type as well as selected mutant forms of choline oxidase are presented, providing a solid background for the medical and biotechnological applications of choline oxidase. In addition, the results obtained in this study have also shed light on other structurally and mechanistically related flavoprotein oxidases.

The correct nucleotide sequence of the *codA* gene encoding for choline oxidase was established in this study. The *codA* gene contains large amount of GC (~70%), resulting in difficulties in PCR amplification. Addition of 2% of DMSO into the PCR reaction mixture

increased the efficiency of denaturation for the double stranded DNA and yielded a full-length PCR product. Sequence analysis was performed independently with two forms of the *codA* gene: the cloned *codA* gene directly from the genomic DNA of *A. globiformis* strain ATCC 8010; and the subcloned *codA* gene (a gift kindly provided by Dr. Norio Murata, National Institute for Basic Biology, Okazaki, Japan), which has been prepared by F. Fan. Similar sequencing results were obtained, both of which showed that the previously reported nucleotide sequence of *codA* in GenBank (13) contained seven flaws. These seven flaws resulted in a translated protein with a significantly altered amino acid sequence between position 298 and 410. The correct newly determined amino acid sequence of choline oxidase corresponds to the mass of the enzyme with one linked FAD (60.612 kDa), consistent with the experimental mass spectral determination (60.614 kDa). For comparison, the calculation of the incorrect previously reported amino acid sequence of the enzyme yields a molecular mass of 59.648 kDa. A significant increase in homology between choline oxidase and other members of the GMC oxidoreductase superfamily was also observed when the newly reported amino acid sequence was used (Figure 3.4 in Chapter III), which further strengthens our sequence analysis. Importantly, the recently solved X-ray crystal structure of choline oxidase clearly showed a covalent linkage between the His99<sup>Nε2</sup> and FAD<sup>C8M</sup> atoms, in contrast to the previously proposed His87<sup>Nε1</sup> determined by mass spectroscopic studies which was based on the previously reported incorrect amino acid sequence of the enzyme (14). The previously reported incorrect nucleotide sequence of *A. globiformis codA* gene was recently replaced with a newer version in the GenBank (accession number X84895.2) that is identical to our sequence.

In this study, our group has established an efficient protocol to express and purify the recombinant choline oxidase to high purity and quantity, allowing detailed biochemical and



mechanistic studies of this enzyme. The same protocol was also applied to express and purify different mutant forms of the enzyme. The cloned *codA* gene from *A. globiformis* was expressed to high quantity in *Escherichia coli* strain Rosetta(DE3)pLysS, which provides tRNAs for rare codons. The *codA* gene contains 27 of such rare codons due to its high GC content. The enzyme was then purified to homogeneity using 30 to 65% ammonium sulfate followed by anion exchange chromatography onto a DEAE-Sepharose Fast Flow column. Typically ~150-200 mg pure choline oxidase could be obtained from 4.5 liters liquid LB culture medium (Table 3.2 in Chapter III).

The recombinant choline oxidase as purified was found to contain large amounts of anionic flavin semiquinone species (35-85%). At pH 8, enzyme-bound flavosemiquinone remains unusually stable when subjected to the treatments with molecular oxygen or oxidizing agents such as ferricyanide, suggesting that the unpaired electron resides in a solvent inaccessible region of the flavin (Figure 4.1 in Chapter IV). The enzyme-bound semiquinone undergoes a slow conversion to the fully oxidized form at pH 6 (Figure 4.4 in Chapter IV), indicating that an increase in proton concentration significantly destabilizes the flavin radical. The spectral studies of the enzyme under turnover showed only two states, i.e., the fully oxidized and reduced forms, indicating that the flavin semiquinone of choline oxidase is catalytically inactive (Figure 4.7 in Chapter IV). The kinetic data further support this conclusion by showing a good correlation between the turnover numbers of the enzyme with choline and betaine aldehyde as substrate and the content of oxidized flavin per active site (Table 4.2 in Chapter IV). The conversion of the kinetically inactive inert semiquinone form of flavin to the active oxidized form increases the specific activity of the purified enzyme at least by 2-folds. The unusual stabilization of flavosemiquinone along with the formation of a tight reversible flavin-N(5)-sulfite adduct in

wild-type choline oxidase was explained as a result of the stabilization of the negative charge that develops on N(1) locus of the flavin by a protein positive charge close to that region. Such protein positive charge was firstly assigned to the dipole of an adjacent  $\alpha$ -helix, which is fully conserved among the GMC oxidoreductase superfamily (15-19). Our recent studies on the active site residue His<sub>466</sub> clearly suggest that the protonated form His<sub>466</sub> stabilizes the negative charge that develops on the N(1) locus of the bound flavin as well as the negative charge of the transient alkoxide intermediate during catalysis (Chapter V and VI) (20, 21). Interestingly, the midpoint reduction-oxidation potential for the oxidized-semiquinone couple in wild-type choline oxidase was 211 mV (Figure 6.8 and Table 6.2 in Chapter VI) (20), which is exceptionally the highest value for such thermodynamic equilibrium reported for a flavoprotein oxidase (22-27), consistent with the unusual stabilization of flavosemiquinone in choline oxidase. In addition, the mutant form of choline oxidase in which the positively charged histidine residue at position 466 was reversed (H466D) lost its ability to either stabilizes the semiquinone species of the bound flavin or the formation of flavin-N(5)-sulfite adduct, consistent with the proposed role of His<sub>466</sub> in stabilizing the negative charge that develops on the N(1) locus of the bound FAD. Furthermore, the midpoint potential for the transfer of the two electrons with CHO-H466D showed a value that was ~130 mV and ~160 mV more negative than the calculated midpoint potentials for the corresponding two-electron transfers in CHO-H466A and CHO-WT, respectively (Figure 6.8 and Table 6.2 in Chapter VI) (20). These data are consistent with a significant effect of the amino acid residue at position 466 on the electrophilicity of the enzyme-bound flavin in choline oxidase (20).

Steady state kinetic studies suggested a sequential mechanism with either choline or betaine aldehyde as substrate over a pH range of 6.5 to 10. The pH dependence of the kinetic

parameters at varying concentrations of both choline and oxygen indicated that a catalytic base with a  $pK_a$  value of 7.5 is required during the reductive-half reaction of both choline and betaine aldehyde oxidation. Based on the amino acid sequence alignment comparison of choline oxidase with other members of the GMC enzyme superfamily, the fully conserved His<sub>466</sub> was firstly proposed to be the catalytic base (28). However, pH-dependent studies with H466A showed similar pH-dependences although the  $pK_a$  value is shifted (Figure 5.7 in Chapter V) (21), suggesting that His<sub>466</sub> might not be the catalytic base. Strong evidence supporting this conclusion comes from the pH dependence of the imidazole effect with CHO-H466A, showing that imidazolium, but not imidazole, is the catalytically relevant species responsible for the partial rescue of the enzymatic activity of the mutant enzyme (Figure 5.6 in Chapter V) (21). These data are clearly difficult to reconcile with the assumption that His<sub>466</sub> is the catalytic base since, if that were the case, maximal rescue of the enzymatic activity of the mutant enzyme would have been observed at increasing pH. In this respect, recent structural data showed that the Nε2 atom of the equivalent histidine residue in the active site of cholesterol oxidase, His<sub>447</sub>, is protonated, suggesting that this conserved residue in the GMC oxidoreductase superfamily may play a role other than acting as a specific base in catalysis (29). In this context, a number of observations presented in this study suggest that in choline oxidase His<sub>466</sub> contributes to catalysis by modulating the electrophilicity of the flavin cofactor (by increasing its reduction-oxidation potential) and the polarity of the active site for efficient proton transfer of the hydroxyl proton from the alcohol substrate to the active site proton acceptor, and by stabilizing the negative charge that is formed in the transition state for the oxidation of choline to betaine aldehyde (Chapter V and VI) (20, 21). An alternative hypothesis arises from the observation of the recently solved X-ray crystallographic data of choline oxidase, which suggest that His<sub>351</sub> may act

as the catalytic base. In agreement with that hypothesis, the X-ray crystal structure of choline oxidase with its substrate choline docked in the active site showed that His<sub>351</sub> is located at a distance of  $\sim 3.3$  Å from the hydroxyl group of choline (Figure 1.27 in Chapter I). However, further biochemical and mechanistic characterization on the His351 mutant enzymes is required to draw conclusions<sup>1</sup>.

His<sub>466</sub> is involved in the oxidation of the choline substrate, but not in the following reduction of molecular oxygen catalyzed by choline oxidase. Evidence supporting this conclusion comes from the steady-state kinetic data with CHO-H466A as compared to those with the wild-type enzyme, showing that the  $k_{\text{cat}}/K_{\text{m}}$  value for choline decreases by three orders of magnitude whereas that for oxygen is not significantly changed in the mutant enzyme. The lack of involvement of His<sub>466</sub> in the oxidative half-reaction agrees well with previous kinetic data on choline oxidase as a function of pH, showing that no ionizable groups with  $\text{p}K_{\text{a}}$  values between 6 and 10 are required for oxidation of the enzyme-bound reduced flavin in catalysis (30).

Recent kinetic and mechanistic studies on the recombinant choline oxidase were carried out in our laboratory by Fan F. (31-33). These studies showed that the overall turnover with choline is limited by both chemical steps for alcohol and aldehyde oxidations (31). For alcohol oxidation, large deuterium isotope effects were observed by both steady state and pre-steady state kinetic approaches, indicating that the chemical step for choline oxidation is not masked by other steps (31). For aldehyde oxidation with betaine aldehyde as substrate, the  $k_{\text{cat}}$  ( $133 \text{ s}^{-1}$  at pH

---

<sup>1</sup> The H351A mutant was constructed and purified in our laboratory. Preliminary kinetic characterization showed a  $\sim 180$  fold decrease in  $k_{\text{cat}}/K_{\text{m}}$  value as compared to the wild type enzyme, indicating the important yet not essential role of His<sub>351</sub> in the catalysis by choline oxidase. In addition, pH-dependence studies with this mutant enzyme revealed a  $\text{p}K_{\text{a}}$  value of  $\sim 7.8$ , which may argue against the notion that His<sub>351</sub> is the catalytic base. Nonetheless, this ongoing study needs to be completed to draw more definitive conclusions (Rungsriruriyachai, K., and Gadda, G.; unpublished data).

10) determined by steady state kinetics is similar to  $k_{\text{red}}$  ( $135 \text{ s}^{-1}$  at pH 10) determined by pre-steady state kinetics, suggesting that the chemical step for betaine aldehyde oxidation is also rate-limiting (31). Both chemical steps of flavin reduction are significantly faster in the forward direction relative to the reverse direction, as suggested by the stopped-flow analyses of the reductive half-reactions with choline and betaine aldehyde (31). Unlike glucose oxidase and cholesterol oxidase, for which the chemical steps has been masked by other steps (34, 35), the rate-limiting chemical steps in choline oxidase allow an opportunity to unambiguously determine the chemical mechanism for catalysis. Primary deuterium and solvent kinetic isotope effects have been used to elucidate the mechanism for substrate oxidation by choline oxidase using both steady state kinetics and rapid kinetics techniques. The oxidation of choline catalyzed by choline oxidase occurs through an asynchronous hydride transfer mechanism, in which the substrate hydroxyl proton is abstracted to form an alkoxide intermediate followed by a hydride transfer to the flavin (31). An in-depth investigation of the hydride transfer in choline oxidation suggested the presence of quantum mechanical tunneling occurring within a highly pre-organized active site, through a process in which environmental vibrations (gating) is minimally involved (32). Evidence for this conclusion is provided by the temperature dependent studies on the  $k_{\text{cat}}/K_{\text{m}}$  and  $^{\text{D}}(k_{\text{cat}}/K_{\text{m}})$  values with choline as substrate (32). The large isotope effect on the preexponential factors ( $A_{\text{H}}'/A_{\text{D}}'$ ) determined from the temperature dependence of the  $k_{\text{cat}}/K_{\text{m}}$  values with choline and 1,2-[- $^2\text{H}_4$ ]-choline, with a value of  $\sim 14$ , rules out a classical over-the-barrier behavior for hydride transfer, for which  $A_{\text{H}}'/A_{\text{D}}'$  values between 0.7 and 1.7 are expected (36). Modeling choline into the active site of choline oxidase revealed an orientation of the substrate with its  $\alpha$ -carbon towards the N5 of flavin isoalloxazine ring, consistent with the proposed hydride transfer mechanism rather than carbanion mechanism. Although the distance between flavin N5 and  $\alpha$ -

carbon ( $\sim 3\text{-}4\text{ \AA}$ ), is rather large when compared to the distance of  $2.7\text{ \AA}$  proposed for tunneling by computational calculations (37), this distance is similar to the donor/acceptor distance observed in liver alcohol dehydrogenase ( $\sim 3.4\text{ \AA}$ ), for which the quantum mechanical tunneling is convincingly suggested (38, 39).

Moreover, the recently solved X-ray crystal structure of choline oxidase at  $1.86\text{ \AA}$  resolution showed dimeric structure (George Lountos, Fan Fan, Giovanni Gadda, and Allen M. Orville; unpublished results). The overall structure of monomeric choline oxidase resembles that of *p*-hydroxy-benzoate hydroxylase, and folds into substrate- and flavin-binding domains as other GMC enzymes. Structural comparison of the choline oxidase with other members of the GMC oxidoreductase superfamily, e.g., cholesterol oxidase (17, 40, 41), glucose oxidase (15, 16, 42), cellobiose dehydrogenase (19, 43), also revealed a highly conserved catalytic site. These structural similarities suggest a similar activation mechanism for the oxidation of their substrates. Mechanistic studies on cholesterol oxidase and glucose oxidase had been hampered since the chemical steps in these enzymes are masked by other kinetic steps (34, 35).

The X-ray crystal structure of choline oxidase also showed that His<sub>466</sub> is located at distance of  $\sim 3.3\text{ \AA}$  from the N(1) locus of the enzyme-bound flavin, consistent with the proposed role of this residue in stabilizing the negative charge that develops on the N(1)-C(2)=O locus of the bound flavin (Chapter V and VI). Interestingly, another active site histidine residue, His<sub>310</sub>, was found to be located at a distance of  $\sim 2.9\text{ \AA}$  from His<sub>466</sub> (His<sub>466</sub><sup>N $\delta$ 1</sup>-His<sub>310</sub><sup>N $\delta$ 1</sup>) (Figure 7.2 in Chapter VII). These structural data strongly suggest the presence of a proton-transfer network between the protonated conserved active site residue His<sub>466</sub> and His<sub>310</sub> (Chapter VII).

In this study, the preliminary results obtained by substituting the active site residue His<sub>310</sub> of choline oxidase with alanine show that the resulting enzyme is completely devoid of any

catalytic activity with choline as substrate. These data suggest that His<sub>310</sub> plays an essential role in the active site of choline oxidase, and consistent with the proposed proton-transfer network between the protonated conserved active site residue His<sub>466</sub> and His<sub>310</sub>.

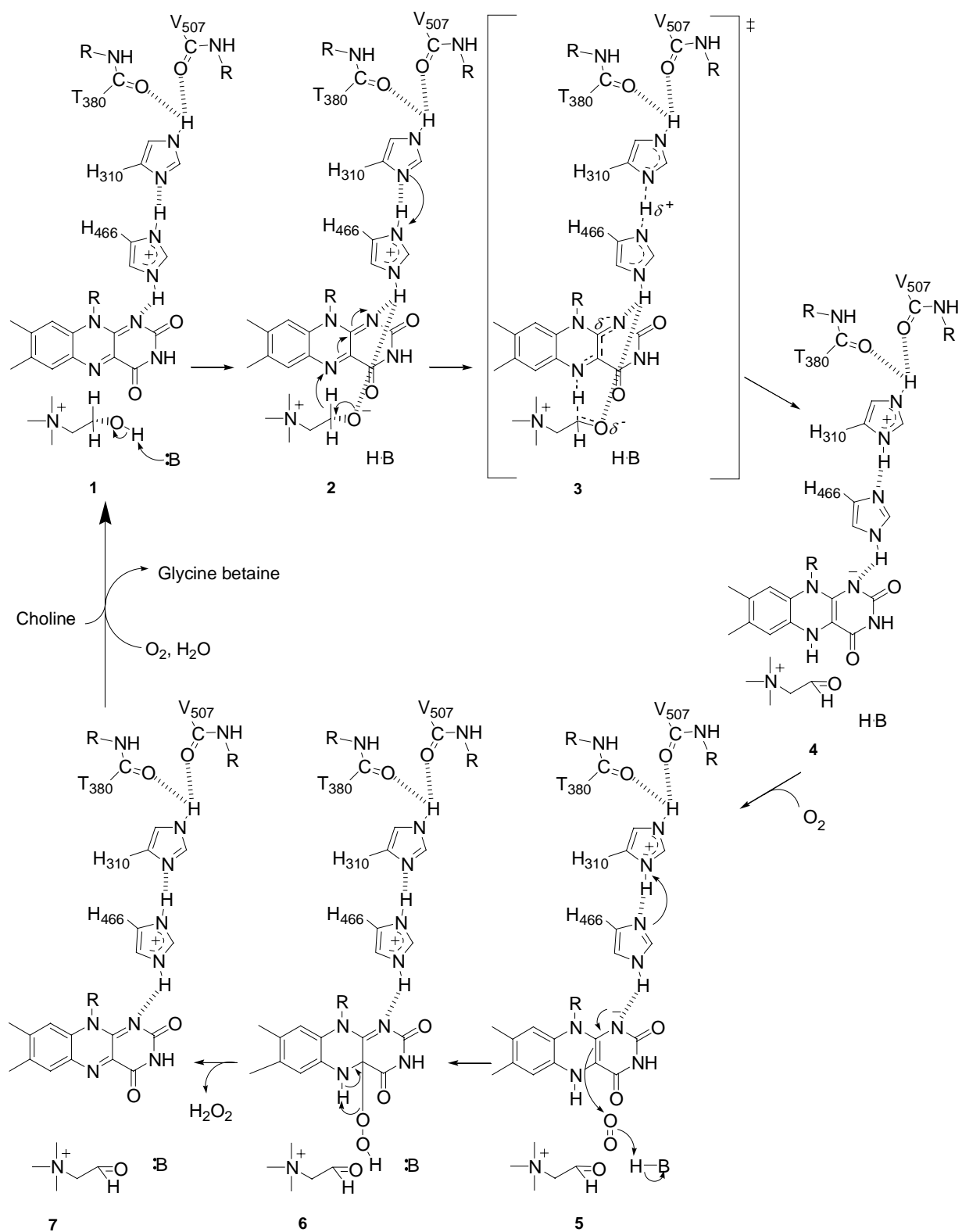
Overall, as shown in Scheme 8.1, and based on the results obtained from this study along with other structural, kinetic, and mechanistic data on wild-type choline oxidase, which have been determined by other members of our research group, the proposed mechanism of reaction for the oxidation of choline to glycine betaine catalyzed by choline oxidase can be summarized as following: 1) during the reductive half-reaction, an unidentified active site base with a  $pK_a$  of 7.5 activates the alcohol substrate with formation of an alkoxide species (species 1 and 2 in Scheme 8.1) (Chapter IV) (30, 31); 2) this alkoxide intermediate is transiently stabilized in the active site through electrostatic interaction with the N $\epsilon$ 2 atom of the protonated side chain of His<sub>466</sub> (species 3 in Scheme 8.1) (Chapter V) (21); 3) similarly, the protonated His<sub>466</sub> also stabilizes electrostatically the negative charge that develops at N(1)-C(2)=O locus of the reduced flavin (anionic species) through its N $\epsilon$ 2 atom (species 3 in Scheme 8.1) (Chapter VI) (20); 4) the hydride transfer from the  $\alpha$ -carbon of the substrate to the N(5) locus of the bound occurs quantum mechanically from the activated choline alkoxide species (species 3 in Scheme 8.1) (32); 5) His<sub>466</sub> is hydrogen bonded to His<sub>310</sub> (His<sub>466</sub><sup>N $\delta$ 1</sup>-His<sub>310</sub><sup>N $\delta$ 1</sup>) and the latter is hydrogen bonded to the main chain carbonyl oxygen atoms of Thr<sub>380</sub> and Val<sub>507</sub>. The main proposed role of such proton-transfer network is to prevent the protonated His<sub>466</sub> from losing its proton during the oxidative half-reaction. Thereby, this proton-transfer network serves to transfer this proton from His<sub>466</sub> to His<sub>310</sub> before the reaction of molecular oxygen. As a result of such proton transfer, the negative charge at the N(1)-C(2)=O locus of the anionic hydroquinone turned to be stabilized through hydrogen bonding with N $\epsilon$ 2 atom of the imidazole side chain of His<sub>466</sub> (species 4 in

Scheme 8.1) (Chapter VII); 6) during the oxidative half-reaction, and after the transfer of the proton from His<sub>466</sub> to His<sub>310</sub>, the electron delocalization from the N(1) locus of the anionic hydroquinone along with the proton transfer from the unidentified catalytic base result in the formation of the C(4a)-hydroperoxo-flavin (species 5 in Scheme 8.1); 7) the highly unstable C(4a)-hydroperoxo-flavin abstracts the second proton from the hydride at N(5) locus of the FAD with the subsequent release of H<sub>2</sub>O<sub>2</sub> and the formation of oxidized enzyme-bound FAD (species 6 and 7 in Scheme 8.1); 8) finally, the oxidation of the hydrated betaine aldehyde occurs through a base catalyzed transfer of a hydride ion from the organic substrate to the enzyme-bound FAD, with a mechanism that is similar to that proposed for the oxidation of choline as proposed recently in a study by our group on the mechanism of aldehyde oxidation (33).

In summary, the results obtained herein from the biochemical, biophysical, and mechanistic characterization of a choline oxidase variants in which the protein charge near the flavin N(1) locus was removed or reversed by site-directed mutagenesis suggest that in wild-type choline oxidase His<sub>466</sub> plays important role in: 1) the transient stabilization of choline alkoxide intermediate during the oxidation of choline to betaine aldehyde; 2) stabilization of the negative charge that develops on the N(1)-C(2)=O locus of the bound flavin; 3) modulation of the electrophilicity of the bound FAD for efficient catalysis by increasing its reduction-oxidation potential; 4) the covalent attachment of the FAD cofactor to the protein moiety for efficient catalysis; 5) modulation of the polarity of the active site for efficient proton transfer of the hydroxyl proton from the alcohol substrate to the active site proton acceptor. In addition the results obtained in this study also suggest that His<sub>310</sub> plays an essential role in the active site of choline oxidase and point out the possibility of its involvement in a proton-transfer network with His<sub>466</sub>. Interestingly, the present study on the biochemical and the mechanistic properties of wild-



type choline oxidase along with its active site mutants can shed light on other functionally and structurally related flavoprotein oxidases. In addition, this study will also provide a foundation for future rational design of efficient transition state analogs and inhibitors that could be used for the development of therapeutic agents that inhibit the formation of glycine betaine, and in turn render pathogenic bacteria susceptible to conventional treatments.



**Scheme 8.1.** Mechanism of oxidation of choline catalyzed by choline oxidase.

## References

- (1) Fan, F., Ghanem, M., and Gadda, G. (2004) Cloning, sequence analysis, and purification of choline oxidase from *Arthrobacter globiformis*: A bacteria enzyme involves in osmotic stress tolerance. *Arch. Biochem. Biophys.* 421, 149-58.
- (2) Gadda, G. (2003) Kinetic mechanism of choline oxidase from *Arthrobacter globiformis*. *Biochim. Biophys. Acta.* 1646, 112-8.
- (3) Ikuta, S., Imamura, S., Misaki, H., and Horiuti, Y. (1977) Purification and characterization of choline oxidase from *Arthrobacter globiformis*. *J. Biochem. (Tokyo)* 82, 1741-9.
- (4) Gorham, J. (1995) Betaines in Higher Plants - Biosynthesis and Role in Stress Metabolism, in *Amino Acids and their Derivatives in Higher Plants* (Wallsgrave, R. M., Ed.) pp 171-203, Cambridge University Press, Cambridge.
- (5) Landfald, B., and Strom, A. R. (1986) Choline-glycine betaine pathwayt confers a high level of osmotic tolerance in *Escherichia coli*. *J. Bacteriol.* 165, 849-55.
- (6) Peddie, B. A., Chambers, S. T., and Lever, M. (1996) Is the ability of urinary tract pathogens to accumulate glycine betaine a factor in the virulence of pathogenic strains? *J. Lab Clin. Med.* 128, 417-22.
- (7) Sleator, R. D., Wouters, J., Gahan, C. G. M., Abee, T., and Hill, C. (2001) Analysis of the role of OpuC, an osmolyte transport system, in salt tolerance and virulence potential of *Listeria monocytogenes*. *Appl. Environ. Microbiol.* 67, 2692-8.
- (8) Park, E. J., Jeknic, Z., Sakamoto, A., DeNoma, J., Yuwansiri, R., Murata, N., and Chen, T. H. (2004) Genetic engineering of glycinebetaine synthesis in tomato protects seeds, plants, and flowers from chilling damage. *Plant J* 40, 474-87.
- (9) Sakamoto, A., Alia, Murata, N., and Murata, A. (1998) Metabolic engineering of rice leading to biosynthesis of glycinebetaine and tolerance to salt and cold. *Plant Mol. Biol.* 38, 1011-9.
- (10) Mohanty, A., Kathuria, H., Ferjani, A., Sakamoto, A., Mohanty, P., Murata, N., and Tyagi, A. K. (2002) Transgenics of an elite indica rice variety *Pusa Basmati 1* harbouring the *codA* gene are highly tolerant to salt stress. *Theor. Appl. Genet.* 106, 51-57.
- (11) Holmstrom, K. O., Somersalo, S., Mandal, A., Palva, T. E., and Welin, B. (2000) Improved tolerance to salinity and low temperature in transgenic tobacco producing glycine betaine. *J Exp Bot* 51, 177-85.
- (12) Fitzpatrick, P. F., Kurtz, K., Gadda, G., Denu, J., Rishavy, M., and Cleland, W. W. (1999) Mechanism of Flavoprotein Oxidase, in *Enzymatic Mechanisms* (Frey, P. A., and Northrop, D. B., Eds.) pp 176-86, IOS Press.

- (13) Deshnum, P., Los, D. A., Hayashi, H., Mustardy, L., and Murata, N. (1995) Transformation of *Synechococcus* with a gene for choline oxidase enhance tolerance to salt stress. *Plant Mol. Biol.* 29, 897-907.
- (14) Rand, T., Halkier, T., and Hansen, O. C. (2003) Structural characterization and mapping of the covalently linked FAD cofactor in choline oxidase from *Arthrobacter globiformis*. *Biochemistry* 42, 7188-7194.
- (15) Hecht, H. J., Kalisz, H. M., Hendle, J., Schmid, R. D., and Schomburg, D. (1993) Crystal structure of glucose oxidase from *Aspergillus niger* refined at 2.3 Å resolution. *J. Mol. Biol.* 229, 153-172.
- (16) Wohlfahrt, G., Witt, S., Hendle, J., Schomburg, D., Kalisz, H. M., and Hecht, H. J. (1999) 1.8 and 1.9 Å resolution structures of the *Penicillium amagasakiense* and *Aspergillus niger* glucose oxidases as a basis for modelling substrate complexes. *Acta Crystallogr. D. Biol. Crystallogr.* 55, 969-977.
- (17) Li, J., Vrielink, A., Brick, P., and Blow, D. M. (1993) Crystal structure of cholesterol oxidase complexed with a steroid substrate: implications for flavin adenine dinucleotide dependent alcohol oxidases. *Biochemistry* 32, 11507-11515.
- (18) Vrielink, A., Lloyd, L. F., and Blow, D. M. (1991) Crystal structure of cholesterol oxidase from *Brevibacterium sterolicum* refined at 1.8 Å resolution. *J. Mol. Biol.* 219, 533-54.
- (19) Hallberg, B. M., Henriksson, G., Pettersson, G., and Divne, C. (2002) Crystal structure of the flavoprotein domain of the extracellular flavocytochrome cellobiose dehydrogenase. *J. Mol. Biol.* 315, 421-434.
- (20) Ghanem, M., and Gadda, G. (2006) Effects of reversing the protein positive charge in proximity of the N(1)-flavin locus of choline oxidase. *Biochemistry* 45, 3437-47.
- (21) Ghanem, M., and Gadda, G. (2005) On the catalytic role of the conserved active site residue His466 of choline oxidase. *Biochemistry* 44, 893-904.
- (22) Barber, M. J., Pollock, V., and Spence, J. T. (1988) Microcoulometric analysis of trimethylamine dehydrogenase. *Biochem. J.* 256, 657-9.
- (23) Efimov, I., Cronin, C. N., and McIntire, W. S. (2001) Effects of noncovalent and covalent FAD binding on the redox and catalytic properties of *p*-cresol methylhydroxylase. *Biochemistry* 40, 2155-66.
- (24) Fraaije, M. W., van den Heuvel, R. H., van Berkel, W. J., and Mattevi, A. (1999) Covalent flavinylation is essential for efficient redox catalysis in vanillyl-alcohol oxidase. *J. Biol. Chem.* 274, 35514-20.

- (25) Gadda, G., Wels, G., Pollegioni, L., Zucchelli, S., Ambrosius, D., Pilone, M. S., and Ghisla, S. (1997) Characterization of cholesterol oxidase from *Streptomyces hygroscopicus* and *Brevibacterium sterolicum*. *Eur. J. Biochem.* 250, 369-76.
- (26) Gomez-Moreno, C., Choy, M., and Edmondson, D. E. (1979) Purification and properties of the bacterial flavoprotein: thiamin dehydrogenase. *J. Biol. Chem.* 254, 7630-5.
- (27) Meyer, T. E., Bartsch, R. G., Caffrey, M. S., and Cusanovich, M. A. (1991) Redox potentials of flavocytochromes c from the phototrophic bacteria, *Chromatium vinosum* and *Chlorobium thiosulfatophilum*. *Arch. Biochem. Biophys.* 287, 128-34.
- (28) Gadda, G. (2003) pH and deuterium kinetic isotope effects studies on the oxidation of choline to betaine-aldehyde catalyzed by choline oxidase. *Biochim. Biophys. Acta.* 1650, 4-9.
- (29) Lario, P. I., Sampson, N., and Vrielink, A. (2003) Sub-atomic resolution crystal structure of cholesterol oxidase: what atomic resolution crystallography reveals about enzyme mechanism and the role of the FAD cofactor in redox activity. *J. Mol. Biol.* 326, 1635-50.
- (30) Ghanem, M., Fan, F., Francis, K., and Gadda, G. (2003) Spectroscopic and kinetic properties of recombinant choline oxidase from *Arthrobacter globiformis*. *Biochemistry* 42, 15179-88.
- (31) Fan, F., and Gadda, G. (2005) On the catalytic mechanism of choline oxidase. *J. Am. Chem. Soc.* 127, 2067-74.
- (32) Fan, F., and Gadda, G. (2005) Oxygen- and temperature-dependent kinetic isotope effects in choline oxidase: correlating reversible hydride transfer with environmentally enhanced tunneling. *J. Am. Chem. Soc.* 127, 17954-61.
- (33) Fan, F., Germann, M. W., and Gadda, G. (2006) Mechanistic studies of choline oxidase with betaine aldehyde and its isosteric analogue 3,3-dimethylbutyraldehyde. *Biochemistry* 45, 1979-86.
- (34) Bright, H. J., and Gibson, Q. H. (1967) The oxidation of 1-deuterated glucose by glucose oxidase. *J. Biol. Chem.* 242, 994-1003.
- (35) Kass, I. J., and Sampson, N. S. (1998) Evaluation of the role of the His447 in the reaction catalyzed by cholesterol oxidase. *Biochemistry* 37, 17990-18000.
- (36) Bell, R. P. (1974) *Chem. Soc. Rev.*, 513-44.
- (37) Billeter, S. R., Webb, S. P., Agarwal, P. K., Iordanov, T., and Hammes-Schiffer, S. (2001) Hydride transfer in liver alcohol dehydrogenase: quantum dynamics, kinetic isotope effects, and role of enzyme motion. *J Am Chem Soc* 123, 11262-72.

- (38) Rubach, J. K., and Plapp, B. V. (2003) Amino acid residues in the nicotinamide binding site contribute to catalysis by horse liver alcohol dehydrogenase. *Biochemistry* 42, 2907-15.
- (39) Rubach, J. K., Ramaswamy, S., and Plapp, B. V. (2001) Contributions of valine-292 in the nicotinamide binding site of liver alcohol dehydrogenase and dynamics to catalysis. *Biochemistry* 40, 12686-94.
- (40) Yue, Q. K., Kass, I. J., Sampson, N. S., and Vrielink, A. (1999) Crystal structure determination of cholesterol oxidase from *Streptomyces* and structural characterization of key active site mutants. *Biochemistry* 38, 4277-4286.
- (41) Lario, P. I., Sampson, N. S., and Vrielink, A. (2003) Sub-atomic resolution crystal structure of cholesterol oxidase: What atomic resolution crystallography reveals about enzyme mechanism and the role of the FAD cofactor in redox activity. *J. Mol. Biol.* 326, 1635-1650.
- (42) Hecht, H. J., Schomburg, D., Kalisz, H., and Schmid, R. D. (1993) The 3D structure of glucose oxidase from *Aspergillus niger*. Implications for the use of GOD as a biosensor enzyme. *Biosens. Bioelectron.* 8, 197-203.
- (43) Hallberg, B. M., Henriksson, G., Pettersson, G., Vasella, A., and Divne, C. (2003) Mechanism of the reductive half-reaction in cellobiose dehydrogenase. *J. Biol. Chem.* 278, 7160-7166.